

UNIVERSIDADE FEDERAL DO PARANÁ  
RIJKUNIVERSITEIT GRONINGEN



TATIANA ROJO MORO

EXTRACTION, CHARACTERIZATION AND BIOLOGICAL EFFECTS OF  
POLYSACCHARIDES FROM MARINE (MICRO)ALGAE

CURITIBA  
2022

TATIANA ROJO MORO

EXTRACTION, CHARACTERIZATION AND BIOLOGICAL EFFECTS OF  
POLYSACCHARIDES FROM MARINE (MICRO)ALGAE

Tese apresentada em cotutela entre a Universidade Federal do Paraná, ao Programa de Pós-graduação em Ciências (Bioquímica), Setor de Ciências Biológicas e a Rijkuniversiteit Groningen, Departament of Molecular Pharmacology, Faculty of Siences and Engineering como requerimento parcial para obtenção do título de Doutor em Ciências (UFPR) e Filosofia (RUG).

Orientadores: Prof. Dr. Miguel Daniel Nosedá (UFPR)  
Prof. Dr. Amalia M. Dolga (RUG)

Coorientadores: Prof. Dr. Maria Eugênia Duarte Nosedá (UFPR)  
Prof. Dr. Sheila Maria Brochado Winnischofer (UFPR)

CURITIBA

2022

DADOS INTERNACIONAIS DE CATALOGAÇÃO NA PUBLICAÇÃO (CIP)  
UNIVERSIDADE FEDERAL DO PARANÁ  
SISTEMA DE BIBLIOTECAS – BIBLIOTECA DE CIÊNCIAS BIOLÓGICAS

Moro, Tatiana Rojo.

Extraction, characterization and biological effects of polysaccharides from marine (micro)algae. / Tatiana Rojo Moro. – Curitiba, 2022.

1 recurso on-line : PDF.

Orientador: Miguel Daniel Nosedá.

Orientadora: Amália M. Dolga.

Coorientadora: Maria Eugênia Duarte Nosedá.

Coorientadora: Sheila Maria Brochado Winnischofer.

Tese (Doutorado) – Universidade Federal do Paraná, Setor de Ciências Biológicas. Programa de Pós-Graduação em Ciências – Bioquímica.

1. Microalga. 2. Algas. 3. Glioma. 4. Glucanas. 5. Citotoxicidade de mediação celular. 6. Fagocitose. I. Título. II. Nosedá, Miguel Daniel. III. Dolga, Amália M. IV. Nosedá, Maria Eugênia Duarte. V. Winnischofer, Sheila Maria Brochado. VI. Universidade Federal do Paraná. Setor de Ciências Biológicas. Programa de Pós-Graduação em Ciências - Bioquímica.

## ATA DE SESSÃO PÚBLICA DE DEFESA DE DOUTORADO PARA A OBTENÇÃO DO GRAU DE DOUTORA EM CIÊNCIAS (BIOQUÍMICA)

No dia trinta e um de janeiro de dois mil e vinte e dois às 08:30 horas, na sala [https://teams.microsoft.com/l/channel/19%3aNilxpscussuoyT5gSqqcj2znMGDWj0lwpRphVKEhGK\\_I1%40thread.tacv2/Geral?groupId=32c03a0c-bb03-4730-a295-83c45b4cef6e&tenantId=c37b37a3-e9e2-42f9-bc67-4b9b738e1df0](https://teams.microsoft.com/l/channel/19%3aNilxpscussuoyT5gSqqcj2znMGDWj0lwpRphVKEhGK_I1%40thread.tacv2/Geral?groupId=32c03a0c-bb03-4730-a295-83c45b4cef6e&tenantId=c37b37a3-e9e2-42f9-bc67-4b9b738e1df0), Defesa Remota - Plataforma Microsoft Teams, foram instaladas as atividades pertinentes ao rito de defesa de tese da doutoranda **TATIANA ROJO MORO**, intitulada: **Extraction, characterization and biological effects of polysaccharides from marine (micro)algae**. A Banca Examinadora, designada pelo Colegiado do Programa de Pós-Graduação CIÊNCIAS (BIOQUÍMICA) da Universidade Federal do Paraná, foi constituída pelos seguintes Membros: JULIANA BELLO BARON MAURER (UNIVERSIDADE FEDERAL DO PARANÁ), SELENE ELIFIO ESPOSITO (PONTIFÍCIA UNIVERSIDADE CATÓLICA DO PARANÁ), MARTINA SCHMIDT (UNIVERSITY OF GRONINGEN), JULIO CESAR DE CARVALHO (UNIVERSIDADE FEDERAL DO PARANÁ). A presidência iniciou os ritos definidos pelo Colegiado do Programa e, após exarados os pareceres dos membros do comitê examinador e da respectiva contra argumentação, ocorreu a leitura do parecer final da banca examinadora, que decidiu pela APROVAÇÃO. Este resultado deverá ser homologado pelo Colegiado do programa, mediante o atendimento de todas as indicações e correções solicitadas pela banca dentro dos prazos regimentais definidos pelo programa. A outorga de título de doutora está condicionada ao atendimento de todos os requisitos e prazos determinados no regimento do Programa de Pós-Graduação. Nada mais havendo a tratar a presidência deu por encerrada a sessão, da qual eu, , lavrei a presente ata, que vai assinada por mim e pelos demais membros da Comissão Examinadora.

CURITIBA, 31 de Janeiro de 2022.

Assinatura Eletrônica  
15/02/2022 14:04:37.0

JULIANA BELLO BARON MAURER  
Avaliador Interno (UNIVERSIDADE FEDERAL DO PARANÁ)

Assinatura Eletrônica  
16/02/2022 11:46:39.0

SELENE ELIFIO ESPOSITO  
Avaliador Externo (PONTIFÍCIA UNIVERSIDADE CATÓLICA DO PARANÁ)

Assinatura Eletrônica  
10/03/2022 11:36:18.0  
MARTINA SCHMIDT

Avaliador Externo (UNIVERSITY OF GRONINGEN)

Assinatura Eletrônica  
15/02/2022 14:25:27.0

JULIO CESAR DE CARVALHO  
Avaliador Externo (UNIVERSIDADE FEDERAL DO PARANÁ)



## TERMO DE APROVAÇÃO

Os membros da Banca Examinadora designada pelo Colegiado do Programa de Pós-Graduação CIÊNCIAS (BIOQUÍMICA) da Universidade Federal do Paraná foram convocados para realizar a arguição da tese de Doutorado de **TATIANA ROJO MORO** intitulada: **Extraction, characterization and biological effects of polysaccharides from marine (micro)algae**, que após terem inquirido a aluna e realizada a avaliação do trabalho, são de parecer pela sua APROVAÇÃO no rito de defesa.

A outorga do título de doutora está sujeita à homologação pelo colegiado, ao atendimento de todas as indicações e correções solicitadas pela banca e ao pleno atendimento das demandas regimentais do Programa de Pós-Graduação.

CURITIBA, 31 de Janeiro de 2022.

Assinatura Eletrônica

15/02/2022 14:04:37.0

JULIANA BELLO BARON MAURER

Avaliador Interno (UNIVERSIDADE FEDERAL DO PARANÁ)

Assinatura Eletrônica

16/02/2022 11:46:39.0

SELENE ELIFIO ESPOSITO

Avaliador Externo (PONTIFÍCIA UNIVERSIDADE CATÓLICA DO PARANÁ)

Assinatura Eletrônica

10/03/2022 11:36:18.0

MARTINA SCHMIDT

Avaliador Externo (UNIVERSITY OF GRONINGEN)

Assinatura Eletrônica

15/02/2022 14:25:27.0

JULIO CESAR DE CARVALHO

Avaliador Externo (UNIVERSIDADE FEDERAL DO PARANÁ)

## ACKNOWLEDGMENTS

Once I have heard from my father, in a casual conversation about goals: “Life is whatever happens to you when you are busy making others plans”. At that time, for being young, I could only understand a part of this particular phrase. But after 13 years, I could fully experience what this phrase really meant. With that, I can state that one of the best parts of live is to see how surprising it can become. Not even in my wildest dreams I taught I would live everything that I have been thought in 5 years of PhD.

As I look back, I can see the PhD itself and an experience abroad was a journey that profoundly changed my life in all ways. The urgency to gain maturity, for being far away from home and in the middle of a pandemic was sure a wake-up call. Being able to experience a new culture, learning new techniques in research; working, studying hard, making mistakes and learning from them; and the opportunity of exchange experiences with different people along the way made me as I am now. So, making an acknowledgments section is always the hardest thing to write about. Because I want so badly to be able to transmit everything that I am grateful for, but I know that words are not enough for that. With an open heart, I will try to write my best here.

I want to thank God for every step of the way that has been made. Thank you for my life, family, friends, love and to plant curiosity inside my heart that has developed into a PhD thesis. In every action and beauty of nature it is possible to see your perfect work. We are only trying to organize your actions for us to understand more about it. I would like to thank my family. Mom, dad and sister, thank you for everything. Mom, you are my rock solid, thank you so much to always fight for your family unit and teach to not give up easily. I learned from you that if you fall 10, you have to stand up 11 times. Dad, they say that the apple doesn't fall far from the tree and that really apply for us. From you, I had learned to study hard, to have curiosity and to be kind with others. Cami, thank you for always showing so much unconditional love for animals and sending me a lot of stickers and memes.

For my “abuela” (grandma) Dolores. Those 6 years living with you were so important for me and it was very strange to be without you in Curitiba. I miss you very much every day, and I dearly hope that you are proud to see what I became. Thank you for teaching me 2 very important things in life: Being fearless, as you were brave enough to leave Madrid to live in Brazil with grandpa (I also packed my bags and left my comfort zone for a while, far away from family, friends and love) and to be truthful at all situations. Y te quiero muchísimo, siempre.

For my love, Phelipe. Baby, we have been together for such a long time now and it was such a ride. You are the most amazing person: caring, loving, kind, and so optimistic in life. Thank you so much for always supporting my dreams, since the beginning. That led us into so many good adventures! Since taking the bus with me to make sure I would not get lost at new places, taking care of me when I wasn't feeling so well, to cross the city just to see me, for all the laughs, to patiently wait for me to come back after a year abroad, for the good advices, lots of love, to be my best friend and to stand by my side. I love you so much. Thank you also for finding and taking care of your baby dog Mille and build your small family. And I also would like to thank my in-laws for always welcomed me so well in their family, to make me feel so loved and for all the good times.

For my supervisors: in order to make dreams turn into reality, work is the bridge between them. And there is no academic work without a team involved. Professor Miguel and Maria Eugênia, thank you so much for accepting me in your lab group. I developed under your orientations so many lessons that I will take for my life as a person and as a professional. Professor Miguel, it is able to see from far your love for research and being such a hard worker! Professor Maria Eugênia, thank you for your observations, contributions for your group. Professor Sheila, thank you so much for your kindness, love, patience and sharing knowledge. And a big thanks for trusting in me (for being for first student abroad) and giving one of my best opportunities of my life, to be able to develop science in the Netherlands and for making me meet Marina and Amalia. Amalia, thank you for being so thoughtful with me, not only at the pandemics, but to be able to be your student. I can really say that I have matured under your guidance and that is something I will never forget.

They say that every person we meet in life is for a particular reason. I truly believe in this statement, even more when from that person we are able to develop the best version of ourselves. Also, when you can look up to emulate in the future. Marina, you were a whole mixed package of the both situations described, along with friendship/family and mentoring for me. There are not enough words to describe the pleasure of being guided from you. You are the most sweet, caring and understandable person. And at the same time, you never let the excellence level of work to be lower down, pushing my boundaries further. I will never forget for all the good things that you, Ricardo, Ruth and Judith did to me in two years, especially in such a dark time as a pandemic. And as a plus, I got great friends/family. I want to take you guys for my life. I am a very lucky girl.

Talking about luck, I want to say a huge thanks to my Brazilian colleagues at Nosedá's lab at the UFPR biochemistry department. It was so great to be able to discuss results and methodologies, in a form to help each other out, but as my good friend Diego points out: one of the highest points of this group was the "polemic topic of the week". It is really good to be able to discuss philosophical issues and being able to go outside of the comfort zone, with so much respect. A sweet thank you to my special friends at E2 lab: Ester, Sarah, Shayla and Isa for all laughter's, good memories, friendship, sharing experiences and treating me so well. A special thank you also to Jenifer Mota, with the partnership in 2019 and to helped me out to make the best professional decision ever made. As well Jean, for the strong friendship built in such a short time. I adore you! Thank you for the good times and standing by my side at the bad ones. Those life encounters are meant to be.

For the Dutch/international colleagues of molecular pharmacology at RUG, thank you so for welcoming me in such a good way. I keep in my heart the days going to "Dot" to relax a bit, the meetings and helping out one and another. From Dolga's lab, I would like to thank in special Asmaa, Alejandro and Melody. Asmaa, such a joy being your office mate. Thank you for always helping me out with the experiments and beign a lovely person. Ale, I have had such a great time with you, thank you for the laughter's. Melody, the most cheerful, amazing parent and a sweetheart girl, it is very joyful to see you develop in the Molecular Pharmacology group as a researcher. Ahya, you are such a sweet woman, it was such a pleasure to have you by my side thought a year. Loved your company for everything, specially to eat bimbimnap on Asia Today and to be able to expand thoughts thought conversations, in so many topics. There are some people that you simply link in a fast way. Rosa, you are exactly this type of person. It is not easy to find someone with the same type of humor, and I founded in you. Thanks so much for everything: specially laughter's, dinner (diet exists?) and translating things from Dutch to English for me. It is so good to be your friends with both of you.

Family is not always composed by blood relations. They are also with the people that we keep in your heart. A huge shout out to my Groningen family: Ayha, Chiara, Ligia, Isabelle, Marina and Ricardo. You guys made my weekends and my period abroad so much lighter. Thanks for routine and all the Friday night dinners in the summer. I love each one of you. And a big thank you for my American family: Karen and Nils Ericson. Those sunny days in St. Peterburg will always be cherish to my heart.

To my beloved friends from the pharmacy undergraduate course: Karina, Matheus, Natan, Reginaldo, Isabelle and Felipe. I miss you all and it is so good to have all of you as

friends! Everyone is on one place, but we are always together, no matter what. Thank you for all the good memories, love all tons. To my good friends from Ponta Grossa, Denise, Jessyca, Cesar, Carlos, Otavio and Jessica Cionek thank you for 15 years of friendship. We are not together every day anymore, but your friendship remains as before. You are all in a safe place in my heart.

I would like to thank for all the staff and technicians from Federal University of Paraná and Rijkuniversiteit Groningen for the usage of equipment's, reagents and infrastructures. I also acknowledge CAPES-PROEX for my brazilian scholarship, CAPES-PrInt for my international scholarship and RUG for my financial support in Groningen.

Well, after all of that, I can state another phrase that I heard in a song, resuming this experienced phase of my life: "It is not about to reach on the top of the world and know that you conquer it, but feel that the way had strengthen you... cause life is a train, and we are only passengers about to departure". But now it is time to go onward, to a new adventure that waits for me. Muito obrigada por tudo.

“From sprinkler splashes to fireplace ashes, I gave my blood, sweat, and tears for this (...) 'Cause there were pages turned with the bridges burned, everything you lose is a step you take. So make the friendship bracelets, take the moment and taste it. You've got no reason to be afraid. You're on your own, kid, yeah, you can face this” - Taylor Swift - You're on your own, Kid.

“Para amar se necessita corage, yo si me atrevo, mira” – Nairobi  
– La Casa de Papel

“Ama sempre, fazendo pelos outros o melhor que possas realizar. Age auxiliando. Serve sem apego. E assim vencerás.” – Chico Xavier.

## RESUMO

Polissacarídeos purificados de algas marinhas possuem alto valor biotecnológico e apresentam diversas ações biológicas, incluindo atividade citotóxica, antiviral, anticoagulante, entre outras. Nesta tese, vários polissacarídeos foram isolados de algas e microalgas marinhas, caracterizados e quimicamente modificados para melhorar seus potenciais efeitos biológicos. O objetivo principal da tese foi caracterizar suas estruturas químicas e vinculá-las a potenciais efeitos biológicos. A  $\beta$ -D-glucana purificada de *Conticribra weissflogii* aumentou a atividade fagocítica de macrófagos. Vários polissacarídeos purificados de *Isochrysis galbana* induziram uma redução do metabolismo mitocondrial ao nível da glicólise, ciclo cítrico, aminoácidos e oxidação de ácidos graxos e reduziram a atividade metabólica geral das células de glioblastoma U251. Dados recentes mostraram um efeito citotóxico de células U87MG em resposta a polissacarídeos e correspondente heterorhammana purificada, oversulfatada de *Gayralia brasiliensis*. Nesta tese, foi investigado os efeitos desses polissacarídeos nas funções mitocondriais. Foi observada a polarização da membrana mitocondrial e o aumento da produção de ROS mitocondrial em resposta à aplicação desses polissacarídeos. Em conclusão, os polissacarídeos exercem vários efeitos biológicos nas células tumorais, e esses efeitos variam desde a morte celular até o metabolismo mitocondrial dependendo do modelo biológico, da estrutura química nativa ou da modificação estrutural induzida. Para estudos futuros, sugere-se investigar as vias moleculares dos polissacarídeos em relação a ligação a receptores e a regulação a proteínas.

Palavras-chave: Microalgas; Algas; Glioma;  $\beta$ -Glucanas; Heterorammana; Citotoxicidade; Respiração celular; Fagocitose.

## ABSTRACT

Polysaccharides purified from marine algae have high biotechnological value and exhibit various biological actions including cytotoxic activity, antiviral, and anticoagulant, among others. In this thesis, various polysaccharides were isolated from marine algae and microalgae, characterized and chemically modified to improve their potential biological effects. The main aim of the thesis was to characterize their chemical structures and link them to potential biological effects.  $\beta$ -D-glucan purified from *Conticribra weissflogii* enhanced phagocytic activity of macrophages. Several polysaccharides purified from *Isochrysis galbana* induced a reduction of the mitochondrial metabolism at the level of glycolysis, the citric cycle, amino acid, and fatty acid oxidation and reduced the overall metabolic activity of U251 glioblastoma cells. Recent data showed a cytotoxic effect of U87MG cells in response to polysaccharides and corresponding oversulfated heterorhamman purified from *Gayralia brasiliensis*. In this thesis, we further investigated the effects of these polysaccharides on the mitochondrial functions. We observed mitochondrial membrane polarization and increased mitochondrial ROS production in response to these polysaccharides application. In conclusion, polysaccharides exert various biological effects in tumor cells, and these effects vary from cell death to mitochondrial metabolism depending on the biological model, the chemical native structure or induced structural modification. For further studies, it would be worth investigating the molecular pathways of polysaccharides in relation to receptor binding and downstream protein regulation.

Keywords: Microalgae; Algae; Glioma;  $\beta$ -Glucans; Heterorhamman; Cytotoxicity; Cell Respiration; Phagocytosis.

## SAMENVATTING

Algen en microalgen hebben hoge biotechnologische waarde. Polysachariden hebben meerdere biologische effecten, zoals onder andere cytotoxische, antivirale en antistolling activiteit. Het doel van dit werk is om polysachariden uit algen en microalgen te isoleren, karakteriseren en chemisch te modificeren en hun immunostimulerende effect op macrofagen (RAW 269.7) en cytotoxische activiteit tegen glioblastoom cellen (U87MG en U251) te onderzoeken. De bestudeerde stammen waren: *Conticribra weissflogii*, *Isocrysis galbana*, en de zee-algen stam *Gayralia brasiliensis*. Chemische en spectroscopische analyse toonde dat microalgen stammen verschillende typen  $\beta$ -D-glucans hadden. *Gayralia brasiliensis* had een heterorhamman, en deze werd overgesulfateerd om de biologische activiteit te verhogen. Biologisch onderzoek gepresenteerd in deze thesis toonde dat  $\beta$ -D-glucan van *Conticribra weissflogii* een verhoogde fagocytotische activiteit van macrofagen van gist induceerde. Een interventie met *Isocrysis galbana* in mitochondrieel metabolisme op het niveau van glycolyse, de citroenzuurcyclus, aminozuren en  $\beta$ -oxidatie verlaagde de metabolische activiteit van U251 glioblastoom cellen. Eerdere data toonde dat *Gayralia brasiliensis* heterorhamman een cytotoxisch effect heeft op U87MG cellen. Verder onderzoek werd uitgevoerd om de effecten op de mitochondriën te bestuderen. Dit polysacharide kan de mitochondriële membraanpolarisatie en de mitochondriële ROS-productie beïnvloeden, wat mogelijk de levensvatbaarheid van de cellen beïnvloedt. In conclusie, polysachariden toonden verschillende biologische effecten op cellen, afhankelijk van het biologische model, de structuur van het natuurlijke polysacharide of de gemodificeerde structuur. Voor toekomstige studies is het interessant om te richten op moleculaire interacties tussen polysachariden en cellen.

Sleutelwoorden: Microalgen; Algen; Glioom;  $\beta$ -glucans; Heterorhamman; Cytotoxiciteit; Celademhaling; Fagocytose.

## FIGURE SUMMARY

### INTRODUCTION

Figure 1. Classification scheme of different algal groups.....	20
Figure 2. A scheme of the biotechnological appliance of algae biomass.....	22
Figure 3. Applications of different biomolecules extracted from algae and microalgae biomass in the biotechnological industry.....	25
Figure 4. Classification of different forms of polysaccharides.....	26
Figure 5. The action of polysaccharides upon different immune cells.....	30

### CHAPTER I - Chemical structure and biological activity of the $\beta$ -D-glucan (1 $\rightarrow$ 3)-linked isolated from marine diatom *Conticribra weissflogii*

Figure 1. HPSEC Elution profile of CAC, obtained with refractive index (RI) detector.....	42
Figure 2. $^{13}\text{C}$ NMR spectrum (a) and $^{13}\text{C}$ NMR DEPT spectrum (b) of the polysaccharide CAC (solvent: $\text{D}_2\text{O}$ , at $70^\circ\text{C}$ ).....	43
Figure 3. HSQC spectrum of polysaccharide CAC.....	43
Figure 4. NMR analyses of the smith-degraded product (CAC-s). $^{13}\text{C}$ (a) and $^{13}\text{C}$ NMR DEPT (b) NMR spectra (solvent: $\text{D}_2\text{O}$ , at $70^\circ\text{C}$ ).....	44
Figure 5. Proposed structure for the smith-degraded product (CAC-s).....	44
Figure 6. Proposed structure for the water-soluble polysaccharide extracted from diatom <i>C. weissflogii</i> . Molar proportions: x: 0.05; y:1 .....	45
Figure 7. Metabolic activity determined by MTT test at glioblastoma cells U87MG (a) and U251 (b) with CAC $\beta$ -D-glucan at 50 and 100 $\mu\text{g. mL}^{-1}$ concentrations at 24, 48 and 72 h treatment time points.....	46
Figure 8. Macrophage RAW 267.4 cells challenged with CAC $\beta$ -D-glucan at 2.5; 5.0; 10 and 25 $\mu\text{g. mL}^{-1}$ concentrations.....	47
Figure S1. Metabolic activity determined by MTT test at mouse hippocampal cell line (HT-22) with CAC at 50; 100; 150 and 200 $\mu\text{g. mL}^{-1}$ concentrations in different time points (24, 48 and 72 h).....	50

CHAPTER II – (1→6, 1→3)-β-D-glucan isolated from *Isochrysis galbana* decreases the mitochondrial activity of human glioblastoma cell lines

Graphical abstract.....	53
Figure 1: Elution profile of IAQ using HPSEC MALLS analysis, obtained with a light scattering (LS) and refractive index (RI) detector (a). Molar mass distribution of IAQ using HPSEC (b). <sup>13</sup> C NMR spectrum (c) and <sup>13</sup> C NMR DEPT spectrum of crude extract IAQ and (d) solvent DMSO-d <sub>6</sub> , at 70 °C.....	61
Figure 2: Elution profiles of IAQ-c using HPSEC-MALLS-RI (a). <sup>13</sup> C NMR spectrum (b) and HSQC correlation spectrum of fraction IAQ-c (c). DMSO-d <sub>6</sub> , 70 °C.....	63
Figure 3: Elution profile of HMW using HPSEC-MALLS-RI (a). HSQC correlation spectrum of fraction HMW (b). DMSO-d <sub>6</sub> , 70 °C.....	64
Figure 4: Elution profile of LMW using HPSEC-MALLS-RI (a). HSQC correlation spectrum of fraction LMW (b). DMSO-d <sub>6</sub> , 70 °C. (c).....	65
Figure 5: Proposed structure for <i>I. galbana</i> extracted polysaccharide.....	67
Figure 6: Metabolic activity at glioblastoma U87MG (a,b,c) and U251 cell lines (d,e,f) in response to of <i>I. galbana</i> extracts treatment. ....	70
Figure 7: Metabolic activity at glioblastoma U87MG (a,b,c) and U251 cell lines (d,e,f) in response to HMW treatment.....	72
Figure 8: Mitoplate heatmap of U251 cell line with consumed substrates (a) and individual diminished substrate consumption after IAQ treatment (b-m). ....	74
Figure 9: Representative mitoplate results from of U87MG cell line. Heatmap with consumed substrates (a) and individual diminished substrate consumption after IAQ treatment ....	75
Figure 10: (1→3,1→6)-β-D-glucan effect in metabolic pathways upon U251 and U87MG cell lines.....	76
Figure S1: HSQC correlation spectrum of fraction IAQ. DMSO-d <sub>6</sub> , 70 °C.....	85
Figure S2: HSQC correlation spectrum of LMW fraction in DMSO-d <sub>6</sub> , 70 °C.....	85
Figure S3: Metabolic activity determined at glioblastoma cell lines U87MG (a,b,c) and U251 (d,e,f) with LMW.....	86

Figure S4: Metabolic activity at hippocampus cell lines HT22 with IAQ (a,b,c) and HMW (d,e,f).....	87
Figure S5: Cell cycle progression with the presence of IAQ (a) and HMW (b). .....	87
Figure S6: Heatmap with analyzed substrates when U251 (a) and U87MG cells (b) are treated with IAQ at 100 ug. mL <sup>-1</sup> , 24 h. ....	88
Figure S7: Representative mitoplate results from of U87MG cell line. Heatmap with consumed substrates (a) and individual diminished substrate consumption after IAQ treatment (100 ug. mL <sup>-1</sup> ). ....	89

CHAPTER III – Mitochondrial effects of an oversulfated heterorhamman from *Gayralia brasiliensis* in glioblastoma cell lines

Graphical abstract.....	91
Figure 1: Cell viability assessed by an MTT assay in glioblastoma cell line U87MG a), b), c) and at hippocampus cell lines HT22 d), e), f) challenged with Gb1 (50; 100; 150 and 200 µg. mL <sup>-1</sup> for 24, 48, and 72 h).....	97
Figure 2: Cell viability assessed by an MTT assay in glioblastoma cell line U87MG a), b), c) and at hippocampus cell lines HT22 d), e), f) challenged with Gb1-OS (50; 100; 150 and 200 µg. mL <sup>-1</sup> for 24, 48, and 72 h).....	98
Figure 3: The effects of GB1 and Gb1-OS on the mitochondrial function. Mitochondrial superoxide levels a), b) and mitochondrial membrane potential c), d) of U87MG cells upon Gb1 and Gb1-OS treatment (100 µg. mL <sup>-1</sup> for 72 h).....	101
Figure 4: Representative image of U87MG cell respiration (control) a) and treated with Gb1 b), Gb1-OS c), at 100 µg. mL <sup>-1</sup> for 72 h.....	103
Figure 5: Analysis of high-resolution respirometry of the treatment of Gb1 and Gb1-OS in U87MG cells. The respiration states: Basal a), ATP linked b), and Uncoupled c). Treatment of the cells with the polysaccharides were at 100 µg. mL <sup>-1</sup> for 72 h.....	104
Figure S1. Cell viability at hippocampus cell lines HT22 with Gb1 a), b), c) and Gb1-OS d), e), f).....	110

## DISCUSSION

Figure 1: $\beta$ -D-glucan immunostimulatory effect. $\beta$ -D-glucan from <i>Conticribra weissflogii</i> microalgae binds with carbohydrate receptors at the cell surface of macrophages.....	112
Figure 2: $\beta$ -D-glucans and heterorhamman effects upon U251 and U87MG glioblastoma cell lines.....	114

## TABLE SUMMARY

CHAPTER I - Chemical structure and biological activity of the  $\beta$ -D-glucan (1 $\rightarrow$ 3)-linked isolated from marine diatom *Conticribra weissflogii*

Table 1. Yield, chemical analyses, and monosaccharide composition of the polysaccharide fraction obtained from diatom *C. weissflogii*.....42

Table 2. NMR chemical shift assignments of polysaccharide CAC isolated from diatom *C. weissflogii*.....43

Table 3.  $^{13}\text{C}$  NMR assignments of polysaccharide CAC (in  $\text{Me}_2\text{SO}_4-d_6$ ) compared with (1 $\rightarrow$ 3)-linked  $\beta$ -glucans from other sources.....43

Table 4. Methylation analysis of polysaccharide fraction CAC from diatom *C. weissflogii*.....44

Table 5. Phagocytic activity of RAW 264.7 cells upon yeast with CAC  $\beta$ -D-glucan.....48

CHAPTER II – (1 $\rightarrow$ 6, 1 $\rightarrow$ 3)- $\beta$ -D-glucan isolated from *Isochrysis galbana* decreases the mitochondrial activity of human glioblastoma cell lines

Table 1.  $^{13}\text{C}$  NMR assignments of polysaccharide IAQ isolated from *I. galbana*.....62

Table 2. Yield, chemical analyses, and monosaccharide composition of polysaccharide fractions obtained from diatom *I. galbana*.....62

Table 3. Monosaccharide composition (%) of polysaccharide ultrafiltration fractions obtained from *I. galbana*.....66

Table 4.  $^{13}\text{C}$  NMR assignments of polysaccharide IAQ<sup>a</sup>, IAQ-c<sup>b</sup> and ultrafiltered fraction (<sup>c</sup>HMW and <sup>d</sup>LMW) in  $\text{Me}_2\text{SO}_4-d_6$ .....66

Table 5. Methylation analysis of polysaccharide obtained from *I. galbana*.....67

## SUMMARY

<b>1. INTRODUCTION.....</b>	<b>20</b>
ALGAE: DEFINITION AND CLASSIFICATION.....	20
ALGAE INDUSTRIAL APPLICATIONS.....	21
<i>Upstream and downstream processes to biomass formation.....</i>	<i>22</i>
<i>Extraction, purification, and fractioning methods.....</i>	<i>23</i>
<i>Applications of algae extracts.....</i>	<i>25</i>
POLYSACCHARIDES.....	26
GLIOBLASTOMA AND POLYSACCHARIDES.....	27
<b>2. OBJECTIVES.....</b>	<b>32</b>
<b>3. CHAPTER I – CHEMICAL STRUCTURE AND BIOLOGICAL ACTIVITY OF THE (1→3)-LINKED β-D-GLUCAN ISOLATED FROM MARINE DIATOM <i>Conticribra weissflogii</i></b>	
ABSTRACT.....	40
INTRODUCTION.....	40
MATERIAL AND METHODS.....	41
<i>Microalgal strain and culture maintenance.....</i>	<i>41</i>
<i>Extraction and purification of C. weissflogii polysaccharide.....</i>	<i>41</i>
<i>Biochemical analysis.....</i>	<i>41</i>
<i>Controlled Smith degradation.....</i>	<i>41</i>
<i>High-pressure size exclusion chromatography (HPSEC) analysis.....</i>	<i>41</i>
<i>Methylation analysis.....</i>	<i>41</i>
<i>Nuclear Magnetic Resonance (NMR) spectroscopy.....</i>	<i>41</i>
<i>Biological activity assays.....</i>	<i>41</i>
<i>Cells and culture conditions.....</i>	<i>41</i>
<i>Cell metabolic activity assay.....</i>	<i>42</i>
<i>Morphology alteration and cell proliferation assay.....</i>	<i>42</i>
<i>Phagocytosis assay.....</i>	<i>42</i>
<i>Flow cytometry assays.....</i>	<i>42</i>
<i>Statistical analysis.....</i>	<i>42</i>

RESULTS AND DISCUSSION.....	42
<i>Extraction and characterization of the water-soluble polysaccharide from C. weissflogii.....</i>	42
<i>NMR spectroscopic analysis.....</i>	42
<i>Methylation analysis of CAC.....</i>	43
<i>Analysis of the Smith-degraded product.....</i>	43
<i>Biological activity of polysaccharide extracted from C. weissflogii.....</i>	45
<i>Effects of CAC <math>\beta</math>-D-glucan on glioblastoma and neuronal cells.....</i>	45
<i>Effect of CAC <math>\beta</math>-D-glucan on the phagocytic activity of macrophages.....</i>	45
CONCLUSION.....	48
ACKNOWLEDGEMENTS.....	48
REFERENCES.....	48
SUPPLEMENTARY DATA.....	50

**4. CHAPTER II – (1→6, 1→3)- $\beta$ -D-GLUCAN ISOLATED FROM *Isochrysis galbana* DECREASES THE MITOCHONDRIAL ACTIVITY OF HUMAN GLIOBLASTOMA CELL LINES**

ABSTRACT.....	52
INTRODUCTION.....	53
MATERIAL AND METHODS.....	54
<i>Microalgae strain, culture maintenance, and biomass formation.....</i>	54
<i>Extraction, purification, and fractioning of <i>Isochrysis galbana</i> polysaccharides.....</i>	55
<i>Biochemical analyses.....</i>	55
<i>Methylation.....</i>	56
<i>High-pressure size exclusion chromatography (HPSEC) analysis.....</i>	57
<i>Nuclear Magnetic Resonance (NMR) spectroscopy.....</i>	57
<i>Cell culture and treatment.....</i>	58
<i>Metabolic activity assay.....</i>	58
<i>Cell cycle analysis.....</i>	58
<i>Cell death analysis.....</i>	59
<i>Mitoplate assay.....</i>	59
<i>Statistical analyses.....</i>	59
RESULTS AND DISCUSSION.....	60
<i><math>\beta</math>-D-Glucan characterization from <i>I. galbana</i>.....</i>	60

<i>Biological activity of polysaccharide extracted from I. galbana</i> .....	68
<i>β-D-glucan suppresses NADH mediated metabolism</i> .....	68
<i>β-D-glucan affects ETC complexes I, III, and IV on U251 and U87MG glioblastoma cell lines</i> .....	73
CONCLUSION.....	79
ACKNOWLEDGEMENTS.....	79
REFERENCES.....	79
SUPPLEMENTARY DATA.....	85

**5. CHAPTER III – MITOCHONDRIAL EFFECTS OF AN OVERSULFATED HETERORHAMMAN FROM *Gayralia brasiliensis* IN GLIOBLASTOMA CELL LINES**

ABSTRACT.....	90
INTRODUCTION.....	92
MATERIAL AND METHODS.....	93
<i>Gb1 and Gb1-OS preparation</i> .....	93
<i>Cell viability MTT assay</i> .....	93
<i>Annexin/PI assay</i> .....	94
<i>Measurement of mitochondrial membrane potential and mitochondrial superoxide production</i> .....	94
<i>High-resolution respirometry</i> .....	95
<i>Statistical analyses</i> .....	95
RESULTS AND DISCUSSION.....	95
<i>Polysaccharide structure</i> .....	95
<i>Gb1-OS affects the U87MG cell viability</i> .....	96
<i>Gb1-OS hyperpolarizes mitochondrial membrane, enhances mitochondrial ROS production, suggesting a reduction in the activity of mitochondrial OXPHOS</i> .....	100
CONCLUSION.....	107
ACKNOWLEDGEMENTS.....	107
REFERENCES.....	108
SUPPLEMENTARY DATA.....	110

<b>6. DISCUSSION.....</b>	<b>111</b>
<b>7. CONCLUSIONS.....</b>	<b>117</b>
<b>8. APPENDIX 1.....</b>	<b>119</b>
<b>9. REFERENCIAS.....</b>	<b>154</b>

# 1. INTRODUCTION

## 1.1 ALGAE: DEFINITION AND CLASSIFICATION.

Algae belong to a large group of photosynthetic prokaryotic and eukaryotic organisms. These unicellular and multicellular organisms are present in aquatic systems (marine and freshwater) and also in terrestrial environments (BARSANTI & GUALTIERI, 2014; DEBIAGI *et al.*, 2017). It is difficult to fit algae into a formal taxonomic position because they are a very diverse group of organisms with polyphyletic origin (DE CLERCK, GUIRY, LELIAERT, SAMYN, & VERBRUGGEN, 2013; MANOYLOV, 2014).

A classic and simple way is to divide them into microalgae and macroalgae (Figure 1). Macroalgae are divided into green algae (Phylum *Chlorophyta*), brown algae (Phylum *Phaeophyta*), and red algae (Phylum *Rhodophyta*). Macroalgae are in general benthic, growing on diverse substrates. Microalgae species are present in the above-mentioned phyla and in several others, such as *Bacillariophyta*, *Haptophyta*, etc. (figure 1). In general, microalgae are floating or suspended in the water column (planktonic), constituting phytoplankton, and they are responsible for about 90% of the photosynthesis that occurs in the oceans. Microalgae have the characteristic to form colonies, and each cell performs all vital functions (JEFFREY, WRIGHT, & ZAPATA, 2011; IBÁÑEZ & CIFUENTES, 2013; WANG, CHEN, HUYNH, & CHANG, 2015).

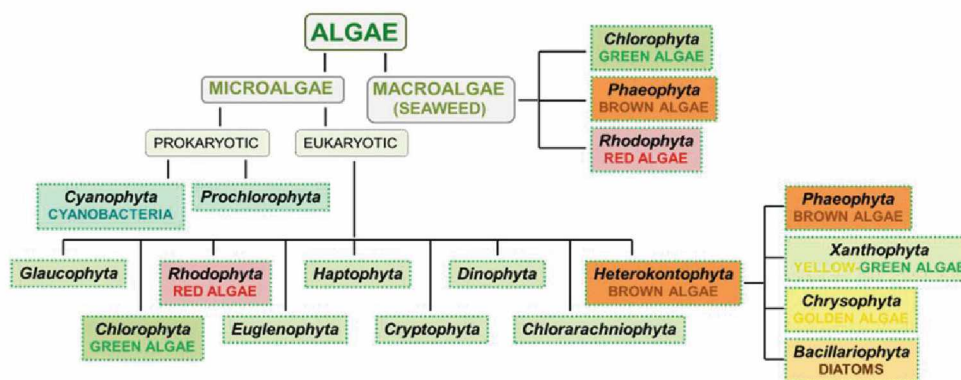


Figure 1. Classification scheme of different algal groups – Reproduced from Niemczyk, Żyszka-Haberecht, Drzyzga, Lenartowicz, and Lipok (2018) with permission.

GRAHAM, WILCOX, and GRAHAM (2009), classified algae into divisions or phyla. What gathers them in groups are aspects that differentiate them according to their reserve products, reproduction, accessory photosynthetic pigments, presence of flagella,

and constituent substances of cell walls (when present) (LEE, 2018). The algae and microalgae species studied in the present thesis are classified in the following groups:

The microalgae *Haptophyta* (or Prymnesiophyta) division has flagella at some stage of its cell cycle and sexual reproduction, with plasma membrane coverage showing calcium carbonate scales or being without it in certain species. The most striking feature of this group is the presence of a wire-shaped structure, known as haptonema, generally located between the two typical flagella and whose function is not yet adequately understood. They have chlorophyll *a* and *c* and beta carotene, and the storage product is chrysolaminarin. There are about 280 species (HEIMANN & HUERLIMANN, 2015; NIEMCZYK *et al.*, 2018).

*Ochrophyta* microalgae division is the most extensive of the groups, subdivided into 13 distinct classes, each class having hundreds or thousands of species. The classes are *Chrysophyceae*, diatoms (or *Bacillariophyceae*, with about 100,000 species), *phaeophytes* (brown algae or *Phaeophyceae*), silicoflagellates, raphidoficeas, eustigmatoficeas, etc. The primary photosynthetic pigments are chlorophyll *a* and *c*, beta carotene, and xanthophylls. As a reserve product, we find lipids and chrysolaminarin. Reproduction is sexual, and there is a flagellum in reproductive cells. As for cell coverage, some do not have it, and others have silica, cellulose, or alginates on the cell membrane. The name derives from the ocher color of most of these algae (BONANNO & ORLANDO-BONACA, 2018; CHAPMAN, 2013; NIEMCZYK *et al.*, 2018).

*Chlorophyta* division corresponds to green macroalgae, containing more than 17,000 species, primarily single-celled, present in freshwater and marine environments. Some species are macroscopic. They have flagellum and sexual reproduction; their reserve product is starch and contains chlorophyll *a* and *b*, beta-carotene, xanthophylls, and other photosynthetic pigments (BONANNO & ORLANDO-BONACA, 2018; CHAPMAN, 2013; HEIMANN & HUERLIMANN, 2015; NIEMCZYK *et al.*, 2018).

## 1.2 ALGAE INDUSTRIAL APPLICATIONS

Scientific research made in the last decades has proven that algae are a valuable source of chemical compounds with a broad spectrum of biological activity. Algal biomass is a renewable source of products with high nutritional value, that can be used as food ingredients, fertilizers, biofuel, biopolymers with extensive cosmetics, medicine and

pharmaceutical applications (Figure 2). It is estimated that there are more than ten million algae species, most of them being microalgae. From that amount, only around 50 species are actually commercially exploited. Identifying new compounds with different biological actions, especially in algae, is an interesting source for new biotechnological products (COLUSSE et al. 2021; LEVASSEUR, PERRE, & POZZOBON, 2020; RAJVANSHI *et al.*, 2019).



Figure 2. A scheme of the biotechnological appliance of algae biomass. Adapted from SKJANES, REBOURS, and LINDBLAD (2013).

### *1.2.1 Upstream and downstream processes to biomass formation.*

One of the essential characteristics of algae is that, because of the photosynthesis process, it can produce significant amounts of biomass in a short period, which turns out to be a very interesting and cheap raw material for industry. It is because they can be cultivated in a great variety of methods and many places as laboratories, outdoors culture tanks, and farms; with freshwater, saltwater, or even wastewater (CORRÊA, DUARTE, & NOSEDA, 2018; SELESU et al., 2016; VALIZADEH & DAVARPANAH, 2020).

Macroalgae can reach large sizes, and their cultivation can be onshore, offshore or integrated. This englobes many techniques: tanks, rock-based farming, off-bottom, submerged, floating line/raft, or net cultivation (GARCÍA-POZA et al., 2020). The assemble will proceed when maximum growth is achieved for macroalgae or the maximum accumulation of a specific biomolecule. This part is called harvesting, and there are many techniques to process algae/microalgae biomass (TAN et al., 2020). Macroalgae methods for harvesting vary from total to partial. Complete harvest happens at the end of the growing season and/or avoids adverse effects from seasonal changes. Partial harvest is made to leave some material behind, collecting only some part of the farming area, and it avoids the complete loss of a single harvest. It can also be used for high production demands. Collecting for both methods can be by mechanical harvesting, nets, or ropes (RADULOVICH et al., 2015).

Since they are small and form colonies, microalgae are cultivated in open and closed photo/bioreactors (TAN et al., 2020). An alternative to outdoors culture is using a photobioreactor for more significant production of microalgae biomass. It provides a protected environment, especially from contamination, and offers controlled parameters as oxygen and carbon dioxide concentration, pH, and temperature, for cultivated species. It can gain eight times more biomass productivity and the biomass concentration is around 16 times higher than open pond production by presenting efficient mass transfer of nutrients and less cross-contamination. Complex and expensive construction are disadvantages of photobioreactors (CORRÊA et al., 2017; NARALA et al., 2016). For microalgae, once the stationary phase on culture reaches its peak, the downstream process is implemented to form biomass. The microalgae harvesting process can be through filtration, centrifugation, flocculation, and flotation (TAN et al., 2020).

#### *1.2.2 Extraction, purification, and fractioning methods*

Once algae and microalgae biomasses are obtained, there are different conversion techniques to achieve bioactive compounds that can be isolated to be used in industry (MICHALAK & CHOJNACKA, 2015). Algae produce both primary and secondary metabolites. Primary metabolites are responsible for the growth, development, or reproduction functions of the algae. They are amino acids, proteins, lipids, and polysaccharides (RICO et al., 2017). Secondary metabolites are obtained under different stress conditions, such as salinity, UV radiation exposure, temperature changes, pH, or environmental contaminants. Secondary metabolites produced in algae are pigments, phenolic compounds, sterols, vitamins (A, B1, B12, C D, and E), and other bioactive agents (ALASSALI et al., 2016; RICO et al., 2017). Contents of primary and secondary metabolites present in each alga will determine its value as a feedstock for different extraction processes (ALASSALI et al., 2016; STIRK et al., 2020).

The extraction process consists of the separation of a specific substance from a based matrix. Traditional methods like maceration, aqueous, and solvent/organic extraction are still used to obtain bioactive compounds (CORRÊA, MORAIS JÚNIOR, MARTINS, CAETANO, & MATA, 2021). Modern extraction methods engage physical or chemical agents to accelerate the process. For chemicals, we can find hydrolytic enzymes, supercritical solvents, osmotic pressure, and isotonic agents. As a physical agent, the most used is microwave-assisted radiation (MAE) and ultrasound-assisted extraction, and there are also the expeller press, bead beating, hot water extraction, and

subcritical water-assisted extraction (HUANG, CHEN, YANG, & HUANG, 2021; SALINAS-SALAZAR et al., 2019). Another method of extraction that is very common is the Soxhlet extraction. This method is used to extract relevant bioactive compounds from natural sources. Soxhlet extraction is frequently used to compare alternative methods (SALINAS-SALAZAR et al., 2019).

The choice of the solvent will depend on the target substance to be extracted and how easy it is to remove it from the extract. It is fundamental that, to obtain the best quality of extraction of active components, the extraction method must correspond to the active component's properties. The relevant point is that the algae cell wall prevents direct contact between the cell wall and the solvent, complicating the process (Miazek et al., 2017). When extracting biomolecules, adding purification and fractioning techniques are necessary to ensure that all impurities from the previous steps were removed. There are many available techniques, as chromatography, dialysis membranes, phase systems, precipitation, filtration, centrifugation, among others. Choosing the best one will depend on the target molecule (CORRÊA et al., 2021).

Chromatography methods are based on the separation of a mixture of molecules, which can be based on their physical properties as adsorption (liquid-solid), partition (liquid-solid), affinity, and molecular weights. This technique requires a stationary phase (a substance at a fixed system that will partially retain the mixture for a certain time) and a mobile phase (a substance that will carry the molecules through the system and the stationary phase). To correctly separate the molecules, each technique will depend on its characteristics. As an example: Gel permeation chromatography bases on molecular polarity, ion-exchange chromatography by charge properties of ionized molecules, size-exclusion chromatography fractions molecules by molar mass, affinity chromatography separates complex mixtures with specific reversible interactions (adsorption of surface-specific sites), and others (REN, BAI, ZHANG, CAI, & DEL RIO FLORES, 2019).

The membrane separation processes are based on the charge, molar mass, and hydrodynamic radius of molecules to separate them through a membrane. Typically, molecules with larger sizes are maintained, and smaller molecules go through the pores. An example is the dialysis process. Ultrafiltration is also a membrane separation, but adding pressure on the system. Another alternative for membrane processes is the electro membrane filtration process. The electric field creates polarity, which helps the electrophoretic force to direct charged biopolymers and form the precipitate more quickly. It has the advantage of being more selective than regular membranes without

pressure. In liquid phase systems, this technique bases on liquid solubility, creating phase-forming components, where one phase aims for the purified molecule and the other has impurities. There are two ways of doing this: by two-phase or three-phase portioning. On the two-phase, for biopolymers, it can be combined between polymer/polymer or polymer/salt as phase-forming components. On the three phases portioning, the interested molecule is in the middle of 2 liquids (CORRÊA et al., 2021; REN et al., 2019).

### 1.2.3 Applications of algae extracts

Algae are known as the richest source of bioactive compounds. Their biomass, especially from microalgae, can be processed to obtain bioactive compounds with significant application in several industry sectors as food, pharmaceutical, cosmetics, nanoscience, energy, and even cancer biology (KUMAR et al., 2021). These compounds with a broad spectrum of biological activity can also be utilized in medical treatment for their antibacterial, antiviral, antifungal, antilipidemic, antitumor, antidiabetic, anticoagulant, antioxidant, and anti-allergic properties. They can also be used in agriculture as fertilizers, biostimulants for plant growth, and animal feeding as additives (CHOJNACKA, WIECZOREK, SCHROEDER, & MICHALAK, 2018). Applications are resumed in Figure 3.

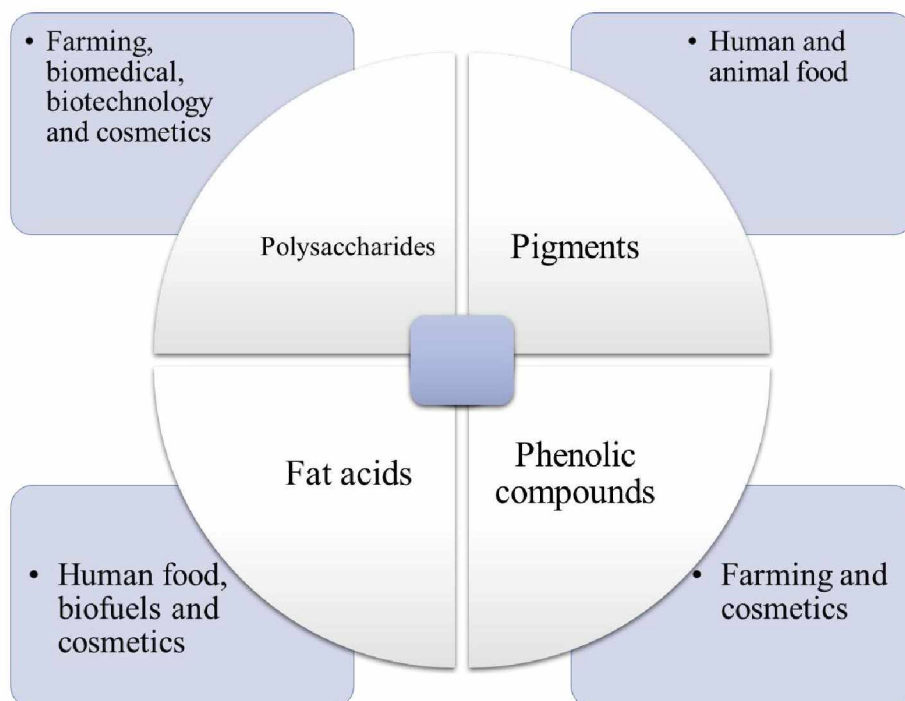


Figure 3. Applications of different biomolecules extracted from algae and microalgae biomass in the biotechnological industry. The author, 2021.

### 1.3 POLYSACCHARIDES

Polysaccharides are macromolecules (biopolymers) constituted by residues of monosaccharides brought together by glycosidic linkages. These biopolymers can be charged (polyanions or polycations) or neutral. Their structural conformation in solution is poorly defined since they can assume various shapes depending on their molecular size, ionic strength on medium, and viscosity. They can be found in plants (gums, cellulose, pectins), animals (chitosan, heparin, chondroitin), fungi ( $\beta$ -glucans, bacteria (leaven, dextran, emulsan), and algae (alginate, carrageenans, agarose) (HARDING et al., 2017; MOHAMMED, NAVEED, & JOST, 2021).

Polysaccharides are often related to various functions in nature, such as energetic reservoir, cell-cell connection, structural support, among others. When compared to other molecules, there is not a simple classification regarding polysaccharides. They can be divided according to their chemical structure or function (Figure 4). They can be branched or unbranched and present the same saccharide residue (homo) or two or more different types of residues (hetero). For homo sequences, they are named after their specific saccharide composition. Glucans are the homopolysaccharides constituted by glucose, mannans by mannose, rhammans by rhamnose, and so on. For heteropolysaccharides, they can be classified based on their sequences of saccharides as heteromannans, heteroxylans, galactoglucomannans, among others (HARDING et al., 2017; MOHAMMED, NAVEED, & JOST, 2021).

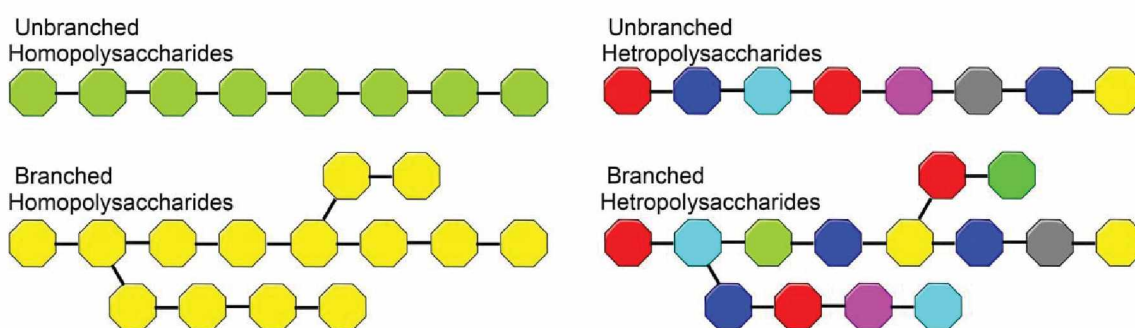


Figure 4. Classification of different forms of polysaccharides – Reproduced from MOHAMMED, NAVEED, & JOST, (2021) with permission.

Polysaccharides have various biotechnological applications. They are used as thickeners, stabilizers, emulsifiers, and gelling agents for the food industry. As farming usage, they can be applied as antibiofilm agents for fungi and microorganisms, fertilizers, bio-elicitor, stimulators,

signaling molecules, and activators of plants. As medical and pharmaceutical application, polysaccharides have been tested for vaccines, drug delivery, tissue engineering, *in vitro* and *in vivo* applications as antioxidant, anticoagulant, antilipidemic, hypoglycemic, antinociceptive, antimicrobial, antiviral, antifungal, and anti-tumor molecules (BOUISSIL et al., 2019; MOHAMMED, NAVEED, & JOST, 2021; RENDUELES, KAPLAN, & GHIGO, 2013; STEPHEN & PHILLIPS, 2006; XIE et al., 2020). Chemically modified polysaccharides can have the potential to enhance their biological properties since the presence and a certain percentage of functional groups are linked to biological responses. This can lead to a more apoptotic activity, a better stabilization for drug delivery, and others. Modifications include sulfation, acetylation, ammoniation, phosphorylation, stearylation, carboxymethylation, among others (COLODI et al., 2021; de CARVALHO et al., 2018, 2020; MAZEPA et al., 2021; XIE et al., 2020).

#### **1.4 GLIOBLASTOMA AND POLYSACCHARIDES**

Cancer is a pathology in which cells present characteristics of disordered cell growth, undifferentiated phenotype and may acquire the capacity of invading other tissues and organs. There are more than 200 types of cancer, and numerous factors are associated with their appearance, such as diet, environmental exposure, genetic predisposition, smoking, among others (COMPTON, 2020).

Glioblastoma multiforme (GBM, astrocytoma grade IV) are the most common form of gliomas, with an annual incidence of 3.19 cases per 100,000 people in the United States of America (ZENG, CUI, & GAO, 2015). They are also the most aggressive and deadliest form of malignant brain tumor in adults. Despite advances in surgical, radiotherapy, and chemotherapy techniques, the average survival for patients with GBM remains a mere 14 months. The current standard treatment for GBM consists of surgery to safely remove as much of the tumor as possible, followed by a combination of radiotherapy with the application of Temozolomide (TMZ). TMZ is a prodrug with the ability to cross the blood-brain barrier. Its effect is due to being a DNA alkylating agent, inducing erroneous pairing of base pairs and, consequently, carrying out the arrest of the cycle and induction of cell death. The adoption of this protocol increased the median survival from 12 to 15 months; however, it did not prevent tumors recurrence (DELGADO-LOPEZ & CORRALES-GARCIA, 2016; PAW, CARPENTER, WATABE, DEBINSKI, & LO, 2015 ). Since this tumor is characterized by high mortality

due to their location, this determines severe repercussions on the patient's quality of life, both for the tumor itself and the consequences of its treatment (WELLER et al., 2015).

Thus, it is necessary to seek new treatments for tumoral cells. Tumor cells present various alterations in cellular metabolism to maintain their characteristics and ensure survival, so it is interesting to target cancer metabolism. Many of the metabolic pathways are linked to tumor initiation and progression (VANDER HEIDEN, 2011). Metabolic adaptation is a crucial survival factor, as cancer cells are present in an environment with poor levels of nutrients and oxygen, also being under immune surveillance (MISSIROLI, PERRONE, GENOVESE, PINTON, & GIORGI, 2020). Cancer cells engage glycolysis and the citric acid cycle (TCA) rates for NADPH, ATP production, and glycolytic intermediates to help biosynthetic reactions. Also, the pentose phosphate pathway is active for ribose and cytosolic NADPH production. Glutaminolysis and TCA intermediates are able to be used at lipids, nucleotide, and amino acid synthesis (VASAN, WERNER & CHANDEL, 2020). This explains some of cancer cells hallmarks: glucose and amino acids uptake (carbon intermediates for macromolecules building blocks, which helps to maintain cellular redox status, among others); usage of mechanisms to enhance nutrients, as aminoacids and lysophospholipids, uptake by macropinocytosis, entosis, and phagocytosis; an increase of nitrogen demand for synthesizing nucleotides, non-essential amino acids, and polyamines; alteration in metabolite-driven gene expression regulation since diverse metabolites are cofactors or substrates for epigenetic marks; and interaction with the microenvironment (PAVLOVA & THOMPSON, 2016).

Mitochondria play a major role in cancer metabolism, influencing malignant transformation, tumoral progression to metastasis. It is also related to cancer cells' metabolic plasticity since alterations are made to guarantee cancer hallmarks (fast proliferation, invasion, among others) through enhancement of cell energy and biosynthesis precursors. This organelle function is linked to cell's bioenergy, as well as controlling cell fate (including cell death) by many signaling mechanisms (as calcium and redox homeostasis) and gene expression regulation (PORPORATO, FILIGHEDDU, PEDRO, KROEMER, & GALLUZZI, 2018). Regarding cancer metabolism, the "Warburg effect" is observed. This is a phenomenon in which glycolysis is preferably used over oxidative phosphorylation (OXPHOS) to produce ATP, with or without the presence of oxygen, and redirects pyruvate to generate lactate (anaerobic glycolysis). Although the ATP yield production is much less (for one molecule of glucose forms 2

ATP mols) when compared with OXPHOS (1 molecule of glucose forms approx. 32 ATP mols), this effect presents its advantages. With anaerobic glycolysis, NADH is converted to NAD<sup>+</sup> more often (recycling); and the intermediates can be used in macromolecules biosynthesis (nucleotides, lipids, and amino acids). The intermediates and enzyme recycling can be applied for other metabolic pathways, such as the pentose phosphate pathway, fatty acid oxidation, among others (MISSIROLI et al., 2020; VASAN et al., 2020). The Warburg effect has been used to predict cancer prognostic as well. Regions with high glucose consumption and metabolization can be detected by Positron emission tomography (PET) to detect malignant lesions at an anatomic place before cell morphology alterations begin (HUNDSHAMMER et al., 2018; PORPORATO et al., 2018). Since cell and mitochondrial metabolism significantly impacts cancer development, new therapies targeting metabolism can be a promising alternative.

Many drugs used for other treatments can affect cancer cell viability through their metabolism (MISSIROLI et al., 2020). TENNANT, DURAN, and GOTTLIEB (2010), in their review paper, show compounds used in many types of cancers, focusing on metabolic therapy. There are compounds able to inhibit: glycolysis (2-deoxyglucose, lonidamine), fatty acid synthesis (Orlistat), electron transport chain (ETC) complexes (complex I, II) (MitoTam, MitoVES), and cell proteins and pathways as Hypoxia-inducible factor - HIF, Insulin-like growth factor 1 - IGF, Protein kinase B - AKT; AMP-activated protein kinase - AMPK (Metformin, Acriflavine, Perifosine). For GBM treatment, some compounds reduced plasma glutamine levels (Phenylacetate), reactivated pyruvate dehydrogenase (PDH) (dichloroacetate), and cell survival pathways as the Mammalian target of rapamycin complex 1 and 2 (mTORC1, 2) (Ridaforolimus). But those molecules have side effects, so there is a problem when aiming for mitochondrial therapy because some immune cells (especially cytotoxic T cells) are very similar in metabolic terms to cancer cells (Warburg effect). So, it is necessary to find a treatment capable of affecting only the cancer cells (PORPORATO et al., 2018).

The main hypothesis is that polysaccharides can increase the immune system response, being called “immunomodulators”. The molecular response is already well described in the literature (figure 5). The immune system response is activated in three ways: by specific receptors as pattern recognition, located intracellularly or on the cell surface, shared by broad groups of agents that are generally absent in the host (for example, *toll-like* receptors, scavengers (SR), complement 3 (CR3), and Dectin-1

receptors); by the complement system, either by the classical, alternative and lectin pathways; and also, by the lectin pathway binding protein. Polysaccharides, when binding to these receptors, trigger signaling pathways that lead to the induction of an inflammatory gene transcription signature, which stimulates the production of cytokines, reactive oxygen species, nitric oxide release, proliferation, and differentiation of immune cells (FERREIRA et al., 2015).

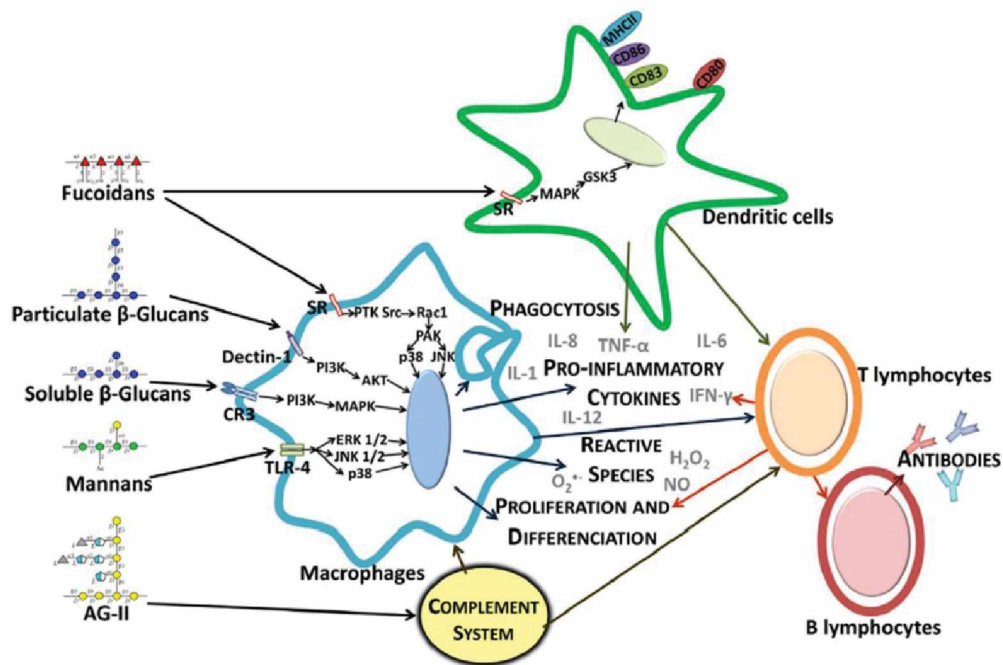


Figure 5. The action of polysaccharides upon different immune cells– Reproduced from FERREIRA *et al.* (2015) with permission.

Polysaccharides can also act directly in cancer cells without involving the immune system. According to KHAN, DATE, CHAWDA, and PATEL (2019), these molecules can perform apoptosis by different mechanisms. The most common ways are cell cycle arrest, alterations on the mitochondrial membrane, and nitric oxide (NO) pathway activation. Cell cycle checkpoints are controlled by specific proteins called cyclins and cyclin-dependent kinases. Whenever there is an interference in the involved regulatory pathways at the cell cycle (causing arrest on G1/S phase) or DNA damage (G2/M), there will be an arrest and it will activate the caspase cascade. CHEN, JIANG, XIE, LI, and SHI (2018) showed a heteropolysaccharide with repetitive β-(1→3), and β-(1→6) linkages from *Ramulus mori* arrested G<sub>0</sub>/G<sub>1</sub> phase in human gastric adenocarcinoma cells. SHAO, LIU, CHEN, FANG, and SUN (2015) reported a β-D-(1→6) side chain linked to a β-D- glucan (1→3) backbone extracted from the brown

seaweed *Sargassum horneri* induced apoptosis and increased the G<sub>2</sub>/M phase in colorectal adenocarcinoma cells.

Other observed effects are the depolarization of the mitochondrial membrane, cytochrome c release, and enhancement of reactive oxygen species (ROS), which will increase p53 and Bax/Bcl-2 expressions. An  $\alpha$ -(1→6) galactomannan with  $\alpha$ -(1→3)-glucan branches was able to reduce mitochondrial membrane potential, releasing cytochrome c and triggering caspase signaling (TIAN, ZHAO, ZENG, ZHANG, & ZHENG, 2016). A (1→3)-glucan extracted from *H. sinensis* caused a mitochondrial membrane collapse and increase of ROS on non-small cell lung cancer (LIU, XIE, SUN, MENG, & ZHU, 2017). Despite the description above with some possible effects, the direct cytotoxic effects of polysaccharides, especially metabolic effects, are not well-defined as the immunomodulatory effects.

## 2. OBJECTIVE

To search for new molecules with biotechnological applications, the marine microalgae *Isocrysis galbana*, *Conticribra weissflogii*, and green macroalga *Gayralia brasiliensis* were studied. As previously described in literature, polysaccharides are molecules that can present multiple biological effects, among them the cytotoxic activity against several tumor lineages, by being immune cell modulators and not affecting healthy cells. As a result, this thesis aimed to study the microalgae and macroalgae polysaccharide's chemical structure and biological effects directed to cytotoxic action, as well as their molecular mechanism.

In **chapter I**, the biological effect on glioblastoma cell lines and macrophages of a (1→3)-linked  $\beta$ -D-glucan isolated from microalga *Conticribra weissflogii* was studied. The chemical structure of the polysaccharide was described, and the effect of this biomacromolecule in the enhancement of phagocytic macrophage activity and in the decrease in mitochondrial metabolism of glioblastoma cells was discussed.

**Chapter II** describes the characterization of a (1→3, 1→6)  $\beta$ -D-glucan from microalga *Isochrysis galbana* and its metabolic effect on two different glioblastoma cell lines. The polysaccharide effects in the reduction of cell mitochondrial metabolism pathways, affecting the TCA cycle, glycolysis, amino acid, and fatty acid oxidation consumption profiles was discussed. A chemically modified heterorhamman (oversulfation) from *Gayralia brasiliensis* previously showed cell death against U87MG glioblastoma cells. In **Chapter III**, the possible ways for this response are examined, focusing on the mitochondrial effects of this polysaccharide. The oversulfated heterorhamman alters the mitochondrial membrane polarization, affecting mitochondrial ROS levels and cell respiration. The main results from this thesis were summarized and discussed and topics for future works were suggested at the discussion section.

## References

- ALASSALI, A., CYBULSKA, I., BRUDECKI, G. P., FARZANAH, R., & THOMSEN, M. H. Methods for Upstream Extraction and Chemical Characterization of Secondary Metabolites from Algae Biomass. **Advanced Techniques in Biology and Medicine**, v.4, n.1, p.16, 2016.
- BARSANTI, L., & GUALTIERI, P. **Algae: Anatomy, Biochemistry and Biotechnology**, 2014.
- BONANNO, G., & ORLANDO-BONACA, M. Trace elements in Mediterranean seagrasses and macroalgae. A review. **Science of The Total Environment**, n. 618, p.1152-1159, 2018.
- BOUISSIL, S., PIERRE, G., ALAOUI-TALIBI, Z. E., MICHAUD, P., EL MODAFAR, C., & DELATTRE, C. Applications of Algal Polysaccharides and Derivatives in Therapeutic and Agricultural Fields. **Current Pharmaceutical Design**, v.25, n.11, p.1187-1199, 2019.
- CHAPMAN, R. L. Algae: the world's most important "plants"—an introduction. **Mitigation and Adaptation Strategies for Global Change**, v. 18, n. 1, p. 1573-1596, 2013.
- CHEN, Y., JIANG, X., XIE, H., LI, X., & SHI, L. Structural characterization and antitumor activity of a polysaccharide from *ramulus mori*. **Carbohydrated Polymers**, v.190, p. 232-239, 2018.
- CHOJNACKA, K., WIECZOREK, P. P., SCHROEDER, G., & MICHALAK, I. **Algae Biomass: Characteristics and Applications**: Springer, Cham, 2018.
- COMPTON, C. **Cancer Initiation, Promotion, and Progression and the Acquisition of Key Behavioral Traits. In Cancer: The Enemy from Within: A Comprehensive Textbook of Cancer's Causes, Complexities and Consequences** (pp. 25-48). Cham: Springer International Publishing, 2020.
- CORRÊA, D. d. O., DUARTE, M. E. R., & NOSEDA, M. D. Biomass production and harvesting of *Desmodesmus subspicatus* cultivated in flat plate photobioreactor using chitosan as flocculant agent. **Journal of Applied Phycology**, v. 31, n. 2, p. 857-866, 2018.
- CORRÊA, P. S., MORAIS JÚNIOR, W. G., MARTINS, A. A., CAETANO, N. S., & MATA, T. M. Microalgae Biomolecules: Extraction, Separation and Purification Methods. **Processes**, v.9, n. 1, p.10, 2021.
- COLUSSE, G.A.; CARNEIRO, J.; DUARTE, M.E.R; DE CARVALHO, J.C.; NOSEDA, M.D. Advances in microalgal cell wall polysaccharides: a review focused on structure, production, and biological application, **Critical**

- COLODI, F. G., DUCATTI, D., NOSEDA, M. D., DE CARVALHO, M. M., WINNISCHOFER, S., & DUARTE, M. (2021). Semi-synthesis of hybrid ulvan-kappa-carrabiose polysaccharides and evaluation of their cytotoxic and anticoagulant effects. **Carbohydrate polymers**, v.267, p.118161. <https://doi.org/10.1016/j.carbpol.2021.118161>
- DE CARVALHO, M. M., DE FREITAS, R. A., DUCATTI, D., FERREIRA, L. G., GONÇALVES, A. G., COLODI, F. G., MAZEPA, E., ARANHA, E. M., NOSEDA, M. D., & DUARTE, M. Modification of ulvans via periodate-chlorite oxidation: Chemical characterization and anticoagulant activity. **Carbohydrate polymers**, v.197, p.631–640, 2018. <https://doi.org/10.1016/j.carbpol.2018.06.041>.
- DE CARVALHO, M. M., NOSEDA, M. D., DALLAGNOL, J., FERREIRA, L. G., DUCATTI, D., GONÇALVES, A. G., DE FREITAS, R. A., & DUARTE, M. Conformational analysis of ulvans from *Ulva fasciata* and their anticoagulant polycarboxylic derivatives. **International journal of biological macromolecules**, v.162, p.599–608, 2020. <https://doi.org/10.1016/j.ijbiomac.2020.06.146>.
- DE CLERCK, O., GUIRY, M. D., LELIAERT, F., SAMYN, Y., & VERBRUGGEN, H. Algal taxonomy: a road to nowhere? **Journal of Phycology**, v. 49, n. 2, p. 215-225, 2013.
- DEBIAGI, P. E. A., TRINCHERA, M., FRASSOLDATI, A., FARAVELLI, T., VINU, R., & RANZI, E. Algae characterization and multistep pyrolysis mechanism. **Journal of Analytical and Applied Pyrolysis**, v.128, p.423-436, 2017.
- DELGADO-LOPEZ, P. D., & CORRALES-GARCIA, E. M. Survival in glioblastoma: a review on the impact of treatment modalities. **Clinical and Translational Oncology**, v.18, n. 11, p. 1062-1071, 2016.
- FERREIRA, S. S., PASSOS, C. P., MADUREIRA, P., VILANOVA, M., & COIMBRA, M. A. Structure-function relationships of immunostimulatory polysaccharides: A review. **Carbohydrate Polymers**, v.132, p.378-396, 2015.
- GARCÍA-POZA, S., LEANDRO, A., COTAS, C., COTAS, J., MARQUES, J. C., PEREIRA, L., & GONÇALVES, A. M. M. The Evolution Road of Seaweed Aquaculture: Cultivation Technologies and the Industry 4.0. **International Journal of Environmental Research and Public Health**, v. 17, n. 18, p. 6528, 2020.
- GRAHAM, J. E., WILCOX, L. W., & GRAHAM, L. E. **Algae**. San Francisco, 2009.

- HARDING, S. E., TOMBS, M. P., ADAMS, G. G., PAULSEN, B. S., INNGJERDINGEN, K. T., & BARSETT, H. **An Introduction to Polysaccharide Biotechnology.** (2nd ed.). Boca Raton, 2017.
- HEIMANN, K., & HUERLIMANN, R. **Chapter 3 - Microalgal Classification: Major Classes and Genera of Commercial Microalgal Species.** In S.-K. Kim (Ed.), **Handbook of Marine Microalgae** (pp. 25-41). Academic Press, 2015.
- HUANG, G., CHEN, F., YANG, W., & HUANG, H. Preparation, deproteinization and comparison of bioactive polysaccharides. **Trends in Food Science & Technology**, v. 109, p. 564-568, 2021.
- HUNDSHAMMER, C., BRAEUER, M., MULLER, C. A., HANSEN, A. E., SCHILLMAIER, M., Duwel, S., . . . SCHWAIGER, M. Simultaneous characterization of tumor cellularity and the Warburg effect with PET, MRI and hyperpolarized (13)C-MRSI. **Theranostics**, v. 8, n. 17, p. 4765-4780, 2018.
- IBAÑEZ, E., & CIFUENTES, A. Benefits of using algae as natural sources of functional ingredients. **Journal of the Science of Food and Agriculture**, v. 93, n. 4, p. 703-709, 2013.
- JEFFREY, S., WRIGHT, S., & ZAPATA, M. **Microalgal classes and their signature pigments.** In C. L. In S. Roy, E. Egeland, & G. Johnsen (Ed.), **Phytoplankton Pigments: Characterization, Chemotaxonomy and Applications in Oceanography** (pp. 3-77), 2011.
- KHAN, T., DATE, A., CHAWDA, H., & PATEL, K. Polysaccharides as potential anticancer agents-A review of their progress. **Carbohydrate Polymers**, v. 210, p. 412-428, 2019.
- KUMAR, B. R., THANGAVEL, M. P. M., SUDHAKAR, K. R., ABDUL-SATTAR, N., BRINDHADEVI, K., & PUGAZHENDHI, A. A state of the art review on the cultivation of algae for energy and other valuable products: Application, challenges, and opportunities. **Renewable and Sustainable Energy Reviews**, v.138, 2021.
- LEE, R. **Basic Characteristics of the Algae.** In **Phycology**.: Cambridge University Press, 2018.
- LEVASSEUR, W., PERRE, P., & POZZOBON, V. A review of high value-added molecules production by microalgae in light of the classification. **Biotechnology Advances**, n. 41, p. 107545, 2020.
- LIU, W. B., XIE, F., SUN, H. Q., MENG, M., & ZHU, Z. Y. Antitumor effect of polysaccharide from *Hirsutella sinensis* on human non-small cell lung cancer and nude mice through intrinsic mitochondrial pathway. **International Journal of Biological Macromolecules**, v. 99, p. 258-264, 2017.

- MANOYLOV, K. M. Taxonomic identification of algae (morphological and molecular): species concepts, methodologies, and their implications for ecological bioassessment. **Journal of Phycology**, v. 50, n. 3, p. 409-424, 2014.
- MAZEPA, E., NOSEDA, M. D., FERREIRA, L. G., DE CARVALHO, M. M., GONÇALVES, A. G., DUCATTI, D., DE L BELLAN, D., GOMES, R. P., DA S TRINDADE, E., FRANCO, C., PELLIZZARI, F. M., WINNISCHOFER, S., & DUARTE, M. Chemical structure of native and modified sulfated heterorhamnans from the green seaweed *Gayralia brasiliensis* and their cytotoxic effect on U87MG human glioma cells. **International journal of biological macromolecules**, v.187, p.710–721, 2021. <https://doi.org/10.1016/j.ijbiomac.2021.07.145>.
- MIAZEK, K., KRATKY, L., SULC, R., JIROUT, T., AGUEDO, M., RICHEL, A., & GOFFIN, D. Effect of Organic Solvents on Microalgae Growth, Metabolism and Industrial Bioproduct Extraction: A Review. **International Journal of Molecular Sciences**, v. 18, n. 7, p. 1429, 2017.
- MICHALAK, I., & CHOJNACKA, K. Algae as production systems of bioactive compounds. **Engineering in Life Sciences**, v. 15, n. 2, p. 160-176, 2015.
- MISSIROLI, S., PERRONE, M., GENOVESE, I., PINTON, P., & GIORGI, C. Cancer metabolism and mitochondria: Finding novel mechanisms to fight tumours. **EBioMedicine**, n. 59, p. 102943, 2020.
- MOHAMMED, A. S. A., NAVEED, M., & JOST, N. Polysaccharides; Classification, Chemical Properties, and Future Perspective Applications in Fields of Pharmacology and Biological Medicine (A Review of Current Applications and Upcoming Potentialities). **Journal of Polymers and the Environment**, p.1-13, 2021.
- NARALA, R. R., GARG, S., SHARMA, K. K., THOMAS-HALL, S. R., DEME, M., Li, Y., & SCHENK, P. M. Comparison of Microalgae Cultivation in Photobioreactor, Open Raceway Pond, and a Two-Stage Hybrid System. **Frontiers in Energy Research**, v. 4, n. 29, 2016.
- NIEMCZYK, E., ŻYSZKA-HABERECHE, B., DRZYZGA, D., LENARTOWICZ, M., & LIPOK, J. **Algae in Biotechnological Processes**. In K. Chojnacka, P. P. Wiczorek, G. Schroeder & I. Michalak (Eds.), **Algae Biomass: Characteristics and Applications: Towards Algae-based Products** (pp. 33-48). Cham: Springer International Publishing, 2018.
- PAVLOVA, N. N., & THOMPSON, C. B. The Emerging Hallmarks of Cancer Metabolism. **Cell Metabolism**, v. 23, n. 1, p. 27-47, 2016.
- PAW, I., CARPENTER, R. C., WATABE, K., DEBINSKI, W., & LO, H. W. Mechanisms regulating glioma invasion. **Cancer letters**, v. 362, n. 1, p. 1–7, 2015.


- PORPORATO, P. E., FILIGHEDDU, N., PEDRO, J. M. B., KROEMER, G., & GALLUZZI, L. Mitochondrial metabolism and cancer. **Cell Research**, v. 28, n. 3, p. 265-280, 2018.
- RADULOVICH, R., NEORI, A., VALDERRAMA, D., REDDY, C. R. K., CRONIN, H., & FORSTER, J. **Farming of seaweeds**. In **D. J. T. Brijesh K. Tiwari (Ed.), Seaweed Sustainability** (pp. 27-59). Academic Press, 2015.
- REN, Y., BAI, Y., ZHANG, Z., CAI, W., & DEL RIO FLORES, A. The Preparation and Structure Analysis Methods of Natural Polysaccharides of Plants and Fungi: A Review of Recent Development. **Molecules**, v. 24, n. 17, p. 3122, 2019.
- RENDUELES, O., KAPLAN, J. B., & GHIGO, J. M. Antibiofilm polysaccharides. **Environmental Microbiology**, v.15, n.2, p.334-346, 2013.
- RICO, M., GONZÁLEZ, A. G., SANTANA-CASIANO, M., GONZÁLEZ-DÁVILA, M., PÉREZ-ALMEIDA, N., & de TANGIL, M. S. **Production of Primary and Secondary Metabolites Using Algae**. In **B. N. Tripathi & D. Kumar (Eds.), Prospects and Challenges in Algal Biotechnology** (pp. 311-326). Singapore: Springer Singapore, 2017.
- SALINAS-SALAZAR, C., SAUL GARCIA-PEREZ, J., CHANDRA, R., CASTILLO-ZACARIAS, C., IQBAL, H. M. N., & PARRA-SALDÍVAR, R. **Methods for Extraction of Valuable Products from Microalgae Biomass**. In **M. A. Alam & Z. Wang (Eds.), Microalgae Biotechnology for Development of Biofuel and Wastewater Treatment** (pp. 245-263). Singapore: Springer Singapore, 2019.
- SELESU, N. F. H., V. DE OLIVEIRA, T., CORRÊA, D. O., MIYAWAKI, B., MARIANO, A. B., VARGAS, J. V. C., & VIEIRA, R. B. Maximum microalgae biomass harvesting via flocculation in large scale photobioreactor cultivation. **The Canadian Journal of Chemical Engineering**, v. 94, n. 2, p. 304-309, 2016.
- SHAO, P., LIU, J., CHEN, X., FANG, Z., & SUN, P. Structural features and antitumor activity of a purified polysaccharide extracted from *Sargassum horneri*. **International Journal of Biological Macromolecules**, v. 73, p. 124-130, 2015.
- SKJANES, K., REBOURS, C., & LINDBLAD, P. Potential for green microalgae to produce hydrogen, pharmaceuticals and other high value products in a combined process. **Critical Reviews in Biotechnology**, v. 33, n. 2, p. 172-215, 2013.
- STEPHEN, A. M., & PHILLIPS, G. O. **Food Polysaccharides and Their Applications** CRC Press, 2006.

- STIRK, W. A., BÁLINT, P., VAMBE, M., LOVÁSZ, C., MOLNÁR, Z., VAN STADEN, J., & ÖRDÖG, V. Effect of cell disruption methods on the extraction of bioactive metabolites from microalgal biomass. **Journal of Biotechnology**, v. 307, 2020.
- TAN, J. S., LEE, S. Y., CHEW, K. W., LAM, M. K., LIM, J. W., HO, S.-H., & SHOW, P. L. A review on microalgae cultivation and harvesting, and their biomass extraction processing using ionic liquids. **Bioengineered**, v. 11, n. 1, p. 116-129, 2020.
- TENNANT, D. A., DURAN, R. V., & GOTTLIEB, E. (2010). Targeting metabolic transformation for cancer therapy. **Nature Reviews Cancer**, v. 10, n. 4, p. 267-277, 2010.
- TIAN, Y., ZHAO, Y., ZENG, H., ZHANG, Y., & ZHENG, B. (2016). Structural characterization of a novel neutral polysaccharide from *Lentinus giganteus* and its antitumor activity through inducing apoptosis. **Carbohydrate Polymers**, v. 154, p. 231-240, 2016.
- VALIZADEH, K., & DAVARPANAH, A. Design and construction of a micro-photo bioreactor in order to dairy wastewater treatment by micro-algae: parametric study. **Energy Sources, Part A: Recovery, Utilization, and Environmental Effects**, v. 42, n. 5, p. 611-624, 2020.
- VANDER HEIDEN, M. G. Targeting cancer metabolism: a therapeutic window opens. **Nature Reviews Drug Discovery**, v. 10, n. 9, p. 671-684, 2011.
- VASAN, K., WERNER, M., & CHANDEL, N. S. Mitochondrial Metabolism as a Target for Cancer Therapy. **Cell Metabolism**, v. 32, n. 3, p. 341-352, 2020.
- WANG, H.-M. D., CHEN, C.-C., HUYNH, P., & CHANG, J.-S. Exploring the potential of using algae in cosmetics. **Bioresource Technology**, v. 184, p. 355-362, 2015.
- WELLER, M., WICK, W., ALDAPE, K., BRADA, M., BERGER, M., PFISTER, S. M., . . . Reifenberger, G. Glioma. **Nature Reviews Disease Primers**, n. 1, p. 15017, 2015.
- XIE, L., SHEN, M., HONG, Y., YE, H., HUANG, L., & XIE, J. Chemical modifications of polysaccharides and their antitumor activities. **Carbohydrate Polymers**, v.229, p.115436, 2020.
- ZENG, T., CUI, D., & GAO, L. Glioma: an overview of current classifications, characteristics, molecular biology and target therapies. **Frontiers in Bioscience (Landmark Ed)**, v. 20, p. 1104-1115, 2015.

### 3. CHAPTER I – Chemical structure and biological activity of the (1→3)-linked $\beta$ -D-glucan isolated from marine diatom *Conticribra weissflogii*

← → ↻ s100.copyright.com/AppDispatchServlet#formTop

CCC RightsLink Home Help Live Chat Sign In Create Account

 **Chemical structure and biological activity of the (1 → 3)-linked  $\beta$ -D-glucan isolated from marine diatom *Conticribra weissflogii***

**Author:** Juliane Rizzi, Tatiana Rojo Moro, Sheila Maria Brochado Winnischofer, Guilherme Augusto Colusse, Camilla Silva Tamiello, Marina Trombetta-Lima, Gullhermina Rodrigues Noleto, Amalia M. Dolga, Maria Eugênia Rabello Duarte, Miguel Daniel Nosedá

**Publication:** International Journal of Biological Macromolecules

**Publisher:** Elsevier

**Date:** Available online 20 October 2022

© 2022 Published by Elsevier B.V.

**Journal Author Rights**

Please note that, as the author of this Elsevier article, you retain the right to include it in a thesis or dissertation, provided it is not published commercially. Permission is not required, but please ensure that you reference the journal as the original source. For more information on this and on your other retained rights, please visit: <https://www.elsevier.com/about/our-business/policies/copyright#Author-rights>

BACK CLOSE WINDOW



Contents lists available at ScienceDirect

International Journal of Biological Macromolecules

journal homepage: [www.elsevier.com/locate/ijbiomac](http://www.elsevier.com/locate/ijbiomac)

## Chemical structure and biological activity of the (1 → 3)-linked $\beta$ -D-glucan isolated from marine diatom *Conticribra weissflogii*

Juliane Rizzi<sup>a,b,1</sup>, Tatiana Rojo Moro<sup>a,b,c,1</sup>, Sheila Maria Brochado Winnischofer<sup>b,\*</sup>,  
Guilherme Augusto Colusse<sup>b,d</sup>, Camila Silva Tamiello<sup>b</sup>, Marina Trombetta-Lima<sup>c</sup>,  
Guilhermina Rodrigues Noleto<sup>b</sup>, Amalia M. Dolga<sup>c,\*</sup>, Maria Eugênia Rabello Duarte<sup>b,\*</sup>,  
Miguel Daniel Nosedá<sup>b,\*</sup>

<sup>a</sup> Postgraduate Program in Sciences (Biochemistry), Federal University of Paraná, Curitiba, Paraná, Brazil

<sup>b</sup> Department of Biochemistry and Molecular Biology, Federal University of Paraná, Av. Cel. Francisco H. dos Santos, 100, CEP 81531-980, PO BOX 19046, Curitiba, Paraná, Brazil

<sup>c</sup> Department of Molecular Pharmacology, Faculty of Science and Engineering, Groningen Research Institute of Pharmacy (GRIP), University of Groningen, 9713 AV Groningen, the Netherlands

<sup>d</sup> Postgraduate Program in Bioprocess Engineering and Biotechnology, Federal University of Paraná, Curitiba, Paraná, Brazil

### ARTICLE INFO

#### Keywords:

Immunological activity  
Glioblastoma  
Microalga  
Phagocytosis  
Polysaccharide

### ABSTRACT

Several polysaccharides are considered to be “biological response modifiers” (BRM) — these refer to biomolecules that augment immune responses and can be derived from a variety of sources. Microalgae produce a diverse range of polysaccharides and could be an excellent source of BRM. Here, we describe the chemical structure and biological activity of water-soluble polysaccharide isolated from the marine diatom *Conticribra weissflogii*. Using chemical and NMR spectroscopic methods, the polysaccharide was identified as a (1 → 3)-linked  $\beta$ -D-glucan with a low proportion of C-6 substitution by single  $\beta$ -glucose units. The biological activity of this low molecular weight  $\beta$ -glucan (11.7 kDa) was investigated with respect to glioblastoma cell lines (U87 MG and U251) and macrophages (RAW 264.7). We observed that this  $\beta$ -D-glucan did not exhibit cytotoxic activity against glioblastoma cells, but did enhance the phagocytic activity of macrophages, suggesting that it possesses immunomodulatory properties.

### 1. Introduction

The potential of microalgae has been the subject of great interest from several areas of research and industry, such as human and animal nutrition. Microalgal biomass represents an additional source of carbohydrates [1], single-cell protein production [2], important fatty acids, natural pigments [3], vitamins, and other substances that can enrich the nutritional value of food while possessing health-promoting effects, such as improved immune responses [4]. Polysaccharides are among the compounds that can be derived from microalgae and are of interest to the food, chemical, and pharmaceutical industries [1,5,6].

$\beta$ -D-(1 → 3) and  $\beta$ -D-(1 → 3, 1 → 6)-glucans are known to have the ability to enhance the immune system and are well-established as

immunostimulants [7]. These polysaccharides are considered biological response modifiers (BRM) due to their interaction with specific cell receptors and proteins, and exhibit antibacterial, antiviral, and antitumor effects [8–11]. The immunological activities of  $\beta$ -glucans obtained from *Euglena gracilis* have been well documented by Barsanti and Gualtieri [12] and Russo et al. [13], and have been shown to mediate Natural Killer (NK) cell activation as well as increase levels of pro-inflammatory mediators.

Gliomas are malignant brain tumors that occur in the central nervous system; they originate in the brain and spread to glial tissue. The global incidence rate of all gliomas is 4.67–5.73 per 100,000 people, regardless of age. Glioblastoma (astrocytoma grade IV) is the most common and most deadly glioma subtype in adults (incidence ranging from 0.59 to

\* Corresponding authors.

E-mail addresses: [juliane.rizzi@gmail.com](mailto:juliane.rizzi@gmail.com) (J. Rizzi), [tatiana.rmoro@gmail.com](mailto:tatiana.rmoro@gmail.com) (T.R. Moro), [sheilambw@ufpr.br](mailto:sheilambw@ufpr.br) (S.M.B. Winnischofer), [guilherme\\_sp\\_92@gmail.com](mailto:guilherme_sp_92@gmail.com) (G.A. Colusse), [camila.taminello@gmail.com](mailto:camila.taminello@gmail.com) (C.S. Tamiello), [m.trombetta.lima@rug.nl](mailto:m.trombetta.lima@rug.nl) (M. Trombetta-Lima), [guinoletto@yahoo.com.br](mailto:guinoletto@yahoo.com.br) (G.R. Noleto), [a.m.dolga@rug.nl](mailto:a.m.dolga@rug.nl) (A.M. Dolga), [eugenia.duarte@pq.cnpq.br](mailto:eugenia.duarte@pq.cnpq.br) (M.E.R. Duarte), [mdn@ufpr.br](mailto:mdn@ufpr.br) (M.D. Nosedá).

<sup>1</sup> These authors equally contributed to this work.

<https://doi.org/10.1016/j.ijbiomac.2022.10.147>

Received 10 January 2022; Received in revised form 8 October 2022; Accepted 16 October 2022

Available online 20 October 2022

0141-8130/© 2022 Published by Elsevier B.V.

3.69 per 100,000 people). It has a poor prognosis, with a low mean survival after surgery (approximately 15 months of survival), and a high mortality rate despite current optimal surgical and chemoradiotherapy regimens. Glioblastoma has many genetic alterations that result in deregulated signaling pathways, the evasion of apoptosis, and increased proliferation. These factors necessitate the search for novel therapies for glioblastoma [14–16]. Microalgae represent an economically viable source of polysaccharides with potential biologic effects [17].

$\beta$ -glucans have been found to have inhibitory effects on different types of tumoral cells, even in the absence of immune cells. Several direct effects have been described in the literature, with apoptosis being the most direct. This can be triggered by the depolarization of the mitochondrial membrane and the activation of the caspase pathway in H1299 cells (human non-small cell lung cancer) [18]; by increasing the expression of p53 and Bax/Bcl-2 in SNU-C4 cells (human colon cancer) [19]; the alteration of the G0 and G1 phases in the cell cycle; and the activation of apoptotic signaling in B16-F10 cells (murine melanoma) [10]. Another potential effect is the alteration of membrane properties by acting as cell adhesion proteins. Zhao et al. [20] reported that the proliferation of B16-BL16 melanoma cells was inhibited due to the interference of  $\beta$ -glucans as cell adhesion proteins. In this study, we isolated and characterized a  $\beta$ -D-glucan extracted from the diatom *Conticribra weissflogii* and evaluated its *in vitro* biological activity with respect to two different biological cell types: glioblastoma and macrophages.

## 2. Material and methods

### 2.1. Microalgal strain and culture maintenance

The *C. weissflogii* microalga strain was obtained from the Elizabeth Aidar Microalgal Culture Collection (Fluminense Federal University, Brazil). The microalgae inoculum was maintained in sterilized f/2 culture medium [21] at  $19 \pm 1$  °C under continuous light.

### 2.2. Extraction and purification of *C. weissflogii* polysaccharide

The extraction of polysaccharide was carried out following the methodology described by Granum and Myklestad [22]. Briefly, dry biomass was extracted with 0.05 M  $H_2SO_4$  at 60 °C for 10 min. The extract was then centrifuged to separate the supernatant, which was dialyzed with distilled water and ultrapure water (cut-off 1 kDa), concentrated, and freeze-dried, producing the *C. weissflogii* acid (CAC) extract. CAC was purified by microfiltration using a 0.1  $\mu$ m membrane (Millipore).

### 2.3. Biochemical analyses

The total carbohydrate content was estimated using the phenol-sulfuric acid method [23] and quantified spectrophotometrically using a standard glucose curve. The protein content was measured using a Folin-Ciocalteu reagent with a bovine serum albumin standard [24].

The monosaccharide composition was determined after acid hydrolysis (2 M TFA at 120 °C for 2 h). Hydrolysis products were reduced with  $NaBH_4$  for 12 h. The  $NaBH_4$  excess in the reaction was converted into boric acid by adding acetic acid to pH 5. Boric acid was eliminated by co-distillation with methanol (4 $\times$ ). After acetylation with acetic anhydride (1 h at 120 °C), the resulting alditol acetate derivatives were analyzed by Gas Chromatography-Mass Spectrometry (GC-MS). GC-MS analyses were performed using a Varian 3800 chromatograph equipped with a fused-silica capillary column (30 m  $\times$  0.25 mm) coated with DB-225 ms (Durabond), and a Varian Saturn 2000 R ITD spectrometer. The chromatograph was programmed to run at 50 °C for 1 min, then ramped from 50 to 215 °C at 40 °C.min<sup>-1</sup>. Helium was used as carrier gas with a flow rate of 1 mL.min<sup>-1</sup> [25].

### 2.4. Controlled Smith degradation

CAC (80 mg) was oxidized with 0.05 M  $NaIO_4$  (40 mL) for 72 h at 25 °C under dark and agitated conditions. Following this, the solution was treated with ethylene glycol, reduced with  $NaBH_4$  for 15 h, neutralized with acetic acid, dialyzed, and freeze-dried [26]. The oxidized and reduced material was subjected to partial acid hydrolysis (TFA, pH 2 at 100 °C for 1 h). After neutralization with NaOH, dialysis (1 kDa cut-off), and freeze-drying, the Smith-degraded fraction (CAC-s; 40 % yield) was obtained.

### 2.5. Methylation analysis

CAC was methylated according to the method described in Ciucanu and Kerek [27]. Briefly, the sample (5 mg) was dissolved in DMSO (1 mL), after which NaOH (30 mg) was added. After being stirred for 30 min at 25 °C, iodomethane (0.2 mL) was added, and the reaction was allowed to proceed. The methylation process was repeated twice, and the reaction was interrupted by the addition of distilled water and neutralized with acetic acid. The methylated polysaccharide was dialyzed and freeze-dried. Partially methylated alditol acetates were generated by hydrolysis using 90 % formic acid (0.5 mL) for 6 h at 100 °C using the method for glucans as described by Bao et al. [28], followed by  $NaBH_4$  reduction and acetylation. The products were analyzed by GC-MS and identified by their mass spectra and retention times [25,29] using the same column and conditions as described in Section 2.3.

### 2.6. High-pressure size exclusion chromatography (HPSEC) analysis

The analysis was performed using 1 mg.mL<sup>-1</sup> of polysaccharide solution in the eluent (0.1 M  $NaNO_3$  solution containing  $NaN_3$  0.2 g.L<sup>-1</sup>) with a Waters high-performance size exclusion chromatography (HPSEC) instrument coupled to a differential refractometer (RI) and a Wyatt Technology Dawn-F multi-angle laser light scattering (MALLS) detector adapted for on-line use. Four Waters Ultrahydrogel columns (2000, 500, 250, and 120) were connected in series and coupled to the multi-detection equipment. The specific refractive index increment (dn/dc) was determined using five concentrations between 0.2 and 1.0 mg.mL<sup>-1</sup> (dn/dc value 0.136). HPSEC data were collected and analyzed using the Wyatt Technology ASTRA program. All experiments were carried out at 25 °C.

### 2.7. Nuclear magnetic resonance (NMR) spectroscopy

Each lyophilized sample was dissolved in deuterium oxide ( $D_2O$ ) (30 mg.mL<sup>-1</sup>) and assessed at 70 °C using a Bruker Advance DRX400 NMR spectrometer equipped with a 5 mm multi-nuclear inverse detection probe; a base frequency of 100.63 MHz and 400 MHz was used for <sup>13</sup>C and <sup>1</sup>H nuclei, respectively. Chemical shifts were expressed in ppm using acetone as an internal standard at 30.2 and 2.225 ppm for <sup>13</sup>C and <sup>1</sup>H, respectively. For <sup>1</sup>H and 2D NMR experiments, samples were deuterium-exchanged by successive freeze-drying steps in  $D_2O$  (99.9 %) and then dissolved in  $D_2O$  (30 mg.mL<sup>-1</sup>). Heteronuclear single quantum coherence spectroscopy (HSQC) spectra were obtained using the pulse program supplied with the Bruker spectrometer. Samples dissolved in dimethyl sulfoxide-*d*<sub>6</sub> ( $Me_2SO-d_6$ , 99.9 %, Sigma-Aldrich) had their spectra calibrated to the solvent peak at 39.51 and 2.50 ppm for <sup>13</sup>C and <sup>1</sup>H, respectively.

### 2.8. Biological activity assays

#### 2.8.1. Cells and culture conditions

The biological activity assays were performed using the mouse macrophage-like cell line RAW 264.7 transformed by the Abelson Leukemia virus [30], the human glioblastoma cell lines U87 MG and U251,

and the mouse hippocampal neuronal-derived cell line HT22. All cell lines were cultivated in DMEM supplemented with 10 % SFB and were maintained in an incubator at 37 °C and 5 % CO<sub>2</sub>.

### 2.8.2. Cell metabolic activity assay

Cell lines were incubated in a culture medium in either the presence or absence of CAC β-D-glucan (50 and 100 μg.mL<sup>-1</sup>) over different lengths of time. Metabolic activity was evaluated using 3-[4,5-dimethylthiazol-2-yl]-2,5-diphenyl-tetrazolium bromide (MTT) (Sigma–Aldrich Chemical Co., St. Luis, MO, USA) as described by Reilly et al. [31]. Absorbance was analyzed by spectrophotometry (Bio-Tek Synergy H1 hybrid reader model) at 570 and 630 nm.

### 2.8.3. Morphology alteration and cell proliferation assay

All macrophages (5 × 10<sup>5</sup> cells per well) were plated in xCELLigence plates and maintained in the presence or absence of CAC β-D-glucan (0.5, 1.0, and 2.5 μg. mL<sup>-1</sup>) for 30 h. An xCELLigence real-time cell impedance system (Aligent Bioscience, San Diego, CA, USA) was used to monitor the changes in the number and morphology of macrophages by varying impedance in the culture media of a 96-well microelectronic plate after treatment with the CAC β-D-glucan. Measurements of macrophage impedance were normalized to the time of treatment (normalized cell index), where *t* = 0 h was defined as the starting point of the experiment.

### 2.8.4. Phagocytosis assay

Phagocytic activity was assessed using yeasts as phagocytic particles [32,33]. Briefly, a macrophage monolayer (5 × 10<sup>5</sup> cells per well) was adhered to a 24-well glass coverslip and was incubated with the standard medium in the absence (control) or presence of varying concentrations of CAC (0.5, 1.0, and 2.5 μg. mL<sup>-1</sup>). After 24 h, cells were washed three times with a MEM medium, following addition of 10 yeast cells per macrophage (macrophage to yeast ratio of 1:5), following incubation under the same conditions for 120 min. After each incubation cycle, the samples were washed with PBS medium to remove non-phagocytic yeasts. Coverslips were fixed with Bouin's fixative, stained with Giemsa for 2 h, and dehydrated in acetone. Slides were mounted with Entellan and examined microscopically. Following this, the total number of macrophages, the number of phagocytic macrophages, and the number of phagocytized yeasts were quantified. The phagocytic activity and index were evaluated by determining the number of yeasts phagocytized by macrophages for every 200 macrophages on each coverslip.

### 2.8.5. Flow cytometry assays

U87 MG cells (4 × 10<sup>4</sup> cells per well) were seeded into a 24-well plate. After 24 h, the cells were treated with CAC β-D-glucan (100 μg. mL<sup>-1</sup>) and incubated for 72 h. To evaluate cell death, the cells were collected and stained with Annexin V FITC and PI from the Dead Cell Apoptosis Kit (Thermo Fisher Scientific, Waltham, US), according to the manufacturer's instructions. For cell cycle analysis, cells were fixed in 4 % PFA for 15 min on ice. The cells were then washed with PBS and stained with DAPI (1 μg.mL<sup>-1</sup> in PBS, 0.01 % TRITON-X-10) on ice for 30 min in the dark. Samples from both techniques were analyzed in a Beckman Coulter CytoFLEX S Flow Cytometer (Beckman Coulter, Woerden, the Netherlands), and the data were reviewed in the FlowJo 10.5 software.

### 2.9. Statistical analyses

A Shapiro-Wilk normality test was used to verify the distribution of the data. Significant differences were determined using a one-way analysis of variance (ANOVA). Differences between mean values were tested using Tukey's *post hoc* test. Data with *p* < 0.05 were considered statistically significant. All graphs were created using GraphPad – Prism 5 and 8.

**Table 1**

Yield, chemical analyses, and monosaccharide composition of the polysaccharide fraction obtained from diatom *C. weissflogii*.

Sample <sup>a</sup>	Yield <sup>b</sup> (%)	Carbohydrate <sup>c</sup> (%)	Protein <sup>c</sup> (%)	Monosaccharides (mol %) <sup>d</sup>			
				Rha	Ara	Xyl	Glc
CAC	29.9	89.9	2.1	2.1	0.3	1.6	95.0

<sup>a</sup> CAC sample is defined in the text.

<sup>b</sup> Percentage based on dried microalgae biomass.

<sup>c</sup> Carbohydrate and protein contents were determined by the Dubois et al. [23] and Lowry et al. [24] methods, respectively.

<sup>d</sup> Monosaccharides quantified in mol% in the acetate alditol form. Rha: rhamnose, Ara: arabinose, Xyl: xylose, Glc: glucose.

## 3. Results and discussion

### 3.1. Extraction and characterization of the water-soluble polysaccharide from *C. weissflogii*

Water-soluble polysaccharide (CAC) was isolated from the marine diatom *C. weissflogii* following the conditions previously reported [22]. The yield, analyses, and monosaccharide composition of CAC are presented in Table 1. The polysaccharide fraction contained glucose as major neutral sugar (95.0 mol%), indicating the presence of a glucan. HPSEC-MALLS-RID analysis of CAC showed a symmetric peak centered at 55 min, suggesting a homogeneous profile (Fig. 1) with a molecular weight of 11.7 kDa.

### 3.2. NMR spectroscopic analyses

The <sup>13</sup>C NMR spectrum of CAC exhibited six main signals (Fig. 2a). The 102.5 ppm signal in the anomeric region was attributed to C-1 in the β-glucosyl units. The resonance at 84.8 ppm was attributed to C-3 in the (1 → 3)-linked β-D-glucosyl units, while the signals at 73.2, 68.4, and 75.7 ppm were assigned to C-2, C-4, and C-5, respectively. The 61.0 ppm signal corresponds to the non-linked C-6 in the (1 → 3)-linked β-D-glucosyl units as confirmed by the inverted signal in the <sup>13</sup>C-DEPT NMR spectrum (Fig. 2b). This NMR spectrum is representative of chrysolaminaran similar to those previously extracted from other diatoms [7,34]. Low-intensity signals observed at 95.9 and 92.2 ppm respectively correspond to the C-1 of β- and α-anomers of the 3-linked glucosyl reducing terminal unit [9]. These results together with HPSEC-RID data, indicate that a (1 → 3)-linked β-D-glucan with a relatively low molecular weight was extracted from the marine diatom *C. weissflogii*.

The main <sup>13</sup>C/<sup>1</sup>H correlations were observed in the HSQC spectrum of CAC (Fig. 3). The C1/H1 anomeric correlation at 102.5/4.78 ppm confirmed the β-anomericity of the glucosyl units. The correlation at 84.8/3.78 ppm was attributed to the substituted C3 and its hydrogen

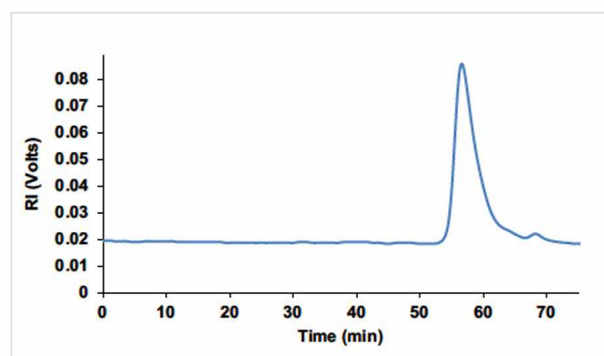


**Fig. 1.** HPSEC elution profile of CAC, obtained with refractive index (RI) detector.

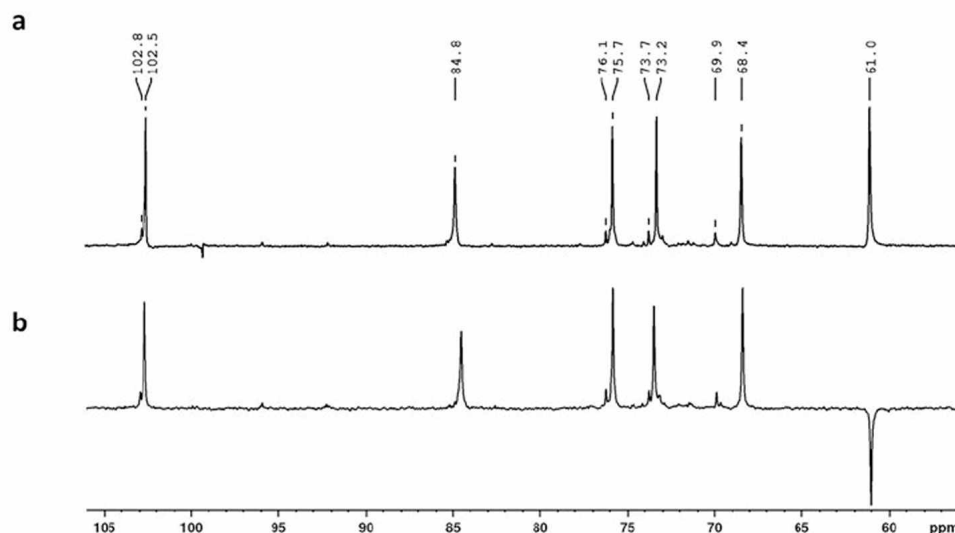


Fig. 2.  $^{13}\text{C}$  NMR spectrum (a) and  $^{13}\text{C}$  DEPT NMR spectrum (b) of the polysaccharide CAC (solvent:  $\text{D}_2\text{O}$ , at  $70^\circ\text{C}$ ).

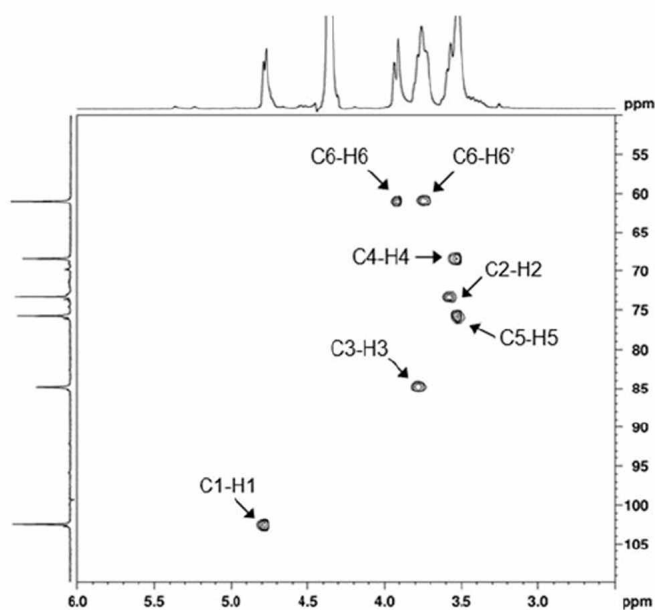


Fig. 3. HSQC spectrum of polysaccharide CAC (solvent:  $\text{D}_2\text{O}$ , at  $70^\circ\text{C}$ ).

(C3/H3), which is consistent with the presence of (1  $\rightarrow$  3)-glycosidic linkages. The carbon at 61.0 ppm (DEPT inverted) was correlated with hydrogens at 3.91 and 3.75 ppm; these correlations were attributed to the unsubstituted C6/H6, H6'. All the other (1  $\rightarrow$  3)-linked glucan correlations observed in the CAC spectrum were assigned and presented in Table 2.

NMR analyses of  $\beta$ -glucans from different sources are frequently carried out using deuterated DMSO ( $\text{Me}_2\text{SO}_4\text{-}d_6$ ) as a solvent. To

Table 2  
NMR chemical shift assignments of polysaccharide CAC isolated from diatom *C. weissflogii*.

Sample	$^{13}\text{C}/^1\text{H}$ chemical shifts (ppm) <sup>a</sup>					
	C1/H1	C2/H2	C3/H3	C4/H4	C5/H5	C6/H6, H6'
CAC	102.5/ 4.78	73.2/ 3.57	84.8/ 3.78	68.4/ 3.52	75.5/ 3.54	61.0/ 3.91, 3.75

<sup>a</sup> Solvent  $\text{D}_2\text{O}$ , temperature:  $70^\circ\text{C}$ .

Table 3

$^{13}\text{C}$  NMR assignments of polysaccharide CAC (in  $\text{Me}_2\text{SO}-d_6$ ) compared with (1  $\rightarrow$  3)-linked  $\beta$ -glucans from other sources.

(1 $\rightarrow$ 3)-linked $\beta$ -glucan source	$^{13}\text{C}$ chemical shifts (ppm)					
	C1	C2	C3	C4	C5	C6
<i>C. weissflogii</i> (marine diatom) <sup>a</sup>	103.1	73.0	86.3	68.6	76.5	61.0
<i>Ganoderma resinaceum</i> (fungus) <sup>b</sup>	102.9	72.8	86.2	68.5	76.4	60.9
<i>Pleurotus tuberregium</i> (fungus) <sup>c</sup>	102.6	72.8	85.9	68.1	75.6	60.3
<i>Chaetoceros mülleri</i> (marine diatom) <sup>d</sup>	102.7	73.4	84.4	68.3	75.8	60.9

<sup>a</sup> Present study.

<sup>b</sup> Amaral et al. [35].

<sup>c</sup> Chenghua et al. [36].

<sup>d</sup> Størseth et al. [7].

compare the  $^{13}\text{C}$  NMR chemical shifts of the (1  $\rightarrow$  3)-linked  $\beta$ -D-glucan extracted from *C. weissflogii* with other  $\beta$ -glucans described in the literature, the CAC fraction was also subjected to NMR analysis using  $\text{Me}_2\text{SO}_4\text{-}d_6$  as a solvent (Table 3). These results show the similarities in the  $^{13}\text{C}$  NMR chemical shifts of  $\beta$ -glucans isolated from different sources.

### 3.3. Methylation analysis of CAC

Results from the methylation analysis were consistent with the NMR experiments. The molecule primarily consists of (1  $\rightarrow$  3)-linked glucopyranosyl units, which account for 92.3 % of the polymer (Table 4). However, methylation also shows a small degree of branching (4.9 %) in C-6. There is also a small amount of (1  $\rightarrow$  4)-linked glucopyranosyl units, which represent 1.8 %.

The results of the  $^{13}\text{C}$  NMR spectroscopy and methylation analyses suggest that the minor signals at 102.8 (C-1), 76.1 (C-5), and 73.7 (C-2) ppm could be attributed to the  $\beta$ -(1  $\rightarrow$  6)-linked units. The presence of  $\beta$ -(1  $\rightarrow$  4)-linked units was not detected by NMR, although they were identified by methylation analysis. These units could be part of the structure or be originated from a minor contamination during the extraction process, as previously reported by Vogler et al. [37] for microalga *Nannochloropsis gaditana*.

### 3.4. Analysis of the Smith-degraded product

To determine the fine structure of the polysaccharide, a CAC-s fraction was produced by subjecting CAC to a controlled Smith degradation. The  $^{13}\text{C}$  NMR spectrum of the CAC-s fraction revealed an abundance of

**Table 4**  
Methylation analysis of polysaccharide fraction CAC from diatom *C. weissflogii*.

Derivative <sup>a</sup>	Rt <sup>b</sup>	Mass fragments ( <i>m/z</i> )	Deduced linkage	CAC (mol %) <sup>c</sup>
2,3,4,6-Me <sub>4</sub> -Glc	1	101; 113,129; 145	Glc-(1→	1.0
2,4,6-Me <sub>3</sub> -Glc	1.269	101; 117; 129; 145	→3)-Glc-(1→	92.3
2,3,6-Me <sub>3</sub> -Glc	1.393	87; 103; 115; 128	→4)-Glc-(1→	1.8
2,4-Me <sub>2</sub> -Glc	1.945	87; 117; 129; 143	→3,6)-Glc-(1→	4.9

<sup>a</sup> 2,3,4,6-Me<sub>4</sub>-Glc analyzed as 1,5-di-*O*-acetyl-2,3,4,6-*O*-methyl glucitol, etc.

<sup>b</sup> Retention time of derivatives in relation to 2,3,4,6-tetra-*O*-methyl-Glc.

<sup>c</sup> mol % of monosaccharide quantified in the form of partially methylated alditol acetate, analyzed by GC-MS.

signals that corresponded to (1 → 3)-linked β-glucopyranosyl units (Fig. 4) that were identical to those observed in the native polysaccharide CAC (Fig. 2). However, the low-intensity signals in the <sup>13</sup>C spectrum differed from those present in the native polysaccharide (CAC). One of these resonances occurred at 63.0 ppm (Fig. 4b) and was attributed to the C-1 of the reducing terminal unit that was reduced with NaBH<sub>4</sub> during the controlled Smith process. Furthermore, the signals at 104.1 and 61.5 ppm were attributed to the C-1 and C-6 of the non-reducing terminal (NRT) units, suggesting that the polysaccharide had partially depolymerized [28]. The presence of (1 → 4)-linked units in the backbone of the native polysaccharide, not confirmed in the present study, could explain the partial depolymerization of the β-glucan. The proposed structure of the controlled Smith-degradation product (CAC-s) is presented in Fig. 5.

The NMR spectra and the results of the methylation analyses indicate that the water-soluble polysaccharide extracted from the microalga *C. weissflogii* is chrysolaminaran, consisting of a (1 → 3)-linked β-D-glucan backbone (97.2 %, 3-linked plus 3,6-linked) with low proportion of substitution in C-6 by single glucose units (Fig. 6).

Polysaccharides in diatoms are often divided into three groups: cell wall polysaccharides, extracellular mucilages, and reserve polysaccharides [22]. The cell wall of diatoms is composed of silica and organic wrappers containing heteropolysaccharides and can vary widely in terms of the proportion of galactose, glucose, mannose (and their corresponding uronic acids), xylose, fucose, rhamnose, and other residues, which vary depending on species [22,38]. Extracellular mucilage has a variable composition; however, glucose is the most abundant monomer as it is excreted during the cultivation exponential phase as

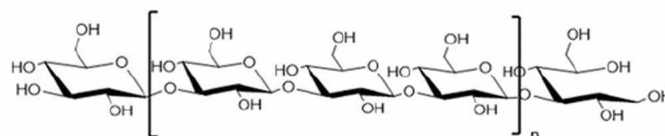


Fig. 5. Proposed structure for the Smith-degraded product (CAC-s).

observed for three diatoms species [39]. Reserve polysaccharides consist of a soluble polysaccharide derivative of glucose formed by β-(1 → 3) glycosidic linkages [40]. β-(1 → 3)-glucan competes with cellulose as the most abundant carbohydrate on earth and is the main food reserve for diatoms [41,42]. β-glucans in diatoms are known as chrysolaminaran (previously known as leucosin) [22]; this differs from laminaran, which is found in brown algae, due to the absence of mannitol [41]. The extraction of diatoms usually involves the disruption of cells by dilute acid treatment, as was the case in this paper. Acid extraction can isolate crystalline laminaran in diatoms, of which 99.5 % is composed of D-glucose [41,42]. However, the extraction of (1 → 3)-linked β-D-glucans from some species of diatoms, such as *Cylindrotheca fusiformis*, *Craspedostauros australis*, and *Thalassiosira pseudonana*, using a hot aqueous medium could indicate the presence of these molecules in the intracellular vacuoles of those organisms [43,44].

In this study, a β-(1 → 3)-glucan with a molecular weight of 11.7 kDa was isolated. According to McConville et al. [5] as well as Paulsen and Myklestad [6], isolated chrysolaminaran is expressed as a β-(1 → 3)-glucan with a molecular weight of 10.1 kDa with a small degree of binding variation in the β-(1 → 2) and (1 → 6) positions. However, the polysaccharide in this strain was found to have a small degree of β-(1 → 4) glycosidic linkages. Vogler et al. [37] characterized a β-(1 → 3), (1 → 6)-glucan from *N. gaditana*, also containing 4 linkage residues (9.1 %). NMR analysis presented in the study as well did not show the presence of (1 → 4) glycosidic linkages although they were detected by methylation analysis and attributed to cellulose contamination. Størseth et al. [7] identified the presence of reserve polysaccharides such as chrysolaminaran in the diatom *Chaetoceros mulleri* and characterized them as a branched β-(1 → 3)-glucan. This suggests that the structure of chrysolaminaran may vary according to species and that the yield varies depending on the stage of microalgae growth. Størseth et al. [7] also identified a (1 → 3)-linked β-glucan present in *Chaetoceros debilis* that contained a large number of (1 → 6)-linked β-glucose units, which had not previously been reported in diatoms. This emphasizes the variety of

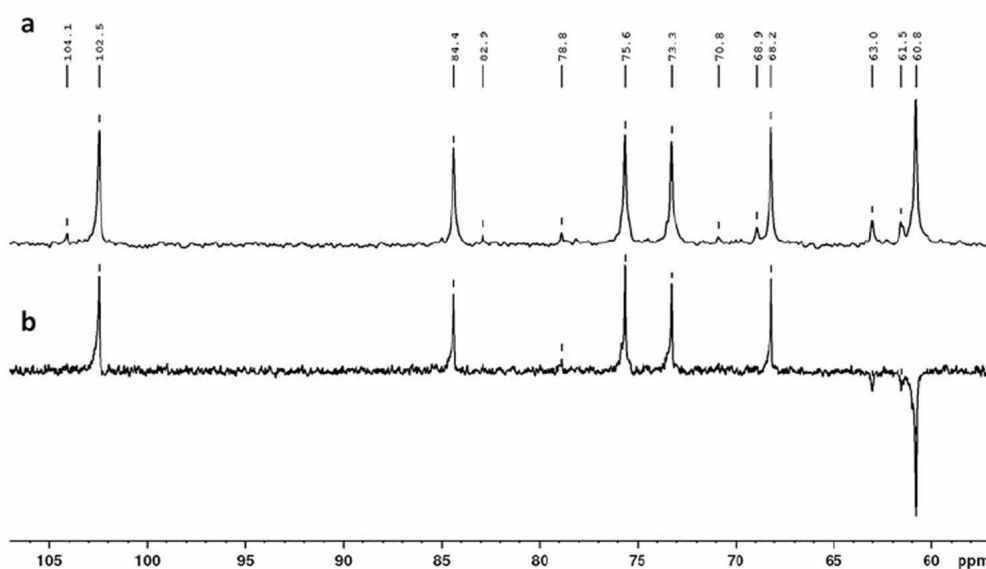


Fig. 4. NMR analyses of the Smith-degraded product (CAC-s). <sup>13</sup>C (a) and <sup>13</sup>C DEPT (b) NMR spectra (solvent: D<sub>2</sub>O, at 70 °C).

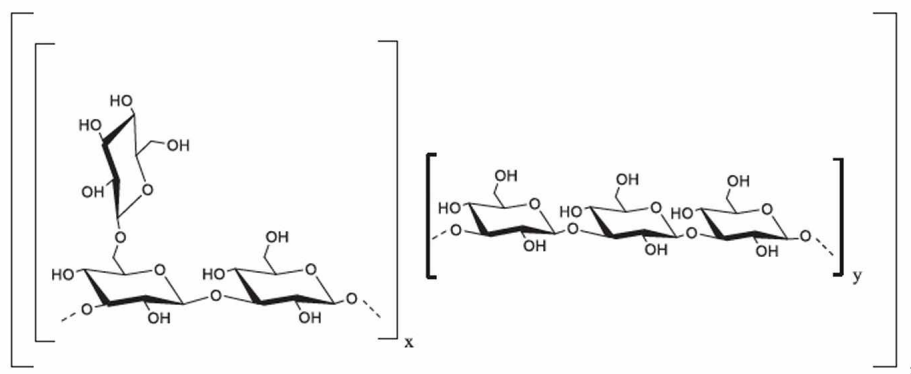


Fig. 6. Proposed structure for the water-soluble polysaccharide extracted from diatom *C. weissflogii*. Molar proportions: x: 0.05; y: 1.

chrysolaminaran structures that can be found within the same micro-algae group.

### 3.5. Biological activity of polysaccharide extracted from *C. weissflogii*

#### 3.5.1. Effects of CAC $\beta$ -D-glucan on glioblastoma and neuronal cells

To investigate whether CAC  $\beta$ -D-glucan affects cell growth and survival, we treated human glioblastoma cell lines (U87 MG and U251) and a mouse hippocampal neuronal-derived cell line (HT22) with different concentrations (50 and 100  $\mu\text{g}\cdot\text{mL}^{-1}$ ) of CAC  $\beta$ -D-glucan for 24, 48, and 72 h. MTT assays and flow cytometric analysis were performed. The results suggested that CAC  $\beta$ -D-glucan had no significant cytotoxic effects on the U87 MG and U251 cells (Fig. 7a, b, c, d). Indeed, after 24 h of CAC  $\beta$ -D-glucan treatment, U87 MG cells in the experimental group exposed to the highest concentration of CAC  $\beta$ -D-glucan (100  $\mu\text{g}\cdot\text{mL}^{-1}$ ) were found to have slightly higher metabolic activity compared to the control group. However, this metabolic effect was not maintained after longer exposure times (48 and 72 h), indicating that there was no statistical difference in the percentage of metabolically active cells observed in the treated groups compared to the control groups for each of the different CAC  $\beta$ -D-glucan concentrations used. Similarly, there was no significant change in the metabolic activity of U251 MG cells and HT22 non-tumor cells under the same conditions (Figs. 7b and S1a, b, c).

In contrast, Pires Ado et al. [45] showed that  $\beta$ -D-glucans derived from mushrooms *Lactarius rufus* and *Agaricus bisporus* exhibited a cytotoxic effect on HepG2 hepatocarcinoma cells without affecting the primary hepatocyte, albeit in higher concentrations than those tested here (>100 and 200  $\mu\text{g}\cdot\text{mL}^{-1}$ , respectively). Interestingly, our data did not show any changes in cell death or alterations to cycle progression in CAC  $\beta$ -D-glucan-treated U87 MG cells even at the highest concentration used (100  $\mu\text{g}\cdot\text{mL}^{-1}$  for 72 h) (Fig. 7c, d, e). Choromanska et al. [46], Hussain et al. [47] reported the cytostatic action of a  $\beta$ -D-glucan extracted from the plant species *Avena sativa* on the Me45 (human melanoma), A431 (epidermal carcinoma), Colo-205 (human colon cancer carcinoma), MCF-7 (human breast carcinoma), and T47D (human ductal breast epithelial tumor) cell lines. There was a drop in cell metabolism without inducing cell death or alterations to the cell cycle when exposed to polysaccharides at concentrations of 50 and 100  $\mu\text{g}\cdot\text{mL}^{-1}$ .

The antitumor mechanisms proposed for most polysaccharides include direct killing as well as indirect antitumor activity by improving immune functions [4,8,10,17,19,20]. There are several examples of polysaccharides in the literature that are non-cytotoxic or exhibit cytotoxicity in higher concentrations (above 400  $\mu\text{g}\cdot\text{mL}^{-1}$ ) that still have clear immunostimulatory effects [48–51]. Li et al. 2019 [48] and 2020 [49] reported that the treatment of MCF7 and 4 T1 breast cancer cells with different concentrations of  $\alpha$ -(1  $\rightarrow$  6)-glucan from the medicinal herb *Astragalus membranaceus* (100 to 1000  $\mu\text{g}\cdot\text{mL}^{-1}$ ) did not inhibit proliferation or increase apoptosis. On the other hand, this glucan was able to activate murine macrophages, promoting up-regulation of TNF- $\alpha$

and NO production, which may lead to repression of cell proliferation in a time- and concentration-dependent manner, cell cycle arrest and apoptosis in MCF7 cells. In addition, Wufuer et al. [50] showed that an  $\alpha$ -(1  $\rightarrow$  4) glucan from the plant species *Brassica rapa* L. showed cytotoxic activity more pronouncedly at high concentrations (500–2000  $\mu\text{g}\cdot\text{mL}^{-1}$ ), leading to apoptosis only on A549 lung adenocarcinoma cells. Interestingly, five different  $\alpha$ -glucans from *B. rapa* L. had no cytotoxic effect even at the highest concentration used (2000  $\mu\text{g}\cdot\text{mL}^{-1}$ ) in both, AGS gastric adenocarcinoma and HepG2 hepatocarcinoma cell lines, showing that cytotoxic effects are dependent of cell-type or cellular context. However, these five  $\alpha$ -glucans were able to promote the growth of murine macrophage cells and also stimulate the released of NO and TNF and IL-6 cytokines.

Concerning  $\beta$ -glucans, Rutchevski et al. [51] showed that  $\beta$ -(1  $\rightarrow$  6)-D-glucan extracted from the mushroom *Agaricus bisporus* inhibit cell viability in MCF-7 breast cancer cells already at 100  $\mu\text{g}\cdot\text{mL}^{-1}$ , while MDA-MB-231 cells (a more aggressive cell line, derived from Triple-negative breast cancer -TNBC) showed more resistance phenotype even at higher concentration (300  $\mu\text{g}\cdot\text{mL}^{-1}$ ). Interestingly, the authors indicate that MCF-7 cell line express estrogen receptors while MDA-MB-231 do not express such receptor [51,52]. According to this data, Xu et al. [53] described that a  $\beta$ -glucan from the mushroom *Lentinus edodes* reduced MCF-7 cell viability in a concentration-dependent manner but did not affect the TNBC cell line, suggesting that cytotoxic-responsiveness to  $\beta$ -glucans could be related to estrogen-receptor expression in breast cancer model. It is important to note that, in addition to direct tumor cell cytotoxicity,  $\beta$ -(1  $\rightarrow$  6)-D-glucan extracted from *A. bisporus* was able to stimulate human THP-1 macrophages, leading to increased levels of pro-inflammatory cytokines (TNF- $\alpha$ , IL-1 $\beta$  and CXCL10) at lower concentrations of the polysaccharide (30 and 100  $\mu\text{g}\cdot\text{mL}^{-1}$ ).

The literature also shows that  $\beta$ -glucans obtained from different sources often exhibit different biological responses despite having the same basic structures, suggesting that there are essential aspects of the  $\beta$ -glucans structures that affects cellular response. These include the degree of polymerization, branching, molecular weight, and the presence, abundance or absence of specific functional groups at the backbone and side chains (as sulfate, phosphate, carboxymethyl, among others) that will rule the primary and spatial structure of those glucans. These features mainly control the interaction between the polysaccharides and carbohydrate receptors or polysaccharide-proteins complexes and trigger different types of responses [54–56].

#### 3.5.2. Effect of CAC $\beta$ -D-glucan on the phagocytic activity of macrophages

We then investigated whether CAC  $\beta$ -D-glucan affected murine macrophages in RAW 264.7 cell lines, which are associated with immunomodulatory processes. An analysis of xCELLigence cell-impedance real-time measurements indicates that CAC  $\beta$ -glucan (2.5  $\mu\text{g}\cdot\text{mL}^{-1}$ ) significantly increases the cell index even after only 14 h

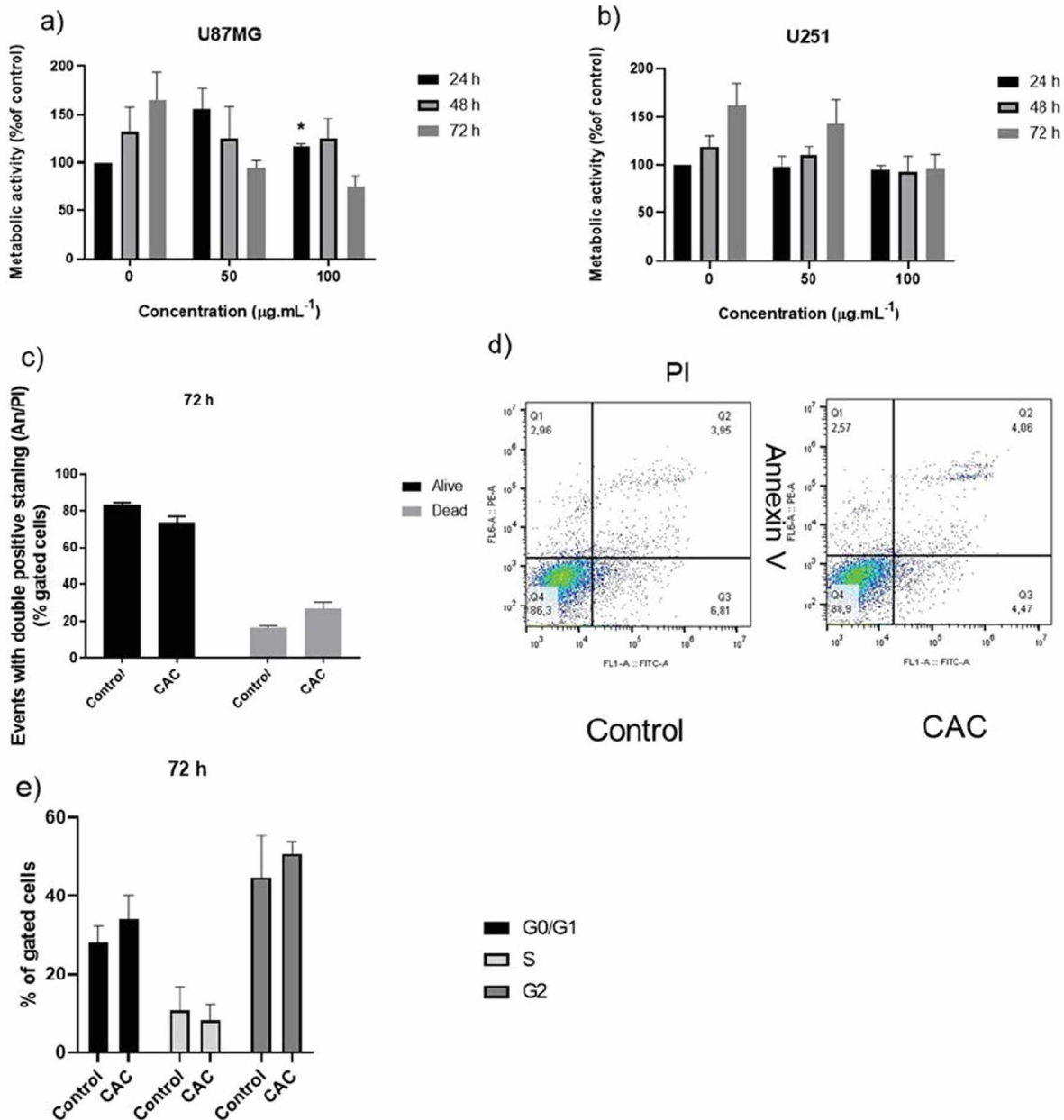


Fig. 7. Metabolic activity determined by MTT test at glioblastoma cells U87 MG (a) and U251 (b) with CAC  $\beta$ -D-glucan at 50 and 100  $\mu\text{g}\cdot\text{mL}^{-1}$  concentrations at 24, 48 and 72 h treatment time points. Zero (control) corresponds to 100 % of metabolic activity, normalized to untreated cells at 24 h. These results are expressed as mean  $\pm$  S.D., three independent experiments with four technical replicates, by ANOVA test. (\*) Significant differences observed compared with the control group by *post-hoc* Tukey test ( $p < 0.05$ ). Cell death assay by An-/PI- and An+/PI+ staining with U87 MG cell line (c, d) and cell cycle progression with U87 MG (e), with presence of CAC  $\beta$ -D-glucan compound at 100  $\mu\text{g}\cdot\text{mL}^{-1}$  concentration for 72 h, expressed as mean  $\pm$  S.D., three independent experiments each with three technical replicates, by ANOVA test.

following treatment when compared with the controls (Fig. 8a); there were also changes in cell attachment, morphology, and/or growth characteristics as a response to CAC  $\beta$ -D-glucan. These results allow for the study of the biomodulating effect of the polymer as well as the evaluation of the phagocytic activity of macrophages in the RAW 264.7 cell line. Using yeasts as phagocytic particles, a clear increase in the phagocytic capacity of RAW 264.7 cells treated with CAC  $\beta$ -D-glucan was observed in terms of the percentage of phagocytosis activity (Table 5), indicating immunostimulatory activity at all tested concentrations (Fig. 8b, c). It must be pointed out that CAC  $\beta$ -D-glucan already showed phagocytic activity at the lowest concentration that was used (0.5  $\mu\text{g}\cdot\text{mL}^{-1}$ ). In the literature, a different  $\alpha$ -(1  $\rightarrow$  4) glucan from *Brassica rapa L* [50] and a branched  $\beta$ -(1  $\rightarrow$  3)-glucan from the

mushroom *Russula vinosa* [57] were able to induce phagocytic ability of RAW264.7 cells, evaluated by neutral red assay, from concentrations of 62.5 and 25  $\mu\text{g}\cdot\text{mL}^{-1}$ , respectively.

Macrophages have an important function in tumoral immunosurveillance. They are present within the tumoral microenvironment and have an important role in tumor immunity. Depending on their activation state, they are capable of phagocytizing cancer cells and presenting tumor-specific antigens to T and B lymphocytes. The activation state of macrophages is modulated by lipopolysaccharides (LPS). LPSs trigger cell signaling events in macrophages, inducing the release of important pro-inflammatory cytokines such as tumor necrosis factor- $\alpha$  (TNF- $\alpha$ ), which stimulates tumoral killing and phagocytosis to produce tumor-specific antigens [58].

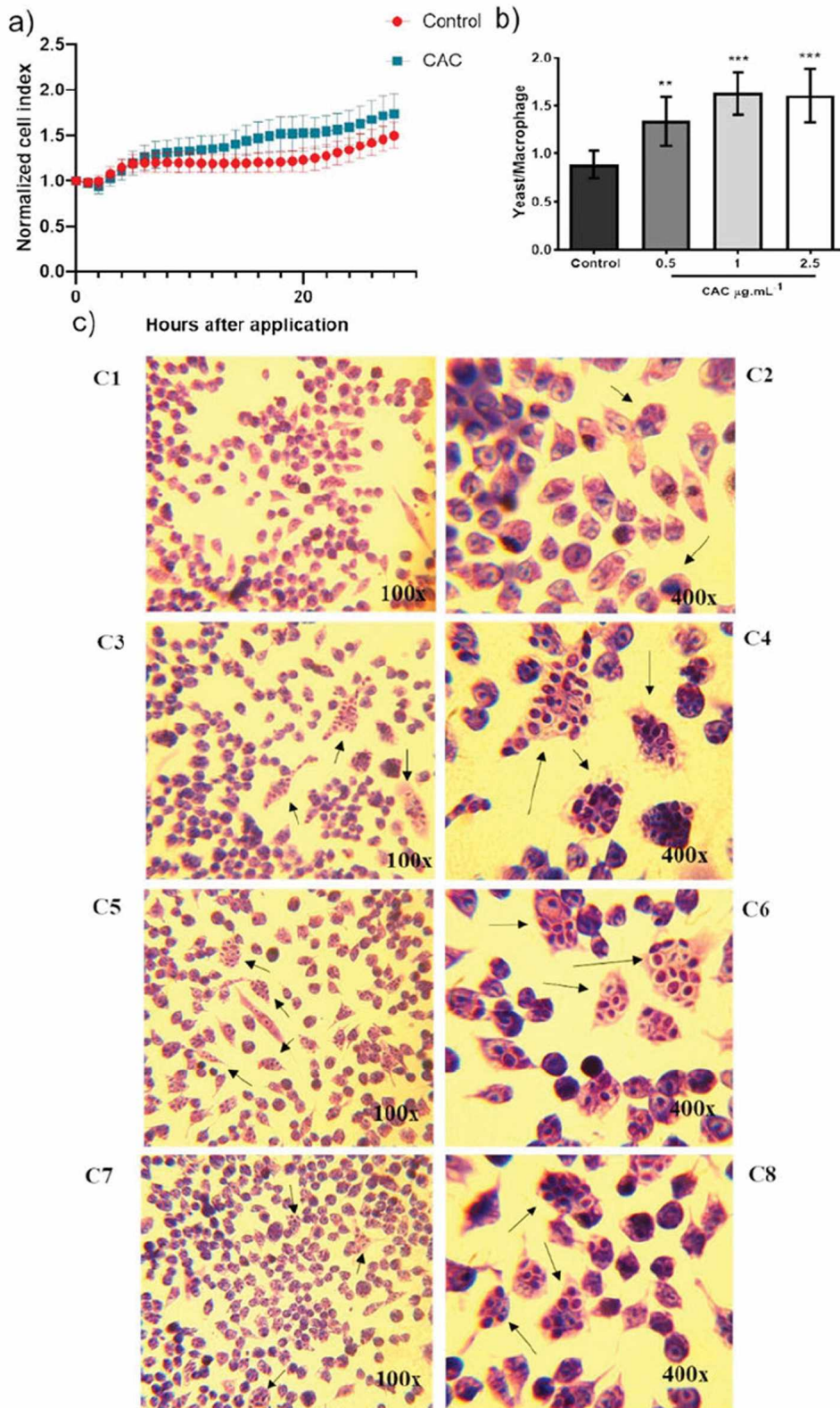


Fig. 8. Macrophage RAW 264.7 cells challenged with CAC  $\beta$ -D-glucan at 2.5; 5.0; 10 and 25  $\mu\text{g}\cdot\text{mL}^{-1}$  concentrations. (a) Cell impedance real-time measurements upon CAC  $\beta$ -D-glucan treatment (2.5  $\mu\text{g}\cdot\text{mL}^{-1}$ , 30 h) (blue curve) and non-treated control (red). (b) Phagocytic index (yeast/macrophage) upon CAC  $\beta$ -D-glucan treatment (0, 0.5, 1.0 and 2.5  $\mu\text{g}\cdot\text{mL}^{-1}$ ) for 24 h. (c) Representative pictures of phagocytic activity. Macrophages were cultivated in absence (control) (C1, C2) or presence of CAC  $\beta$ -glucan 0.5 (C3, C4), 1 (C5, C6) and 2.5 (C7, C8)  $\mu\text{g}\cdot\text{mL}^{-1}$  for 24 h. After treatment, the medium was removed and yeasts (1:5) were added following incubation for 1 h. Arrows point yeasts being phagocytized by macrophages. Original magnification:  $\times 400$  (C1, C3, C5, C7) and  $\times 1000$  (C2, C4, C6, C8). All results are expressed as mean  $\pm$  s.d., three independent experiments in triplicate to each concentration. (\*\*\*) Significant differences between treatment groups and the control group by Tukey *post-hoc* test ( $p < 0.01$ ) (\*\*\*) Significant differences between treatment groups and the control group by the Tukey test ( $p < 0.001$ ).

It is important to note that CAC  $\beta$ -D-glucan is a partially branched (1  $\rightarrow$  3)-linked  $\beta$ -D-glucan with low molecular weight. Many studies have reported the immunostimulating capacity of  $\beta$ -glucans and have related this immunostimulatory activity to their chemical structure [48–51]. Kulicke et al. [58] compared the influence of the molecular structure of four different  $\beta$ -glucans on immune activity and found that  $\beta$ -glucans

with low molecular weight are more efficient at activating the immune system by increasing the amount of TNF- $\alpha$  and superoxide radicals released by human monocytes. Furthermore, higher immunomodulatory activities were observed in (1  $\rightarrow$  3)-linked  $\beta$ -D-glucans with a lower degree of branching compared to those with higher degrees of branching [28,59].  $\beta$ -glucans have received increased attention in recent decades

**Table 5**  
Phagocytic activity of RAW 264.7 cells upon yeast with CAC  $\beta$ -D-glucan.

Concentration ( $\mu\text{g. ml}^{-1}$ )	Phagocytic activity (Mean $\pm$ SD)	% of enhancement compared with control
Control (0)	0.88 $\pm$ 0.1	–
0.5	1.34 $\pm$ 0.3*	54.3
1.0	1.61 $\pm$ 0.3***	84.7
2.5	1.63 $\pm$ 0.2***	88.8

Three independent experiments in triplicate for each concentration. Significant differences from control group by Dunnett *post-hoc* test (\*) ( $p < 0.05$ ) and (\*\*\*) ( $p < 0.01$ ). Phagocytic activity was calculated as described in the methods section.

as they can be recognized by macrophage-specific receptors and, consequently, can activate this type of cell. The  $\beta$ -D-glucans are phagocytized after activation [60,61]. Consequently, determining the structural characteristics of  $\beta$ -glucans is an essential prerequisite for understanding how glucans are recognized by the immune system.

Immunomodulators primarily operate based on the stimulation of specific and non-specific functions of the native and adaptative immune system [58,59].  $\beta$ -D-glucans are engulfed by macrophages and carried to the marrow and the endothelium reticular system. There, small fragments from the polymer are released and bind to different receptors such as Dectin-1, toll-like receptor (TLR) 2, 3, 4, and 6, complement receptor 3 (CR3), carbohydrate-binding modules, and the cluster of differentiation 5 (CD5). They also can bind to proteins and glycoproteins [62–66]. The activation of these receptors triggers molecular pathways such as phosphoinositide 3-kinase (PI3K), macrophage inflammatory protein 2 (MIP-2), tyrosine-protein kinase (PTK), releasing diverse cytokines [61,65,66]. In addition, another (1  $\rightarrow$  3), (1  $\rightarrow$  6)-linked  $\beta$ -D-glucan from the seaweed *Durvillaea antarctica* increased the activation of RAW 264.7 cells by binding to TLR4 and mediating the release of nitric oxide (NO), reactive oxygen species (ROS), MCP-1, TNF- $\alpha$ , and interleukin-1 beta (IL-1 $\beta$ ) [67].

#### 4. Conclusion

A (1  $\rightarrow$  3)-linked  $\beta$ -D-glucan with a small proportion of C-6 substitution by single  $\beta$ -glucose units was isolated from the marine diatom *C. weissflogii*. This water-soluble polysaccharide, which had a molecular weight of 11.7 kDa, did not had cytotoxic effect on glioblastoma cell lines at any of the tested concentrations. However, this microalgal  $\beta$ -D-glucan was able to enhance the phagocytic activity of the macrophage RAW 264.7 at low concentrations, suggesting that it exhibited important immunostimulatory activity and was thus of biotechnological interest. Further studies are necessary to evaluate its *in vivo* immunostimulating potential.

Supplementary data to this article can be found online at <https://doi.org/10.1016/j.ijbiomac.2022.10.147>.

#### CRediT authorship contribution statement

Conceptualization, J.R., G.R.N. and M.D.N; Writing – Original Draft Preparation, J.R., M.E.D. and M.D.N; Writing – Review & Editing, T.R.M., G.A.C., M.T.L., M.E.D., G.R.N. S.M.B.W., M.D.N., and A.M.D.; Supervision, M.D.N., M.E.D., G.R.N. and A.M.D.; Project Administration, M.D.N., M.E.D., G.R.N. and A.M.D.; Funding Acquisition, M.D.N., M.E.D., G.R.N. and A.M.D.; All the authors have read, approved and made substantial contributions to the manuscript.

#### Declaration of competing interest

The authors declare that they have no known competing financial interests or personal relationships that could have appeared to influence the work reported in this paper.

#### Data availability

Data will be made available on request.

#### Acknowledgements

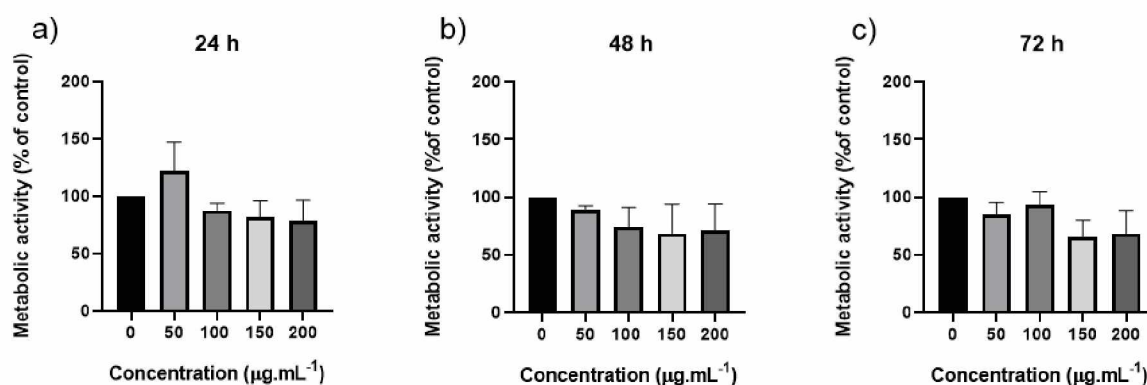
This work was supported by the Conselho Nacional de Desenvolvimento Científico e Tecnológico (CNPq, Brazil) (Universal Call grant #: 462414/2014-0 and Process # 306568/2018-7) and by Coordenação de Aperfeiçoamento de Pessoal de Nível Superior (CAPES, Brazil) (Finance code 001). M.T.L. was a recipient of CAPES scholarship (Process # 88887.321693/2019-00). T.R.M. acknowledge a doctoral scholarship from CAPES (Process # 88882.344138/2019-01), a doctoral sandwich scholarship from CAPES PrInt program (Process # 88887.468902/2019-00). M.E.D., M.D.N., and S.M.B.W. are Research Members of the National Research Council of Brazil (CNPq). A.M.D. is the recipient of a Rosalind Franklin Fellowship co-funded by the European Union and the University of Groningen. The authors acknowledge the NMR Center of Federal University of Paraná (UFPR) for data acquisition and also Dr. Frank Kruyt from Rijkuniversiteit Groningen (RUG) for donating the U87MG and U251 cell lines.

#### References

- [1] G.A. Colusse, J. Carneiro, M.E.R. Duarte, J.C. De Carvalho, M.D. Nosedá, *Advances in microalgal cell wall polysaccharides: a review focused on structure, production, and biological application*, *Crit. Rev. Biotechnol.* 42 (2022) 562–577.
- [2] T.M.M. Bernaerts, L. Gheysen, C. Kyomugasho, Z. Jamsazzadeh Kermani, S. Vandionant, I. Foubert, A.M. Van Loey, Comparison of microalgal biomasses as functional food ingredients: focus on the composition of cell wall related polysaccharides, *Algal Res.* 32 (2018) 150–161.
- [3] D.Y. Rahman, F.D. Sarian, A. Van Wijk, M. Martínez-García, M.J.E.C. Van der Maarel, Thermostable phycocyanin from the red microalga *Cyanidioschyzon merolae*, a new natural blue food colorant, *J. Appl. Phycol.* 29 (3) (2017) 1233–1239.
- [4] G. Riccio, C. Lauritano, Microalgae with immunomodulatory activities, *Mar. Drugs* 18 (1) (2019).
- [5] F. Boukid, M. Castellari, Food and beverages containing algae and derived ingredients launched in the market from 2015 to 2019: a front-of-pack labeling perspective with a special focus on Spain, *Foods* 10 (1) (2021) 173.
- [6] A. Kartik, D. Akhil, D. Lakshmi, K. Panchamoorthy Gopinath, J. Arun, R. Sivaramakrishnan, A. Pugazhendhi, A critical review on production of biopolymers from algae biomass and their applications, *Bioresour. Technol.* 329 (2021) 124868.
- [7] T. Størseth, K. Hansen, J. Skjermo, J. Krane, Characterization of a  $\beta$ -D-(1 $\rightarrow$ 3)-glucan from the marine diatom *Chaetoceros mulleri* by high-resolution magic-angle spinning NMR spectroscopy on whole algal cells, *Carbohydr. Res.* 339 (2004) 421–424.
- [8] J. Bohn, J. Bemiller, (1 $\rightarrow$ 3)- $\beta$ -D-glucans as biological response modifiers: a review of structure-functional activity relationships, *Carbohydr. Polym.* 28 (1995) 3–14.
- [9] Y.T. Kim, E.H. Kim, C. Cheong, D.L. Williams, C.W. Kim, S.T. Lim, Structural characterization of  $\beta$ -D-(1 $\rightarrow$ 3, 1 $\rightarrow$ 6)-linked glucans using NMR spectroscopy, *Carbohydr. Res.* 328 (2000) 331–341.
- [10] S.H. Young, J. Ye, D.G. Frazer, X. Shi, V. Castranova, Molecular mechanism of tumor necrosis factor- $\alpha$  production in (1 $\rightarrow$ 3)- $\beta$ -D-glucan (zymosan)-activated macrophages, *J. Biol. Chem.* 276 (2001) 20781–20787.
- [11] J. Skjermo, T. Størseth, K. Hansen, A. Handá, G. Øie, Evaluation of  $\beta$ -(1 $\rightarrow$ 3, 1 $\rightarrow$ 6)-glucans and high-M alginate used as immunostimulatory dietary supplement during first feeding and weaning of Atlantic cod (*Gadus morhua* L), *Aquaculture* 261 (2006) 1088–1101.
- [12] L. Barsanti, P. Gualtieri, Paramylon, a potent immunomodulator from WZSL mutant of *Euglena gracilis*, *Molecules* 24 (17) (2019) 3114.
- [13] R. Russo, L. Barsanti, V. Evangelista, A.M. Frassanito, V. Longo, L. Pucci, P. Gualtieri, *Euglena gracilis* paramylon activates human lymphocytes by upregulating pro-inflammatory factors, *Food Sci. Nutr.* 5 (2) (2017) 205–214.
- [14] R. Chen, M. Smith-Cohn, A.L. Cohen, H. Colman, Glioma subclassifications and their clinical significance, *Neurotherapeutics* 14 (2) (2017) 284–297.
- [15] T. Zeng, D. Cui, L. Gao, Glioma: an overview of current classifications, characteristics, molecular biology and target therapies, *Front. Biosci. (Landmark Ed)* 20 (2015) 1104–1115.
- [16] Q.T. Ostrom, L. Bauchet, F.G. Davis, I. Deltour, J.L. Fisher, C.E. Langer, M. Pekmezci, J.A. Schwartzbaum, M.C. Turner, K.M. Walsh, M.R. Wrensch, B.S. JS, The epidemiology of glioma in adults: a “state of the science” review, *Neuro-Oncol.* 16 (7) (2014) 896–913.
- [17] M.F. de Jesus Raposo, A.M.M.B. de Moraes, R.M.S.C. de Moraes, Bioactivity and applications of polysaccharides from marine microalgae, in: K. Ramawat, J. M. Mérillon (Eds.), *Polysaccharides*, Springer, Cham, 2014, pp. 1–38.
- [18] W.B. Liu, F. Xie, H.Q. Sun, M. Meng, Z.Y. Zhu, Anti-tumor effect of polysaccharide from *hirsutella sinensis* on human non-small cell lung cancer and nude mice

- through intrinsic mitochondrial pathway, *Int. J. Biol. Macromol.* 99 (2017) 258–264.
- [19] M.J. Kim, S.Y. Hong, S.K. Kim, C. Cheong, H.J. Park, H.K. Chun, K.H. Jang, B. D. Yoon, C.H. Kim, S.A. Kang,  $\beta$ -glucan enhanced apoptosis in human colon cancer cells SNU-C4, *Nutr. Res. Pract.* 3 (2009) 180–184.
- [20] L. Zhao, Y. Chen, S. Ren, Y. Han, H. Cheng, Studies on the chemical structure and antitumor activity of an exopolysaccharide from rhizobium sp. N613, *Carbohydr. Res.* 345 (2010) 637–643.
- [21] R.R.L. Guillard, Culture of Phytoplankton for Feeding Marine Invertebrates, in: W. L.S.M.H. Chanley (Ed.), *Culture of Marine Invertebrate Animals: Proceedings*, Springer, US, Boston, MA, 1975, pp. 29–60.
- [22] E. Granum, S.M. Mykkestad, A simple combined method for determination of  $\beta$ -(1 $\rightarrow$ 3)-glucan and cell wall polysaccharides in diatoms, *Hydrobiologia* 477 (2002) 155–161.
- [23] M. Dubois, K. Gilles, P. Rebers, F. Smith, Colorimetric method for determination of sugars and related substances, *Anal. Chem.* 3 (1956) 350–356.
- [24] O. Lowry, N. Rosebrough, A. Faar, R. Randall, Protein measurement with the Folin phenol reagent, *J. Biol. Chem.* 193 (1951) 265–275.
- [25] G.L. Sassaki, P.A. Gorin, L.M. Souza, P.A. Czelusniak, M. Iacomini, Rapid synthesis of partially O-methylated alditol acetate standards for GC-MS: some relative activities of hydroxyl groups of methyl glycopyranosides on purdie methylation, *Carbohydr. Res.* 340 (2005) 731–739.
- [26] R.H. Furneaux, T.T. Stevenson, The xylogalactan sulfate from *Chondria macrocarpa* (Ceramiales, Rhodophyta), *Hydrobiologia* 204 (1990) 615–620.
- [27] I. Ciucanu, F. Kerek, A simple and rapid method for the permethylation of carbohydrates, *Carbohydr. Res.* 131 (1984) 209–217.
- [28] X. Bao, C. Liu, J. Fang, X. Li, Structural and immunological studies of a major polysaccharide from spores of *Gracilaria lucidum* (Fr.) Karst, *Carbohydr. Res.* 332 (2001) 67–74.
- [29] P.E. Janson, L. Kenne, H. Liedgren, B. Lindberg, J. Lonngren, A practical guide to the methylation analysis of carbohydrates, Stockholm, 1976.
- [30] W.C. Raschke, S. Baird, P. Ralph, I. Nakoinz, Functional macrophage cell lines transformed by abelson leukemia virus, *Cell* 15 (1978) 261–267.
- [31] T. Reilly, F. Bellevue, P. Woster, C. Svensson, Comparison of the in vitro cytotoxicity of hydroxylamine metabolites of sulfamethoxazole and dapsone, *Biochem. Pharmacol.* 55 (1998) 803–810.
- [32] H.P. Ramesh, K. Yamaki, T. Tsushida, Effect of fenugreek (*trigonella foenum-graecum* L.) galactomannan fractions on phagocytosis in rat macrophages and on proliferation and IgM secretion in HB4C5 cells, *Carbohydr. Polym.* 50 (2002) 79–83.
- [33] D.D.F. Buchi, W. de Souza, Internalization of surface components during Fc-receptor mediated phagocytosis by macrophages, *Cell Struct. Funct.* 18 (1993) 399–407.
- [34] S.A. Alekseeva, N.M. Shevchenko, M.I. Kusaikin, L.P. Ponomorenko, V.V. Isakov, T. N. Zviagintseva, E.V. Likhoshvai, Polysaccharides of diatoms occurring in lake baikal, *Prikl. Biokhim. Mikrobiol.* 41 (2005) 213–219.
- [35] A.E. Amaral, E.R. Carbonero, R.D.C.G. Simao, M.K. Kadowaki, G.L. Sassaki, C. A. Osaku, P.A.J. Gorin, M. Iacomini, An unusual water-soluble  $\beta$ -glucan from the basidiocarp of the fungus *Ganoderma resinaceum*, *Carbohydr. Polym.* 72 (3) (2008) 473–478.
- [36] D. Chenghua, Y. Xiangliang, G. Xiaoman, W. Yan, Z. Jingyan, X. Huibi, A  $\beta$ -D-glucan from the sclerotia of *Pleurotus tuber-regium* (Fr.) Sing, *Carbohydr. Res.* 328 (2000) 629–633.
- [37] B.W. Vogler, J. Brannum, J.W. Chung, M. Seger, M.C. Posewitz, Characterization of the *Nannochloropsis gaditana* storage carbohydrate: a 1,3-beta glucan with limited 1,6-branching, *Algal Res.* 36 (2018) 152–158.
- [38] C.W. Ford, E.E. Percival, Carbohydrates of *Phaeodactylum tricornutum*, *J. Chem. Soc.* 7042–7046 (1965).
- [39] R. Urbani, E. Magaletti, P. Sist, A. Cicero,  $\beta$ -D-glucans in the induction of cytokine production from macrophages in vitro, *Biol. Pharm. Bull.* 18 (2006) 1320–1327.
- [40] S.E. Harding, M.P. Tombs, G.G. Adams, B.S. Paulsen, K.T. Inngjerdigen, H. Barsett, An Introduction to Polysaccharide Biotechnology, 2nd, CRC Press, 2018, pp. 1–239.
- [41] T.J. Painter, Algal polysaccharides, in: G.O. Aspinall (Ed.), *The Polysaccharides*, 1st 2, Academic Press, 1983, pp. 195–285.
- [42] M. McConville, A. Bacic, A. Clarke, Structural studies of chrysolaminaran from the ice diatom *Stauroneis amphioxys* (Gregory), *Carbohydr. Res.* 153 (1986) 330–333.
- [43] A. Chiviotti, P. Molino, S.A. Crawford, R. Teng, T. Spurck, R. Wetherbee, The glucans extracted with warm water from diatoms are mainly derived from intracellular chrysolaminaran and not extracellular polysaccharides, *Eur. J. Phycol.* 39 (2004) 117–128.
- [44] B.S. Paulsen, S. Mykkestad, Structural studies of the reserve glucan produced by the marine diatom *Skeletonema costatum* (Grev.) Cleve, *Carbohydr. Res.* 62 (1978) 386–388.
- [45] R. Pires Ado, A.C. Ruthes, S.M. Cadena, A. Acco, P.A. Gorin, M. Iacomini, Cytotoxic effect of *Agaricus bisporus* and *Lactarius rufus* b-D-glucans on HepG2 cells, *Int. J. Biol. Macromol.* 58 (2013) 95–103.
- [46] A. Choromanska, J. Kulbacka, N. Rembialkowska, J. Pilat, R. Oledzki, J. Harasym, J. Saczko, Anticancer properties of low molecular weight oat beta-glucan - an in vitro study, *Int. J. Biol. Macromol.* 80 (2015) 23–28.
- [47] P.R. Hussain, S.A. Rather, P.P. Suradkar, Structural characterization and evaluation of antioxidant, anticancer and hypoglycemic activity of radiation degraded oat (*Avena sativa*)  $\beta$ -glucan, *Radiat. Phys. Chem.* 144 (2018) 218–230.
- [48] W. Li, K. Song, S. Wang, C. Zhang, M. Zhuang, Y. Wang, T. Liu, Anti-tumor potential of astragalus polysaccharides on breast cancer cell line mediated by macrophage activation, *Mater. Sci. Eng. C Mater. Biol. Appl.* 98 (2019) 685–695.
- [49] W. Li, X. Hu, S. Wang, Z. Jiao, T. Sun, T. Liu, K. Song, Characterization and anti-tumor bioactivity of astragalus polysaccharides by immunomodulation, *Int. J. Biol. Macromol.* 145 (2020) 985–997.
- [50] R. Wufuer, J. Bai, Z. Liu, K. Zhou, H. Taoerdahong, Biological activity of *Brassica rapa* L. polysaccharides on RAW 264.7 macrophages and on tumor cells, *Bioorg. Med. Chem.* 28 (7) (2020), 115330.
- [51] R. Rutckeviski, C.R. Corso, Y. Román-Ochoa, T.R. Cipriani, A. Centa, F.R. Smiderle, *Agaricus bisporus*  $\beta$ -(1 $\rightarrow$ 6)-D-glucan induces M1 phenotype on macrophages and increases sensitivity to doxorubicin of triple negative breast cancer cells, *Carbohydr. Polym.* 278 (2022), 118917.
- [52] N.A. Razaq, N. Abu, W.Y. Ho, et al., Cytotoxicity of eupatorin in MCF-7 and MDA-MB-231 human breast cancer cells via cell cycle arrest, anti-angiogenesis and induction of apoptosis, *Sci. Rep.* 9 (2019) 1514.
- [53] H. Xu, S. Zou, X. Xu, The  $\beta$ -glucan from lentinus edodes suppresses cell proliferation and promotes apoptosis in estrogen receptor positive breast cancers, *Oncotarget* 8 (2017) 86693–86709.
- [54] W. Qiang, S. Xiaojing, S. Aimin, H. Hui, Y. Ying, L. Li, F. Ling, L. Hongzhi, B-glucans: relationships between modification, conformation and functional activities, *Molecules* 22 (2017) 257–269.
- [55] V.E. Ooi, F. Liu, Immunomodulation and anti-cancer activity of polysaccharide-protein complexes, *Curr. Med. Chem.* 7 (2000) 715–729.
- [56] X. Zhou, X. Liu, L. Huang, Macrophage-mediated tumor cell phagocytosis: opportunity for nanomedicine intervention, *Ad. Funct. Mater.* 31 (2021) 1–18.
- [57] H. Zhang, C. Li, P.F.H. Lai, J. Chen, F. Xie, Y. Xia, L. Ai, Fractionation, chemical characterization and immunostimulatory activity of  $\beta$ -glucan and galactoglucon from *Russula vinosa* Lindblad, *Carbohydr. Polym.* 256 (2021), 117559.
- [58] W.M. Kulicke, A. Lettau, H. Thielking, Correlation between immunological activity, molar mass, and molecular structure of different (1 $\rightarrow$ 3)- $\beta$ -D-glucans, *Carbohydr. Res.* 297 (1997) 135–143.
- [59] M. Okazaki, Y. Adachi, N. Ohno, T. Yadamae, Structure-activity relationship of (1 $\rightarrow$ 3)- $\beta$ -D-glucans in the induction of cytokine production from macrophages in vitro, *Biol. Pharm. Bull.* 18 (1995) 1320–1327.
- [60] M. Moretao, A.R. Zampronio, P.A.J. Gorin, M. Iacomini, M.B.M. Oliveira, Induction of secretory and tumoricidal activities in peritoneal macrophages activated by an acidic heteropolysaccharide (ARAGAL) from the gum of *Anadenanthera colubrina* (angico branco), *Immunol. Lett.* 93 (2004) 189–197.
- [61] G.C. Chan, W.K. Chan, D.M. Sze, The effects of b-glucan on human immune and cancer cells, *J. Hemat. Oncol.* 2 (2009) 25.
- [62] S.S. Ferreira, C.P. Passos, P. Madureira, M. Vilanova, M.A. Coimbra, Structure-function relationships of immunostimulatory polysaccharides: a review, *Carbohydr. Polym.* 132 (2015) 378–396.
- [63] M. Novak, V. Vetricka, Glucans as biological response modifiers, *Endocr. Metab. Immune Disord. Drug Targets* 9 (2009) 67–75.
- [64] L. Legentil, F. Paris, C. Ballet, S. Trouvelot, X. Daire, V. Vetricka, V. Ferrières, Molecular interactions of  $\beta$ -(1 $\rightarrow$ 3)-glucans with their receptors, *Molecules (Basel, Switzerland)* 20 (2015) 9745–9766.
- [65] Y. Jin, P. Li, F. Wang,  $\beta$ -glucans as potential immunoadjuvants: a review on the adjuvanticity, structure-activity relationship and receptor recognition properties, *Vaccine* 36 (2018) 5235–5244.
- [66] X. Zheng, S. Zou, H. Xu, Q. Liu, J. Song, M. Xu, X. Xu, L. Zhang, The linear structure of  $\beta$ -glucan from baker's yeast and its activation of macrophage-like RAW264.7 cells, *Carbohydr. Polym.* 148 (2016) 61–68.
- [67] Y. Yin, X. Zhao, H. Jia Li, X. Jiang, Y. Shan, W. Wang, J. Ma, G.Yu. Hao, A  $\beta$ -glucan from *Durivillaea antarctica* has immunomodulatory effects on RAW 264.7 macrophages via toll-like receptor 4, *Carbohydr. Polym.* 191 (2018) 255–265.

## Supplemental Data



Supplementary figure 1. Metabolic activity determined by MTT test at mouse hippocampal cell line (HT-22) with CAC at 50; 100; 150 and 200  $\mu\text{g.mL}^{-1}$  concentrations in different time points (24, 48 and 72 h). Control corresponds to 100% metabolic activity normalized by the non-treated control. Results are expressed as mean  $\pm$  s.d., three independent experiments in quadruplicate, by ANOVA test. (\*\*\*) Significant differences from control group by post-hoc Tukey test ( $p < 0.001$ ).

#### **4. CHAPTER II – (1→6, 1→3)-β-D-glucan isolated from microalga *Isochrysis galbana* decreases the mitochondrial activity of human glioblastoma cell lines**

Tatiana Rojo Moro<sup>a,c,1</sup>, Marina Trombetta-Lima<sup>c,1</sup>, Asmaa Oun<sup>c</sup>, Melissa van den Veen<sup>c</sup>, Maria Eugênia Rabello Duarte<sup>d</sup>, Sheila M.B. Winnischofer<sup>d,e</sup>, Miguel Daniel Nosedá<sup>\*d</sup>, Amalia M. Dolga<sup>\*c</sup>

<sup>a</sup> *Postgraduate Program in Biochemistry, Biochemistry and Molecular Biology Department, Federal University of Paraná, Av. Cel. Francisco H. dos Santos, 100, CEP 81531-980, PO BOX 19046, Curitiba, Brazil.*

<sup>b</sup> *Biochemistry and Molecular Biology Department, Federal University of Paraná, Av. Cel. Francisco H. dos Santos, 100, CEP 81531-980, PO BOX 19046, Curitiba, Paraná, Brazil.*

<sup>c</sup> *Faculty of Science and Engineering, Department of Molecular Pharmacology, Groningen Research Institute of Pharmacy (GRIP), University of Groningen, 9713 AV Groningen, the Netherlands.*

<sup>d</sup> *Biochemistry and Molecular Biology Dept., Federal University of Paraná, Av. Cel. Francisco H. dos Santos, 100, P.O. Box 19046, Curitiba 81531-980, Paraná, Brazil*

<sup>e</sup> *Department of Cell Biology, Federal University of Paraná, Curitiba 81531-980, Paraná, Brazil*

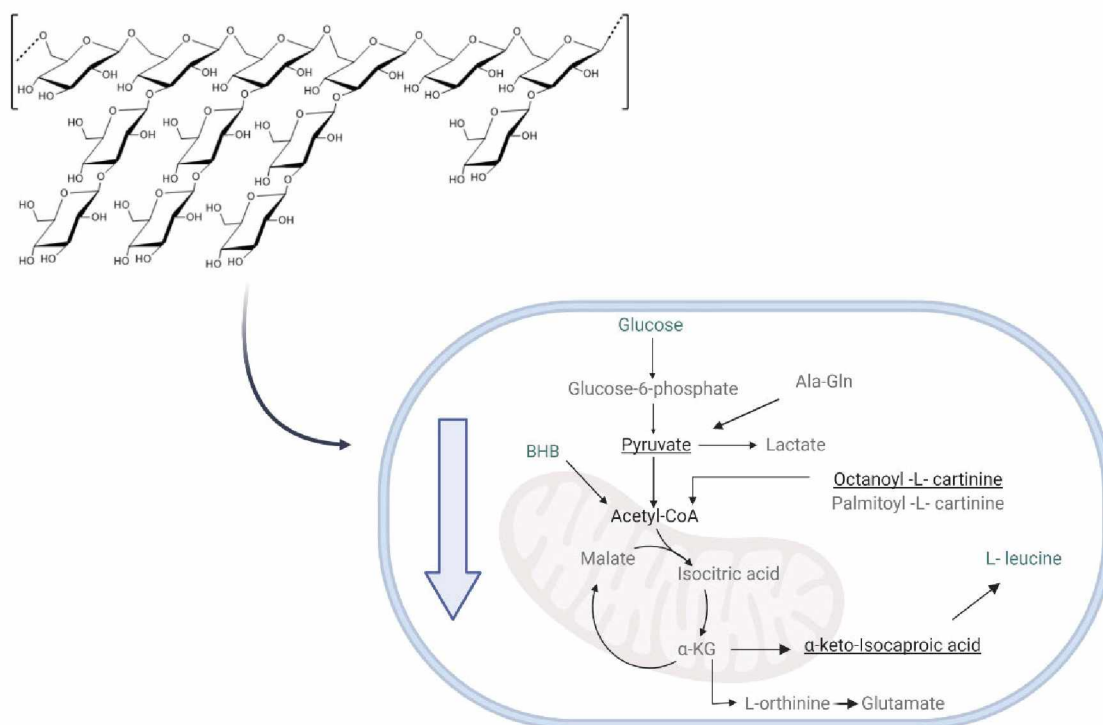
1 These authors equally contributed to this work.

\* Shared senior authorship

**Abstract:** Glioblastoma multiforme is the most aggressive and deadliest type of brain tumor. Even with current therapy, the survival average is less than two years. Therefore, elucidating the molecular pathways that contribute to the pathology of the disease is of paramount importance. Several studies have shown that mitochondrial metabolism is associated with genesis and maintenance of tumorigenicity. In fact, targeting mitochondrial metabolism has been proposed as a strategy to prevent or stop cancer progression. Polysaccharides are natural polymers with the capacity of targeting tumoral cells. Marine microalgae are a biotechnological source for polysaccharides. This work aims to isolate and characterize *Isochrysis galbana* microalgae polysaccharide and investigate its influence on the metabolic activity of two glioblastoma cell lines, U251 and U87 MG. Here we report by NMR, methylation, HPSEC, and ultrafiltration techniques the presence of two fractions (high (<1000 KDa) and low molecular weight (5KDa)), both being a  $\beta$ -D-glucans (1 $\rightarrow$ 6)-linked structure, with branches of (1 $\rightarrow$ 3)-linked in C-3. In-depth analysis of the cell metabolic profile showed that (1 $\rightarrow$ 3,1 $\rightarrow$ 6)- $\beta$ -D-glucan treatment reduces the consumption rate of mitochondrial metabolites without inducing a cytotoxic response. Our study demonstrates that (1 $\rightarrow$ 3,1 $\rightarrow$ 6)- $\beta$ -D-glucan isolated from *Isochrysis galbana* has potential anti-tumoral activity by modulating the mitochondrial metabolism of glioblastoma cells.

**Keywords:** *Isochrysis galbana*;  $\beta$ -glucan; glioblastoma; cell metabolism

## Graphical abstract:



Legend: (1→3,1→6)-β-D-glucan isolated from *Isochrysis galbana* decreases mitochondrial metabolism. At U251 cells, there is a decrease of glucose-6-phosphate, lactate, alanine-glutamine (Ala-Gln), isocitric acid, α-ketoglutaric acid, malate, L-orthinine, glutamate and palmitoyl -L- carnitine substrates (gray color). U87MG cells diminishes glucose, β-hydroxybutyrate (BHB) and L-leucine substrates (cyan color). Pyruvate, α-ketoisocaproic acid and octanoyl-L-carnitine substrates were diminished by both cell lines (underline) Created with [www.BioRender.com](http://www.BioRender.com)

## 1. Introduction

Cancer is a multifactorial disease, being considered one of the biggest public health problems due to its epidemiological, social, and economic magnitude [1]. Glioblastomas (GBM) are the most aggressive and most common form of malignant brain tumor in adults. Despite advances in surgical, radiotherapy, and chemotherapy techniques, the survival range for GBM patients, is in average, 14 months [2, 3]. GBM present dysfunctional mitochondria, showing physiological alterations in membrane potential, hemodynamic (fission and fusion cycles), genes (mitogenic), and apoptosis control [4]. Regarding bioenergetic signaling, GBM display enhanced oxidative stress and undergoes metabolic reprogramming from an oxidative phosphorylation (OXPHOS) profile towards glycolysis. This metabolic shift is also reflected in an alteration in the expression profile of genes involved in the citric acid cycle (TCA) [4]. Mitochondria is involved in all important steps

of the initiation of cancer growth and progression. This organelle produces important intermediates that affect tumor anabolism, control cell homeostasis (redox and calcium balance), gene regulation, and cell death [5]. Therefore, targeting mitochondrial metabolism represents a promising opportunity against cancer progression.

Marine algae and microalgae are promising biotechnological sources of polysaccharides due to their feasible culture conditions and biomass extraction. Although there was an increase in identifying and exploring novel molecules with biological activity (such as terpenes or peptides) isolated from marine organisms (including Porifera, bacteria, and macroalgae) in the last 28 years [6], studies exploring polysaccharides from marine microalgae with biological activities are still scarce [7].

Polysaccharides of different origins have been shown to display different biological activities, such as immunomodulation, anticoagulant, angiogenic, antiviral, antivenom, and antitumoral. [8-12]. Previous studies with marine algae polysaccharides (fucans, ulvans, galactans, among others) showed interference in cell viability affecting cell metabolism [13-15]. The present study describes the extraction, and structural characterization of the (1→3,1→6)-β-D-glucan purified from the marine microalga *Isochrysis galbana* and evaluates its metabolic activity in the human GBM cell lines U251 and U87MG.

## 2. Material and methods

### 2.1 Microalgae strain, culture maintenance, and biomass formation

The *I. galbana* microalga strain was obtained from the Aidar and Kutner Microorganism Bank (BMAK - Collection of Marine Microalgae - University of São Paulo, Brazil) and cultivated at the Microalgae Biotechnology Laboratory (LABMA, Federal University of Paraná, Brazil) with batch cultures. Microalgae inoculum was maintained in sterilized f/2 culture medium [16] with the addition of 35 g.L<sup>-1</sup> of artificial marine salt Salinity® (Aquavitro, Madison, GA, USA), under continuous compressed air supply (0.25 vvm without supplementary CO<sub>2</sub>) and, pH adjusted to 8.0. The cultures were grown and maintained individually in 2,000 mL flasks at 23 ± 1 °C under a 12:12 light/dark cycle (155 μmol m<sup>-2</sup> s<sup>-1</sup>). Biomass formation was downstreamed until the number of cells reached the stationary phase (9 days). Cell growth measurements were carried out by cell counting in a Neubauer hemocytometer by optical microscopy. For the final obtainment of biomass, microalgae suspension was isolated from the culture medium by Novatecnica

centrifuge (Piracicaba, SP, BR) at 2,600 x G, for 20 min at 4 °C. The precipitate (biomass) was separated from the supernatant and then freeze-dried.

## 2.2 *Extraction, purification, and fractioning of Isochrysis galbana polysaccharides*

Freeze-dried biomass of microalgae *Isochrysis galbana* was solubilized in distilled water (2.0 g %) and subjected to aqueous extraction for 2 h at 80 °C, under mechanical agitation. After extraction, the solution was centrifuged at 2.607 G for 20 min, whereas the supernatant of the extract was separated, and the residue was frozen and lyophilized. Three volumes of cold ethanol were added with the supernatant, forming a precipitate and isolated by centrifugation at 2.607 G for 15 min at 4 °C. The residue was resolubilized in water, dialyzed against distilled H<sub>2</sub>O, and later in ultrapure H<sub>2</sub>O in a membrane with an exclusion limit of 6-8 KDa and lyophilized to obtain *Isochrysis* aqueous extract (termed in the manuscript IAQ).

For the fractioning of polysaccharides present in native fractions, centrifugation and ultrafiltration were performed on membranes of 1,000, 500, 300, 100, 30, 10, and 5 KDa (Spectra/Por Repligen – Boston, MA, USA and Merck Millipore - Burlington, MA, USA). The centrifugation process was performed with 10.410 G for 20 min at 4 °C. Ultrafiltration procedures were performed using a SARTORIUS filtration system model 16249 (Göttingen, DE), coupled with a compressed air cylinder. In this method, polysaccharides were solubilized in water at a concentration of 1 mg. mL<sup>-1</sup> and subjected to cylinder filtration. Ultrafiltered material was lyophilized and stored in a dissector.

## 2.3 *Biochemical analyses*

Total carbohydrate content was estimated by phenol-sulfuric methodology (CH<sub>6</sub>H<sub>5</sub>OH 99.0-100.5%, and H<sub>2</sub>SO<sub>4</sub>, 95-97% - Merck) [17] and quantified spectrophotometrically using a standard glucose curve, while protein content was measured using Folin-Ciocalteu reagent with bovine serum albumin (BSA, ≥99% - Sigma-Aldrich) as standard [18]. According to Dodgson and Price [19] and Filisetti-Cozzi and Carpita [20], sulfate and uronic acid contents were determined, respectively.

Monosaccharide composition of polysaccharide samples was performed with 1 mL of 2 M trifluoroacetic acid (TFA 99% – Sigma Aldrich - St. Louis, MO, USA) at 120 °C for

2 h [21]. Hydrolysis products were reduced with sodium borohydride ( $\text{NaBH}_4 \geq 98\%$  - Sigma Aldrich) for 12 h. Excess  $\text{NaBH}_4$  was converted into boric acid by adding acetic acid to pH 5. Then boric acid was eliminated by 4x co-distillation with methanol ( $\text{MeOH}$ , 99% - Alphatec Cachoerinha, RS, BR). After acetylation with acetic anhydride (1 mL, for 1 h at 120 °C), the resulting alditol acetate derivatives were analyzed by Gas Chromatography-Mass Spectrometry (GC-MS). GC-MS analyses were performed using an Agilent Varian 3800 chromatograph (Santa Clara, CA, USA), equipped with a fused silica capillary column (30m x 0.25mm) coated with DB-225ms (Durabond) and a Varian Saturn 2000 R ITD spectrometer. The chromatograph ran at 50 °C for 1 min, then 50 – 215 °C at 40 °C.  $\text{min}^{-1}$ , using helium as carrier gas at 1 mL.  $\text{min}^{-1}$ .

#### 2.4 Methylation

Methylation of *Isochrysis* aqueous extract was performed according to Ciucanu and Kerek [22]. Samples were dissolved in 1 ml of dimethyl sulfoxide ( $\text{DMSO}$ ,  $\geq 99\%$  - Merck - Kenilworth, NJ, USA), and ~30 mg, of Sodium hydroxide ( $\text{NaOH}$ , 99% - Alphatec) was added. After 30 min stirring (at 25 °C), 0.2 mL of iodomethane ( $\text{CH}_3\text{I}$ ,  $\geq 99\%$  - Sigma Aldrich) was added. The reaction proceeded twice more, as described above. The reaction was interrupted by the addition of distilled water and neutralized with glacial acetic acid ( $\text{AcOH}$ ,  $\geq 99\%$  - Merck). Products were dialyzed and freeze-dried. Partially methylated alditol acetates were generated by hydrolysis using 90% formic acid (0.5 mL) for 6 h at 100 °C as described by Bao *et al.* (2001) for glucans followed by  $\text{NaBDH}_4$  reduction and acetylation. Products were analyzed by GC-MS and identified by their electron impact mass spectra and retention times [21, 23] using SHIMADZU gas chromatograph, model 2010-plus with AOC 5000 plus auto-sampler, coupled to a SHIMADZU mass spectrometer, model T08040 (Kyoto, JP). This equipment is fused with silica capillary column (30 m x 0.25 d.i) model SH-Rtx-5MS, SHIMADZU. Injector temperature was 250 °C, and the initial temperature was 100 °C, followed by a gradual increase of 10 °C per min, until reaching 210 °C for alditol acetates partially methylated, remaining constant after 25 and 30 min, respectively. The carrier gas used was helium, with a flow of 1 mL.  $\text{min}^{-1}$ . Mass spectra were obtained by electron impact at 70 meV, repeating every 1/10 of a second, and with a mass/charge ratio ( $m/z$ ) of 90 to 220. Chromatograms were analyzed, and peak areas of interest were determined by integration, using software Lab solutions GCMS solution post-run analysis 4.20 (SHIMADZU).

### *2.5 High-pressure size exclusion chromatography (HPSEC) analysis*

Analysis was performed using 1 mg. mL<sup>-1</sup> of polysaccharide solution and a Waters high-performance size exclusion chromatography (HPSEC) apparatus coupled to a differential refractometer (RI) and a Wyatt Technology Dawn-F multi-angle laser light scattering (MALLS) detector adapted online (Santa Barbara, CA, USA). Four Waters Ultrahydrogel columns (2000, 500, 250, and 120) (Santa Barbara, CA, USA) were connected in series and coupled with multi-detection equipment. A 0.1 M NaNO<sub>3</sub> solution containing NaN<sub>3</sub> (0.5 g. L<sup>-1</sup>) was used as an eluent. The value of molar weight was determined by molecular mass distribution (Mw). HPSEC data were collected and analyzed by the Wyatt Technology ASTRA program (Santa Barbara, CA, USA). All experiments were carried out at 25 °C.

### *2.6 Nuclear Magnetic Resonance (NMR) spectroscopy*

Nuclear magnetic resonance analyzes (NMR-<sup>13</sup>C, NMR-<sup>13</sup>C-DEPT, NMR-<sup>1</sup>H, <sup>13</sup>C / <sup>1</sup>H HSQC) were performed on a BRUKER spectrometer, model DRX 400, series Avance (Billerica, MA, USA), at 70 °C temperature. Samples dissolved in Dimethyl sulfoxide-d<sub>6</sub> (DMSO-d<sub>6</sub>, 99.9%, Sigma-Aldrich) had spectra calibrated with the solvent peak at 39.51 and 2.50 ppm for <sup>13</sup>C and <sup>1</sup>H, respectively. <sup>13</sup>C NMR and <sup>13</sup>C DEPT NMR spectra were obtained using the base frequency of 100.61 MHz, with a signal acquisition interval of 0.6 seconds, made from 4.000 - 70.000 acquisitions, using an interval of 0.1 seconds between wrists. <sup>1</sup>H NMR spectra were obtained at a base frequency of 400.13 MHz. HSQC spectra (Heteronuclear Single Quantum Correlation Spectroscopy) were obtained using a heteronuclear technique, which allows determining which hydrogen atoms (<sup>1</sup>H) are attached to the respective carbon atoms (<sup>13</sup>C) from known <sup>13</sup>C or <sup>1</sup>H signals already determined. Acquisition parameters were carried out using the pulse programs supplied with the Bruker manual. The data were analyzed using Topspin 4.0.5 (Bruker).

## 2.7 Cell culture and treatment

U87MG and U251 human glioblastoma cells were kindly provided by Prof. Dr. Frank Kruyt (University of Groningen). The cells used in our study had a passage number between 30 and 50. Cells were cultivated in DMEM supplemented with 10 % fetal bovine serum (Gibco - Amarillo, TX, USA), penicillin at 100 U. mL<sup>-1</sup> (Sigma-Aldrich), and streptomycin 100 µg. mL<sup>-1</sup> (Sigma-Aldrich), and maintained at 37 °C with 5 % CO<sub>2</sub>.

In order to evaluate the impact of (1→3,1→6)-β-D-glucan treatment on GBM cells, 4000 cells/ p96 well were seeded and treated with different concentrations of the polysaccharide following 24 h of culturing. Cells were treated with (1→3,1→6)-β-D-glucan in the range of 50 to 200 µg. mL<sup>-1</sup>, for 24, 48, or 72 h. Polysaccharides samples were dissolved in PBS buffer (5 mg mL<sup>-1</sup>, pH = 7), filtered (0.22 µm) and stored (-20 °C) until use.

## 2.8 Metabolic activity assay

Cell metabolic activity was evaluated using 3- [4,5-dimethylthiazol-2-yl]- 2,5 diphenyl-tetrazolium bromide (MTT) (Sigma – Aldrich) according to Reilly, Bellevue, Woster and Svensson [24]. Absorbance at 570 and 630 nm was determined using the Bio-Tek Synergy H1 hybrid plate reader by BioTek (Winooski, VT, USA). Control cells (treated with PBS vehicle) represents 100% of the cell metabolic activity. Each treatment had 4 technical replicates, and was repeated at least three times with cells at different passage numbers.

## 2.9 Cell cycle analysis

Cells were treated with 100 µg. mL<sup>-1</sup> (1→3,1→6)-β-D-glucan for 72 h. Cells were fixed in PFA 4% for 15 min on ice. Next, the cells were washed with PBS and stained with DAPI (C<sub>16</sub>H<sub>15</sub>N<sub>5</sub> · 2HCl, >90% - Sigma-Aldrich) at 1µg. mL<sup>-1</sup> in PBS and 0.01 % TRITON<sup>™</sup>-X-100 (*t*-Oct-C<sub>6</sub>H<sub>4</sub>-(OCH<sub>2</sub>CH<sub>2</sub>)<sub>x</sub>OH, x= 9-10- Sigma-Aldrich) on ice for 30 min in the dark. Fluorescence was measured in Beckman Coulter CytoFLEX S Flow Cytometer (Beckman Coulter, Woerden, The Netherlands) and analyzed with FlowJo 10.5 software from BD life Sciences (Ashland, CA, USA).

### *2.10 Cell death analysis*

Cells were treated with 100  $\mu\text{g. mL}^{-1}$  (1 $\rightarrow$ 3,1 $\rightarrow$ 6)- $\beta$ -D-glucan for 72 h and afterwards stained with the Dead cell apoptosis kit with Annexin V and PI followed by analysis using flow cytometry (Invitrogen Thermo Fisher – Waltham, MA, USA) according to the manufacturer's instructions. Fluorescence was measured in Beckman Coulter CytoFLEX S Flow Cytometer and analyzed with FlowJo 10.5 software of BD Life Sciences (Franklin Lakes, NJ, USA).

### *2.11 Mitoplate assay*

The consumption of different metabolic intermediates was determined using the MitoPlate-S1 assay (BIOLOG INC., Hayward, CA, USA). The MitoPlate-S1 hydration was performed in the presence of 25  $\mu\text{g. mL}^{-1}$  saponin according to the manufacturer's instructions. Cells were treated with 100  $\mu\text{g. mL}^{-1}$  (1 $\rightarrow$ 3,1 $\rightarrow$ 6)- $\beta$ -D-glucan for 24 h, detached and seeded (75000 cells/ well) to the MitoPlate-S1. Absorbance was measured at 590 nm and 750 nm every 15 min for 3 h using Bio-Tek Synergy H1 hybrid plate reader. The substrate consumption profile in each metabolic pathway was analyzed by comparing the non-treated cells (depicted as control condition) with treated cells.

### *2.12 Statistical analyses*

Shapiro-Wilk normality test was used to verify the data distribution. For parametrical data, significant differences were determined using one-way analysis of variance (ANOVA) followed by Tukey's post-hoc test. For non-parametrical data, Mann-Whitney U test was used. Data with  $p < 0.05$  were considered statistically significant. All graphs were created using GraphPad - Prism 8.0.1 from GraphPad Software Inc. (San Diego, CA, USA).

### 3. Results and discussion

#### 3.1 $\beta$ -D-Glucan characterization from *I. galbana*

The polysaccharide sample ( $\beta$ -D-Glucan) from *I. galbana*, named in this study IAQ, was extracted and purified as reported in the methods section. IAQ was evaluated by the HPSEC-MALLS analysis to determine chromatogram and molar mass distribution (**Fig. 1a** and **b**), and this analysis rendered a heterogeneous profile. From 30 - 40 min of the assay, IAQ extract analysis showed a small fraction with a molar mass varying between  $1.88 \times 10^{+5}$  -  $1.37 \times 10^{+9}$  g.mol<sup>-1</sup>. At 42-60 min of the assay, the compound showed that a large fraction of the compound had a molar mass varying between  $5.16 \times 10^{+2}$  -  $1.36 \times 10^{+8}$  g.mol<sup>-1</sup>. Based on this analysis, IAQ molecular weight average was estimated as  $6.4 \times 10^{+4}$  g.mol<sup>-1</sup> (**Fig. 1b**). <sup>13</sup>C and <sup>13</sup>C-DEPT NMR analyzes were also performed (**Figs. 1c** and **d**). The analysis of the corresponding spectrum demonstrated the presence of 2 signals at 103.9 and 102.7 ppm, indicating two anomeric carbons in different chemical environments, which were attributed to  $\beta$ -D-glucopyranose units. In addition, (1 $\rightarrow$ 3) binding was observed at 87.8 and 87.1 ppm signals, while in the range of 72.2 to 68.3 ppm, signals referred to carbons 2, 4, and 5 of the ring. In <sup>13</sup>C-DEPT NMR spectrum (**Fig. 1d**), we could observe an inversion of signals in 61.0 ppm of -CH<sub>2</sub>, demonstrating the presence of free C-6. Additionally, the presence of (1 $\rightarrow$ 6) bond was determined in 68.6 ppm, where the carbon 6 substitution occurs.

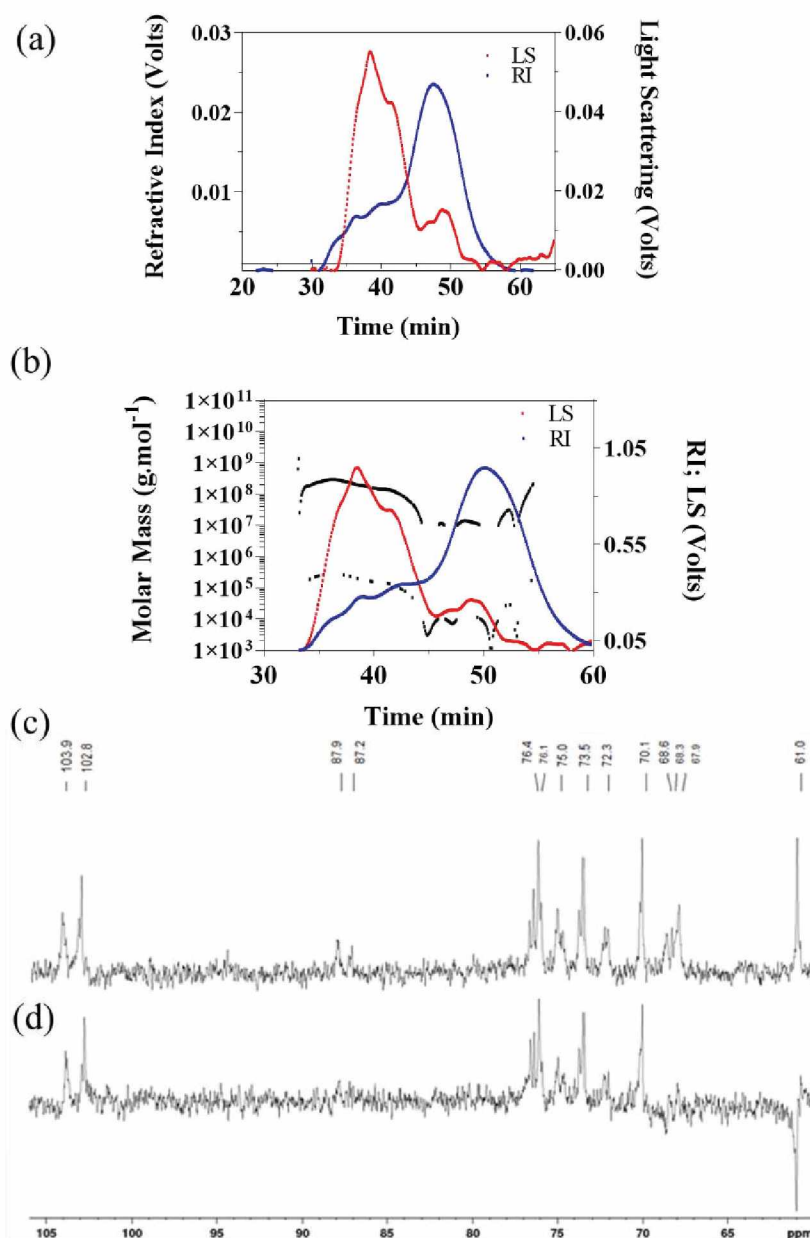


**Fig. 1** Elution profile of the polysaccharide isolated from *I. galbana* IAQ using HPSEC MALLS analysis, obtained with a light scattering (LS) and refractive index (RI) detector (a). Molar mass distribution of IAQ using HPSEC (b).  $^{13}\text{C}$  NMR spectrum (c) and  $^{13}\text{C}$  NMR DEPT spectrum of crude extract IAQ and (d) solvent  $\text{DMSO-d}_6$ , at  $70^\circ\text{C}$ .

To better identify the molecule, two-dimensional analysis of HSQC  $^{13}\text{C}$ - $^1\text{H}$  was performed, shown in **Fig. S1**. In this two-dimensional spectrum, it was observed that there are two correlations in 103.9/4.38 and 102.7/4.24 ppm corresponding to C-1 at low and relatively high frequency for H-1, confirming  $\beta$  position. Correlations at 61.0/3.70 and 61.0/3.50 ppm correspond to the C-6/H-6 and C-6/H-6' of the glucose units not replaced in C-6 and other correlations in 76.1/3.25 and 76.4/3.16 ppm referring to C/H of the ring. **Table 1** below shows chemical shifts of  $\beta$ -D-glucan with (1 $\rightarrow$ 3) - and (1 $\rightarrow$ 6) binding.

**Table 1.**  $^{13}\text{C}$  NMR assignments of polysaccharide IAQ isolated from *I. galbana*.

Polysaccharide	$^{13}\text{C}$ chemical shifts (ppm)						
	C1	C2	C3	C3'	C4	C5	C6
$\beta$ -Glucan (1 $\rightarrow$ 3)	102.8	72.2	87.9	87.2	68.3	76.1	61.0
$\beta$ -Glucan (1 $\rightarrow$ 6)	103.9	73.5	76.4	-	70.1	75.0	68.6

Solvent:  $\text{Me}_2\text{SO}d_6$ , temperature: 80 °C.

As the heterogeneous IAQ sample profile was demonstrated by the HPSEC-MALLS analysis and NMR signals, the IAQ sample was submitted to a centrifugation process to purify the sample and termed IAQ-c (IAQ centrifuged). HPSEC-MALLS analysis of IAQ-c has been performed once again (**Fig. 2a**). The chromatogram of IAQ-c retains the heterogeneous profile as observed for the extract IAQ alone. Regarding chemical characterization of obtained IAQ-c fraction (**Table 2**), it is observed that the centrifugation process provided a higher percentage in carbohydrate content and showing an increase by about two times when compared to the initial fraction, followed by contents of sulfate, proteins, and uronic acids.

**Table 2.** Yield, chemical analyses, and monosaccharide composition of polysaccharide fractions obtained from diatom *I. galbana*.

Sample <sup>a</sup>	Carbohydrate (%)	Protein (%)	Monosaccharides (mol%)						
			Glc	Rha	Xyl	Ara	Gal	Man	Fuc
IAQ	36.7	11.6	68.2	1.2	3.8	9.0	9.1	6.7	1.9
IAQ-c	68.3	13.2	87.6	1.0	6.5	-	3	-	1.9

<sup>a</sup>Fractions are defined in the text. <sup>b</sup>Percentage based on dried microalgae biomass. - Not detected.

Next, IAQ-c was analyzed by  $^{13}\text{C}$  NMR and HSQC (**Figs. 2b** and **c**) to compare signals that would appear in this fraction compared to the native one. As observed in the  $^{13}\text{C}$  spectrum (**Fig. 2b**), most signals had the same profile as those initially characterized (**Fig. 1c**), with only differences of 68.6 and 68.3 ppm signals that were no longer present. In

the HSQC spectrum (Fig. 2c), the same signal correlations presented in Table 1 were observed.

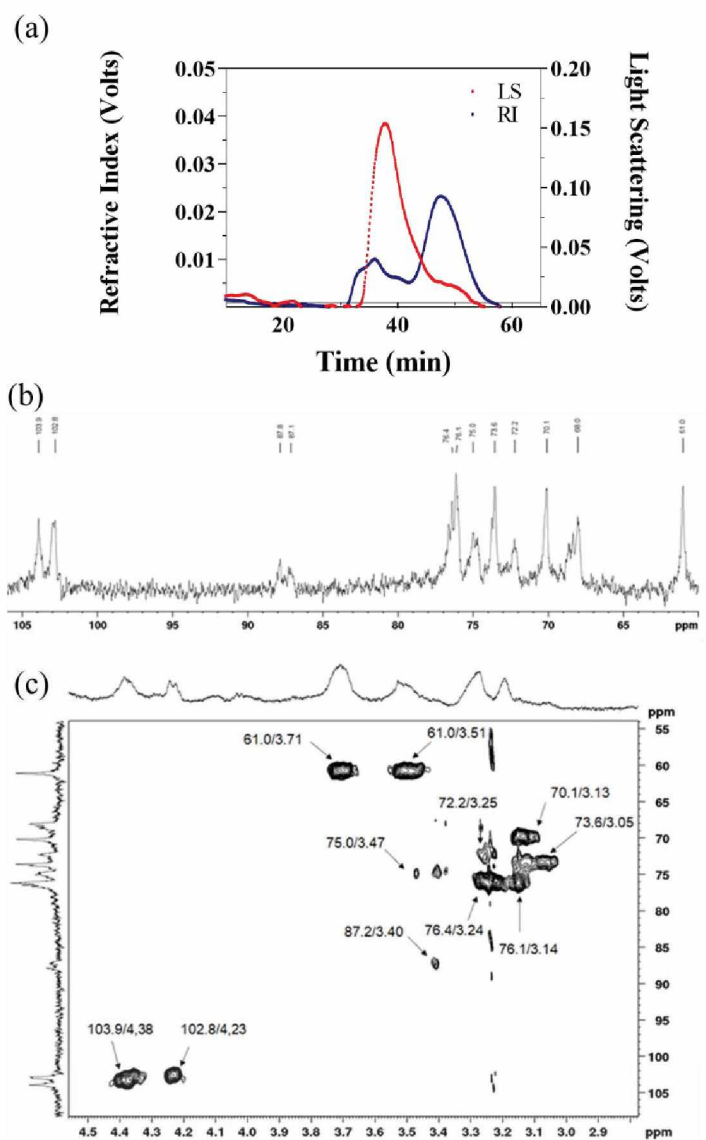


**Fig. 2** Elution profiles of IAQ-c using HPSEC-MALLS-RI (a).  $^{13}\text{C}$  NMR spectrum (b) and HSQC correlation spectrum of fraction IAQ-c (c). DMSO- $d_6$ , 70 °C.

Based on the analysis of IAQ-c rendering a heterogeneous profile, we further performed fractionation by ultrafiltration with membranes of 1.000, 500, 300, 100, 30, 10, and 5 kDa to obtain homogeneous fractions. Fractions retained at 1.000 Kda (high molecular weight - HMW) and retained at 5 Kda, (low molecular weight - LMW) showed the highest yields (41.5 and 21.7 %, respectively). Retained samples in 500, 300, 100, 30, and 10 kDa showed a low yield (1.4; 1.5; 2.2; 0.9 and 3 % respectively), so further HPSEC and NMR analyzes were not performed. For HMW and LMW fractions, HPSEC-MALLS

analysis was performed again to verify the purity of the novel compounds (Figs. 3a and 4a).

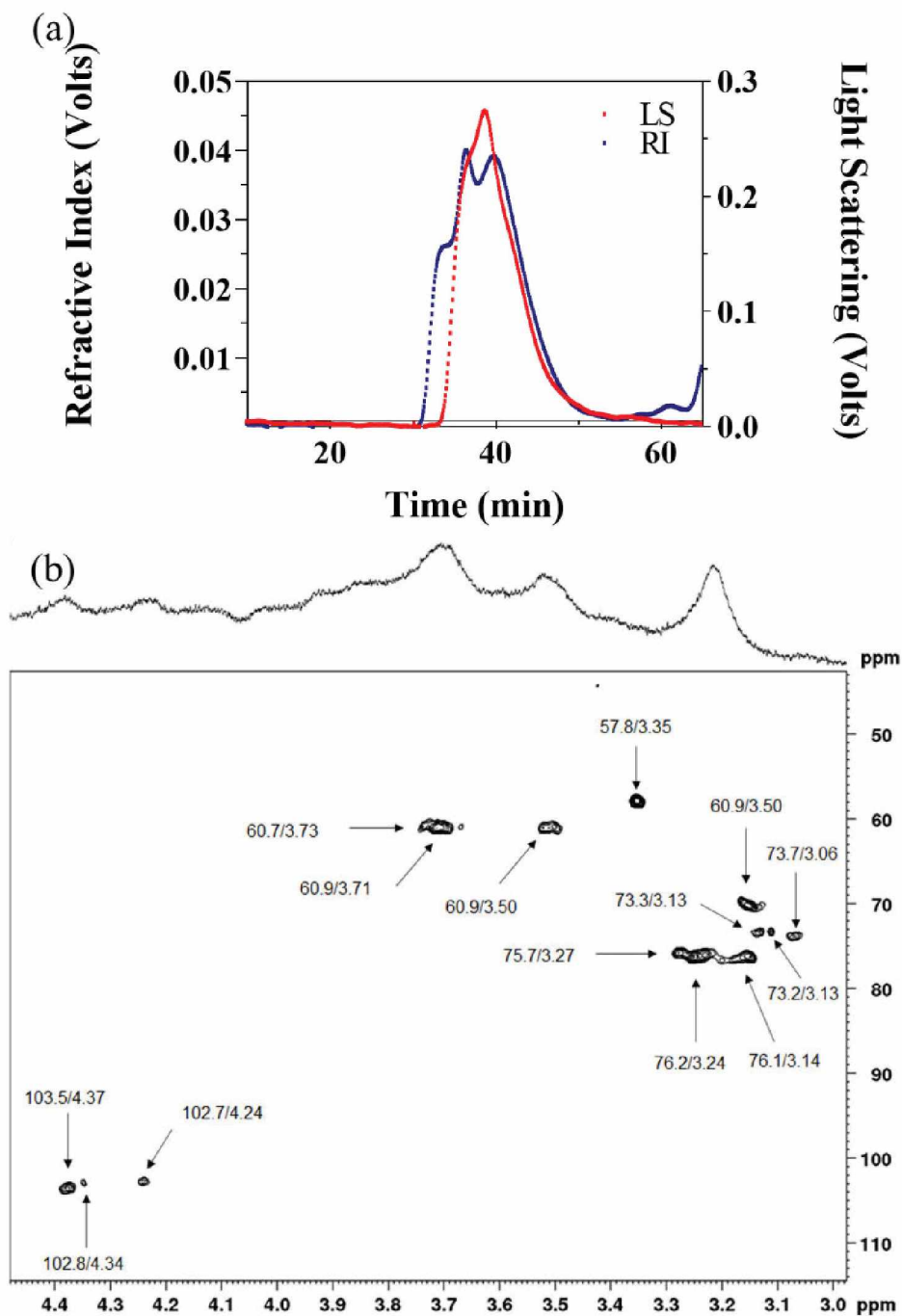


**Fig. 3** Elution profile of HMW using HPSEC-MALLS-RI (a). HSQC correlation spectrum of fraction HMW (b). DMSO- $d_6$ , 70 °C.

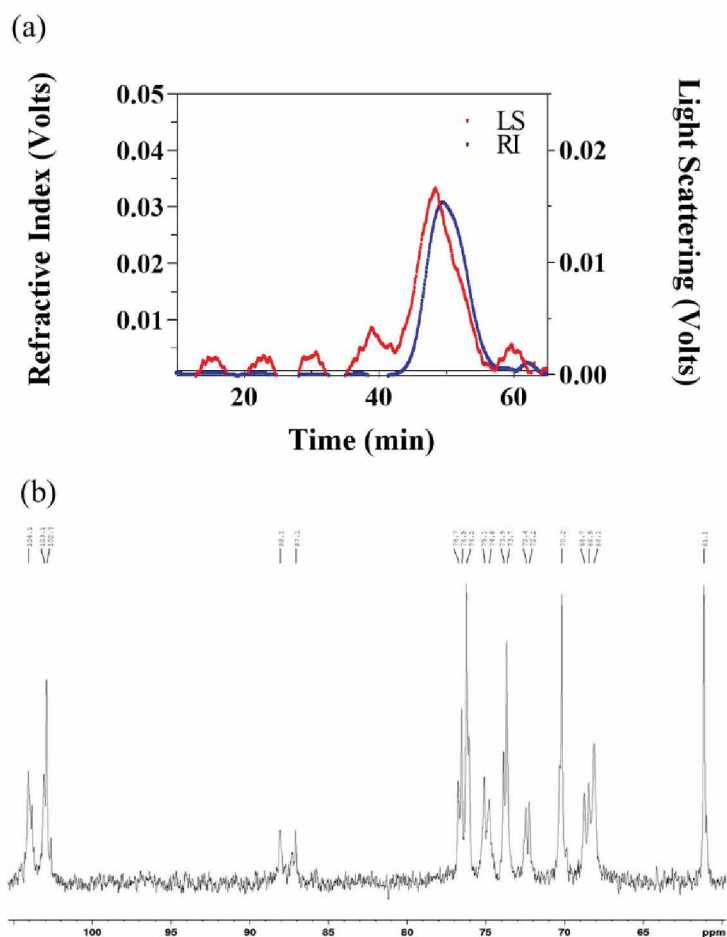


**Fig. 4** Elution profile of LMW using HPSEC-MALLS-RI (a). HSQC correlation spectrum of fraction LMW (b). DMSO- $d_6$ , 70 °C. (c)

Next, monosaccharide composition, NMR, and methylation analyses of the fractions HMW and LMW were performed. Those fractions contain a high percentage of glucose (**Table 3**). In the two-dimensional NMR spectrum of HMW (**Fig. 3b**), we further corroborated the initial findings, showing the same signals in the anomeric region (103.5, 102.8, and 102.7 ppm), ring region (73.3 - 76.2 ppm), and free C6 (60.9 and 60.7 ppm). In  $^{13}\text{C}$  and HSQC spectra of LMW fraction (**Figs. 4b** and **S2**), the pattern was more complex, containing similar signals as in the initial analysis and additional new signals (see **Table 4**).

**Table 3.** Monosaccharide composition (%) of polysaccharide ultrafiltration fractions obtained from *I. galbana*.

Sample <sup>a</sup>	Monosaccharides (mol%)							
	Glc	Rha	Xyl	Ara	Gal	Man	Fuc	Rib
HMW	50.7	3.8	16.4	-	6.8	18.0	4.0	-
LMW	94.1	0.2	0.9	1.6	2.2	1.0	0.2	-

- Not detected <sup>a,b</sup> Fractions are defined in the text.

**Table 4.** <sup>13</sup>C NMR assignments of polysaccharide IAQ<sup>a</sup>, IAQ-c<sup>b</sup> and ultrafiltered fraction (<sup>c</sup>HMW and <sup>d</sup>LMW) in Me<sub>2</sub>SO<sub>4</sub>-d<sub>6</sub>.

Polysaccharide	<sup>13</sup> C chemical shifts (ppm)						
	C1/H1	C2/H2	C3/H3	C3'	C4/H4	C5/H5	C6/H6
<b>β-Glucan (1→3)</b> <sup>a</sup>	102.8	72.2	87.9	87.2	68.3	76.1	61.0
<b>β-Glucan (1→3)</b> <sup>b</sup>	102.8	72.2	87.8	87.1	68.0	76.1	61.0
<b>β-Glucan (1→3)</b> <sup>c</sup>	102.7/102.8	73.2/73.3	-	-	-	76.1	60.9
<b>β-Glucan (1→3)</b> <sup>d</sup>	102.9	72.2/72.4	88.1	87.1	68.2/68.1	76.2	61.1
<b>β-Glucan (1→6)</b> <sup>a</sup>	103.9	73.5	76.4	-	70.1	75.0	68.6
<b>β-Glucan (1→6)</b> <sup>b</sup>	103.9	73.6	76.4	-	70.1	75.0	-
<b>β-Glucan (1→6)</b> <sup>c</sup>	103.5	73.7	76.2	-	-	75.7	-
<b>β-Glucan (1→6)</b> <sup>d</sup>	103.1/104.1	73.7/73.9	76.5/76.7	-	70.2	75.1/74.8	68.7/68.5

For a better structural determination of these IAQ-related molecules, methylation technique was performed on all the fractions, IAQ native, HMW, and LMW. Results are presented in **Table 5**. Methylation for all fractions confirmed that the structure of the polymer is composed of glucose units as non-reducing terminals (NRT) and glucose units

(1→6) -linked, (1→3) - (1→6) -linked, and (1→3)-linked. The highest percentage of (1→3) - (1→6) -linked units is connected to the native polysaccharide. HMW and LMW presented more (1→6)-links than (1→3) -links. NRT linkage was further enhanced during the fractioning process.

**Table 5** - Methylation analysis of polysaccharide obtained from *I. galbana*

Derivative <sup>a</sup>	Deduced linkage	IAQ <sup>b</sup>	HMW <sup>b</sup>	LMW <sup>b</sup>
2,3,4,6-Me <sub>4</sub> -Glc	Glc <sub>p</sub> -(1→	2.1	12.5	34.8
2,4,6-Me <sub>3</sub> -Glc	→3)-Glc <sub>p</sub> -(1→	8.5	15.5	7.5
2,3,4-Me <sub>3</sub> -Glc	→6)-Glc <sub>p</sub> -(1→	55.0	50.0	48.6
2,4-Me <sub>2</sub> -Glc	→3,6)-Glc <sub>p</sub> -(1→	34.4	22.0	9.1

<sup>a</sup>2,3,4,6-Me<sub>4</sub>-Glc analyzed as 1,5-di-*O*-acetyl-2,3,4,6-*O*-methyl glucitol, etc. <sup>b</sup> mol% of monosaccharide quantified in the form of partially methylated alditol acetate, analyzed by GC-MS.

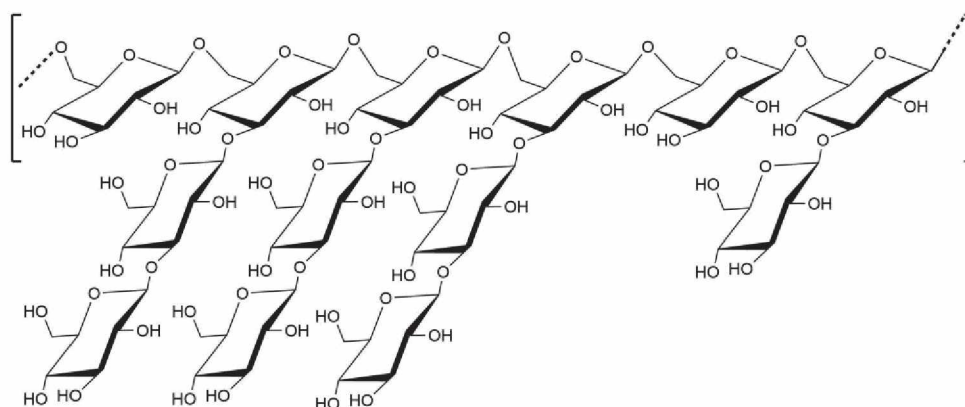


**Fig. 5** Proposed structure for *I. galbana* extracted polysaccharide.

The native extract IAQ is a  $\beta$ -D-glucan, presenting two molecular fractions with high molecular weight (above 1000 KDa) and another between 10-5KDa. The proposed structure is presented in Fig 5. (1→6)-linked  $\beta$ -D-glucans backbone with (1→3), (1→6) branches are often found in mushrooms, presenting diverse biological effects, as showed by Pires Ado, Ruthes, Cadena, Acco, Gorin and Iacomini [25], Abreu, Simas, Smiderle, Sovrani, Dallazen, Maria-Ferreira, Werner, Cordeiro and Iacomini [26], Palacios, Garcia-Lafuente, Guillamon and Villares [27]. Brown algae present  $\beta$ -D-glucans as reserve polysaccharides, often with (1→3)-linked backbone [28-30].

Regarding marine microalgae polysaccharides, Sadovskaya and colleagues (Sadovskaya, Souissi, Souissi, Grard, Lencel, Greene, Duin, Dmitrenok, Chizhov, Shashkov and Usov [31]) worked with *Isochrysis galbana*. Our study corroborates the native structure by NMR and methylation analysis, while the size-exclusion chromatography (SEC) data shows a different profile. Our HPSEC-MALLS data already presents a heterogeneous profile (with high and low molecular weight fractions) from the native polysaccharide, and Sadovskaya, Souissi, Souissi, Grard, Lencel, Greene, Duin, Dmitrenok, Chizhov, Shashkov and Usov [31] show a homogeneous profile. Polysaccharides are polydisperse molecules because the molecular mass can differ once they are synthesized. Molecular mass conditions are responsible for their properties and behavior, and any degradation can modify those characteristics. Therefore, it is essential to investigate and determine those distributions. The SEC technique fractionates by their size but not by their molecular weight. Thus, the multi-angle laser technique (MALLS) coupled with HPSEC allows verifying the molar mass weight average in each elution volume of the chromatogram. For  $\beta$ -glucans, HPSEC is the prevailing technique used [32]. This method is used to analyze the marine microalgae polysaccharides extracted from *Isochrysis galbana* can explain the data differences.

Sadovskaya et al. (2014) obtained the high and low fractions after the Smith-controlled reaction. This reaction has the purpose of modifying the polysaccharide structure to elucidate more precisely the chemical structure. It excludes the branches of the polysaccharides from the main chain, also causing a decrease in the polymer's molecular weight [33]. Any reaction able to modify the real structure can directly affect the chemical-physical properties of the polymer. For example, cellulose is a  $\beta$ -glucan (1 $\rightarrow$ 4) linked, and modification of their chain length directly affects the product properties [32].

### 3.2 *Biological activity of polysaccharide extracted from I. galbana*

#### 3.2.1 *$\beta$ -D-glucan suppresses NADH mediated metabolism.*

To evaluate the impact of *I. galbana* extracts (native, HMW, and LMW) treatment on tumoral and normal cells, we performed a kinetic of 24, 48, and 72 h of treatment with 50, 100, 150, and 200  $\mu\text{g. mL}^{-1}$ . We investigated the effects on the metabolic activity of two tumoral cell lines, namely U251 and U87MG, and one non-tumoral neuronal cell line, hippocampal-derived HT22. The cell metabolic activity was evaluated by MTT

assay. Interestingly, native and HMW fractions mediated an alteration of the cell metabolism of U251 cells after 24 h (**Figs. 6d, e, f** and **7d, e, f**). While LMW only presented a small decrease at 48 and 72 h (**Fig. S3d, e, f**). In contrast, U87MG cells only displayed metabolic alterations at 72 h following treatment without a clear dose-dependent effect (**Figs. 6c** and **7c**). HT22 cell line did not show alterations with any fractions (**Fig. S4**). A similar effect between various molecular fractions of polysaccharides is also described by Choromanska, Kulbacka, Harasym, Oledzki, Szewczyk and Saczko [34]. A  $\beta$ -D-glucan with a high molecular weight from oat reduced 30 to 40 % cell metabolic activity. The polysaccharides with low molecular weight reduced 20% cell metabolism in two human epithelial lung cancer cell lines. Those analyzed fractions did not affect normal cells, similarly to the present study.

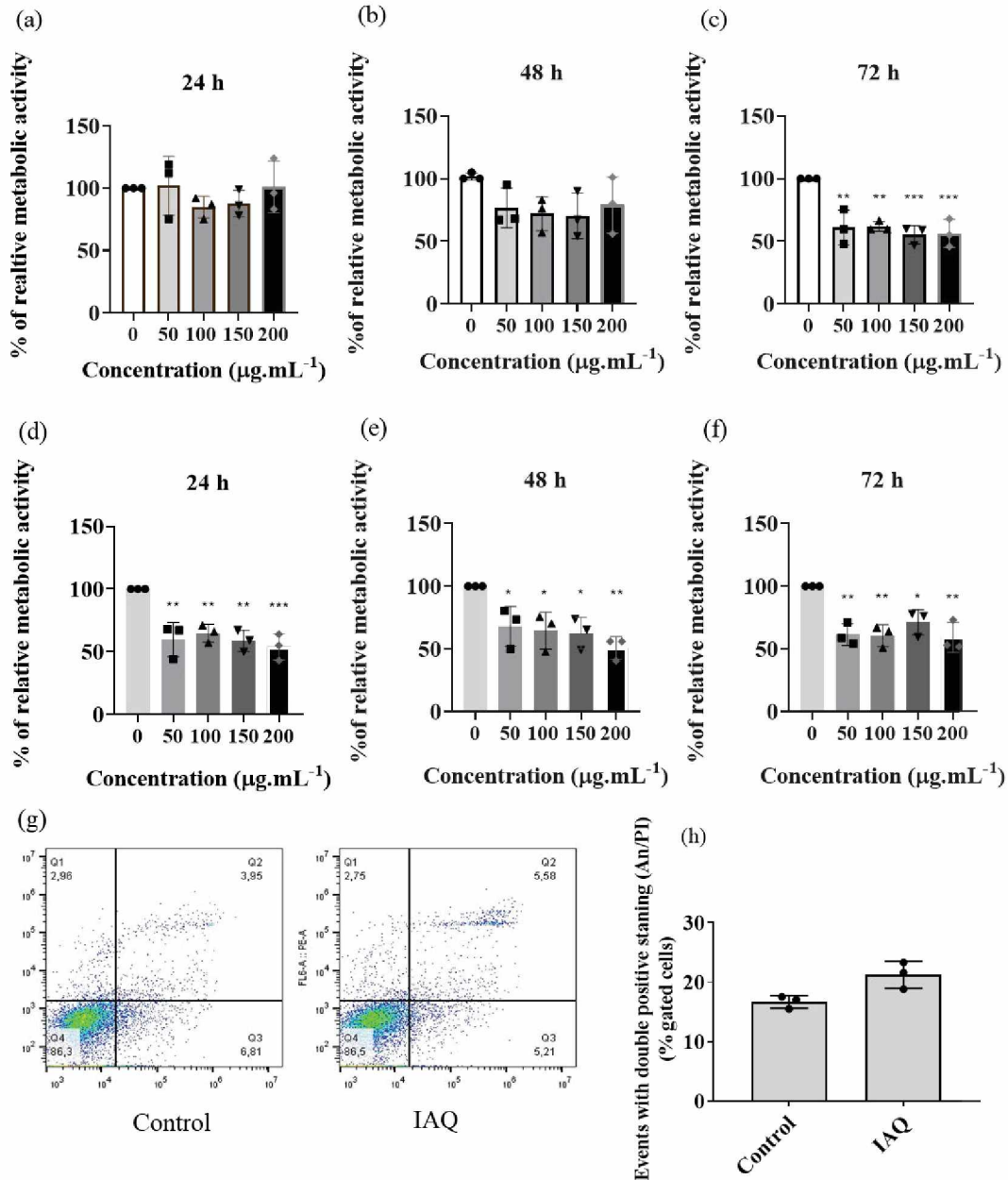


**Fig. 6** Metabolic activity at glioblastoma U87MG (a,b,c) and U251 cell lines (d,e,f) in response to of *I. galbana* extracts treatment. Concentrations of 50; 100; 150 and 200  $\mu\text{g. mL}^{-1}$  were applied to cells for various time points and analyzed by an MTT assay after 24, 48, and 72 h of treatment. Control cells correspond to cells incubated with the solvent in DMEM medium and normalized to 100%. These results are expressed as mean  $\pm$  s.d., three independent experiments with 4 technical replicates, with statistical significance (\* stands for  $p < 0.05$ , \*\* for  $p < 0.01$ ). (g) Representative plots of FACS analysis of An/PI staining of U87 MG cells treated with IAQ (100  $\mu\text{g. mL}^{-1}$  for 72 h). (h) The analysis of the FACS measurements of U87 MG cells (un)- treated for 72h with IAQ the native extract (100  $\mu\text{g. mL}^{-1}$ ), the values are expressed as mean  $\pm$  s.d., three independent experiments in triplicate, ANOVA test.

Next, to investigate if the metabolic decreasing observed in the  $\beta$ -D-glucan presence is related to cell death, we performed analysis of Annexin V and propidium iodide (depicted as Annexin V/PI) cell staining challenged with native IAQ or HMW-related fractions ( $100 \mu\text{g. mL}^{-1}$ ) for 72 h in U87MG cells. These data show that despite a decrease in the metabolic activity showed by an MTT assay (Fig. 6c; Fig 7c), native IAQ and HMW did not induce an increase in double-positive Annexin V/PI (Fig. 6g, h and Fig 7g, h).

To investigate if the decreasing of the observed MTT absorbance could be attributed to a potential cell cycle arrest, we evaluated DNA content by flow cytometry (Fig S5). The analysis of the FACS data showed no detectable alteration in the cell cycle progression in the presence of the (1 $\rightarrow$ 3,1 $\rightarrow$ 6)- $\beta$ -D-glucan. Several studies also reported that  $\beta$ - glucans could decrease cell metabolism without apoptosis nor cell cycle alterations in breast cancer, hepatocarcinoma, and oral cancer cells (Abdullah, Sharif, Azizan, Hafidz, Supramani, Usuldin, Ahmad and Wan-Mohtar [35], Al-Saffar, Hadi and Khalaf [36], Baranoski, Tempesta Oliveira, Semprebon, Niwa, Ribeiro and Mantovani [37]).

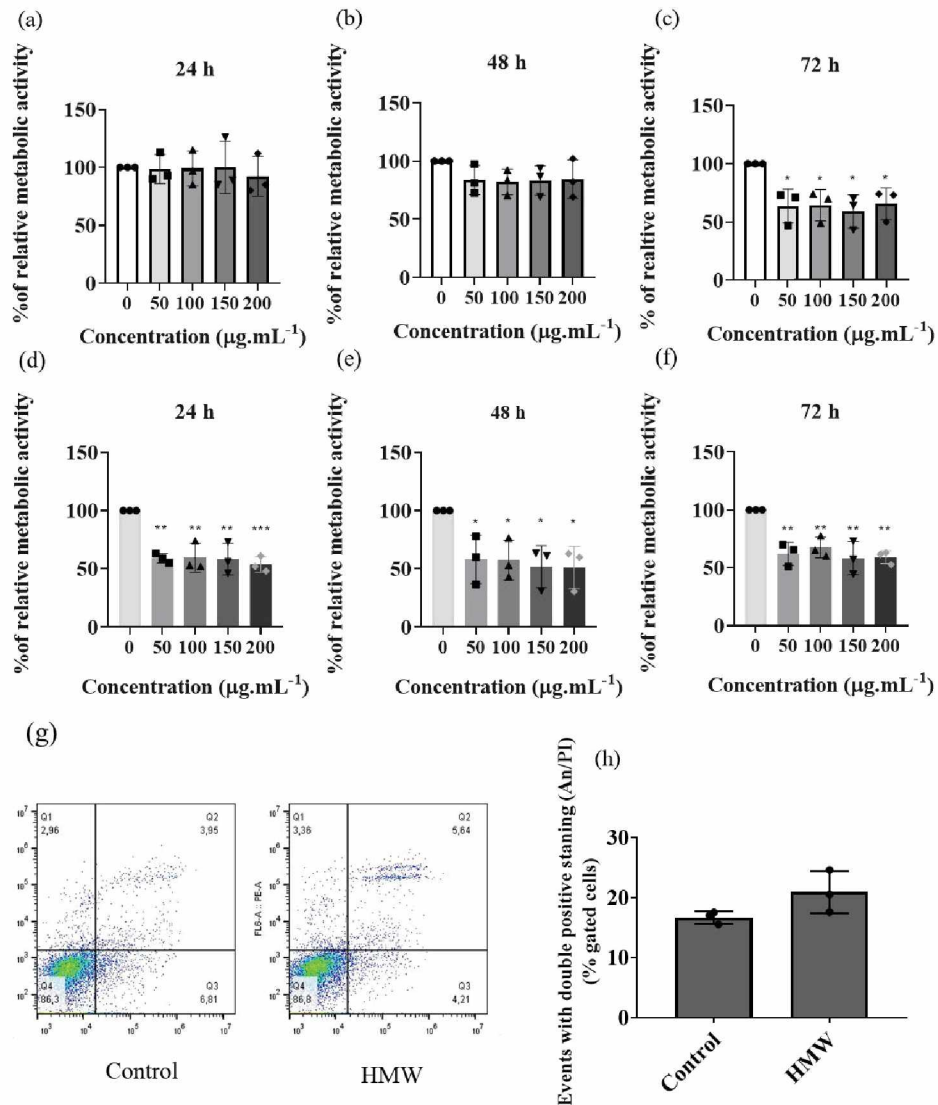


**Fig. 7** Metabolic activity at glioblastoma U87MG (a,b,c) and U251 cell lines (d,e,f) in response to HMW treatment. Concentrations of 50; 100; 150 and 200  $\mu\text{g. mL}^{-1}$  were applied to cells for various time points and analyzed by an MTT assay after 24, 48, and 72 h of treatment. Control cells correspond to cells incubated with the solvent in DMEM medium and normalized to 100%. These results are expressed as mean  $\pm$  s.d., three independent experiments with 4 technical replicates, with statistical significance (\* stands for  $p < 0.05$ , \*\* for  $p < 0.01$ ). (g) Representative plots of FACS analysis of An/PI staining of U87 MG cells treated with the native extract (100  $\mu\text{g. mL}^{-1}$  for 72 h). (h) The analysis of the FACS measurements of U87 MG cells (un)- treated for 72h with HMW (100  $\mu\text{g. mL}^{-1}$ ), the values are expressed as mean  $\pm$  s.d., three independent experiments in triplicate, ANOVA test.

### 3.2.2 $\beta$ -D-glucan affects ETC complexes I, III, and IV on U251 and U87MG glioblastoma cell lines.

Based on the cell metabolic data acquired using an MTT assay, both the native extract IAQ and HMW reduced cell metabolic activity in U251 cells already after 24h of treatment. In contrast, in U87MG cells, the reduction was detected only after 72 hours. Interestingly, cell death was not observed with either IAQ native or HMW extract treatment even after 72h of application. Therefore, to get further insight into the cell metabolic status, we performed a Mitoplate-S1 assay at 24 hours with IAQ treatment in both U251 and U87MG cells. This assay allows to investigate cell metabolic pathways based on substrate consumption. The analysis of these measurements showed that in U251 cells (**Fig. 8, Fig. S6a**), IAQ decreased the substrate consumption of metabolic intermediates presented in the citric acid cycle (TCA). In U87MG (**Fig. 9, Fig. S7b**), IAQ decreased ketone body. For both cell lines, glycolysis, fat acid oxidation, and amino acid pathways were diminished. A scheme of cell metabolic pathways shows that (1 $\rightarrow$ 3,1 $\rightarrow$ 6)- $\beta$ -D-glucan interfered with the metabolic pathways of the studied cell lines (**Fig. 10**).

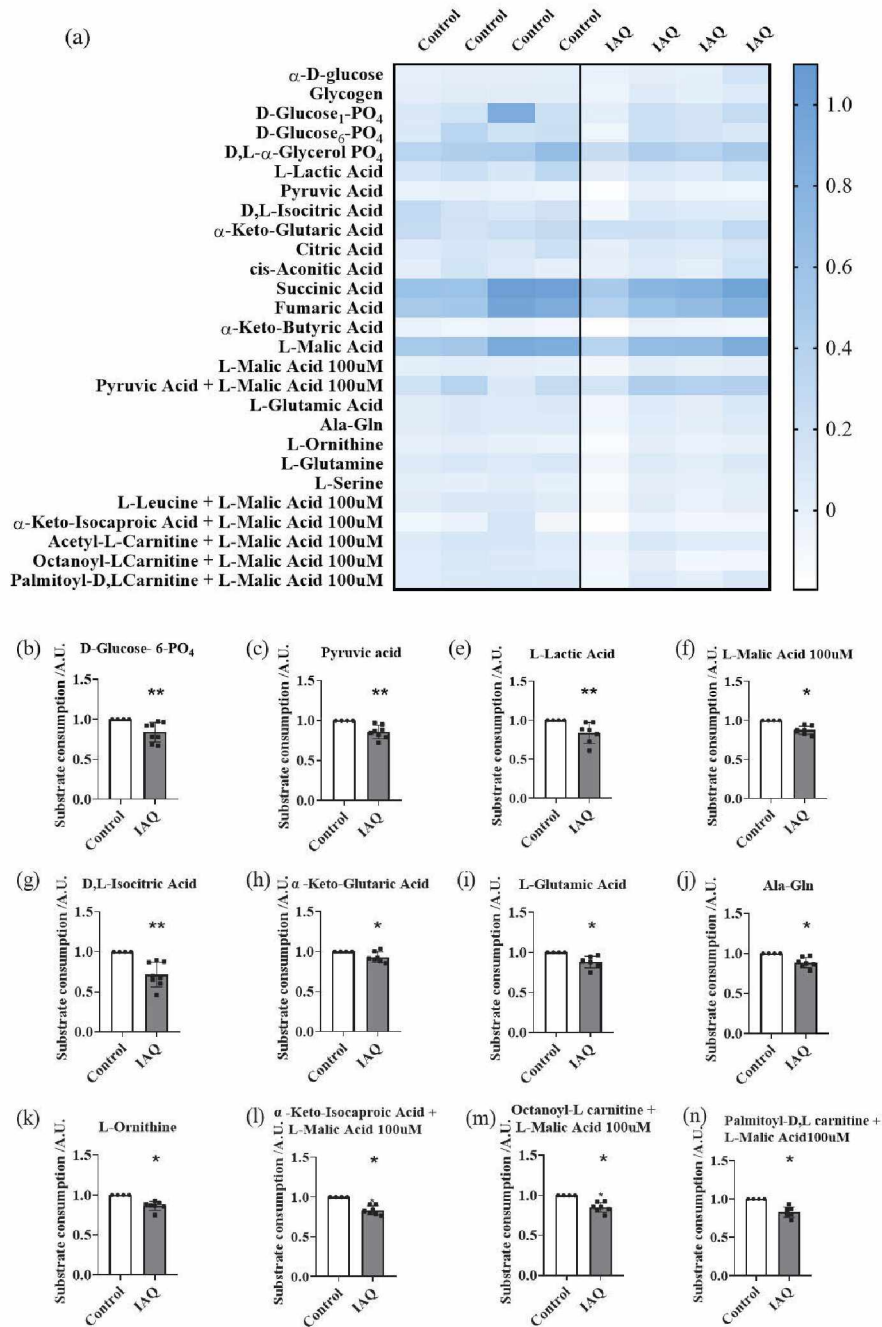


**Fig. 8** Mitoplate heatmap of U251 cell line with consumed substrates (a) and individual diminished substrate consumption after IAQ treatment (b-m). Metabolic drop in glycolysis (b, c), TCA (d,e,f,g), amino acid (h,i,j,k) and fat acid oxidation (l,m) intermediates consumption when U251 cells are treated with the native extract IAQ at 100  $\mu\text{g} \cdot \text{mL}^{-1}$ , 24 h, 4 independent experiments. Data are represented as Mean  $\pm$  SD; \* $p < 0.05$ , \*\*  $p < 0.01$ . Heatmap shows significant and not significant substrates, and graphs only show significant substrates.

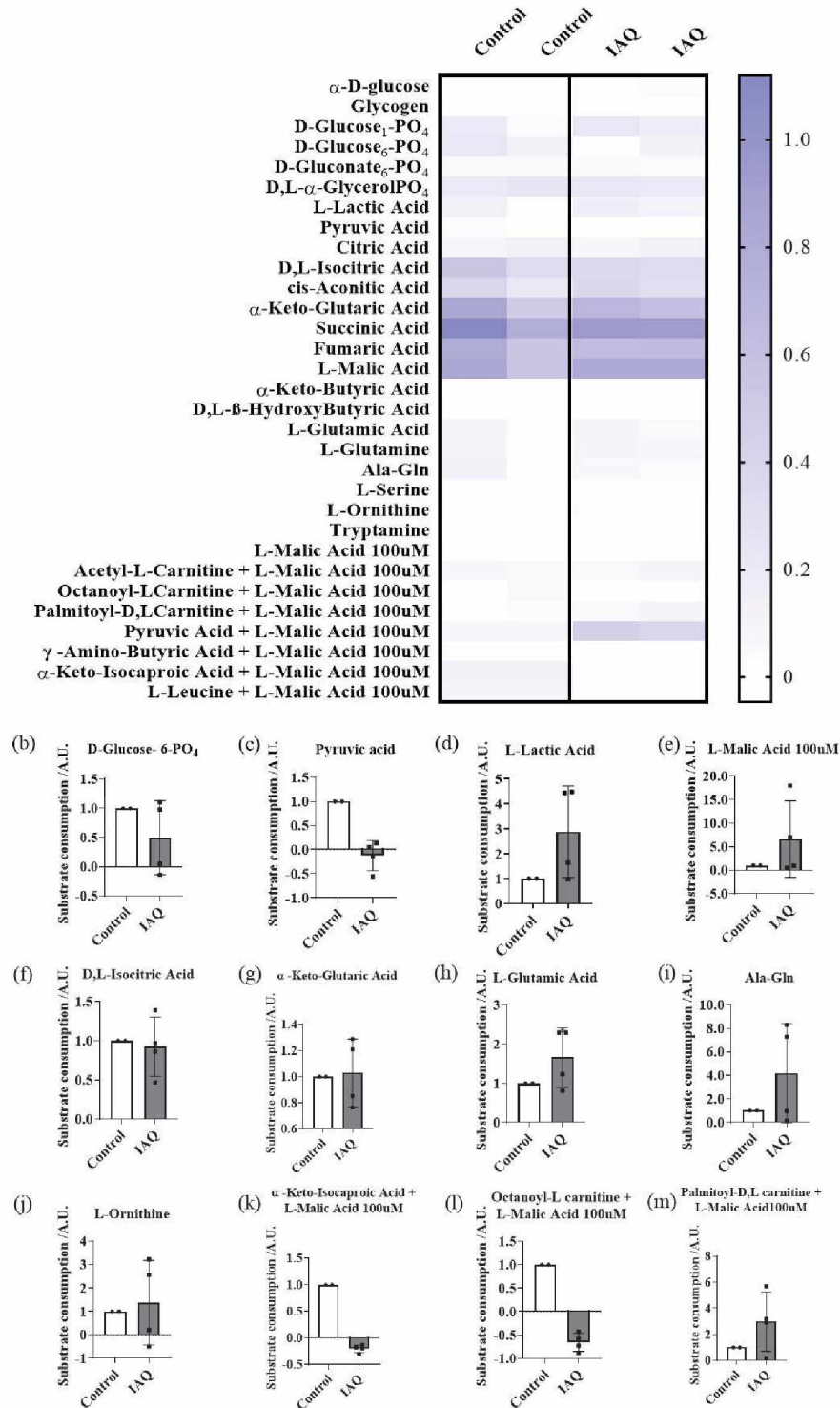


**Fig. 9** Representative mitoplate results from of U87MG cell line. Heatmap with consumed substrates (a) and individual diminished substrate consumption after IAQ treatment (100 ug. mL<sup>-1</sup>). Metabolic drop in ketone body, amino acid, and fat acid oxidation intermediates consumption when U87MG cells are treated with IAQ at 100 ug. mL<sup>-1</sup>, 24 h. 2 independent experiments.

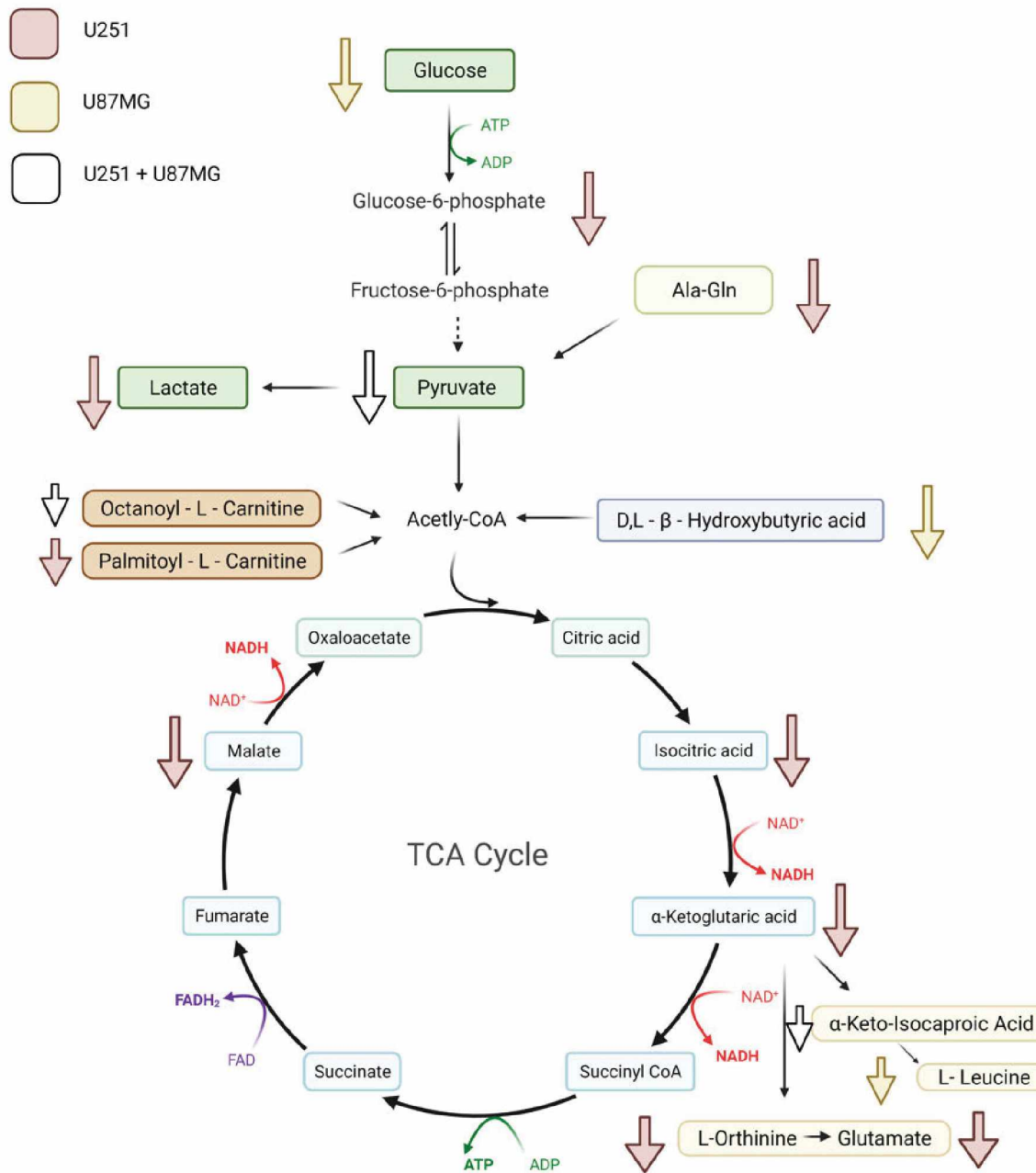


**Fig. 10** (1→3,1→6)-β-D-glucan effect in metabolic pathways upon U251 and U87MG cell lines. Adapted from “Krebs cycle” and “Glycolysis” (2021). Created using BioRender.com <https://app.biorender.com/biorendertemplates>

(1→3,1→6)-β-D-glucan (native) was able to interfere with the pathway of mitochondrial metabolism intermediates. Glycolysis reduction of α-D-glucose (U87MG), D-glucose-6-PO<sub>4</sub> (U251), pyruvic acid (both), and lactate (U251) is possibly correlated with an interference of the monocarboxylate transporter 1 (MCT1) and glucose transporter 1 (GLUT -1), along with hexokinase 2 (HK2) enzyme. GLUT -1 captures glucose from the environment and brings it to the cell and, HK2 will phosphorylate glucose to glucose-6-phosphate. GLUTs and HKs are proteins that mediate glucose

metabolism in tumors [38, 39]. MCT1 is a transporter of lactate and pyruvate and, it is mostly located at the plasma membrane, but it is expressed at the mitochondrial membranes. MCT1 and HK2 are overexpressed in GBM cells, so an interference on those proteins would lead to a decrease of substrates [40]. For U87MG cells, the decrease of ketone body  $\beta$ -hydroxybutyrate (BHB) could also be related to the MCT1, and MCT2 since those transporters are responsible for carrying and control BHB's uptake in the brain [41]. An overall diminishing those intermediates can affect the complexes I and IV of the electron transport chain (ETC), therefore reducing cell metabolic activity.

Regarding the TCA cycle, (1 $\rightarrow$ 3,1 $\rightarrow$ 6)- $\beta$ -D-glucan induced an alteration of the consumption of malate, isocitrate, and  $\alpha$ -Ketoglutarate intermediates. This could be attributed to a reduction of glycolysis, which could affect the TCA cycle. Another hypothesis could be related to an alteration of the malate-citrate antiporter (CIC) or the malate- $\alpha$ -ketoglutarate antiporter (OGCP). Those antiporters will affect the entry of malate on the mitochondrial matrix, consequently affecting 3 enzymes: the multi-enzyme complex 2-oxoglutarate dehydrogenase (OGDHC), isocitrate dehydrogenase (IDH), and malate dehydrogenase (MDH) [42]. IDH converts isocitrate to  $\alpha$ -ketoglutarate, and it is related to the occurrence and development of glioma by upregulating vascular endothelial growth factor (VEGF) and hypoxia-inducible factor-1 $\alpha$  (HIF-1 $\alpha$ ) [43]. OGDHC regulates the conversion of  $\alpha$ -ketoglutarate to succinyl-CoA, strictly regulating the TCA cycle by controlling the metabolic flux. MDH is responsible for converting malate to oxaloacetate. All of those enzymes are linked to NADH production and can lead to an alteration in the activity of mitochondrial complexes I and III of ETC [44]. Those intermediates directly affect the amino acid pathway [45].

Concerning the amino acid pathway, (1 $\rightarrow$ 3,1 $\rightarrow$ 6)- $\beta$ -D-glucan mediated a decrease in the consumption of L-glutamic acid, alanine – glutamine, L-orthinine and L-leucine, and  $\alpha$ - ketoisocaproic acid. A possible explanation for the decrease of those intermediates would be the result in an upregulation of amino acid membrane transporters. Ala-serine cysteine, preferring transporter 2 (ASCT2/SLC1A5) and essential membrane protein (SLC3A2), are located in the plasma membrane. Both of them take amino acids from the extracellular environment, being essential to the pro-survival phenotype, and are overexpressed in glioblastoma cells [46]. ASCT2 transporter uptakes glutamine for the TCA cycle. SLC3A2 also activates transport neutral aminoacids (LAT 1/2/3), guanine nucleotide-binding (ASC1), and cystine/glutamate antiporter (xCT). LAT 1 transports the

essential amino acids for growth enhancement via the mammalian target-of-rapamycin (mTOR) kinase, being essential to cancer cells [47]. ASC1 regulates cellular adhesion. xCT plays a major role in glutathione synthesis, diminishes caspase 3 activity, and can lead to resistance to cell death of cancer cells [48]. (1→3,1→6)-β-D-glucan also induced a decrease of fatty acid oxidation intermediates: octanoyl - L- carnitine, and palmitoyl - D, L- carnitine. Tumor cells collect extracellular amino acid substrates, thought-specific transporters, for the amino acid intermediates maintain the tumoral metabolism. A possibility for this event might be related to the decrease of aminoacid intermediates since acetyl-CoA supplies carbons for lipid biosynthesis and the TCA cycle [46].

Overall, (1→3,1→6)-β-D-glucan shows a cytostatic effect, affecting the cell metabolic state. These results were corroborated by the MTT assay and mitoplate results. Both assays evaluate cellular oxidoreduction reactions. MTT evaluates the reduction of tetrazolium salt to formazan, observing the NADH and dihydroflavine-adenine dinucleotide (FADH<sub>2</sub>) enzymes activity in the cell. Mitoplate also evaluates the tetrazolium reduction by electron flow through the ETC, but with specific substrates consumption rates that produce NADH and FADH<sub>2</sub>. Those oxidoreduction enzymes are re-used in several metabolic pathways of the cell. NAD<sup>+</sup> is reduced to NADH at the TCA cycle, glycolysis, fat acid oxidation, and glutamine metabolism (amino acid metabolism). A diminished conversion of NADH directly affects ETC's complexes I, III, and IV. Once the electron transport from NADH is affected, there is no electron flow on ETC's complex I, and the other complexes stop working. Consequently, this leads to a direct reduction of ATP production at the oxidative phosphorylation (OXPHOS) [49, 50].

Mitoplate results show a difference in substrate consumption between the U87MG and U251 glioblastoma lines. This could be attributed to the tumor intertumoral heterogeneity (tumors from different patients) of the GBM [51]. U251 and U87MG cell lines present differences in their protein and metabolic pathway expression. U251 cells highly express nicotinamide nucleotide and oxidoreduction coenzyme proteins compared to U87MG cells [52]. Another interesting fact is that the U251 glycolysis pathway is more enhanced than U87MG cells [52], while (1→3,1→6)-β-D-glucan increased lactate consumption in U87MG cells.

#### **4. Conclusion**

Extracts from *Isochrysis galbana* provide a mixture of polymers, constituted of high and low molecular weights, and both of them are  $\beta$ -D-glucans with a (1 $\rightarrow$ 6) backbone and (1 $\rightarrow$ 3), (1 $\rightarrow$ 6) branches in the third carbon. The native fraction was able to reduce cellular metabolism of two glioblastoma cell lines, affecting more metabolic mitochondrial intermediates in the U251 cell line (glycolysis, TCA cycle, amino acids, and fat acid oxidation) and less in the U87 MG line. We can, therefore, conclude that this compound has a cytostatic effect upon U251 cells, and propose the IAQ polysaccharide fraction, with further studies, to be used as adjuvant therapy in patients with U251 genotype.

#### **Acknowledgments**

This work was supported by Fundação Araucária/CNPq (PRONEX-Carboidratos), MCT/CNPq/CT-PETRO, CNPq and CAPES. M.T.L. was a recipient of CAPES (Process # 88887.321693/2019-00). T.R.M. acknowledges a doctoral scholarship from CAPES (Process # 88882.344138/2019-01), a doctoral sandwich scholarship from the CAPES PrInt program (Process # 88887.468902/2019-00). M.E.D., M.D.N., and S.M.B.W. are Research Members of the National Research Council of Brazil (CNPq). A.M.D. is the recipient of a Rosalind Franklin Fellowship co-funded by the European Union and the University of Groningen. The authors acknowledge the NMR Center of Federal University of Paraná (UFPR) for the NMR data acquisition and also Dr. Frank Kruyt from Rijkuniversiteit Groningen (RUG) for providing the U87MG and U251 cell lines.

#### **Conflicts of Interest**

The authors declare no conflict of interest.

#### **CRedit authorship contribution statement:**

Conceptualization, T.R.M, M.T.L., S.M.B.W., A.M.D, M.E.D and M.D.N.; Data collection, T.R.M and M.T.L., Data analysis and interpretation, T.R.M, M.T.L., S.M.B.W., A.M.D, M.E.D, and M.D.N.; Drafting the article, T.R.M.; Critical revision of the article, M.T.L., S.M.B.W., A.M.D, M.E.D, and M.D.N.; Final approval of the version to be published, M.T.L., S.M.B.W., A.M.D, M.E.D and M.D.N. Project Administration,

M.D.N., M.E.D, and A.M.D.; Funding Acquisition, M.D.N., M.E.D, and A.M.D. All the authors have read, approved, and made substantial contributions to the manuscript.

## References

- [1] C. Compton, Cancer Initiation, Promotion, and Progression and the Acquisition of Key Behavioral Traits, *Cancer: The Enemy from Within: A Comprehensive Textbook of Cancer's Causes, Complexities and Consequences*, Springer International Publishing, Cham, 2020, pp. 25-48.
- [2] P.D. Delgado-Lopez, E.M. Corrales-Garcia, Survival in glioblastoma: a review on the impact of treatment modalities, *Clin Transl Oncol* 18(11) (2016) 1062-1071.
- [3] I. Paw, R.C. Carpenter, K. Watabe, W. Debinski, H.W. Lo, Mechanisms regulating glioma invasion, *Cancer Lett* 362(1) (2015) 1-7.
- [4] L. Guntuku, V.G. Naidu, V.G. Yerra, Mitochondrial Dysfunction in Gliomas: Pharmacotherapeutic Potential of Natural Compounds, *Curr Neuropharmacol* 14(6) (2016) 567-83.
- [5] P.E. Porporato, N. Filigheddu, J.M.B. Pedro, G. Kroemer, L. Galluzzi, Mitochondrial metabolism and cancer, *Cell Res* 28(3) (2018) 265-280.
- [6] Y. Hu, J. Chen, G. Hu, J. Yu, X. Zhu, Y. Lin, S. Chen, J. Yuan, Statistical research on the bioactivity of new marine natural products discovered during the 28 years from 1985 to 2012, *Marine drugs* 13(1) (2015) 202-21.
- [7] K.A. Martínez Andrade, C. Lauritano, G. Romano, A. Ianora, Marine Microalgae with Anti-Cancer Properties, *Marine drugs* 16(5) (2018) 165.
- [8] J.E. Cassolato, M.D. Nosedá, C.A. Pujol, F.M. Pellizzari, E.B. Damonte, M.E. Duarte, Chemical structure and antiviral activity of the sulfated heterorhamnan isolated from the green seaweed *Gayralia oxysperma*, *Carbohydr Res* 343(18) (2008) 3085-95.
- [9] M.M. de Carvalho, R.A. de Freitas, D.R.B. Ducatti, L.G. Ferreira, A.G. Goncalves, F.G. Colodi, E. Mazepa, E.M. Aranha, M.D. Nosedá, M.E.R. Duarte, Modification of ulvans via periodate-chlorite oxidation: Chemical characterization and anticoagulant activity, *Carbohydrate polymers* 197 (2018) 631-640.
- [10] G.S. Mendes, M.E. Duarte, F.G. Colodi, M.D. Nosedá, L.G. Ferreira, S.D. Berte, J.F. Cavalcanti, N. Santos, M.T. Romanos, Structure and anti-metapneumovirus activity of sulfated galactans from the red seaweed *Cryptonemia seminervis*, *Carbohydrate polymers* 101 (2014) 313-23.
- [11] L.G. Ferreira, A.C.R. da Silva, M.D. Nosedá, A.L. Fuly, M.M. de Carvalho, M.T. Fujii, E.F. Sanchez, J. Carneiro, M.E.R. Duarte, Chemical structure and snake antivenom properties of sulfated agarans obtained from *Laurencia dendroidea* (Ceramiales, Rhodophyta), *Carbohydrate polymers* 218 (2019) 136-144.

- [12] S.D.C. Amaral, S.F. Barbieri, A.C. Ruthes, J.M. Bark, S.M. Brochado Winnischofer, J.L.M. Silveira, Cytotoxic effect of crude and purified pectins from *Campomanesia xanthocarpa* Berg on human glioblastoma cells, *Carbohydr Polym* 224 (2019) 115140.
- [13] O.S. Vishchuk, S.P. Ermakova, T.N. Zvyagintseva, Sulfated polysaccharides from brown seaweeds *Saccharina japonica* and *Undaria pinnatifida*: isolation, structural characteristics, and antitumor activity, *Carbohydrate research* 346(17) (2011) 2769-76.
- [14] P. Shao, Y. Pei, Z. Fang, P. Sun, Effects of partial desulfation on antioxidant and inhibition of DLD cancer cell of *Ulva fasciata* polysaccharide, *Int J Biol Macromol* 65 (2014) 307-13.
- [15] B. Nikolova, S. Semkova, I. Tsoneva, G. Antov, J. Ivanova, I. Vasileva, P. Kardaleva, I. Stoineva, N. Christova, L. Nacheva, L. Kabaivanova, Characterization and potential antitumor effect of a heteropolysaccharide produced by the red alga *Porphyridium sordidum*, *Eng Life Sci* 19(12) (2019) 978-985.
- [16] R.R.L. Guillard, Culture of Phytoplankton for Feeding Marine Invertebrates., in: W.L.S.M.H. Chanley (Ed.) *Culture of Marine Invertebrate Animals: Proceedings --- 1st Conference on Culture of Marine Invertebrate Animals Greenport*, Springer US. , Boston, MA, 1975, pp. 29–60.
- [17] M. Dubois, K. Gilles, P. Rebers, F. Smith, Colorimetric method for determination of sugars and related substances. , *Analytical Chemistry* 3 (1956) 350–356.
- [18] O.H. Lowry, N.J. Rosebrough, A.L. Farr, R.J. Randall, Protein measurement with the Folin phenol reagent, *The Journal of biological chemistry* 193(1) (1951) 265-75.
- [19] K.S. Dodgson, R.G. Price, A note on the determination of the ester sulphate content of sulphated polysaccharides, *The Biochemical journal* 84(1) (1962) 106-10.
- [20] T.M.C.C. Filisetti-Cozzi, N.C. Carpita, Measurement of uronic acids without interference from neutral sugars, *Analytical Biochemistry* 197(1) (1991) 157-162.
- [21] P.E. Jansson, *A Practical Guide to the Methylation Analysis of Carbohydrates*, Univ.1976.
- [22] I. Ciucanu, F. Kerek, A simple and rapid method for the permethylation of carbohydrates, *Carbohydrate Research* 131 (1984) 209-217.
- [23] G.L. Sasaki, P.A. Gorin, L.M. Souza, P.A. Czelusniak, M. Iacomini, Rapid synthesis of partially O-methylated alditol acetate standards for GC-MS: some relative activities of hydroxyl groups of methyl glycopyranosides on Purdie methylation, *Carbohydr Res* 340(4) (2005) 731-9.
- [24] T.P. Reilly, F.H. Bellevue, 3rd, P.M. Woster, C.K. Svensson, Comparison of the in vitro cytotoxicity of hydroxylamine metabolites of sulfamethoxazole and dapsone, *Biochem Pharmacol* 55(6) (1998) 803-10.
- [25] R. Pires Ado, A.C. Ruthes, S.M. Cadena, A. Acco, P.A. Gorin, M. Iacomini, Cytotoxic effect of *Agaricus bisporus* and *Lactarius rufus* beta-D-glucans on HepG2 cells, *Int J Biol Macromol* 58 (2013) 95-103.

- [26] H. Abreu, F.F. Simas, F.R. Smiderle, V. Sovrani, J.L. Dallazen, D. Maria-Ferreira, M.F. Werner, L.M.C. Cordeiro, M. Iacomini, Gelling functional property, anti-inflammatory and antinociceptive bioactivities of beta-D-glucan from the edible mushroom *Pholiota nameko*, *Int J Biol Macromol* 122 (2019) 1128-1135.
- [27] I. Palacios, A. Garcia-Lafuente, E. Guillamon, A. Villares, Novel isolation of water-soluble polysaccharides from the fruiting bodies of *Pleurotus ostreatus* mushrooms, *Carbohydr Res* 358 (2012) 72-7.
- [28] S.C. Raimundo, S. Pattathil, S. Eberhard, M.G. Hahn, Z.A. Popper, beta-1,3-Glucans are components of brown seaweed (Phaeophyceae) cell walls, *Protoplasma* 254(2) (2017) 997-1016.
- [29] A.A. Salmean, D. Duffieux, J. Harholt, F. Qin, G. Michel, M. Czjzek, W.G.T. Willats, C. Herve, Insoluble (1 → 3), (1 → 4)-beta-D-glucan is a component of cell walls in brown algae (Phaeophyceae) and is masked by alginates in tissues, *Sci Rep* 7(1) (2017) 2880.
- [30] Y. Cui, L. Zhu, Y. Li, S. Jiang, Q. Sun, E. Xie, H. Chen, Z. Zhao, W. Qiao, J. Xu, C. Dong, Structure of a laminarin-type beta-(1→3)-glucan from brown algae *Sargassum henslowianum* and its potential on regulating gut microbiota, *Carbohydrate polymers* 255 (2021) 117389.
- [31] I. Sadvskaya, A. Souissi, S. Souissi, T. Grard, P. Lencel, C.M. Greene, S. Duin, P.S. Dmitrenok, A.O. Chizhov, A.S. Shashkov, A.I. Usov, Chemical structure and biological activity of a highly branched (1 → 3,1 → 6)-beta-D-glucan from *Isochrysis galbana*, *Carbohydrate polymers* 111 (2014) 139-48.
- [32] A. Rolland-Sabaté, High-Performance Size-Exclusion Chromatography coupled with on-line Multi-angle Laser Light Scattering (HPSEC-MALLS), in: Martin Masuelli, D. Renard. (Eds.), *Advances in Physicochemical Properties of Biopolymers (Part 1)*, Bentham Science Publisher 2017, pp. 92-136.
- [33] R.H. Furneaux, T.T. Stevenson, The xylogalactan sulfate from *Chondria macrocarpa* (Ceramiales, Rhodophyta). , *Hydrobiologia* 204. (1990) 615-620.
- [34] A. Choromanska, J. Kulbacka, J. Harasym, R. Oledzki, A. Szewczyk, J. Saczko, High- and low-Molecular Weight oat Beta-Glucan Reveals Antitumor Activity in Human Epithelial Lung Cancer, *Pathology oncology research : POR* 24(3) (2018) 583-592.
- [35] N.R. Abdullah, F. Sharif, N.H. Azizan, I.F.M. Hafidz, S. Supramani, S.R.A. Usuldin, R. Ahmad, W. Wan-Mohtar, Pellet diameter of *Ganoderma lucidum* in a repeated-batch fermentation for the trio total production of biomass-exopolysaccharide-endopolysaccharide and its anti-oral cancer beta-glucan response, *AIMS microbiology* 6(4) (2020) 379-400.
- [36] A.Z. Al-Saffar, N.A. Hadi, H.M. Khalaf, Antitumor Activity of β-glucan Extracted from *Pleurotus eryngii*, *Indian Journal of Forensic Medicine & Toxicology* 14(3) (2020) 2492-2499.
- [37] A. Baranoski, M. Tempesta Oliveira, S.C. Semprebon, A.M. Niwa, L.R. Ribeiro, M.S. Mantovani, Effects of sulfated and non-sulfated beta-glucan extracted from *Agaricus brasiliensis*

in breast adenocarcinoma cells - MCF-7, *Toxicology mechanisms and methods* 25(9) (2015) 672-9.

[38] A.K. Koyande, K.W. Chew, K. Rambabu, Y. Tao, D.-T. Chu, P.-L. Show, Microalgae: A potential alternative to health supplementation for humans, *Food Science and Human Wellness* 8(1) (2019) 16-24.

[39] A. Wolf, S. Agnihotri, J. Micallef, J. Mukherjee, N. Sabha, R. Cairns, C. Hawkins, A. Guha, Hexokinase 2 is a key mediator of aerobic glycolysis and promotes tumor growth in human glioblastoma multiforme, *J Exp Med* 208(2) (2011) 313-26.

[40] S.J. Park, C.P. Smith, R.R. Wilbur, C.P. Cain, S.R. Kallu, S. Valasapalli, A. Sahoo, M.R. Guda, A.J. Tsung, K.K. Velpula, An overview of MCT1 and MCT4 in GBM: small molecule transporters with large implications, *Am J Cancer Res* 8(10) (2018) 1967-1976.

[41] J.C. Newman, E. Verdin,  $\beta$ -Hydroxybutyrate: A Signaling Metabolite, *Annu Rev Nutr* 37 (2017) 51-76.

[42] J.B. Spinelli, M.C. Haigis, The multifaceted contributions of mitochondria to cellular metabolism, *Nat Cell Biol* 20(7) (2018) 745-754.

[43] J. Huang, J. Yu, L. Tu, N. Huang, H. Li, Y. Luo, Isocitrate Dehydrogenase Mutations in Glioma: From Basic Discovery to Therapeutics Development, *Front Oncol* 9(506) (2019).

[44] E.L. Allen, D.B. Ulanet, D. Pirman, C.E. Mahoney, J. Coco, Y. Si, Y. Chen, L. Huang, J. Ren, S. Choe, M.F. Clasquin, E. Artin, Z.P. Fan, G. Cianchetta, J. Murtie, M. Dorsch, S. Jin, G.A. Smolen, Differential Aspartate Usage Identifies a Subset of Cancer Cells Particularly Dependent on OGDH, *Cell Rep* 17(3) (2016) 876-890.

[45] P. Karki, V. Angardi, J.C. Mier, M.A. Orman, A Transient Metabolic State In Melanoma Persister Cells Mediated By Chemotherapeutic Treatments, *bioRxiv* (2021) 2021.02.21.432154.

[46] R.K. Gandhirajan, D. Meyer, S.K. Sagwal, K.D. Weltmann, T. von Woedtke, S. Bekeschus, The amino acid metabolism is essential for evading physical plasma-induced tumour cell death, *Br J Cancer* 124(11) (2021) 1854-1863.

[47] B.C. Fuchs, B.P. Bode, Amino acid transporters ASCT2 and LAT1 in cancer: partners in crime?, *Semin Cancer Biol* 15(4) (2005) 254-66.

[48] S. Bekeschus, S. Eisenmann, S.K. Sagwal, Y. Bodnar, J. Moritz, B. Poschkamp, I. Stoffels, S. Emmert, M. Madesh, K.D. Weltmann, T. von Woedtke, R.K. Gandhirajan, xCT (SLC7A11) expression confers intrinsic resistance to physical plasma treatment in tumor cells, *Redox Biol* 30 (2020) 101423.

[49] N. Xie, L. Zhang, W. Gao, C. Huang, P.E. Huber, X. Zhou, C. Li, G. Shen, B. Zou, NAD(+) metabolism: pathophysiologic mechanisms and therapeutic potential, *Signal transduction and targeted therapy* 5(1) (2020) 227.

[50] L. Vettore, R.L. Westbrook, D.A. Tennant, New aspects of amino acid metabolism in cancer, *Br J Cancer* 122(2) (2020) 150-156.

[51] K. Anjum, B.I. Shagufta, S.Q. Abbas, S. Patel, I. Khan, S.A.A. Shah, N. Akhter, S.S.U. Hassan, Current status and future therapeutic perspectives of glioblastoma multiforme (GBM) therapy: A review, *Biomedicine & pharmacotherapy = Biomedecine & pharmacotherapie* 92 (2017) 681-689.

[52] H. Li, B. Lei, W. Xiang, H. Wang, W. Feng, Y. Liu, S. Qi, Differences in Protein Expression between the U251 and U87 Cell Lines, *Turk Neurosurg* 27(6) (2017) 894-903.

Supplemental Data

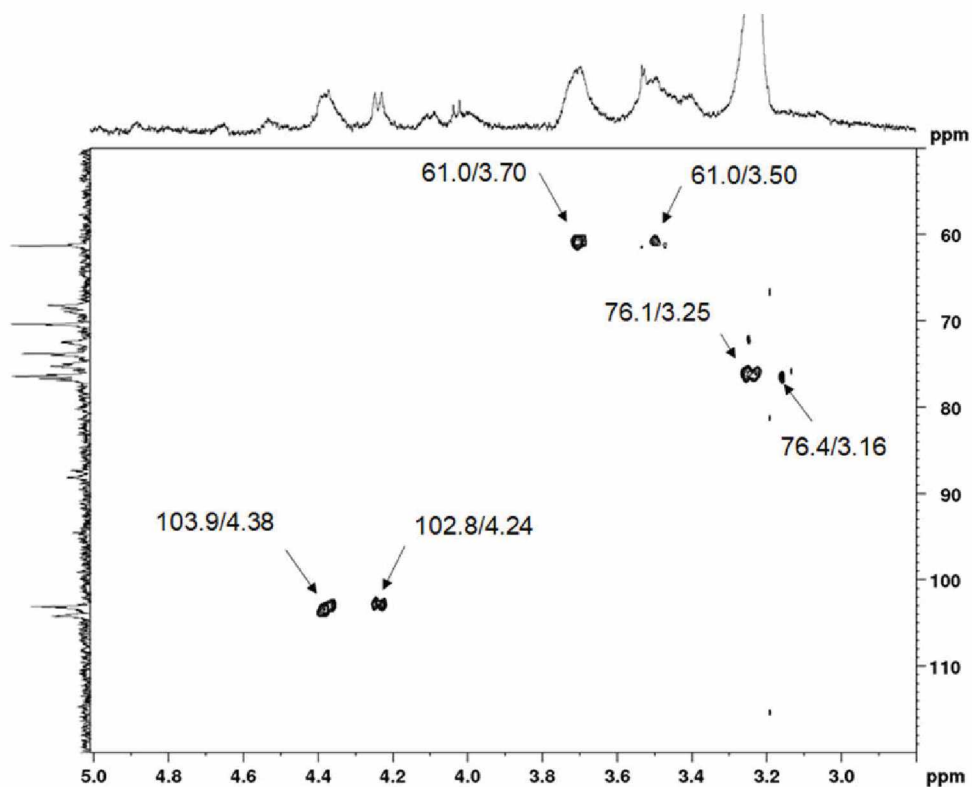


Fig. S1 HSQC correlation spectrum of fraction IAQ. DMSO- $d_6$ , 70 °C.

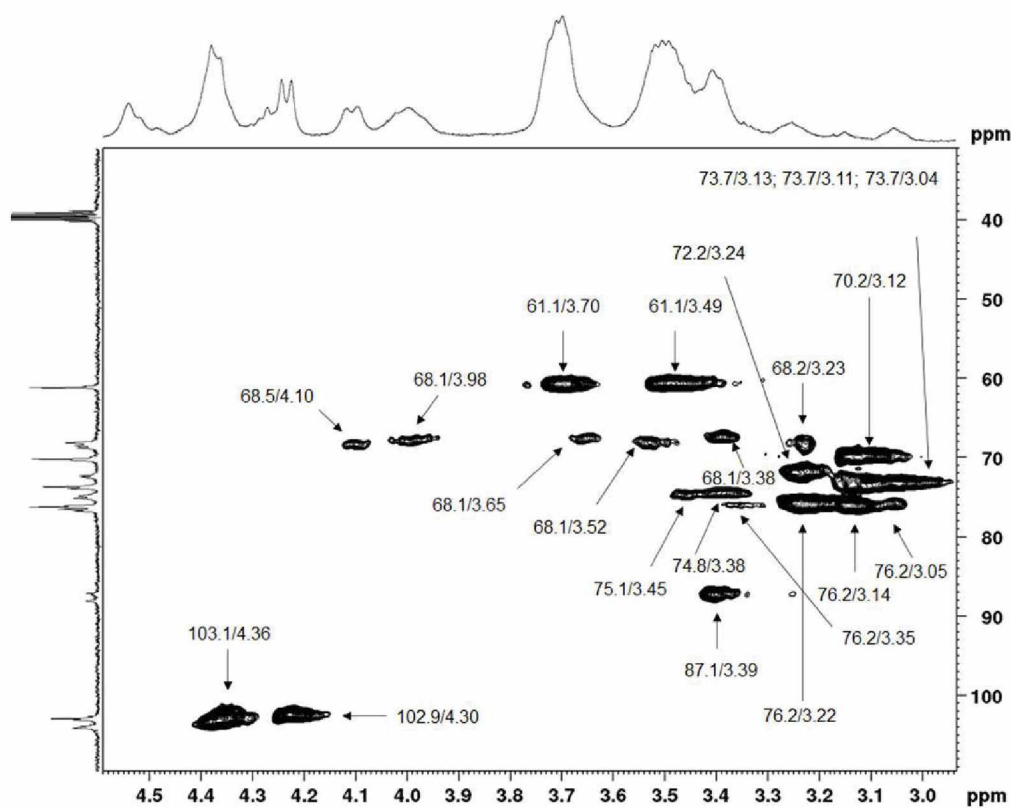
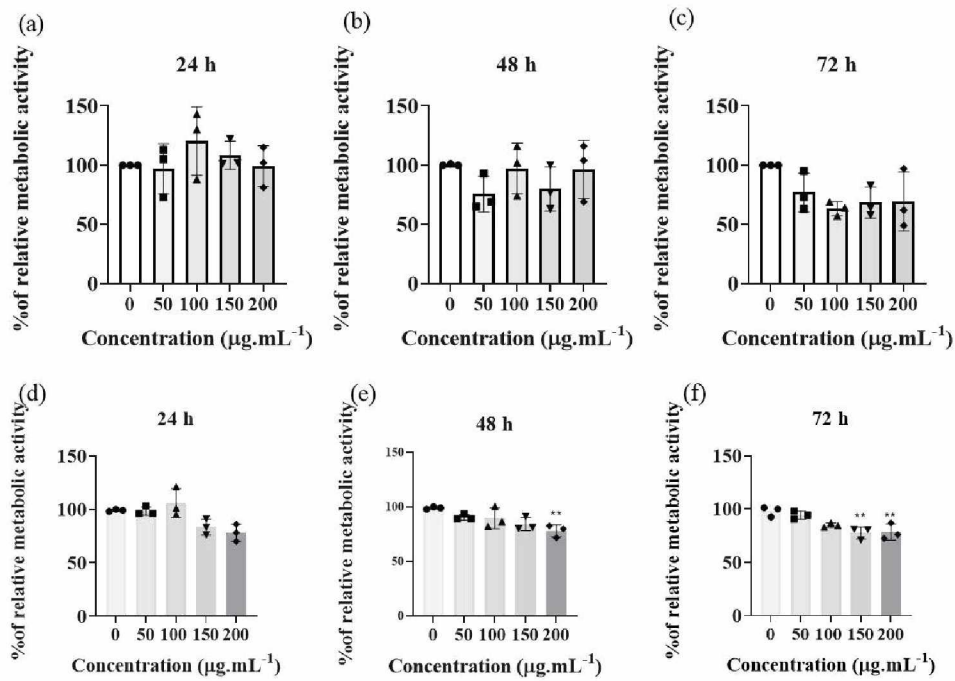
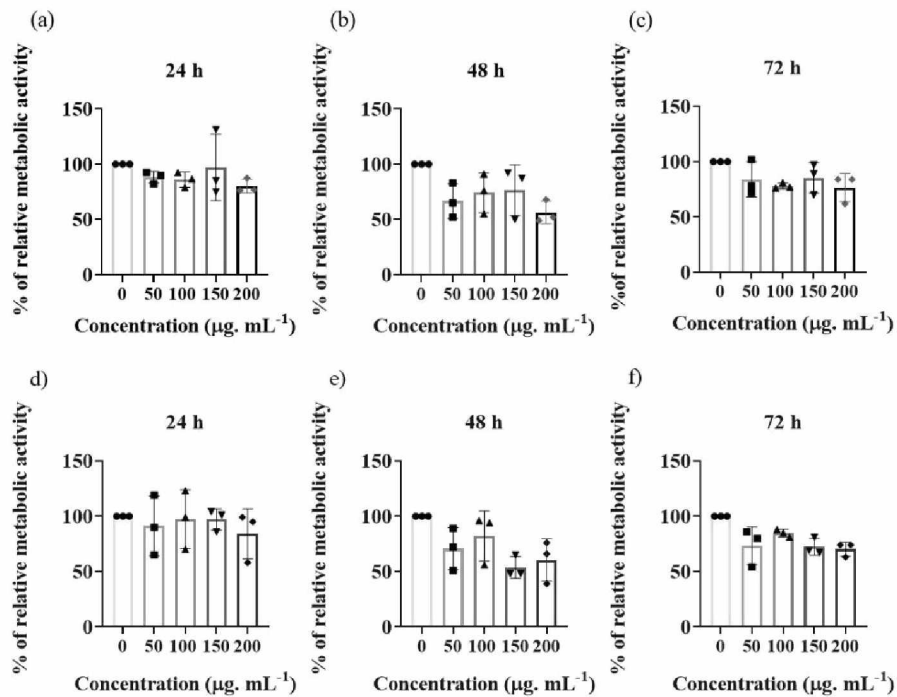


Fig. S2 HSQC correlation spectrum of LMW fraction in DMSO- $d_6$ , 70 °C.



**Fig. S3** Metabolic activity determined at glioblastoma cell lines U87MG (a,b,c) and U251 (d,e,f) with LMW. Concentrations of 50; 100; 150 and 200 µg. mL<sup>-1</sup> at time points of 24, 48, and 72 h. Control corresponds to 100% of cells incubated at DMEM medium. These results are expressed as mean ± s.d., three independent experiments with four technical replicates, with statistical significance (p<0.05).



**Fig. S4** Metabolic activity at hippocampus cell lines HT22 with IAQ (a,b,c) and HMW (d,e,f). Concentrations of 50; 100; 150 and 200  $\mu\text{g. mL}^{-1}$  at time points of 24, 48, and 72 h. Control corresponds to 100% of cells incubated at DMEM medium. These results are expressed as mean  $\pm$  s.d., three independent experiments with four technical replicates, with statistical significance ( $p < 0.05$ ).

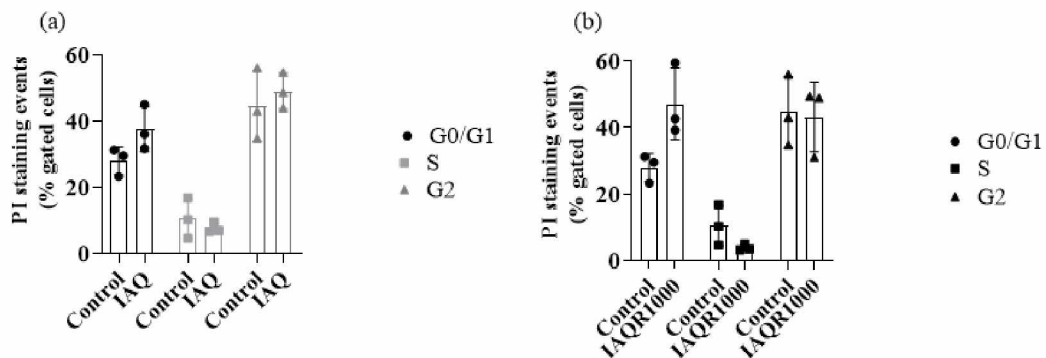


**Fig. S5** Cell cycle progression with the presence of IAQ (a) and HMW (b). Cell cycle was performed with U87MG cell line at a concentration of 100  $\mu\text{g. mL}^{-1}$  for 72 h, expressed as mean  $\pm$  s.d., three independent experiments in triplicate, by ANOVA test.

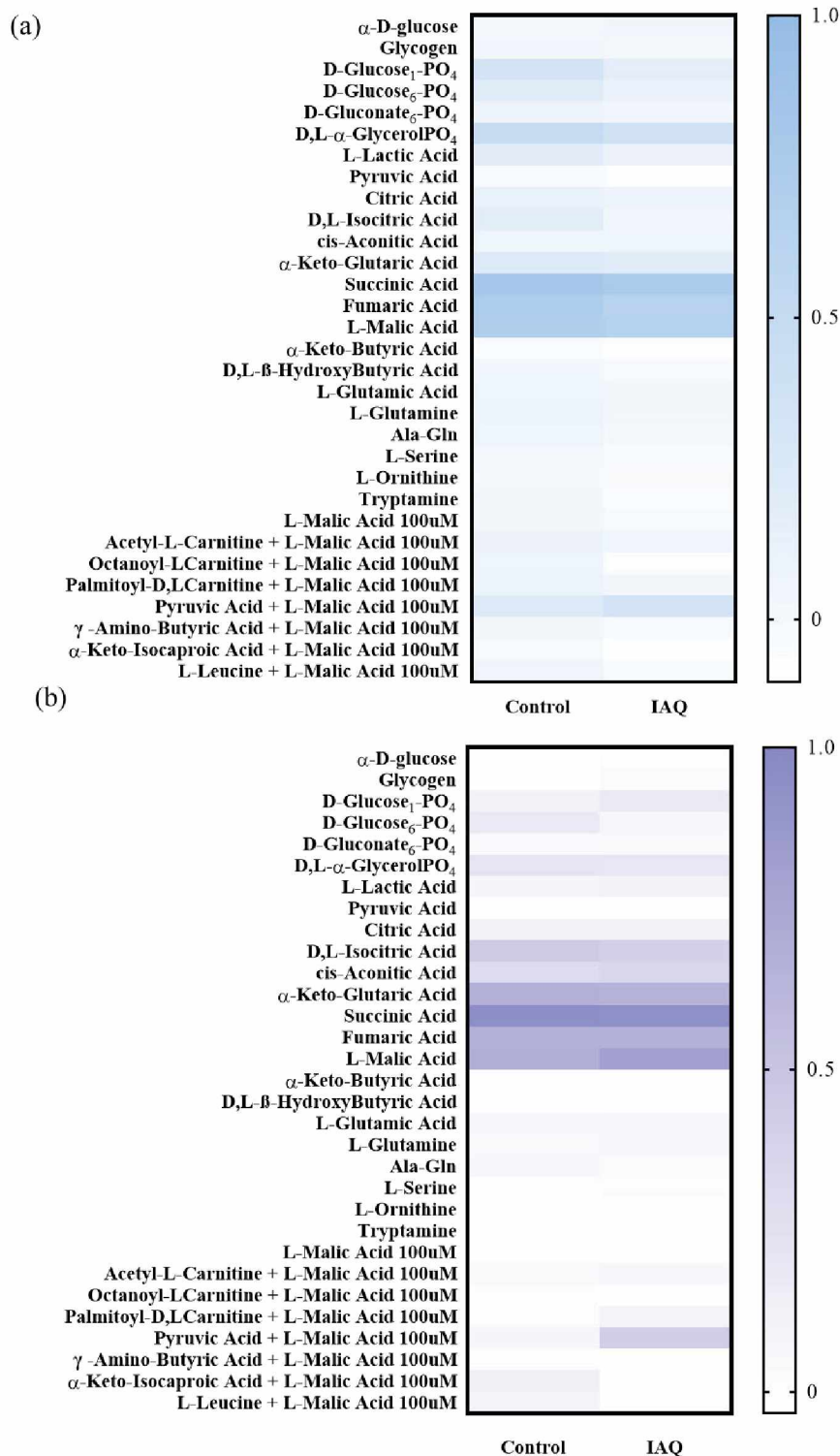


**Fig. S6** Heatmap with analyzed substrates when U251 (a) and U87MG cells (b) are treated with IAQ at 100  $\mu\text{g} \cdot \text{mL}^{-1}$ , 24 h. Three independent experiments for U87MG and four independent experiments for U251. Data are represented as Mean  $\pm$  SD; \* $p < 0.05$ , \*\*  $p < 0.01$ . Heatmap shows significant and not significant substrates, and graphs only show significant substrates.

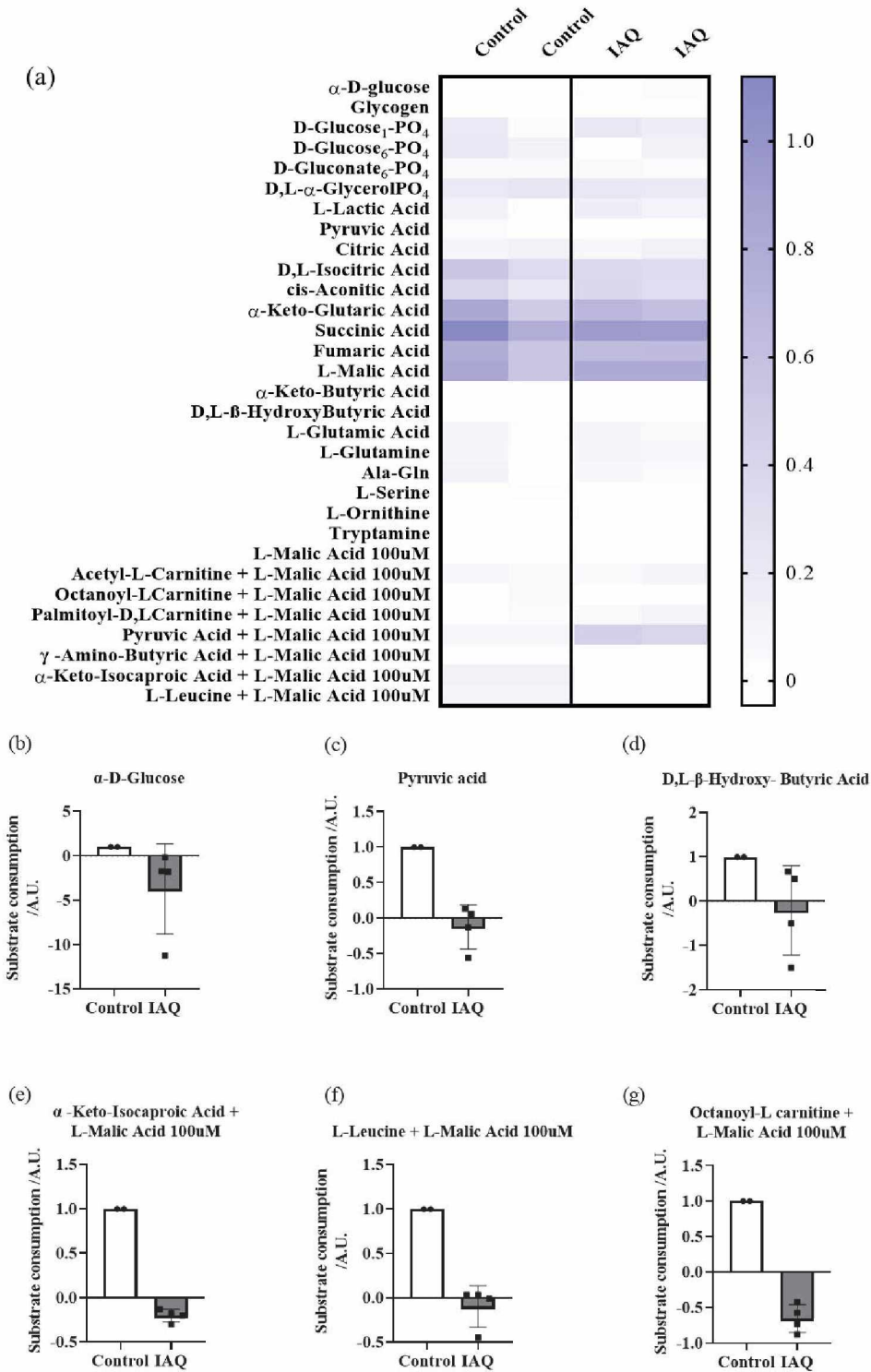


**Fig. S7** Representative mitoplate results from of U87MG cell line. Heatmap with consumed substrates (a) and individual diminished substrate consumption after IAQ treatment (100  $\mu\text{g. mL}^{-1}$ ). Metabolic drop in glycolysis, ketone body, amino acid, and fat acid oxidation intermediates consumption when U87MG cells are treated with IAQ at 100  $\mu\text{g. mL}^{-1}$ , 24 h. 2 independent experiments.

#### 4. CHAPTER III - Mitochondrial effects of an oversulfated heterorhamman from *Gayralia brasiliensis* in glioblastoma cell lines

Tatiana Rojo Moro<sup>a,c,1</sup>, Marina Trombetta-Lima<sup>c,1</sup>, Marília Locatelli Correa Ferreira<sup>a</sup>, Ester Mazepa<sup>a</sup>, Silvia Maria Suter Correia Cadena<sup>d</sup>, Sheila Maria Brochado Winnischofer<sup>d</sup>, Miguel Daniel Nosedá<sup>d</sup> Maria Eugênia Rabello Duarte<sup>d\*</sup>, Amalia M. Dolga<sup>c\*</sup>

<sup>a</sup> *Postgraduate Program in Biochemistry Sciences, Sector of Biological Sciences, Federal University of Paraná, Curitiba, Paraná, Brazil.*

<sup>b</sup> *Biochemistry and Molecular Biology Department, Federal University of Paraná, Av. Cel. Francisco H. dos Santos, 100, CEP 81531-980, PO BOX 19046, Curitiba, Paraná, Brazil.*

<sup>c</sup> *Department of Molecular Pharmacology, Faculty of Science and Engineering, Groningen Research Institute of Pharmacy (GRIP), University of Groningen, 9713 AV Groningen, the Netherlands.*

<sup>d</sup> *Postgraduate Program in Cellular and Molecular Biology, Sector of Biological Sciences, UFPR, Curitiba, Paraná, Brazil.*

<sup>1</sup> These authors equally contributed to this work.

\* Shared senior authorship

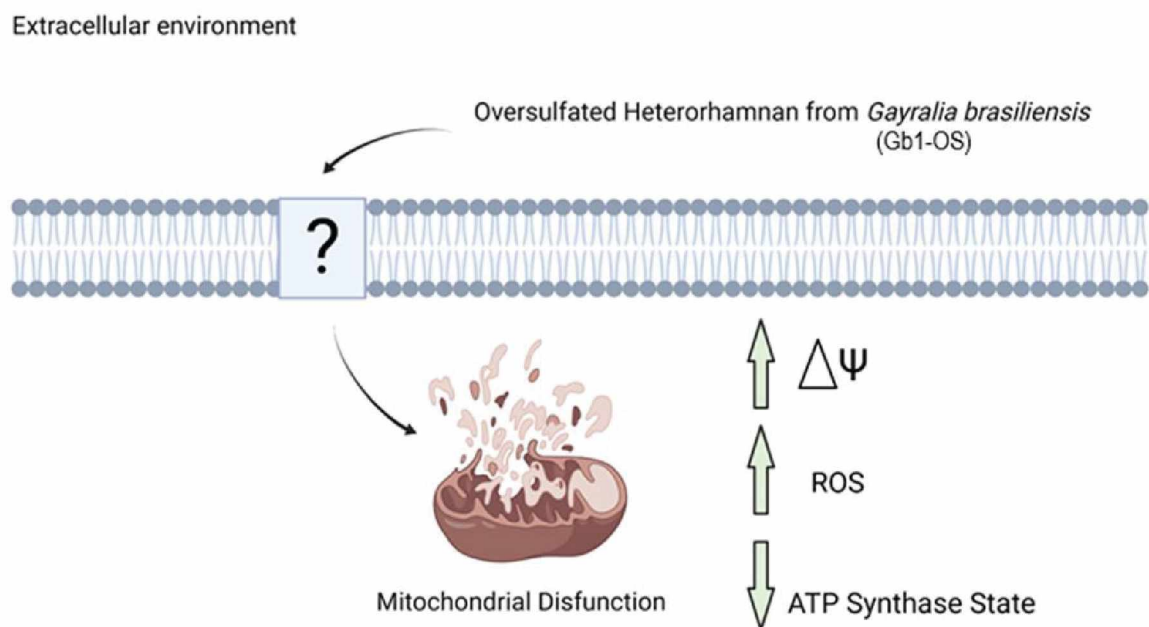
**Abstract:** Glioblastoma multiforme is the deadliest form of brain cancer because of its aggressiveness and poor recovery. Mitochondria is important in cancer development since this organelle regulates metabolic and signaling pathways to guarantee cell endurance. Therapies targeting mitochondria hold great potential for cancer treatment. Polysaccharides are natural polymers able to target cancer cells. Chemical modification of polysaccharides can enhance biological effects when compared with natural polysaccharides. Recent findings showed that oversulfated form of a heterorhamman extracted from *Gayralia brasiliensis* (Gb1-OS) mediated a reduction of U87MG glioblastoma cell viability. Our study aims to further investigate the underlying molecular mechanism for cell death mediated by Gb1-OS polysaccharide in glioblastoma cell lines. Gb1-OS caused an alteration of the mitochondrial respiration and decreased basal respiration, mostly ATP-linked respiration in U87MG cells. In addition, Gb1-OS

mediated hyperpolarization of mitochondrial membrane and augmentation of mitochondrial reactive oxygen species (ROS). Our study shows that Gb1-OS polysaccharide mediates cell death by altering the mitochondrial functions, suggesting that targeting mitochondrial metabolism might be a viable option to prevent cancer cell growth and progression.

### Highlights:

- Gb1-OS induces cell death of the U87MG glioblastoma cells.
- Gb1-OS cell death effect might be related to the oxidative phosphorylation impairment.
- Gb1-OS cell death effect is also related to an increase of the mitochondrial ROS.

### Graphical abstract:



Legend: Gb1-OS affects mitochondrial respiration, leading to apoptosis. Created with BioRender.com

**Keywords:** *Green macroalga, Polysaccharide sulfation, Glioblastoma Multiform, Mitochondrial hyperpolarization, Cell respiration*

## 1. Introduction

Cancer is the second worldwide cause of death [1]. Glioblastoma (GBM) is the most common type of glioma, corresponding to more than 60 % of all brain tumors among adults. It has a poor prognosis, being distinctly aggressive. The most challenging part of the disease is related to treatment. Even after surgical removal, application of chemo/radiotherapy combined with Temozolomide (TMZ), the mean survival rate of patients varies between 8 and 15 months after diagnosis [2]. GBM's unsatisfactory results on therapies are linked with alteration of complex signaling pathways to ensure cell survival [3].

Mitochondria play essential roles in cancer genesis, maintenance, and cell fate. It is also responsible for tumoral hallmarks by metabolic reprogramming and flexibility. Cancer cells undergo a metabolic reprogramming, by increasing aerobic glycolysis (Warburg effect) and decreasing oxidative phosphorylation (OXPHOS), concomitant with alterations in the citric acid cycle (TCA). Mitochondria is also termed the "motor of cell death" because of the decisive role in programmed cell death by regulating redox and ion signaling [3, 4].

Polysaccharides are polymers from natural sources (plants, fungi, bacteria, among others) with diverse biological effects, presenting advantageous characteristics of having fewer side effects compared to other cancer treatments in healthy cells [5]. Macroalgae represent a biotechnological source of polysaccharides because of their fast growth and easy cultivation [6]. Green macroalgae-derived polysaccharides (ulvans, heterorhamman) are not as well studied as red and brown-derived polysaccharides since they have complex structures and do not have many industrial applications [7]. Polysaccharides from macroalgae can present antitumoral effects by affecting mitochondria. Recent findings showed sulfated carrageenan extracted from *Laurencia papillosa* (red macroalga) was able to provoke apoptosis by increasing reactive oxygen species (ROS) production and releasing cytochrome-c from mitochondria, in MDA-MB-231 human breast cancer cells [8].

Chemical modification of polysaccharides is a strategy to increment biological effects since native molecules sometimes do not reach a satisfying pharmacological result. Biological effects of polysaccharides are directly linked to the chemical composition, *i.e.* the presence of groups sulfate, uronic acids, and others; and their molecular structure, *i.e.* molar mass solution, conformation, and others [9]. A recent study of our group generated a chemically modified form of the native sulfated heterorhamman from green macroalga

*Gayralia oxysperma*, using the Smith-controlled reaction (reducing the polysaccharide's size chain) [10]. This modified polysaccharide has induced an alteration of the expression of *p21* and *p53* genes, and increased the G1 phase of the cell cycle in U87MG glioblastoma cells. Mazepa, Nosedá, Ferreira, de Carvalho, Gonçalves, Ducatti, Bellan, Gomes, Trindade, Franco, Pellizzari, Winnischofer and Duarte [11] increased the sulfate content by chemical sulfation of another heterorhamman extracted from *Gayralia brasiliensis*. This modified heterorhamman reduced the cell viability of U87MG cells, possibly by apoptosis-related mechanisms. Therefore, our current study aims to further investigate the molecular mechanisms underlying the cell death response caused by the oversulfated heterorhamman from *Gayralia brasiliensis*, with a focus on the mitochondrial function in the glioblastoma U87MG cells.

## 2. Material and methods

### 2.1 Gb1 and Gb1-OS preparation

Gb1 and Gb1-OS stock solutions were prepared as previously described by Mazepa, Nosedá, Ferreira, de Carvalho, Gonçalves, Ducatti, de, Gomes, da, Franco, Pellizzari, Winnischofer and Duarte [11].

### 2.2 Cell viability MTT assay

Cell viability assays were performed using U87MG and U251 cells, kindly provided by Dr. Frank Kruyt (University of Groningen) and Dr. Mari C. Sogayar (University of São Paulo). The cells were Mycoplasma negative and we used them in passage number 48. Adherent cells were cultivated in DMEM (Gibco, Thermo Fisher Scientific, the Netherlands) and supplemented with 10% fetal bovine serum (Gibco, Thermo Fisher Scientific, the Netherlands) and incubated at 37 °C, 5 % CO<sub>2</sub>. For experiments, cells were first seeded at 4x10<sup>3</sup> cells/well, for 24 h, in a 96 well plate. For Gb1 and Gb1-OS treatments, cells were treated in the absence (control-vehicle H<sub>2</sub>O) or presence of polysaccharide (Gb1 and Gb1-OS) at concentrations of 50, 100, 150, and 200 µg. mL<sup>-1</sup> for 24, 48 and 72 h at 37 °C and 5 % CO<sub>2</sub>. Cell viability was evaluated using MTT (3-[4,5-dimethylthiazol-2-yl]- 2.5 diphenyl-tetrazolium bromide by Sigma-Aldrich (St. Louis, MO, USA) according to Ruijter, Ramakers, Hoogaars, Karlen, Bakker, van den

Hoff and Moorman [12]. Absorbance was measured by spectrophotometry using microplate reader Bio-Tek Synergy H1 hybrid reader model (Biotek, LA, USA) at 570 and 630 nm. Non-treated cells are used as the control and were normalized to 100 % of cell viability. Cell viability was determined by comparing the percentage of control cells with the treatment, using quadruplicates in each independent experiment. Three independent experiments were performed.

### *2.3 Annexin/PI assay*

Annexin V (ann V) and propidium iodide (PI) technique was performed. Dead-cell kit with Annexin V and PI was purchased from Invitrogen Thermo Fisher Scientific (Carlsbad, CA, USA). After 72 h of 100  $\mu\text{g. mL}^{-1}$  treatment with Gb1, Gb1-OS, and control cells ( $4 \times 10^4$  p/well in a p24 plate) were collected and centrifuged. Treated pellets were resuspended in binding buffer and stained with ann V and PI. As positive control for double staining, DMSO 10 % v/v well was used (Dimethyl sulfoxide (DMSO,  $\geq 99\%$ )). Samples were run in a Beckman Coulter CytoFLEX S Flow Cytometer (Beckman Coulter, Woerden, the Netherlands). The data were analyzed with FlowJo 10.5 software by BD life Sciences (Franklin Lakes, NJ, USA).

### *2.4 Measurement of mitochondrial membrane potential and mitochondrial superoxide production*

For both assays, U87MG cells were treated with Gb1-OS 100  $\mu\text{g. mL}^{-1}$  for 72 h. The seeding density of U87MG cells was similar as in the section 2.3. To evaluate the mitochondrial membrane potential (MMP), tetramethylrhodamine-ethyl ester (TMRE) was used. Cells were collected, centrifuged and, incubated for 30 min at 37 °C with 200 nM of the TMRE dye. For the measurement of mitochondrial superoxide production, U87MG cells were treated with Gb1-OS 100  $\mu\text{g. mL}^{-1}$  for 72 h and incubated at 37 °C with 2.5  $\mu\text{M}$  Red Mitochondrial Superoxide Indicator (MitoSOX) dye for 30 min. Both fluorescences were excited at 488 nm and detected at 690/50 nm using Beckman Coulter CytoFLEX S Flow Cytometer. TMRE and MitoSOX dyes were purchased from Fisher Scientific (Landsmeer, Netherlands).

## 2.5 High-resolution respirometry

Respiration of intact U87MG cells ( $1 \times 10^6$  cells) were analyzed by high-resolution respirometry with the oxygraphy-2K (OROBOROS INSTRUMENTS, Innsbruck, Austria). The assay was performed as described by Brandt, Gozzi, Pires Ado, Martinez, Dos Santos Canuto, Echevarria, Di Pietro and Cadena [13]. Antimycin, Carbonyl cyanide p-trifluoromethoxyphenylhydrazone (FCCP), Oligomycin, Rotenone were purchased from Sigma-Aldrich (St. Louis, MO, USA).

## 2.6 Statistical analyses

Shapiro-Wilk normality test was used to verify the distribution of data. Significant differences were determined using a one-way analysis of variance (ANOVA). Differences between mean values were tested using Tukey's posthoc test. Data with  $p < 0.05$  were considered statistically significant. All graphs were generated using GraphPad - Prism 8 version from GraphPad Software Inc (San Diego, CA, USA).

# 3. Results

## 3.1 Polysaccharide structure

Recently our group isolated and characterized a sulfated polysaccharide heterorhamman from *Gayralia brasiliensis* [11]. This polysaccharide consisted mainly of rhamnose (<70 %), followed by glucose, uronic acids (galacturonic and glucuronic acids), xylose, and galactose units. The sulfate content of the polysaccharide was 29.3 %. The glycosidic linkages of this polysaccharide had multiple variations. Rhamnose presented (1→3,4), (1→2,3), (1→2,4) linkage and non-reducing terminals (NRT). Glucose has (1→4), (1→4,6) and NRT; uronic acids showed (1→2), (1→4) and (1→2,4); xylose presented (1→3), (1→4); galactose showed NRT.

In order to compare if the chemical modification could improve the biological effect on cancer cells, sulfate units were inserted at the polysaccharide backbone. The chemical sulfation consisted of substituting hydrogen from free hydroxyl groups of the chain, while leaving unchanged the main chain polysaccharide structure. The overall sulfate content was enhanced to approximately 2.5-fold higher of sulfated units. At rhamnose units, they

were primarily present at carbons 4 and 2. NMR spectrum could not identify sulfate positions of other saccharide units, since these signals were overlapped by the sulfate positions of the rhamnose units.

### *3.2 Gb1-OS affects the U87MG cell viability*

To observe Gb1 and Gb1-OS cellular effects, we used two different glioblastoma cell lines U87MG and U251, and a neuronal cell line, HT22 (mouse hippocampal neuronal-derived cell line). A kinetics performance with Gb1 and Gb1-OS were applied in concentrations ranging from 50 to 200  $\mu\text{g. mL}^{-1}$  for 24,48 and 72 h. Gb1 treatment mediated a minimal effect on the cell viability of U87MG cells (at 100, 150 and 200  $\mu\text{g. mL}^{-1}$ , at 72 h) (**Fig. 1**), while Gb1-OS reduced cell viability at all measured concentrations in U87MG cells following 72 h challenge (**Fig. 1 and 2a, b, c**). Interestingly, there was no significant alteration at any concentration or time point for Gb1 and Gb1-OS in HT22 or U251 cell lines (**Fig. 1 and 2d, e, f, and Fig. S1**). To assess whether the cell viability MTT assay, which is in fact measuring the metabolic activity of the cells, corresponds to a potential cell death mediated by Gb1-OS in U87MG cells, we performed FACS experiments with annexin V/PI. Analysis of the FACS data in glioblastoma cells challenged with Gb1 and Gb1-OS (100  $\mu\text{g. mL}^{-1}$ ) for 72 h showed an increase of cell death in U87MG cells challenged with Gb1-OS, from 17 (control cells) to 44.7 % (challenged cells) (**Fig. 2h**). Gb1 treatment did not cause any apoptotic effect in U87MG cells (**Fig. 1g, h**). Representative bright field images of U87MG cell morphology indicate that Gb1 treatment do not alter the cell morphology, while Gb1-OS largely affect the U87MG cell morphology and induced more rounded-shaped cells. These data corroborate with the cell metabolic MTT assay and FACS analysis of annexin V/PI, indicating that Gb1-OS treatment could initiate cell death pathways.

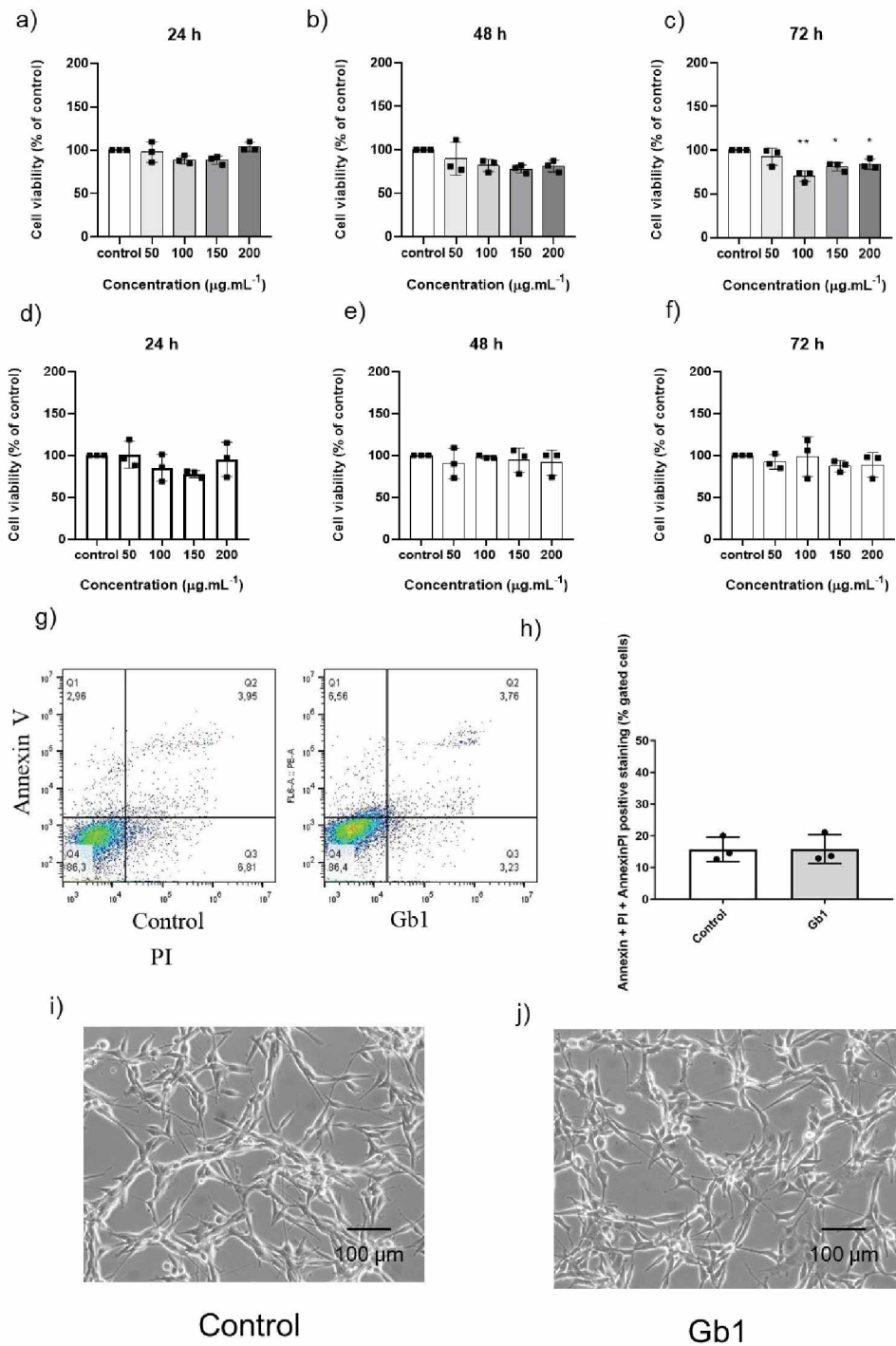


**Fig. 1** Cell viability assessed by an MTT assay in glioblastoma cell line U87MG a), b), c) and at hippocampus cell lines HT22 d), e), f) challenged with Gb1 (50; 100; 150 and 200  $\mu\text{g.mL}^{-1}$  for 24, 48, and 72 h). Control cells correspond to 100% of cells incubated only with DMEM medium. These results are expressed as mean  $\pm$  s.d., three independent experiments with four technical replicates ( $p < 0.05$ ). FACS analysis of the An/PI staining g), h) of U87MG cells challenged with Gb1 (100  $\mu\text{g.mL}^{-1}$  for 72 h). The values are expressed as mean  $\pm$  S.D., three independent experiments in triplicate, by ANOVA test with Tukey's h posthoc test. i-j) Bright-field images of U87MG glioblastoma cells cultivated in DMEM (control) and in the presence of Gb1 100  $\mu\text{g.mL}^{-1}$  for 72 h. Original magnification: 10x, with scale bar of 100  $\mu\text{m}$ .

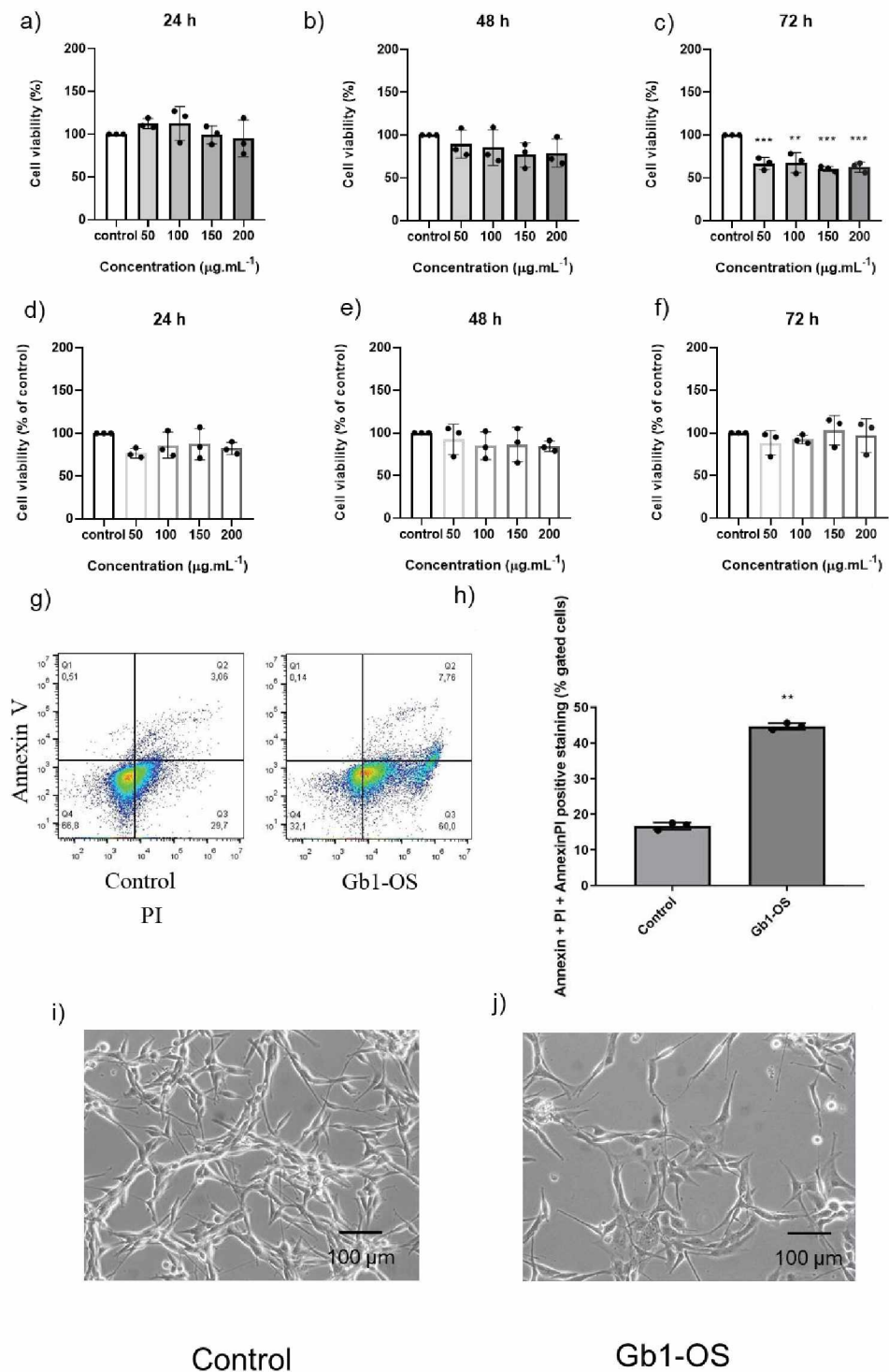


**Fig. 2** Cell viability assessed by an MTT assay in glioblastoma cell line U87MG a), b), c) and at hippocampus cell lines HT22 d), e), f) challenged with Gb1-OS (50; 100; 150 and 200  $\mu\text{g.mL}^{-1}$  for 24, 48, and 72 h). Control cells correspond to 100% of cells incubated only with DMEM medium. These results are expressed as mean  $\pm$  s.d., three independent experiments with four technical replicates ( $p < 0.05$ ). FACS analysis of the An/PI staining g), h) of U87MG cells challenged with Gb1-OS (100  $\mu\text{g.mL}^{-1}$  for 72 h). The values are expressed as mean  $\pm$  S.D., three independent experiments in triplicate, by ANOVA test with Tukey's h posthoc test. i-j) Bright-field images of U87MG glioblastoma cells cultivated in DMEM (control) and in the presence of Gb1-OS 100  $\mu\text{g.mL}^{-1}$  for 72 h. Original magnification: 10x, with scale bar of 100  $\mu\text{m}$ .

Marine macroalgae produce sulfated polysaccharides as an adaptation against the environment's ionic state [14]. They are anionic polysaccharides, and their composition and structure are highly variable and complex. The structural differences can be attributed to the monosaccharide constituents, linearity of their backbones, uronic acid residues, homogeneity, and sulfate content. Environmental factors and gene expression of each phyllo are responsible for the different polysaccharide biosynthesis of each macroalga. *Gayralia brasiliensis* belongs to *Chlorophyta* phyllo (green macroalgae) and to the Ulotrichales order. This order produces sulfated polysaccharides with significant amounts of rhamnose and uronic acids on their backbone, varying on the quantities and positions of sulfate units [14].

Although *Gayralia oxysperma* and *Gayralia brasiliensis* are macroalgae from Ulotrichales order, their derived sulfated heterorhamman contain significant differences in their structure and function. The polysaccharide derived from *Gayralia oxysperma* is composed of rhamnose 2- and 3-linked at the backbone, with non-reducing terminals containing uronic acids and xylose, with approx. 26 % of sulfate content [15]. *Gayralia brasiliensis*-derived polysaccharides contain a rhamnose backbone, linked in different positions and other monosaccharide units, as described before [11]. Different structures and contents of sulfate units are correlated with the biological effect [16]. A recent study generated a reduced heterorhamman size chain of the polysaccharide extracted from *Gayralia oxysperma*, separating it into two homogenous fractions, and resulting into an increased percentage of sulfate units in each fraction (33.5 and 41 %, respectively, compared to 26 % of the crude polysaccharide). When comparing the products, the polysaccharide fractions with a higher percentage of sulfate mediated a higher cytotoxic action in U87MG cells [10].

Gb1 and Gb1-OS polysaccharides showed to elicited differential effects between glioblastoma lines. These effects could be related to the intertumoral heterogeneity of glioblastoma [2] and attributed to the role of specific gene and cell phenotype that are dependent on glioblastoma degree and progression status [17]. Indeed, the transcriptome analysis of three different types of glioblastoma cell lines (U87MG, U251, and U373) and their responses following the temozolomide (TMZ) treatment showed a differential gene expression [18]. U87MG cells present an increased cell death susceptibility to TMZ treatment, exhibit a more proliferative profile, and overexpress the genes related to the cell cycle, *i.e.* the G protein-coupled receptor 84 (GPR84), when compared with U251 and U373 cells. U251/U373 cell lines show a lower proliferative rate, while they are less

vulnerable to TMZ treatment. The differential effects among these glioblastoma cells could be attributed to the high expression of genes related to cell survival in U251 and U373 cells, including immediate early response 3 (IR3), and colony-stimulating factor 2 (CSF2), among others [18].

### *3.3 Gb1-OS hyperpolarizes mitochondrial membrane, enhances mitochondrial ROS production, suggesting a reduction in the activity of mitochondrial OXPHOS*

The mitochondrial function was further evaluated to delineate the cell death molecular pathways induced by Gb1-OS treatment in U87MG cells. Mitochondrial ROS levels and mitochondrial membrane potential were measured by mitoSOX and TMRE fluorescence, respectively. The analysis of the FACS data showed a higher production of mitochondrial ROS (depicted as mtROS) (**Fig. 3 a), b**) and a hyperpolarization state of mitochondrial membrane potential (**Fig. 3 c) and d**) caused by the Gb1-OS challenge when compared with control cells.

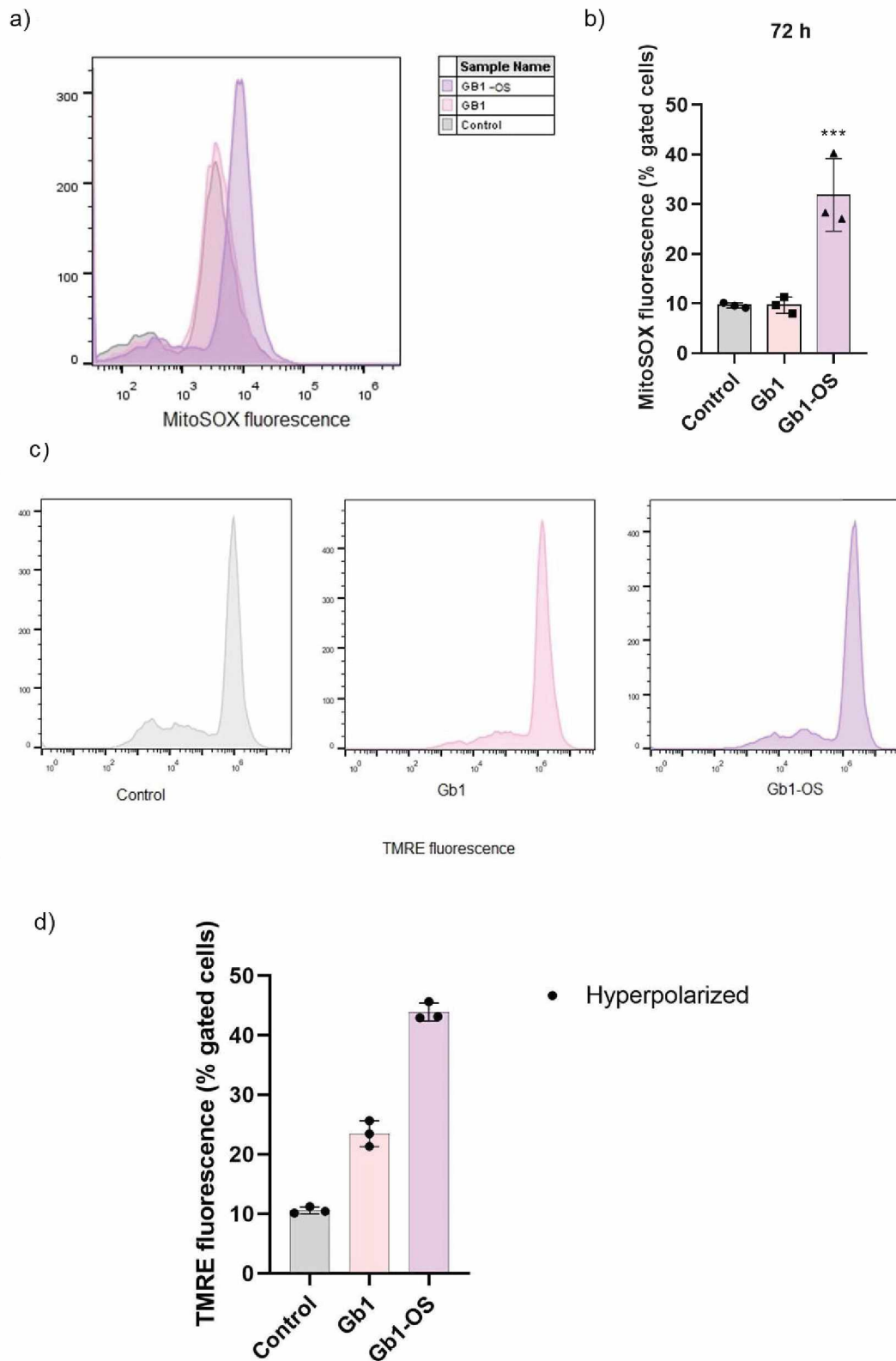


**Fig. 3** The effects of GB1 and Gb1-OS on the mitochondrial function. Mitochondrial superoxide levels a), b) and mitochondrial membrane potential c), d) of U87MG cells upon Gb1 and Gb1-OS treatment ( $100 \mu\text{g. mL}^{-1}$  for 72 h). MitoSOX and TMRE probes were used, and data was determined by FACS analysis. Data are presented as mean  $\pm$  SD, in triplicates, \*\*\* $p < 0.001$ . All experiments were performed independently three times.

Hyperpolarization of mitochondrial membrane and increased production of mitochondrial ROS can be related to ATP production by OXPHOS to support O<sub>2</sub> consumption/respiration [19]. Therefore, we then next performed high-resolution respirometry to evaluate the oxygen consumption using Oroboros oxygraphy. **Fig. 4** presents a representative experiment of the cell respiration measurement of U87MG cells in the presence or absence (a) of Gb1 (b), and Gb1-OS (c). Treatment with Gb1 and Gb1-OS induced a drop of oxygen flow, however the analysis of the cell respiration revealed that mostly Gb1-OS reduced the cell respiration status. We investigated the respiration states (basal, ATP-linked respiration, and uncoupled) in cells challenged with both Gb1 and Gb1-OS (**Fig. 5**). Analysis of the high-resolution respirometry data showed that only the treatment with Gb1-OS induced a significant drop in ATP-linked respiration, while the basal respiration state and uncoupled respiration states were not changed. In addition, Gb1 did not affect mitochondrial respiration of U87MG cells, further corroborating the MTT metabolic activity assay, the mitochondrial ROS and the mitochondrial potential data.

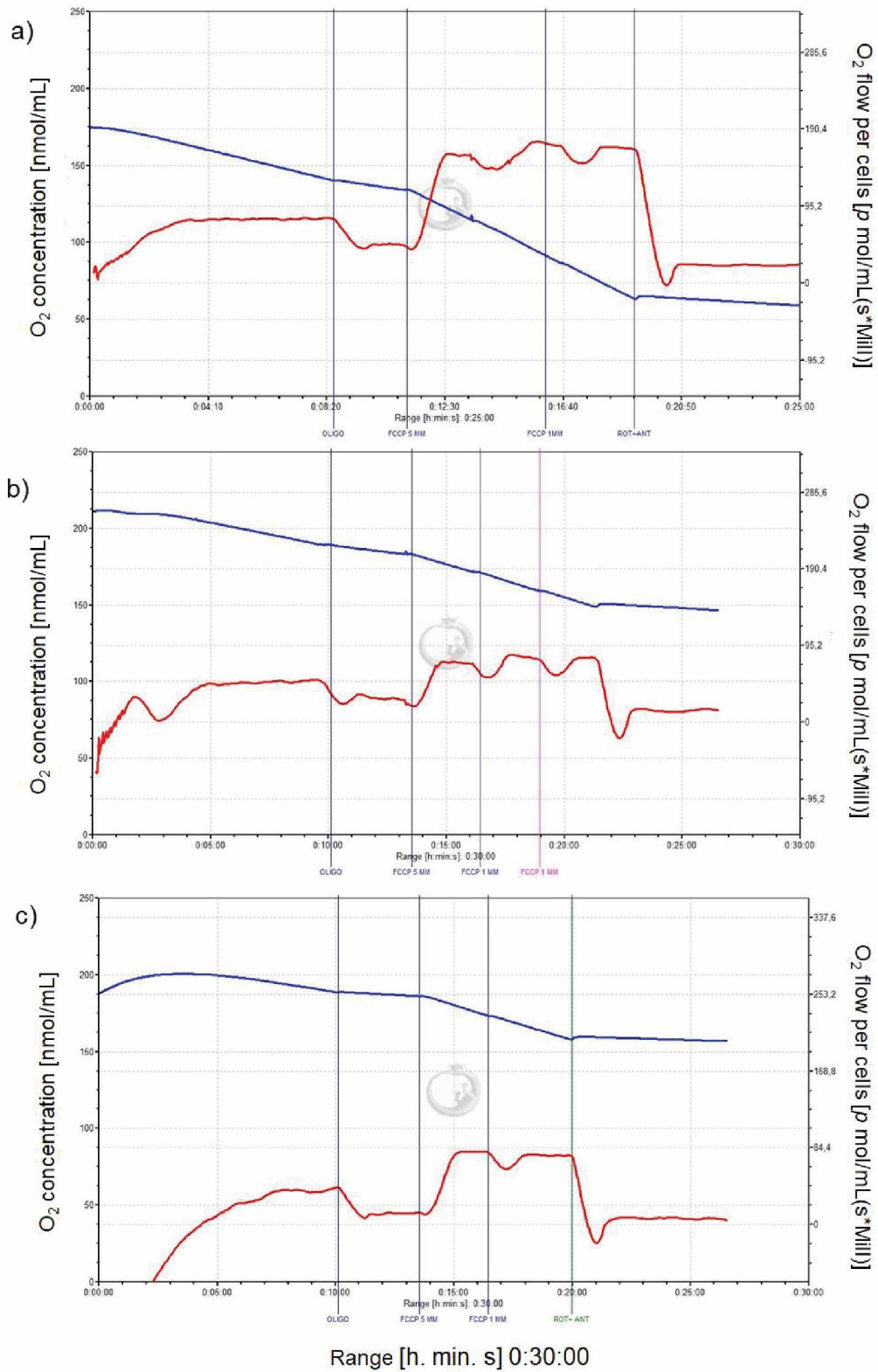


**Fig. 4** Representative image of U87MG cell respiration (control) a) and treated with Gb1 b), Gb1-OS c), at 100  $\mu\text{g} \cdot \text{mL}^{-1}$  for 72 h. Results were performed at OROBOROS-2K oxygraphy. Legends: OLIGO - oligomycin; ROT - rotenone; ANT - antimycin. Blue line: oxygen concentration; Red line: oxygen flow.

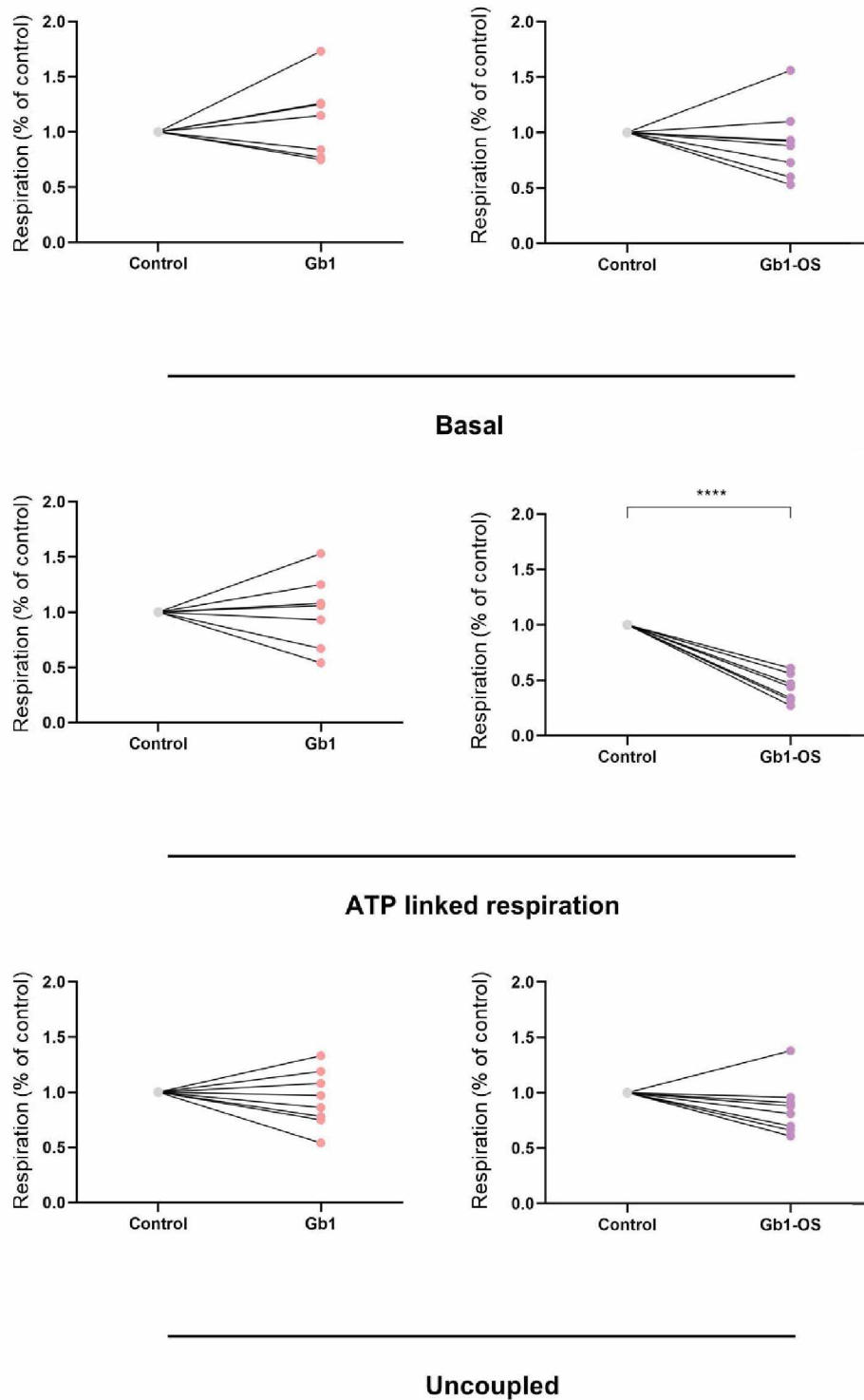


**Fig. 5** Analysis of high-resolution respirometry of the treatment of Gb1 and Gb1-OS in U87MG cells. The respiration states: Basal a), ATP linked b), and Uncoupled c). Treatment of the cells with the polysaccharides were at  $100 \mu\text{g. mL}^{-1}$  for 72 h. The results were displayed as a paired plot, showing respiration (in  $\text{pmolO}_2/\text{mg protein}$ ), normalized by the control. Values represent the mean  $\pm$  S.D. of three independent experiments. Values significantly different from the control at \*\*\*\* $p < 0.001$ .

Mitochondria is responsible for many essential cellular processes. One of them is related to the production of the cell energy, OXPHOS being the final step of glucose oxidation to produce adenosine triphosphate (ATP). OXPHOS operates with the electron transport chain (ETC) complex and uncoupling protein, using mitochondrial matrix and intercellular space. The ETC oxidizes the nicotinamide adenine dinucleotide (NADH) and flavin adenine dinucleotide (FADH<sub>2</sub>) co-enzymes to return them to the TCA cycle. Via the oxidation reaction, at the ETC complex, protons are pumped to the intermembrane space, creating a membrane potential. So, the protons at the intermembrane space returns to the mitochondrial matrix through the F<sub>0</sub>F<sub>1</sub>-ATP-synthase (complex V), coupling with adenosine diphosphate (ADP) to form ATP. The electrons from the oxidation reaction are transferred through the ETC complex (I, II, III and, IV) and couple with O<sub>2</sub>. This reaction typically forms H<sub>2</sub>O, but some of the electrons do not couple, which could result in mtROS. So, for the best functioning of OXPHOS and maintenance of cellular homeostasis, mitochondria need to find a balance between the operation of the proton pump and electron discharge [19].

Based on the analysis of the cellular O<sub>2</sub> consumption results, Gb1-OS diminished overall cellular respiration, significantly affecting the ATP-linked respiration. The F<sub>0</sub>F<sub>1</sub>-ATP-synthase enzyme transports protons from the intermembrane to the mitochondrial matrix, allowing ATP formation and stabilizing membrane potential. The protons cannot leave the intermembrane space when there is a dysfunction of this enzyme or any others from ETC complex I-IV and the adenine nucleotide translocase (ANT). This leads to a hyperpolarization of the mitochondrial membrane, and it is harmful to the organelle. Hyperpolarization status significantly produces more mtROS since there is lower hydrogen coupling with oxygen [20].

Mitochondrial antioxidant enzymes such as glutathione, thioredoxin, and pyridine nucleotide redox couples can neutralize a certain level of mtROS. Yet still, excessive mtROS can go to the cytosol and oxidate essential cellular macromolecules as lipids, proteins, or DNA. With that, cytochrome c and apoptosis-inducing factors can be released to the cytosol and trigger the intrinsic apoptosis pathway [21].

Chemical modification of polysaccharides and their potential effects on cancer cell's respiration have been previously studied. A xyloglucan complexed with oxovanadium was shown to induce a reduction of murine melanoma (B16-F10) viability [22]. This polysaccharide was able to diminish the basal and uncoupled state of cell respiration. Another study used the same polysaccharide as mentioned above and showed a reduced

cell viability of hepatocarcinoma (HepG2) cells [23]. In HepG2 cells, the treatment with this polysaccharide induced a decreased mitochondrial membrane potential and the basal cell respiration. A treatment with galactomannan (composed of galactose and mannose) complexed with oxovanadium induced a depolarization of the mitochondrial membrane, an increase of mtROS and of all states of the cell respiration in HepG2 cells [24].

Furthermore, a sulfation at a galactomannan polysaccharide resulted in a low level of sulfate units (one sample had 6.2 % and the other had 8.2 % of sulfate group [25]). Treatment of HepG2 cells with this modified polysaccharide led to different responses of cell respiration states. The polysaccharide with the lowest sulfate group affected all respiration states, especially uncoupled respiration. Interestingly, the polysaccharide with high sulfate units also affected all cell respiration states [25], indicating that sulfation process, in general, affect cell respiration.

Cytotoxic effects of polysaccharides rely on their chemical structure and sulfate unit levels [9], [25]. Backbone chain monosaccharide composition, as well the glycosylic bound, molar mass, and sulfate content could differentially affect cell viability, as mentioned in previous studies. The sulfation reaction used by Cunha de Padua and colleagues [25] caused a degradation of the backbone chain, while Mazepa [11] sulfation method did not cause alteration at the main chain, as observed with HPSEC-MALLS-RID. Modifying structures of polysaccharides can compromise their biological effects by changing their interaction with specific receptors/proteins or how they can be internalized by cells [25].

A recent study by Li, Wei, Zhao, Yu, Huang and Li [26] showed very interesting results regarding a possible transport mechanism of a polysaccharide and accumulation in mitochondria. A Rhamnogalacturonan – I, from *Cucurbita Moschata*, was tested with Caco-2 cells (intestinal epithelium cells). This polysaccharide has a molecular weight average of  $2.26 \times 10^5$  g.mol<sup>-1</sup> (Gb1-OS ranges between  $1.81 \times 10^5$  and  $2.19 \times 10^6$  g.mol<sup>-1</sup>). The authors inserted Fluorescein Isothiocyanate (FITC) at the polysaccharide, without modifying the structure. The study suggests that polysaccharide with concentration ranges varying between 250 - 1500  $\mu\text{g mL}^{-1}$ , showed it was moderately-absorbed at the cells, with the highest absorption peak of 1 h. The entrance route seems to be by the clathrin/caveolin, as pointed out by the flow-cytometry results. Normal cells containing inhibitors of clathrin-related route as Dynasore, Chlorpromazine and M $\beta$ CD; and cells transfected with gene silencing clathrin heavy chain siRNA (CLTC), dynamin II (DNM2) siRNA, caveolin-1 (CAV1) siRNA significantly decrease their fluorescence, when

compared with control. Cells with the fluorescent polysaccharide were also stained with Hoechst 33342 (nucleus), EndoTracker (endoplasmic reticulum, ER) and MitoTracker (mitochondria) and were observed at a Laser scanning fluorescent microscope. Images showed the polysaccharide was accumulated at the RE and mitochondria, by FITC and Endo/MitoTracker fluorescence overlap in the cells.

The effect of Gb1-OS at mitochondria can be hypothesized by the link of sulfate with iron-sulfur clusters (FeS) at ETC complex I [27]. Forkink, Manjeri, Liemburg-Apers, Nibbeling, Blanchard, Wojtala, Smeitink, Wieckowski, Willems and Koopman [20] showed that the inhibition of ETC complex I could leave unaffected the oxidative phosphorylation process, while it could enhance glycolysis in kidney embryonic (HEK293) cells [20]. Mitochondrial complex I inhibition could lead to a prominent inhibition of O<sub>2</sub> consumption. This triggers the low activity of complexes III and IV (that reduced matrix proton efflux), F<sub>0</sub>F<sub>1</sub>-ATP-synthase (reduced proton influx), and ANT (reduced mediated influx of positive charge), resulting in the hyperpolarization status. These observations corroborate our results.

#### **4. Conclusion**

The oversulfated heterorhamman isolated from *Gayralia brasiliensis* caused cell death in U87MG but not in U251 glioblastoma cells. U87MG cells treated with Gb1-OS show a decrease in the cell respiration and enhanced mitochondrial ROS. Further studies are necessary to observe the effects of this polysaccharide in U87MG glioblastoma cells.

#### **Acknowledgments**

This work was supported by Fundação Araucária/CNPq (PRONEX-Carboidratos), MCT/CNPq/CT-PETRO, CNPq and CAPES. M.T.L. was a recipient of CAPES (Process # 88887.321693/2019-00). T.R.M. acknowledges a doctoral scholarship from CAPES (Process # 88882.344138/2019-01), a doctoral sandwich scholarship from the CAPES PrInt program (Process # 88887.468902/2019-00). M.E.D., M.D.N., and S.M.B.W. are Research Members of the National Research Council of Brazil (CNPq). A.M.D. is the recipient of a Rosalind Franklin Fellowship co-funded by the European Union and the University of Groningen. The authors acknowledge the NMR Center of Federal University of Paraná (UFPR) for the NMR data acquisition and also Dr. Frank

Kruyt from Rijkuniversiteit Groningen (RUG) for kindly providing the U87MG and U251 cell lines.

### Conflicts of Interest

The authors declare no conflict of interest.

### CRedit authorship contribution statement:

Conceptualization, T.R.M, M.T.L., S.M.B.W., A.M.D., M.E.D., and M.D.N.; Data collection, T.R.M, M.T.L., and M.L.C.F. Data analysis and interpretation, T.R.M, M.T.L., M.L.C.F., E.M., S.M.B.W., S.M.S.C.C., A.M.D, M.E.D, and M.D.N.; Drafting the article, T.R.M.; Critical revision of the article, M.T.L., M.L.C.F., E.M., S.M.B.W., S.M.S.C.C., A.M.D, M.E.D and M.D.N. Final approval of the version to be published, T.R.M, M.T.L., M.L.C.F., E.M., S.M.B.W., S.M.S.C.C., A.M.D, M.E.D and M.D.N. Project Administration, M.D.N., M.E.D., S.M.S.C.C., and A.M.D.; Funding Acquisition, M.D.N., M.E.D., S.M.S.C.C., and A.M.D. All the authors have read, approved, and made substantial contributions to the manuscript.

### References

- [1] F. Bray, J. Ferlay, I. Soerjomataram, R.L. Siegel, L.A. Torre, A. Jemal, Global cancer statistics 2018: GLOBOCAN estimates of incidence and mortality worldwide for 36 cancers in 185 countries, *CA: A Cancer Journal for Clinicians*, 68 (2018) 394-424.
- [2] K. Anjum, B.I. Shagufta, S.Q. Abbas, S. Patel, I. Khan, S.A.A. Shah, N. Akhter, S.S.U. Hassan, Current status and future therapeutic perspectives of glioblastoma multiforme (GBM) therapy: A review, *Biomedicine & pharmacotherapy = Biomedecine & pharmacotherapie*, 92 (2017) 681-689.
- [3] M.B. Leão Barros, D.D.R. Pinheiro, B.D.N. Borges, Mitochondrial DNA Alterations in Glioblastoma (GBM), *International journal of molecular sciences*, 22 (2021).
- [4] L. Guntuku, V.G. Naidu, V.G. Yerra, Mitochondrial Dysfunction in Gliomas: Pharmacotherapeutic Potential of Natural Compounds, *Curr Neuropharmacol*, 14 (2016) 567-583.
- [5] A.S.A. Mohammed, M. Naveed, N. Jost, Polysaccharides; Classification, Chemical Properties, and Future Perspective Applications in Fields of Pharmacology and Biological Medicine (A Review of Current Applications and Upcoming Potentialities), *Journal of polymers and the environment*, (2021) 1-13.
- [6] S. García-Poza, A. Leandro, C. Cotas, J. Cotas, J.C. Marques, L. Pereira, A.M.M. Gonçalves, The Evolution Road of Seaweed Aquaculture: Cultivation Technologies and the Industry 4.0, *International Journal of Environmental Research and Public Health*, 17 (2020) 6528.
- [7] V. Stiger, N. Bourgougnon, E. Deslandes, Chapter 8 - Carbohydrates From Seaweeds. , in: I.L. Joël Fleurence (Ed.) *Seaweed in Health and Disease Prevention*, Academic Press, 2016.
- [8] H. Murad, M. Hawat, A. Ekhtiar, A. AlJapawe, A. Abbas, H. Darwish, O. Sbenati, A. Ghannam, Induction of G1-phase cell cycle arrest and apoptosis pathway in MDA-MB-231 human breast cancer cells by sulfated polysaccharide extracted from *Laurencia papillosa*, *Cancer Cell International*, 16 (2016) 39.
- [9] L. Xie, M. Shen, Y. Hong, H. Ye, L. Huang, J. Xie, Chemical modifications of polysaccharides and their anti-tumor activities, *Carbohydr Polym*, 229 (2020) 115436.
- [10] J. Ropellato, M.M. Carvalho, L.G. Ferreira, M.D. Nosedo, C.R. Zuconelli, A.G. Goncalves, D.R.B. Ducatti, J.C.N. Kenski, P.L. Nasato, S.M.B. Winnischofer, M.E.R. Duarte, Sulfated heterorhamnans from the green seaweed *Gayralia oxysperma*: partial depolymerization, chemical structure and antitumor activity, *Carbohydrate polymers*, 117 (2015) 476-485.
- [11] E. Mazepa, M.D. Nosedo, L.G. Ferreira, M.M. de Carvalho, A.G. Goncalves, D.R.B. Ducatti, L.B.D. de, R.P. Gomes, S.T.E. da, C.R.C. Franco, F.M. Pellizzari, S.M.B. Winnischofer, M.E.R. Duarte, Chemical

- structure of native and modified sulfated heterorhamnans from the green seaweed *Gayralia brasiliensis* and their cytotoxic effect on U87MG human glioma cells, *Int J Biol Macromol*, 187 (2021) 710-721.
- [12] J.M. Ruijter, C. Ramakers, W.M. Hoogaars, Y. Karlen, O. Bakker, M.J. van den Hoff, A.F. Moorman, Amplification efficiency: linking baseline and bias in the analysis of quantitative PCR data, *Nucleic Acids Res*, 37 (2009) e45.
- [13] A.P. Brandt, G.J. Gozzi, R. Pires Ado, G.R. Martinez, A.V. Dos Santos Canuto, A. Echevarria, A. Di Pietro, S.M. Cadena, Impairment of oxidative phosphorylation increases the toxicity of SYD-1 on hepatocarcinoma cells (HepG2), *Chem Biol Interact*, 256 (2016) 154-160.
- [14] M. Ciancia, P.V. Fernández, F. Leliaert, Diversity of Sulfated Polysaccharides From Cell Walls of Coenocytic Green Algae and Their Structural Relationships in View of Green Algal Evolution, *Frontiers in Plant Science*, 11 (2020).
- [15] J.E. Cassolato, M.D. Nosedá, C.A. Pujol, F.M. Pellizzari, E.B. Damonte, M.E. Duarte, Chemical structure and antiviral activity of the sulfated heterorhamnan isolated from the green seaweed *Gayralia oxysperma*, *Carbohydr Res*, 343 (2008) 3085-3095.
- [16] Z. Wang, J. Xie, M. Shen, S. Nie, M. Xie, Sulfated modification of polysaccharides: Synthesis, characterization and bioactivities, *Trends in Food Science & Technology*, 74 (2018) 147-157.
- [17] J. Liu, H. Dang, X.W. Wang, The significance of intertumor and intratumor heterogeneity in liver cancer, *Exp Mol Med*, 50 (2018) e416.
- [18] H. Motaln, A. Koren, K. Gruden, Z. Ramsak, C. Schichor, T.T. Lah, Heterogeneous glioblastoma cell cross-talk promotes phenotype alterations and enhanced drug resistance, *Oncotarget*, 6 (2015) 40998-41017.
- [19] L.D. Zorova, V.A. Popkov, E.Y. Plotnikov, D.N. Silachev, I.B. Pevzner, S.S. Jankauskas, V.A. Babenko, S.D. Zorov, A.V. Balakireva, M. Juhaszova, S.J. Sollott, D.B. Zorov, Mitochondrial membrane potential, *Anal Biochem*, 552 (2018) 50-59.
- [20] M. Forkink, G.R. Manjeri, D.C. Liemburg-Apers, E. Nibbeling, M. Blanchard, A. Wojtala, J.A. Smeitink, M.R. Wieckowski, P.H. Willems, W.J. Koopman, Mitochondrial hyperpolarization during chronic complex I inhibition is sustained by low activity of complex II, III, IV and V, *Biochim Biophys Acta*, 1837 (2014) 1247-1256.
- [21] H. El-Osta, M.L. Circu, Mitochondrial ROS and Apoptosis, in: L.M. Buhlman (Ed.) *Mitochondrial Mechanisms of Degeneration and Repair in Parkinson's Disease*, Springer International Publishing, Cham, 2016, pp. 1-23.
- [22] C.L.A. Farias, G.R. Martinez, S. Cadena, A.L.R. Merce, C.L. de Oliveira Petkowicz, G.R. Noleto, Cytotoxicity of xyloglucan from *Copaiifera langsdorffii* and its complex with oxovanadium (IV/V) on B16F10 cells, *Int J Biol Macromol*, 121 (2019) 1019-1028.
- [23] L. Escalante, B. Busato, C.L.O. Petkowicz, S. Cadena, G.R. Noleto, Cytotoxic effect of xyloglucan and oxovanadium (IV/V) xyloglucan complex in HepG2 cells, *Int J Biol Macromol*, 185 (2021) 40-48.
- [24] M.M. Cunha-de Padua, S.M. Suter Correia Cadena, C.L. de Oliveira Petkowicz, G.R. Martinez, M.E. Merlin Rocha, A.L.R. Merce, G.R. Noleto, Toxicity of native and oxovanadium (IV/V) galactomannan complexes on HepG2 cells is related to impairment of mitochondrial functions, *Carbohydrate polymers*, 173 (2017) 665-675.
- [25] M.M. Cunha de Padua, S.M. Suter Correia Cadena, C.L. de Oliveira Petkowicz, G.R. Martinez, G. Rodrigues Noleto, Galactomannan from *Schizolobium amazonicum* seed and its sulfated derivatives impair metabolism in HepG2 cells, *Int J Biol Macromol*, 101 (2017) 464-473.
- [26] F. Li, Y. Wei, J. Zhao, G. Yu, L. Huang, Q. Li, Transport mechanism and subcellular localization of a polysaccharide from *Cucurbita Moschata* across Caco-2 cells model, *Int J Biol Macromol*, 182 (2021) 1003-1014.
- [27] D. Nolfi-Donagan, A. Braganza, S. Shiva, Mitochondrial electron transport chain: Oxidative phosphorylation, oxidant production, and methods of measurement, *Redox Biol*, 37 (2020) 101674.

## Supplemental Data

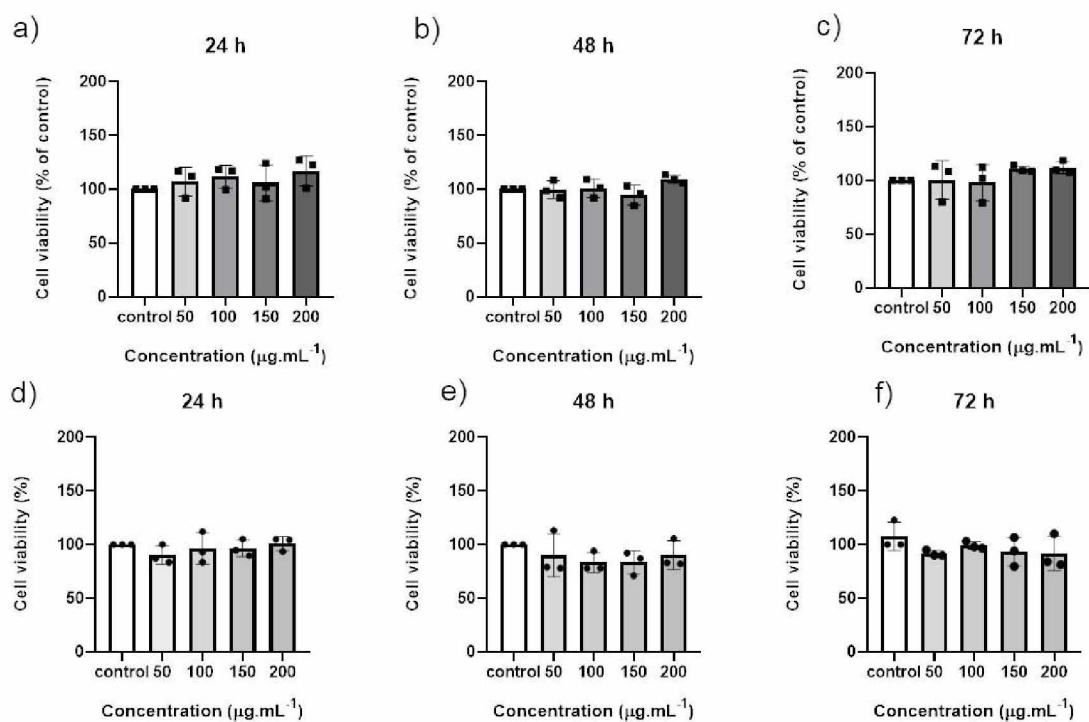


**Fig. S1** Cell viability at hippocampus cell lines HT22 with Gb1 a), b), c) and Gb1-OS d), e), f). Concentrations of 50; 100; 150 and 200  $\mu\text{g.mL}^{-1}$  at timepoints of 24, 48 and 72 h. Control corresponds to 100% of cells incubated at DMEM medium. These results are expressed as mean  $\pm$  s.d., three independent experiments with 4 technical replicates, with statistical significance ( $p < 0.05$ ).

## 5. DISCUSSION

Polysaccharides represent the major biopolymer group produced by natural resources, including algae, fungi, bacteria, and plants. Polysaccharides contain extensive chains of twenty or more sequences of polyhydroxy aldehydes or polyhydroxy ketones bound together. Since at least twenty monosaccharides could be linked in different ways, the combination of different polymers can reach billions. The structure-activity relationship of polysaccharides in biological models is still not well defined, and this can be attributed to their differences in building their structures (MOHAMMED et al., 2021).

Polysaccharides' structure in solution directly depends on their physical-chemical properties, such as the monosaccharide composition, glycosylic bound, the amount of specific functional groups, molecular weight, ramifications, and the molecular conformation. The monosaccharide composition rules the primary structure, and the secondary structure depends on the organization of oligosaccharide units at the chain (HARDING et al., 2017). Tertiary structures depend on the rotational degree of freedom from the glycosidic bond. The molecular weight of polysaccharides also modulates the polysaccharide's tertiary structures since this represents the most crucial physical propriety regarding polysaccharide behavior in solutions. The molecular weight will influence the polysaccharide's hydrodynamic parameters (intrinsic viscosity, gyration radius, diffusion coefficient) and shape the conformation that the molecule can acquire in solution. A quaternary structure can also be formed when an interchain complex is connected with another ligand or molecule (HARDING et al., 2017).

Polysaccharides' chemical modification is an interesting field to study, and the insertion method can modify molecular weight and affect the polysaccharide's structure and response. The tertiary structures represent an essential factor in addressing and understanding their biological activity since they determine the interactions of proteins and polysaccharides (HARDING et al., 2017). Several findings on the association between polysaccharides chemical structure and their biological effects will be further described below.

Cells exhibit a pattern of oligosaccharides on their surface membrane, associated with protein and lipids. Those molecules are essential for many physiological functions since they are responsible for cell-cell, cell-matrix communications, cell adhesion, cell differentiation, signaling, and others. Cells also present surface proteins that bind with various degree of specificity from high to moderate affinity for saccharides, termed carbohydrate-binding receptors (CHEN *et. al.*, 2017; KIM, RAHHAL, & RADEMACHER, 2021).

In **chapter 1**, the microalgae from Bacillariophyta phylum *Conticribra weissflogii* formed another linear (1→3)-linked β-D-glucan. Those β-glucans are widespread in microalgae, classified as reserve polysaccharides (located at the cell wall) called laminarans. Carbohydrate-

binding receptors (**Fig. 1**) are present in normal and cancer cells.  $\beta$ -D-glucans can bind to carbohydrate receptors as lectins, toll-like (TLR), scavengers, and complement receptor 3 (CR3). This chapter showed that the linear  $\beta$ -D-glucan had an immunostimulatory effect on macrophages. Polysaccharides are well known in the literature to produce this effect by binding to macrophages, dendritic cells, and other immune cells through those receptors. By that, immune cells decode the polysaccharide's particular carbohydrate sequence and activate signaling pathways for immunostimulation, causing cytokine release, cell maturation, and other actions (KIM et. al., 2021).

As polysaccharides bind to receptors, signaling pathways are activated to elicit biological effects. The immunostimulatory effect of the  $\beta$ -D-glucan in macrophages presented in **chapter 1** is an example of that. In macrophages, when glucans bind lectins and CR3, they will trigger activation of a series of signaling proteins, such as the phosphatidylinositol-3 kinase (PI3K), followed by protein kinase B (Akt) and p38mitogen-activated protein kinase (MAPK). By those signaling proteins, there is an activation and release of cytokines and cell differentiation as the reactive oxygen species (ROS), interleukins (IL), gamma-interferon ( $\gamma$ -IFN), tumoral necrosis factor (TNF- $\alpha$ ), among others (FERREIRA, PASSOS, MADUREIRA, VILANOVA, & COIMBRA, 2015).

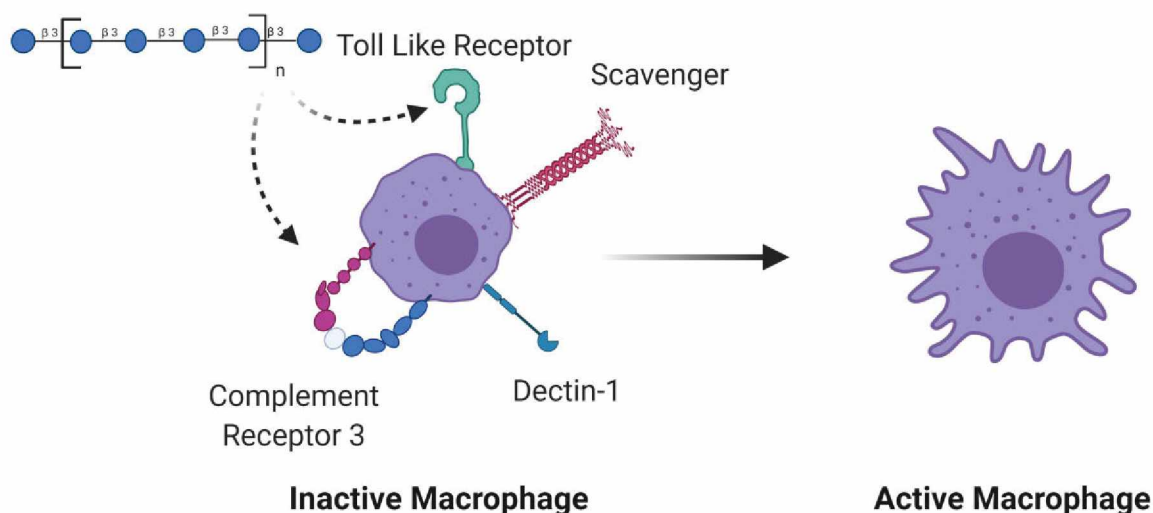


**Fig. 1:**  $\beta$ -D-glucan immunostimulatory effect.  $\beta$ -D-glucan from *Conticribra weissflogii* microalga binds with carbohydrate receptors at the cell surface of macrophages. After binding, cell signaling is triggered, activates macrophages, and leads to immunostimulatory effect. Adapted from "How Dendritic Cells Become Competent to Stimulate T Cells" by BioRender.com (2021). Retrieved from <https://app.biorender.com/biorendertemplates>.

In **chapter 2**, we describe another type of polysaccharide isolated from *Isochrysis galbana* microalgae containing a (1 $\rightarrow$ 3)-linked  $\beta$ -D-glucan backbone with branches of

(1→3),(1→6)-linked. In **chapter 3**, a sulfated heterorhamman was extracted from the macroalgae *Gayralia brasiliensis* (phylum *Chlorophyta*) and later chemically modified to enhance the sulfate content to potentially increase the polymer's biological effect. Rhamnose was the main unit present (~70 %), followed by glucose, uronic acids, xylose, and galactose units. The glycosidic linkage between the rhamnose units varied, dependent on the source of algae. Those polysaccharides were tested in glioblastoma cell lines and diminished mitochondrial metabolism (**chapter 2**), and induced cell death (**chapter 3**).

Regarding the direct polysaccharide's effects on cancer cells, one of the possibilities for those effects is the regulation of signal pathways transduction and gene expressions (CHEN & HUANG, 2018). One of the hypotheses is based on the binding affinity of the polysaccharides to the carbohydrate-binding receptors', as it was shown in immune cells. Glioblastoma cells overexpressing carbohydrate receptors such as TLR 2 and 4, and lectins (Biray Avci et al., 2016; T. Chen et al., 2019; Polisetty et al., 2016; Sarrazy et al., 2011). XU *et al.* (2017) showed that the  $\beta$ -D-glucan from *Lentinus edodes* was able to inhibit PI3K pathways (PI3K/Akt/MDM2/p53 and PI3K/Akt/mTOR), to activate the ERK-dependent pathway and caspase-3, along with inducing cell cycle arrest at G2/M phase via MDM2/p53- and ER $\alpha$ -dependent pathways, in MCF-7 cells. In **chapter 3**, the heterorhamman interaction could also be related to those receptors by the action of glucose and galactose units. There is no specific receptor for the rhamnose unit in human glycoproteins (**Fig. 2**).

Another hypothesis can be related to intermolecular interactions between polysaccharides and proteins. For **chapters 1, 2, and 3**, a possible explanation of biological activity might rely on electrostatic interactions.  $\beta$ -D-glucans do not form covalent bonds and are slightly negatively charged. Heterorhamman is heavily negatively charged because of the sulfate content (the same effect observed in heparan sulfate). It can form an interaction with surface glycoproteins positively charged, forming a physical cross-linkage between them (CAGNO, TSELIGKA, JONES, & TAPPAREL, 2019; ZIELKE, LU, POINSOT, & NILSSON, 2018). The last hypothesis is related to endocytosis. When polysaccharides bind to receptors, they can be recognized as pathogen-associated molecular patterns (PAMPs) and be internalized by some cells. XU, ZOU, XU (2017) observed the internalization of an  $\beta$ -(1→6) branched  $\beta$ -(1→3)-glucan from *Lentinus edodes* in breast cancer cells (MCF-7). SINGH *et al.* (2018) also observed the same effect on glioblastoma (LN-18) and rat glioma Initiating stem-like cells (C6) at a  $\beta$ -(1→3)-glucan anchored with chitosan nanocarrier loaded with paclitaxel.  $\beta$ -D-glucans (**chapters 1 and 2**) could be endocytosed when linked with the receptors. For **chapter 3**, the glucose and galactose units from the heterorhamman connected with receptors could be responsible for endocytosis. LI *et al.* (2021) presented a Rhamnogalacturonan I ([ $\rightarrow$ 4)- $\alpha$ -GalpA-(1  $\rightarrow$  2)- $\alpha$ -Rhap-(1  $\rightarrow$  4)- $\alpha$ -GalpA-(1 $\rightarrow$ )] isolated from *Cucurbita Moschata*, was endocytosed by the clathrin/caveolin routes in

Caco-2 cells (these cells mimic intestinal epithelium). With fluorescence assays, the subcellular location of the polysaccharide was found, and it was accumulated at the endoplasmic reticulum (ER) and mitochondria. The two hypotheses for those actions could be related to activation of signaling pathways related to the cell fate either by direct interaction with various receptors; or by the endocytic transport and accumulation in mitochondria, causing alterations of metabolic pathways.

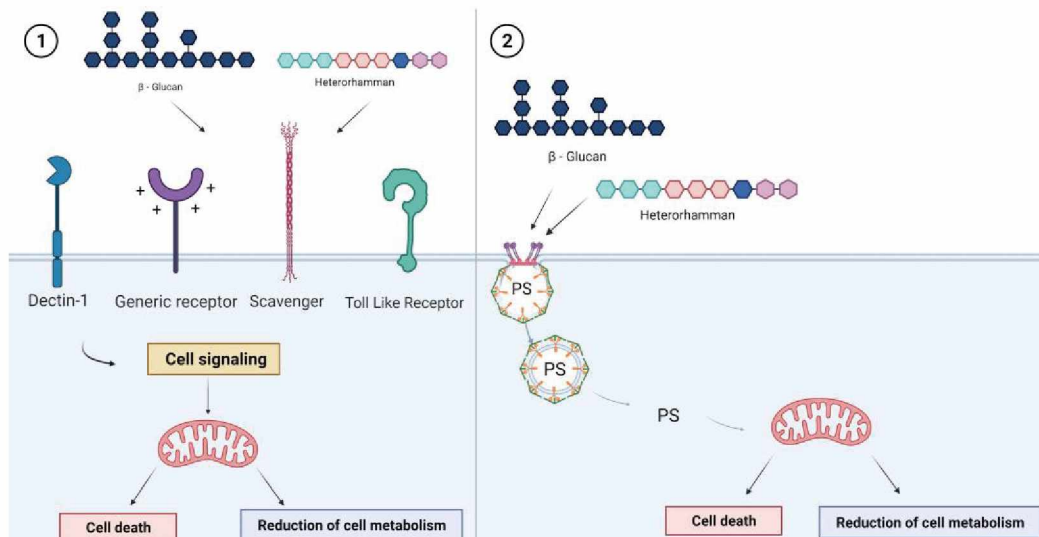


**Fig. 2:**  $\beta$ -D-glucans and heterorhamman effects upon U251 and U87MG glioblastoma cell lines. Polysaccharides can affect glioblastoma cells by two hypotheses. 1) Bidding with carbohydrate receptors or other proteins triggers cell signaling. 2) The polysaccharides could be endocytosed and causes biological effects. PS: polysaccharide. Adapted from "Targeting B Cell Co-Receptors for Vaccine Design" and "Clathrin-Mediated Endocytosis" by BioRender.com (2021). Retrieved from <https://app.biorender.com/biorendertemplates>

## References

- BIRAY AVCI, C., KURT, C. C., TEPEDELEN, B. E., OZALP, O., GOKER, B., MUTLU, Z., . . . GUNDUZ, C. Zoledronic acid induces apoptosis via stimulating the expressions of ERN1, TLR2, and IRF5 genes in glioma cells. **Tumour Biology**, v.37, n.5, p.6673-6679, 2016.
- CAGNO, V., TSELIGKA, E. D., JONES, S. T., & TAPPAREL, C. Heparan Sulfate Proteoglycans and Viral Attachment: True Receptors or Adaptation Bias? **Viruses**, v.11, p.7, 2019.
- CHEN, J., THAN, A., LI, N., ANANTHANARAYANAN, A., ZHENG, X., XI, F., . . . CHEN, P. Sweet graphene quantum dots for imaging carbohydrate receptors in live cells. **FlatChem**, v.5, p.25-32, 2017.
- CHEN, L., & HUANG, G. (2018). Antitumor Activity of Polysaccharides: An Overview. **Current Drug Targets**, v.19, n.1, p.89-96.
- CHEN, T., CHEN, J., ZHU, Y., LI, Y., WANG, Y., CHEN, H., . . . KE, Y. (2019). CD163, a novel therapeutic target, regulates the proliferation and stemness of glioma cells via casein kinase 2. **Oncogene**, v.38, n.8, p.1183-1199.
- FERREIRA, S. S., PASSOS, C. P., MADUREIRA, P., VILANOVA, M., & COIMBRA, M. A. (2015). Structure-function relationships of immunostimulatory polysaccharides: A review. **Carbohydrate Polymers**, v.132, p.378-396, 2015.
- HARDING, S. E., TOMBS, M. P., ADAMS, G. G., PAULSEN, B. S., INNGJERDINGEN, K. T., & BARSETT, H. **An Introduction to Polysaccharide Biotechnology**. (2nd ed.). Boca Raton, 2017.
- KIM, D., RAHHAL, N., & RADEMACHER, C. Elucidating Carbohydrate-Protein Interactions Using Nanoparticle-Based Approaches. **Frontiers in Chemistry**, v.9, p.265, 2021.
- LI, F., WEI, Y., ZHAO, J., YU, G., HUANG, L., & LI, Q. Transport mechanism and subcellular localization of a polysaccharide from *Cucurbita Moschata* across Caco-2 cells model. **International Journal of Biological Macromolecules**, 182(182), 1003-1014, 2021.
- MENSHOVA, R. V., ERMAKOVA, S. P., ANASTYUK, S. D., ISAKOV, V. V., DUBROVSKAYA, Y. V., KUSAYKIN, M. I., . . . ZVYAGINTSEVA, T. N. (2014). Structure, enzymatic transformation and anticancer activity of branched high molecular weight laminaran from brown alga *Eisenia bicyclis*. **Carbohydrate Polymers**, v.99, p.101-109, 2014.
- MOHAMMED, A. S. A., NAVEED, M., & JOST, N. Polysaccharides; Classification, Chemical Properties, and Future Perspective Applications in Fields of Pharmacology and Biological Medicine (A Review of Current

Applications and Upcoming Potentialities). **Journal of Polymers and the Environment**, p.1-13, 2021.

POLISETTY, R. V., GAUTAM, P., GUPTA, M. K., SHARMA, R., GOWDA, H., RENU, D., . . . SIRDESHMUKH, R. Microsomal membrane proteome of low grade diffuse astrocytomas: Differentially expressed proteins and candidate surveillance biomarkers. **Scientific Reports**, v.6, p.26882, 2016.

SARRAZY, V., VEDRENNE, N., BILLET, F., BORDEAU, N., LEPREUX, S., VITAL, A., . . . DESMOULIERE, A. TLR4 signal transduction pathways neutralize the effect of Fas signals on glioblastoma cell proliferation and migration. **Cancer Letters**, v.311, n.2, p.195-202, 2011.

SINGH, P. K., SRIVASTAVA, A. K., DEV, A., KAUNDAL, B., CHOUDHURY, S. R., & KARMAKAR, S. 1, 3beta-Glucan anchored, paclitaxel loaded chitosan nanocarrier endows enhanced hemocompatibility with efficient anti-glioblastoma stem cells therapy. **Carbohydrate Polymers**, v.180, p.365-375, 2018.

XU, H., ZOU, S., & XU, X. The beta-glucan from *Lentinus edodes* suppresses cell proliferation and promotes apoptosis in estrogen receptor positive breast cancers. **Oncotarget**, v.8, n.49, p.86693-86709, 2017.

ZIELKE, C., LU, Y., POINSOT, R., & NILSSON, L. Interaction between cereal beta-glucan and proteins in solution and at interfaces. **Colloids Surface B Biointerfaces**, v.162, p.256-264, 2018.

## 6. CONCLUSIONS

- The microalgae *Isochrysis galbana* and *Conticribra weissflogii*, produced different types  $\beta$ -D-glucans. The macroalga *Gayralia brasiliensis* produced a sulfated heterorhamman, a complex polysaccharide with multiple monosaccharides as rhamnose, xylose, galactose, and glucose. All those polysaccharides showed different glycosidic linkage between them.
- Polysaccharides have different biological effects, and the construction of the polymeric blocks can contribute to these biological effects. Different block association can be arranged between the monosaccharide's units and the presence of other atoms (sulfate, phosphate, among others). The glycosidic linkage will assist the arrangement of the saccharide blocks. These factors will influence the molecular weight, conformation, and the complexity of the chain complex and potential interaction with other macromolecules and receptors.
- The linear (1 $\rightarrow$ 3)  $\beta$ -D-glucan from *Conticribra weissflogii* did not have a cytotoxic response against glioblastoma cell lines U87MG and U251. On the other hand, this polysaccharide enhanced the phagocytosis of macrophages, leading to an immunostimulatory activity in macrophages.
- The branched (1 $\rightarrow$ 6), (1 $\rightarrow$ 3)  $\beta$ -D-glucan from *Isochrysis galbana* could exhibit a high molecular weight (HMW) and a low molecular weight (LMW) profile. Native and HMW interfere with the cellular metabolism of glioblastoma cell lines (U87MG and U251), do not lead to cell death, or affect the cell cycle either. However, it affects many of the mitochondrial intermediates used in metabolic pathways, reducing the cellular metabolism of the U251 line following 24 h treatment and the U87MG line following 72 h treatment.
- The oversulfated (chemically modified) heterorhamman from *Gayralia brasiliensis* previously presented cellular death at the U87MG cell line. The oversulfated molecule appears to affect the mitochondrial membrane potential, cell respiration, ATP respiration state, and mediates an increase of mitochondrial ROS production.
- Polysaccharides' biological responses are related to the interaction with cell receptors. This can explain the adhesion properties, the immunostimulatory effect of macrophages,

and the interference on the cellular metabolism of the glioblastoma cells following treatment with these polysaccharides.

- For future perspectives, it would be worthwhile investigating the interaction of polysaccharides with the cell membranes, to better understand their mechanism of action and their associated biological effects on cancer cells.

## APPENDIX 1 – PUBLISHED PAPER DURING THE DOCTORAL PERIOD:

### **Marine Microalgae Biomolecules and Their Adhesion Capacity to *Salmonella enterica* sv. Typhimurium**

*Applied Sciences*, 10, 2239 (2020)

Tatiane Winkler Marques Machado<sup>1,2,†</sup>, Jenifer Mota Rodrigues<sup>2,3,†</sup>, Tatiana Rojo Moro<sup>1,2</sup>, Maria Eugênia Rabello Duarte<sup>2,\*</sup> and Miguel Daniel Nosedá<sup>2,\*</sup>

<sup>1</sup>Postgraduate Program in Sciences (Biochemistry), Federal University of Paraná (UFPR), Curitiba 81531-980, Paraná, Brazil

<sup>2</sup>Biochemistry and Molecular Biology Dept., UFPR, Av. Cel. Francisco H. dos Santos, 100, P.O. Box 19046, Curitiba 81531-980, Paraná, Brazil

<sup>3</sup>Postgraduate Program in Bioprocesses and Biotechnology Engineering, UFPR, Curitiba 81531-990, Paraná, Brazil

\* Authors to whom correspondence should be addressed.

† These authors equally contributed to this work.

Publication at Applied Sciences Journal. Citation: Machado, T.W.M.; Rodrigues, J.M.; Moro, T.R.; Duarte, M.E.R.; Nosedá, M.D. Marine Microalgae Biomolecules and Their Adhesion Capacity to *Salmonella enterica* sv. Typhimurium. Appl. Sci. 2020, 10, 2239. <https://doi.org/10.3390/app10072239>

## Abstract

Different molecules have been tested as analog receptors due to their capacity to bind bacteria and prevent cell adhesion. By using in vitro assays, the present study characterized the aqueous and alkaline extracts from microalgae *Pavlova lutheri* and *Pavlova gyrans* and evaluated the capacity of these extracts to adhere to enterobacteria (*Salmonella* Typhimurium). The aqueous and alkaline extracts of both species were fractionated via freeze-thawing, giving rise to soluble and insoluble (precipitate) fractions in cold water. The obtained fractions were studied using thermogravimetric, methylation analyses, and using 1D and 2D NMR techniques. The cold-water-soluble fractions obtained from the aqueous extracts were mainly composed of highly branched (1→3), (1→6)-β-glucans, whereas the cold-water-precipitate fractions were constituted by (1→3)-β-glucans. The alkaline extract fractions showed similar compositions with a high protein content, and the presence of glycosides (sulfoquinovosylglycerol (SQG), digalactosylglycerol (DGG), and free fatty acids. The linear (1→3)-β-glucans and the alkaline extract fractions showed an adhesion capacity toward *Salmonella*. The chemical composition of the active fractions suggested that the presence of three-linked β-glucose units, as well as microalgal proteins and glycosides, could be important in the adhesion process. Therefore, these microalgal species possess a high potential to serve as a source of anti-adhesive compounds.

Keywords: microalgae; *Pavlova*; β-glucans; glycosides; adhesion capacity; enterobacteria

## Introduction

Microalgae are photosynthetic microorganisms capable of producing a wide variety of biomolecules in accordance with the division or class to which they belong. The large biodiversity encompasses about 200,000–800,000 species, of which only 50,000 have been taxonomically defined and over 15,000 novel compounds have so far been associated with algae biomass, including carotenoids, sterols, phycobiliproteins, phycotoxins, and polysaccharides [1,2,3]. Phylum Haptophyta comprises two classes, *Coccolithophyceae* and *Pavlovophyceae* [4], where the latter includes the two marine species under study, *Pavlova lutheri* and *Pavlova gyrams*. Since they can be easily grown, quickly ingested and digested and exhibit a high nutritional value, these species, as well as some other microalgae, are widely used as raw material in the aquaculture of fish, mollusks, and crustaceans [5,6,7]. All these characteristics have also aroused the interest of the biotechnology sector for the potential use of these microorganisms in nutritional and pharmaceutical bioproducts [8].

Polysaccharides and oligosaccharides from different microalgal sources have widely diverse chemical structures and are known to have multiple biological activities [9,10]. Numerous investigations have suggested that some types of carbohydrates can avoid enteric infections by inhibiting adhesion of enteropathogens to the host tissue [11,12,13,14,15]. Adhesion is the first step in a bacterial infection process and it is mediated via adhesins expressed by bacteria that recognize and adhere to ligand-like carbohydrates located on the surface of host epithelial cells [16]. Thus, carbohydrates can act as analog receptors, mimicking the host receptors and participating in binding with specific bacterial adhesins. Therefore, anti-adherence therapies act to reduce infections and diseases, as well as the risk of transmission via the food chain. In addition, its application acts as an alternative to the inappropriate and excessive use of antibiotics with the added benefit of reducing selective pressure since pathogens are not killed, they are only impeded from attaching to host cells [17].

Commercial products with anti-adhesive properties that are derived from yeast cell walls and contain mannose have been sold worldwide for a long time and employed in animal feed to bind pathogens and prevent bacterial adhesion [18,19]. Few studies examining the anti-adhesive properties of polysaccharides derived from microalgae are available in the literature. Guzman-Murillo and Ascencio [20] reported that sulfated exopolysaccharides from *Tetraselmis sp.*, *Neochloris oleoabundans*, and *Phaeodactylum*

*tricornutum* caused a 50% inhibition of adhesion of *Helicobacter pylori* to HeLa S3 cells. According to Loke et al. [21], polysaccharides obtained from *Spirulina* and *Chlorella* were capable of preventing *H. pylori* from binding to gastric mucin. Thus, the present study aimed to obtain and characterize aqueous and alkaline extracts from microalgae *P. lutheri* and *P. gyrams* and evaluate, using an *in vitro* assay, the ability of these extracts to adhere to enterobacteria *Salmonella enterica* sv. Typhimurium.

## Materials and Methods

### Algae Culture Conditions

Haptophyte species *P. gyrams* (UTEX LB 992, Culture Collection of Algal at The University of Texas, Austin, TX, USA) and *P. lutheri* (Elizabeth Aidar Microalgae Collection, Fluminense Federal University, Niteroi, RJ, Brazil) were cultivated in Erlenmeyer flasks (2 L) with Guillard f/2 culture medium [22]. The culture medium was prepared using filtered seawater or synthetic seawater ( $30 \text{ g} \cdot \text{L}^{-1}$ ), sterilized at  $120 \text{ }^\circ\text{C}$  for 15 min before inoculation. Microalgal growth was performed at  $18\text{--}20 \text{ }^\circ\text{C}$  under constant light ( $100 \mu\text{mol} \cdot \text{m}^{-2} \cdot \text{s}^{-1}$ ), and the air was supplied at a flow rate of  $3 \text{ L} \cdot \text{min}^{-1}$  (without supplementary  $\text{CO}_2$ ). After fourteen days, we removed the microalgal biomass using centrifugation ( $10,000 \times g$ , 20 min,  $4 \text{ }^\circ\text{C}$ ) and lyophilized it for further analysis ( $0.4$  and  $0.7 \text{ g} \cdot \text{L}^{-1}$  yield for *P. gyrams* and *P. lutheri*, respectively).

### Microalgae Extraction

Sequential extractions were performed for both species, *P. gyrams* and *P. lutheri*, where the procedures are summarized in Figure 1. Dry biomasses were submitted to aqueous extraction ( $20 \text{ g} \cdot \text{L}^{-1}$ ) under magnetic stirring at  $80 \text{ }^\circ\text{C}$  for 2 h ( $2 \times$ ), followed by alkaline extraction with  $0.5 \text{ M NaOH}$  ( $20 \text{ g} \cdot \text{L}^{-1}$ ) and  $\text{NaBH}_4$  (5 % w/w) at  $80 \text{ }^\circ\text{C}$  for 2 h. After each extraction, the residual biomasses were removed via centrifugation ( $12,000 \times g$ , 20 min,  $4 \text{ }^\circ\text{C}$ ) and submitted to the next extraction. Combined aqueous extracts and alkaline extracts (after neutralization with  $0.5 \text{ M HCl}$ ) were concentrated and submitted to ethanol precipitation (EtOH 99 %, 3:1 v/v) at  $4 \text{ }^\circ\text{C}$  overnight. The precipitates obtained via centrifugation ( $12,000 \times g$ , 15 min,  $4 \text{ }^\circ\text{C}$ ) were dissolved in water and submitted to fractionation using freeze-thawing [23]. The fractions that were soluble in cold water (W-s and A-s) were separated from the insoluble fractions (W-p and A-p) using centrifugation ( $12,000 \times g$ , 20 min,  $4 \text{ }^\circ\text{C}$ ). All the fractions obtained were dialyzed (1–2 kDa molecular

weight (MW) cut-off for aqueous fractions and 12–14 kDa MW cut-off for alkaline fractions; Spectra/Por Dialysis Membrane, Repligen Corporation, Rancho Dominguez, CA, USA) against distilled water and freeze-dried.

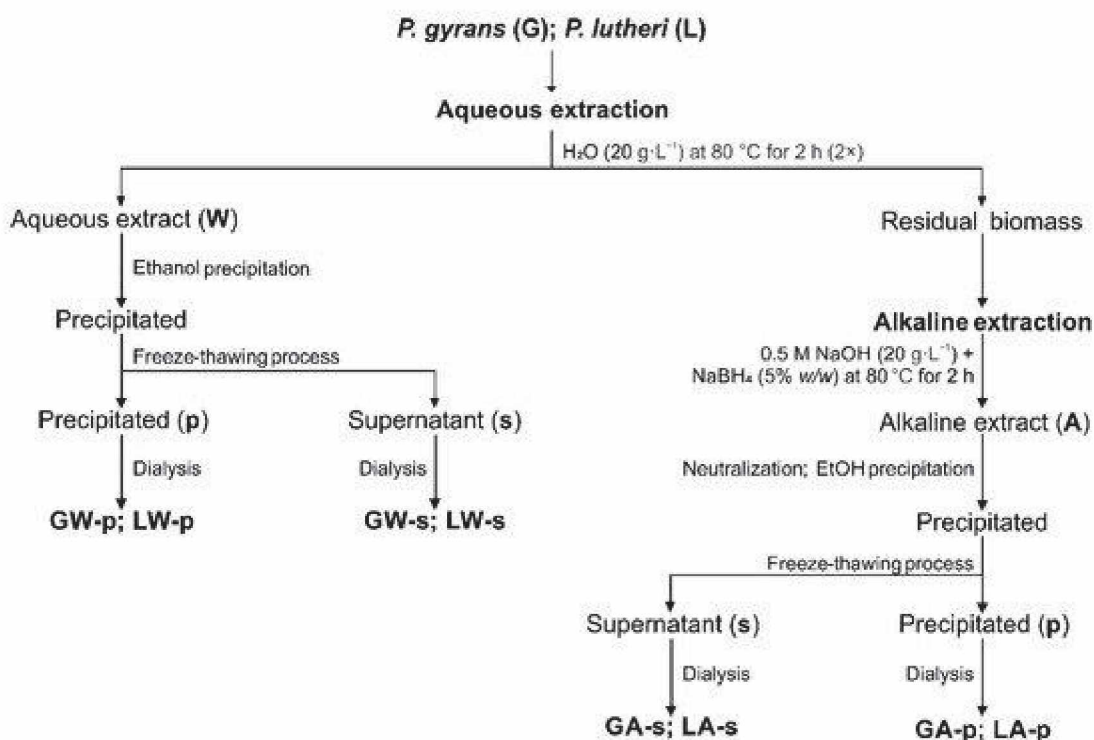


**Figure 1. Extraction sequence and fractionation of crude extracts from microalgae *P. gyrans* and *P. lutheri*. G and L fractions correspond to *P. gyrans* and *P. lutheri*, respectively; W and A correspond to aqueous and alkaline extracts, respectively; and p and s correspond to precipitated and supernatant extracts, respectively.**

## Characterization of Microalgal Extracts and Fractions

### General Methods

The total carbohydrate and protein contents were determined according to previously reported methods [24,25] using glucose and bovine serum albumin as standards, respectively. Thermogravimetric analyses (TGA) were carried out using a thermal analyzer STA 449 F3—Jupiter (NETZSCH-Gerätebau GmbH, Selb, BY, Germany) with an alumina sample pan, a sample mass of 15.0 mg, and under a nitrogen atmosphere with a temperature program from 20 – 800 °C at the heating rate of 10 °C·min<sup>-1</sup>. For the monosaccharide composition, fractions were hydrolyzed (2 M TFA (trifluoroacetic acid), 100 °C, 2 h), reduced with NaBH<sub>4</sub> and acetylated with Ac<sub>2</sub>O (120 °C, 1 h). The resulting alditol acetate derivatives were analyzed using gas

chromatography–mass spectrometry (GC–MS) and identified using their typical electron-impact breakdown profiles and retention times [26]. GC–MS analyses were performed using a Varian 3800 gas chromatograph (Agilent Technologies Inc., Santa Clara, CA, USA) connected to a Varian Saturn 2000R ITD mass spectrometer with an Agilent J&W DB-225 capillary column (30 m × 0.25 mm i.d.), programmed to heat up from 50 to 220 °C at 40 °C.min<sup>-1</sup>, and using helium as the carrier gas (1 mL.min<sup>-1</sup>).

### **Methylation Analyses**

Methylation analysis was carried out in accordance with Ciucanu and Kerek [27]. Polysaccharides (5 mg) were dissolved in Me<sub>2</sub>SO<sub>4</sub> (1 mL), followed by the addition of powdered NaOH (30 mg). After 30 min, under magnetic stirring at 25 °C, CH<sub>3</sub>I (0.2 mL) was added, and the reaction remained for another 30 min. Except for the Me<sub>2</sub>SO<sub>4</sub> addition, the above-mentioned process was repeated twice, and the reaction was interrupted via the addition of water and neutralized with 50 % (v/v) aq. AcOH. Methylation products were dialyzed against distilled water, freeze-dried, and submitted to two more steps of methylation in the same way as described above. Products (1.5 mg) were then hydrolyzed with 90 % (v/v) aq. formic acid (0.5 mL) at 100 °C for 6 h and then with 2 M TFA (0.5 mL) for 2 h at 80 °C [28]. The resulting mixtures of partially O-methylated aldoses were reduced with NaBD<sub>4</sub> and acetylated as described above for the monosaccharide composition to give a mixture of partially O-methylated alditol acetates, which were analyzed using GC–MS and identified using their typical electron-impact breakdown profiles and retention times [26,29].

### **Nuclear Magnetic Resonance Spectroscopy (NMR).**

NMR spectroscopic analyses were performed using a Bruker AVANCE III 400 NMR spectrometer (Bruker BioSpin Corporation, Billerica, MA, USA) equipped with a 5-mm inverse probe, operating at 400.13 and 100.63 MHz for <sup>1</sup>H and <sup>13</sup>C, respectively, at 70 °C. <sup>1</sup>H, <sup>13</sup>C, and <sup>13</sup>C-DEPT-135 (Distortionless Enhancement by Polarization Transfer 135°) acquisition parameters were previously reported [30]. 2D <sup>1</sup>H/<sup>13</sup>C HSQC (Heteronuclear Single Quantum Coherence) experiments were performed using pulse programs supplied by the Bruker manual. Samples were solubilized in Me<sub>2</sub>SO<sub>4</sub>-d<sub>6</sub> at 15

and 40 mg. mL<sup>-1</sup> for <sup>1</sup>H and <sup>13</sup>C, respectively. Chemical shifts are expressed in ppm relative to Me<sub>2</sub>SO-d<sub>6</sub> resonances at 2.50 and 39.5 ppm for <sup>1</sup>H and <sup>13</sup>C, respectively.

### **Adhesion Assay**

A microplate method, previously described by Becker et al. [31] and Ganner et al. [32], and adapted by Rodrigues, Duarte, and Nosedá [15], was used to determine the ability of microalgal molecules to specifically adhere to *Salmonella* Typhimurium.

### **Bacteria Strain and Culture Conditions**

*Salmonella enterica* sv. Typhimurium ATCC 14028 strain was maintained at 4 °C in Brain Heart Infusion Agar (HiMedia Laboratories Ltd., Mumbai, MH, India) under aerobic conditions and subcultured at 15-day intervals. Bacteria were transferred to Tryptic Soy Broth (TSB, HiMedia Laboratories Ltd.), incubated overnight at 37 °C under aerobic conditions, and subcultured to a fresh medium for 2 h at 37 °C. The optical density (OD) of the bacterial suspension was adjusted to 0.01 (at 690 nm) with PBS (phosphate-buffered saline: 10 mmol. L<sup>-1</sup> sodium phosphate, 0.15 mol. L<sup>-1</sup> sodium chloride, pH 7.0) for the experiments.

### **Calibration Curve**

Serial dilutions of freshly prepared cultures were plated in triplicate on Tryptic Soy Agar (HiMedia Laboratories Ltd.) and incubated for 24 h prior to CFU enumeration. Simultaneously, eight replicates of each bacterial suspension were incubated, 200 µL per well, in a microplate reader (SpectraMax 340, Molecular Devices LLC, San Jose, CA, USA) for 18 h at 37 °C. The OD at 690 nm was determined at intervals of 15 min, with automatic shaking taking place for 3 s prior to every reading. A calibration curve (linear regression) was produced by plotting the time in hours necessary for bacterial solutions to reach an OD of 0.1 (tOD) versus the number of counted bacteria on an agar plate (CFU.mL<sup>-1</sup>) to calculate the number of bacteria originally connected to the studied fractions.

## Assay

Microalgal extracts were suspended in PBS (1 % m/v) and subsequently homogenized in an ultrasonic bath (three times for 30 s each) (coating solutions). For coatings, 300  $\mu\text{L}$ /well of the coating solutions were pipetted into flat-bottom wells of a high-binding microtitration plate (Costar 3590, Corning Inc., Corning, NY, USA) and incubated overnight at 4 °C. The plate was washed three times with 300  $\mu\text{L}$  of PBS, and subsequently, wells were blocked with 300  $\mu\text{L}$  of 1 % (m/v) bovine serum albumin (BSA) in PBS at 4 °C for 1 h. Thereafter, the plate was washed three times with PBS and bacterial suspension OD 0.01 was added (300  $\mu\text{L}$ /well). Bacteria were allowed to adhere for 1 h at 37 °C, and then, wells were washed six times with PBS. Finally, 200  $\mu\text{L}$  of TSB and one drop of paraffin-oil were added, and the bacterial growth was monitored using the OD (690 nm) at 37 °C, for 16 h at intervals of 15 min, with automatic shaking taking place for 3 s prior to every reading. All readings were performed for three independent assays and in triplicate per assay.

Blank samples, negative controls, growth controls, positive controls, and media controls were also assessed on each plate. Blank samples consisted of coating solutions and BSA but without bacteria. A negative control consisted of BSA and bacteria but without coating solutions. A growth control consisted of non-coated wells containing a suspension of bacteria (OD 0.01) in TSB. A commercially available yeast cell wall-derived product was used as the positive control. Blank and media controls showed no growth during the experimental time (16 h) and the negative control showed growth after 7 h.

## Data Processing and Statistics

Data generated using the photometer software (Soft-Max Pro version 2.2.1; Molecular Devices LLC) were converted into text files and analyzed using R Software (version 2.15.1; The R Foundation for Statistical Computing, Vienna, Austria). All OD data were processed using non-linear regression analysis employing a bacterial kinetic model [31]. The tOD (h) were transformed into  $\log \text{CFU}\cdot\text{mL}^{-1}$  by means of fitted linear regressions:  $y = -0.7693x + 9.0485$  ( $R^2 = 995$ ), where “y” corresponds to tOD and “x” to the log of CFU/well (see the calibration curve) [32]. The data were statistically evaluated by applying an analysis of variance (ANOVA) and differences between the mean values

were tested using Tukey's test. Data with a p-value lower than 0.05 was considered statistically significant.

## Results

### Extraction and Characterization of Polysaccharides from *P. gyrans* and *P. lutheri*

Dried biomasses of *P. gyrans* and *P. lutheri* were extracted under sequential aqueous extraction followed by alkaline extraction. Crude aqueous and alkaline extracts were treated with EtOH, and ethanolic precipitates were submitted to freeze-thawing and dialysis, producing the fractions GW-p (0.9%), GW-s (3.8%), GA-p (1.2%), and GA-s (0.4%) from *P. gyrans*, and LW-p (0.6%), LW-s (4.7%), LA-p (1.0%), and LA-s (0.9%) from *P. lutheri* (Figure 1) (G and L fractions correspond to *P. gyrans* and *P. lutheri*, respectively; W and A correspond to aqueous and alkaline extracts, respectively; and p and s correspond to precipitated and supernatant extracts, respectively). Table 1 shows the chemical analyses and monosaccharide compositions of these fractions. The aqueous fractions from *P. gyrans* (GW-p, GW-s) and *P. lutheri* (LW-p, LW-s) showed a high content of carbohydrates, with contents varying from 55.6 % in LW-p to 83.5 % in GW-p. These fractions were mainly constituted by glucose (85.4–100 mol %), indicating the presence of glucans. The alkaline fractions (GA-p, GA-s, LA-p, LA-s) were predominantly composed of proteins, with contents varying from 30.0 % in GA-p to 49.1% in LA-p. The carbohydrate contents varied from 11.6 % in GA-p to 17.5 % in LA-s, and the monosaccharide analysis indicated three main sugars: glucose, galactose, and mannose. Other monosaccharides were present in lower amounts in these fractions.

**Table 1. Chemical analyses and monosaccharide composition of fractions from *P. gyrans* and *P. lutheri*.**

Fraction	Carbohydrate (%)	Protein (%)	Monosaccharides (mol%)						
			Rha	Fuc	Ara	Xyl	Man	Gal	Glc
<i>P. gyrans</i>									
GW-p	83.5	10.7	tr	tr	tr	tr	tr	tr	100
GW-s	68.6	18.1	1.4	1.2	1.1	tr	2.8	2.7	90.8
GA-p	11.6	30.0	5.2	6.5	3.7	10.6	21.6	16.0	36.4
GA-s	15.3	38.4	4.1	6.6	8.9	11.5	12.2	24.2	32.5
<i>P. lutheri</i>									
LW-p	55.6	14.5	2.1	2.5	tr	tr	1.5	2.0	91.8
LW-s	59.9	17.9	1.4	3.7	1.8	tr	3.4	4.3	85.4
LA-p	15.2	49.1	8.3	7.8	3.0	5.1	14.2	17.6	44.0
LA-s	17.5	34.7	5.5	7.7	8.2	8.1	15.4	24.9	30.2

tr: Percentages lower than 1 mol%.

Thermogravimetric analyses were performed to complement the chemical composition of the microalgal fractions. Thermogravimetric (TG) curves, derivative thermogravimetric (DTG) curves, and characteristics of the microalgal extracts in the TGA process are shown in Table 2 and Figure 2. Although the fractions have different chemical compositions, three stages could be identified for all microalgal fractions that were similar to the previously published works [33,34].

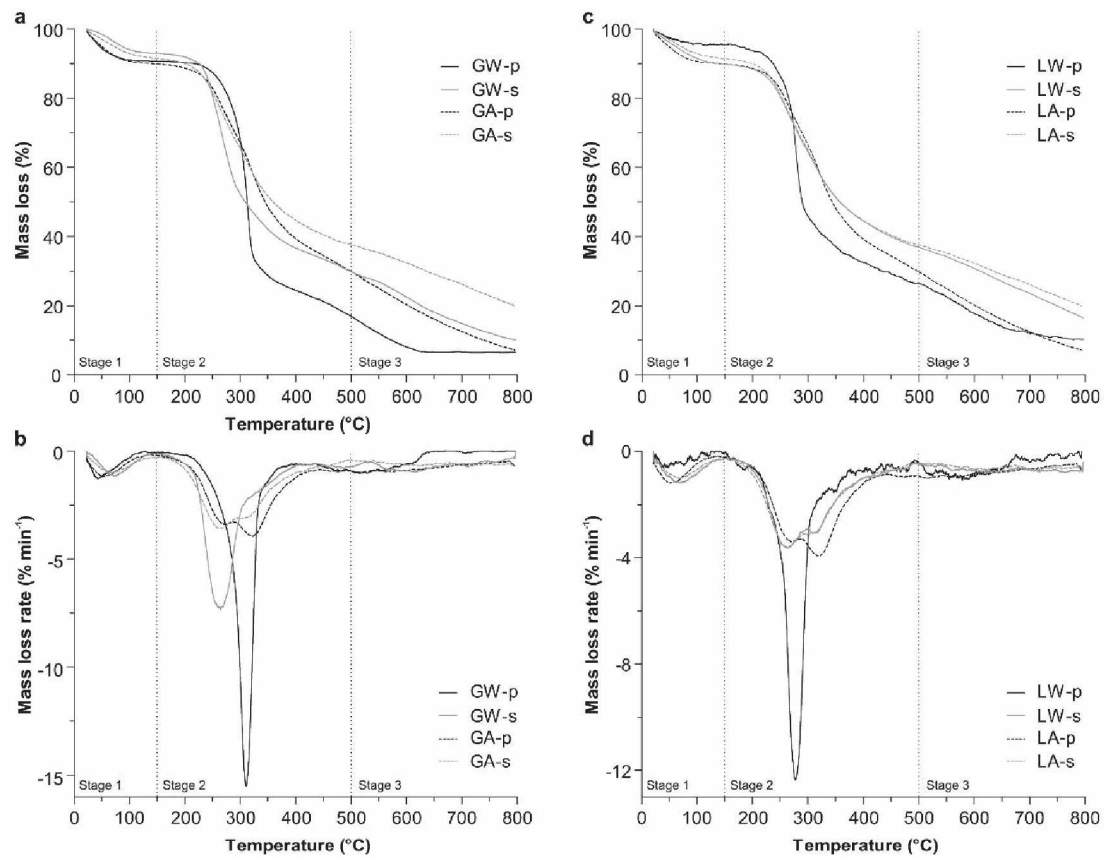


**Figure 2.** Thermogravimetric (a,c) and derivative thermogravimetric curves (b,d) of aqueous and alkaline fractions from *P. gyrans* (GW-p, GW-s, GA-p, GA-s) and *P. lutheri* (LW-p, LW-s, LA-p, LA-s) at a heating rate of 10 °C.min<sup>-1</sup> under a nitrogen atmosphere.

**Table 2. Characteristic total volatile matter content (%) of the different stages for microalgal extracts at a heating rate of 10 °C.min<sup>-1</sup>.**

Fraction	Total Volatile Matter Content (%) <sup>a</sup>			Ash and Fixed Carbon (%) <sup>b</sup>
	Stage 1	Stage 2	Stage 3	
<i>P. gyrans</i>				
GW-p	9.2	78.7	5.5	6.5
GW-s	7.0	66.1	16.8	10.1
GA-p	8.8	63.6	17.4	10.1
GA-s	8.6	58.0	22.5	10.8
<i>P. lutheri</i>				
LW-p	4.6	72.8	12.3	10.3
LW-s	10.1	55.6	17.8	16.5
LA-p	10.0	64.7	18.1	7.1
LA-s	8.3	56.1	15.4	20.1

<sup>a</sup> Stage 1: Range from 20 to 150 °C; Stage 2: Range from 150 to 500 °C; Stage 3: Range from 500 to 800 °C. <sup>b</sup> Non-degradable residue at 800 °C.

In the first stage of the decomposition process, ranging from 20 – 150 °C, a slight mass loss in the TG curves was observed (4.6 % – 10.1 %) due to water loss (free and loosely bound water) and some light volatile compounds. By comparing the first stage in the DTG curves (Figure 2b,d), the results showed subtle differences in the peak temperatures between 41.8 and 70.6 °C. These differences might have been due to the location and intermolecular forces between water molecules and the carbonaceous matrix that influenced the water elimination, and consequently, the peak temperatures [35]. The second stage of decomposition, between 150 and 500 °C, represented the main devolatilization reaction, where most of the sample mass was released as volatile matter. This stage involved the decomposition of microalgae organic substances, including proteins and carbohydrates, present in all the studied fractions (Table 1). The percentages of volatile matter (Table 2) were between 55.6 % and 66.1 % of the initial mass, except for GW-p and LW-p, which showed higher values (78.7 % and 72.8 %, respectively). The GW-p and LW-p DTG curves showed one intense sharp peak, indicating a high mass-loss rate; however, for GW-p, the inflection point was observed at 310 °C, while for LW-p, the inflection point was at 277 °C. One peak was also distinguished in this stage for GW-s at 264 °C. These differences in the thermal profiles may have been due to different

chemical compositions, or differences in the linkage pattern of glucans present in these fractions [36,37]. Stage 2 in the DTG curves (Figure 2b,d) of alkaline fractions (GA-p, GA-s, LA-p, LA-s) was complex as multiple overlapping peaks and wide shoulders were visible, in agreement with the chemical composition complexity observed for these fractions (Table 1). In the third stage, at temperatures higher than 500 °C, the carbonaceous materials retained in the solid residues were decomposed at a slow rate, resulting in the formation of a non-degradable residue. For nearly all the fractions, the percentage of non-degradable residue at 800 °C (Table 2) accounted for 6.5 % – 10.8 % of the initial mass, with a higher value for LW-s and LA-s (16.5 % and 20.1 %, respectively).

To elucidate the linkage pattern of the polysaccharides, present in the aqueous fractions, GW-p and GW-s were submitted to methylation analysis, and the results are shown in Table 3. The methylation analysis of fraction GW-p revealed the major presence of the derivative 2,4,6-tri-O-methyl glucitol (90.0 %), suggesting the presence of a main linear backbone constituted by 3-O-substituted glucopyranosyl units. In addition, the methylation analysis showed minor proportions of non-reducing terminal units, as well as 6- and 3,6-di-O-substituted glucopyranosyl units. The relative amount of nonbranched and disubstituted *GlcP* residues indicated one branching point for every  $\approx 20$  *GlcP* residues. In contrast, GW-s showed a highly branched structure, with non-reducing terminal, 3-, 6-, and 3,6-di-O-substituted glucopyranosyl units, indicating the presence of a (1 $\rightarrow$ 3), (1 $\rightarrow$ 6)-linked glucan, with one branching point every approximately four *GlcP* residues.

**Table 3. Methylation analysis of GW-p and GW-s.**

Sugar Derivative <sup>a</sup>	Deduced Linkages <sup>b</sup>	Molar Ratio <sup>c</sup>	
		GW-p	GW-s
2,3,4,6-Me <sub>4</sub> -Glc <sup>d</sup>	Glc <sub>p</sub> -(1→	7.3	38.0
2,4,6-Me <sub>3</sub> -Glc	→3)-Glc <sub>p</sub> -(1→	90.0	26.7
2,3,4-Me <sub>3</sub> -Glc	→6)-Glc <sub>p</sub> -(1→	2.5	11.2
2,4-Me <sub>2</sub> -Glc	→3,6)-Glc <sub>p</sub> -(1→	5.3	24.1

<sup>a</sup> Monosaccharide bearing a methyl group in the indicated position. <sup>b</sup> Based on derived *O*-methyl alditol acetates. <sup>c</sup> Expressed in mol% of the total *O*-methylalditol acetates. <sup>d</sup> 2,3,4,6-Me<sub>4</sub>-Glc analyzed as 1,5-di-*O*-acetyl-2,3,4,6-tetra-*O*-methyl glucitol.

Fractions were also examined using NMR spectroscopy. <sup>1</sup>H and <sup>13</sup>C NMR assignments were determined using spectral information from 1D and 2D NMR experiments and previously reported data. The <sup>13</sup>C NMR spectra of GW-p (Figure 3a) and LW-p (data not shown) demonstrated six major signals at 102.4, 72.3, 85.6, 67.9, 75.8, and 60.4 ppm, which were assigned to the six-membered ring of β-D-Glc<sub>p</sub> units (residue GL), the major component of these fractions. The anomeric signal at 4.53 ppm ( $J_{H1,H2}$  7.7 Hz) in the <sup>1</sup>H NMR spectrum confirmed the β-anomerism of these units. The cross-peak in the HSQC spectrum (Figure 4a) at 3.49/85.6 ppm indicated the 3-*O*-substitution of β-D-Glc<sub>p</sub> residues. The non-substitution at *O*-6 was confirmed by the <sup>13</sup>C-DEPT inverted resonance at 60.4 ppm. All the <sup>1</sup>H and <sup>13</sup>C NMR assignments of GW-p are shown in Table 4. The spectroscopic analyses indicated the occurrence of a (1→3)-linked β-glucan in the GW-p fraction.



**Table 4.  $^1\text{H}$  and  $^{13}\text{C}$  NMR chemical shifts of GW-p and GW-s.**

Fraction	Glycosyl Residues		Chemical Shifts <sup>a</sup>					
			H-1/C-1	H-2/C-2	H-3/C-3	H-4/C-4	H-5/C-5	H-6;H-6'/C-6
GW-p	$\rightarrow 3$ )- $\beta$ -D-Glcp-(1 $\rightarrow$	G <sub>L</sub>	4.53/102.4	3.32/72.3	3.49/85.6	3.28/67.9	3.28/75.8	3.72; 3.48/60.4
	$\rightarrow 3$ )- $\alpha$ -D-Glcp	G <sub><math>\alpha</math></sub>	5.00/91.5	nd	nd	nd	nd	nd
	$\rightarrow 3$ )- $\beta$ -D-Glcp	G <sub><math>\beta</math></sub>	4.39/96.1	nd	nd	nd	nd	nd
	$\beta$ -D-Glcp-(1 $\rightarrow 3$	G <sub>3t</sub>	4.38/103.5	3.11/73.5	3.24/75.6	3.12/69.7	3.12/75.8	3.72;3.47/60.7
GW-s	$\beta$ -D-Glcp-(1 $\rightarrow 6$	G <sub><math>\alpha</math></sub>	4.23/102.5	3.05/73.3	3.23/75.6	3.13/69.7	3.19/nd	3.71;3.49/60.7
	$\rightarrow 3$ )- $\beta$ -D-Glcp-(1 $\rightarrow$	G <sub>A</sub>	4.49/102.4	3.32/72.2	3.46/85.6	3.26/67.9	3.29/75.8	3.72; 3.48/60.4
	$\rightarrow 6$ )- $\beta$ -D-Glcp-(1 $\rightarrow$	G <sub>B</sub>	4.28/102.6	3.05/73.3	3.23/75.8	3.15/69.7	3.34/74.4	4.00; 3.61/67.9
	$\rightarrow 3,6$ )- $\beta$ -D-Glcp-(1 $\rightarrow$	G <sub>C</sub>	4.36/102.4	3.25/72.0	3.40/87.0	3.33/67.8	3.42/74.4	4.00; 3.66/67.9

nd: Not determined. <sup>a</sup> In ppm relative to Me<sub>2</sub>SO-*d*<sub>6</sub> resonances.

The  $^{13}\text{C}$  NMR analyses of fractions GW-s (Figure 3b) and LW-s (data not shown) showed signals of (1 $\rightarrow 3$ )-linked  $\beta$ -Glc<sub>p</sub> residues at 102.4, 72.2, 85.6, 67.9, 75.8, and 60.4 ppm, which were attributed to C-1–C-6, respectively. Additionally, the HSQC spectrum (Figure 4b) contained anomeric correlations (H-1/C-1) at 4.38/103.5 and 4.23/102.5 ppm, corresponding to non-reducing end units (residues G<sub>3t</sub> and G<sub>6t</sub>, respectively), and others at 4.28/102.6 and 4.36/102.4 ppm, corresponding to 6- (G<sub>B</sub>) and 3,6-di-O-substituted Glc<sub>p</sub> residues (G<sub>C</sub>), respectively. Furthermore, the HSQC cross-peaks at 5.00/91.5 and 4.39/96.1 ppm were attributed to H-1/C-1 of  $\alpha$ - (G <sub>$\alpha$</sub> ) and  $\beta$ -reducing end Glc<sub>p</sub> residues (G <sub>$\beta$</sub> ), respectively. The correlation at 3.40/87.0 ppm arose from a substitution at O-3 in (1 $\rightarrow 3,6$ )-linked  $\beta$ -D-Glc<sub>p</sub> units, while those at 3.23/75.6, 3.24/75.6, and 3.23/75.8 ppm were from free O-3 of non-reducing ends and (1 $\rightarrow 6$ )-linked  $\beta$ -D-Glc<sub>p</sub> units. The  $^{13}\text{C}$  DEPT-135 inverted resonance at 67.9 ppm corresponded to substituted CH<sub>2</sub>-6 of  $\beta$ -D-Glc<sub>p</sub> units, while the inverted signals at 60.7 and 60.4 ppm, could be attributed to unsubstituted CH<sub>2</sub>-6 of  $\beta$ -D-Glc<sub>p</sub> units. All the  $^1\text{H}$  and  $^{13}\text{C}$  NMR assignments, based on HSQC (Figure 4), COSY (Figure S1), and TOCSY (Figure S2) spectra, presented in Table 4 are in agreement with previously reported resonances [38,39,40,41]. In accordance with the methylation analysis, the NMR data suggest the presence of a highly branched  $\beta$ -D-glucan constituted by a (1 $\rightarrow 3$ )-linked main chain substituted at O-6 by single units of D-Glc<sub>p</sub> or (1 $\rightarrow 6$ )-linked  $\beta$ -D-Glc<sub>p</sub> branches.

The HSQC NMR spectrum (Figure 5a) of the alkaline fraction LA-p, showed an anomeric correlation at 4.59/98.4 ppm ( $J_{\text{H1,H2}}$  3.7 Hz), which is consistent with an  $\alpha$ -

glycosidic configuration. Correlations at an unusual high field region (2.89;2.64/54.9 ppm) indicated the presence of a  $-\text{CH}_2\text{-SO}_3^-$  group of 6-sulfoquinovose units. The  $^{13}\text{C}$ -DEPT inverted signal at 54.9 ppm ( $\text{CH}_2$ ) confirmed the S-substituted C-6 (Figure 5c'). The H-2/C-2–H-5/C-5 correlations at 3.22/71.3, 3.4/72.6, 3.02/74.3, and 3.82/68.1 ppm, respectively, also confirmed the presence of a quinovosyl structure (residue SQ). Furthermore, the HSQC spectrum (Figure 5a) contained correlations at 3.87;3.46/64.7, 5.14/69.7, and 4.35;4.15/62.0, which were attributed, respectively, to H-1;H-1'/C-1, H-2/C-2, and H-3;H-3'/C-3 of linked glycerol (Gly), indicating the presence of the glycoside sulfoquinovosylglycerol (SQG). Moreover, the anomeric region contained two low-intensity correlations at 4.14/103.5 ppm ( $J_{\text{H}_1,\text{H}_2}$  7.1 Hz) and 4.72/99.0 ppm ( $J_{\text{H}_1,\text{H}_2}$  3.3 Hz), which were attributed to  $\beta$ -Galp and  $\alpha$ -Galp units, respectively, suggesting the presence of a second glycoside in this fraction, namely digalactosylglycerol (DGG) [42,43,44]. The  $\text{CH}_3$  correlations at 0.86/13.3 ppm,  $\text{CH}_2$  at 1.20/21.1 to 2.3/36.6 ppm with a predominant one at 1.25/28.5 ppm (inverted resonances in the  $^{13}\text{C}$ -DEPT spectrum, Figure 5c'), and carboxylic signals at 171–175 ppm in the  $^{13}\text{C}$  NMR spectra (Figure 5c), as well as double-bond correlations from 5.05/119.8 to 5.50/137.3 ppm, indicated the presence of unsaturated free fatty acid chains [45].

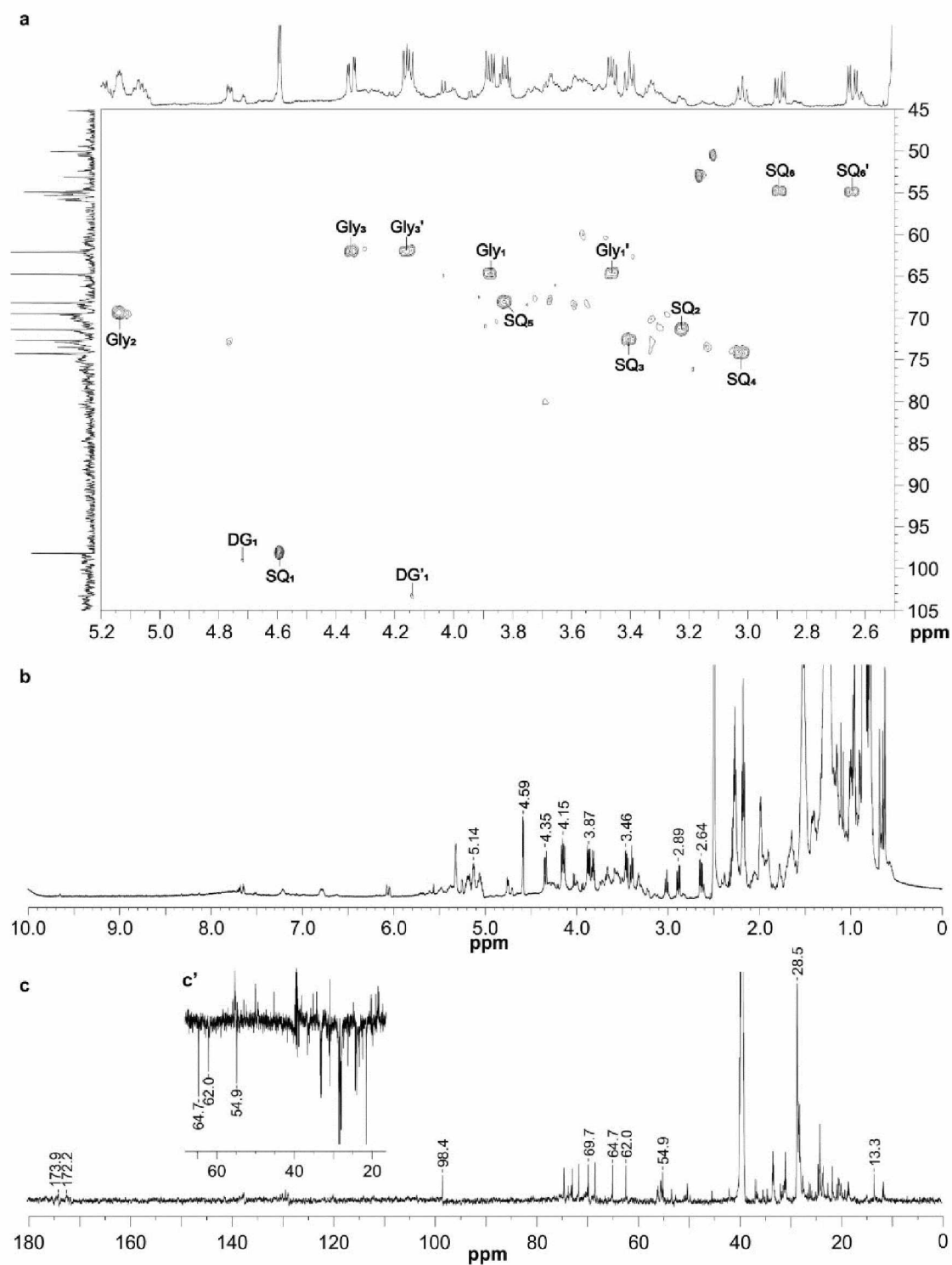


**Figure 5.** NMR analyses of the LA-p fraction.  $^1\text{H}$ - $^{13}\text{C}$  HSQC (a),  $^1\text{H}$  NMR (b),  $^{13}\text{C}$  NMR (c), and partial  $^{13}\text{C}$ -DEPT-135 spectra (c') ( $\text{Me}_2\text{SO}_4\text{-d}_6$ , 70 °C). DG, SQ, and Gly correspond to the glycosyl moiety of digalactosylglycerol and sulfoquinovosylglycerol, and the linked glycerol units, respectively.

Additional to glycosides and free fatty acid signals, the  $^1\text{H}$  and  $^{13}\text{C}$  NMR spectra of LA-p (Figure 5) showed protein signals in accordance with the high protein content (49.1 %) observed in the chemical analyses. Overlapping was expected for some of the protein and free fatty acid resonances. The  $^1\text{H}$  NMR spectrum (Figure 5b) showed signals in the region of the backbone amide protons (10.0–7.0 ppm), aromatic and side-chain amide protons (8.0–6.0 ppm),  $\alpha$ -proton (5.5–3.5 ppm), methine, methylene (3.5–1.0 ppm), and methyl protons (2.0–0 ppm) of the aliphatic side chains [46]. The  $^{13}\text{C}$  NMR spectrum (Figure 5c) showed signals corresponding to the carbonyl carbon of the main chain and carboxylic groups of the acidic amino acids side chain (180–165 ppm), aromatic amino acids (140–115 ppm),  $\alpha$  and  $\beta$  carbons (65–45 ppm and 45–25 ppm, respectively), and methylene and methyl groups of the aliphatic side chains (25–10 ppm) [47].

The  $^1\text{H}$  NMR spectra of the other alkaline fractions, LA-s, GA-s, and GA-p (data not shown), presented the same characteristic protein resonances that were described for the LA-p fraction. Free fatty acid NMR signals were also observed in the GA-p fraction. The LA-s and GA-s fractions showed a low-intensity anomeric resonance at 4.53 ppm ( $J_{\text{H1,H2}}$  7.6 Hz), which was attributed to H-1 of (1→3)-linked  $\beta$ -glucan; however, no other signal in the carbohydrate region could be detected.

### Adhesion Test

The ability of microalgal fractions to adhere to *Salmonella* Typhimurium was determined using an *in vitro* assay and the results are shown in Figure 6. The quantitative adhesion numbers (CFU) between bacteria and microalgal fractions were determined using linear regression, where a higher number of bound bacteria results in an earlier entry into the exponential phase and indicates a higher adhesion capacity. The results indicated three different levels of adhesion, which involved binding between  $1.28 \times 10^3$  and  $1.52 \times 10^4$  CFU. The group including alkaline fractions GA-s and LA-s showed the lower detection times of  $\approx 6.5$  h and exhibited the highest adhesion capacity, adhering between 98% and 140% more bacteria than the positive control (yeast cell wall-derived product). The precipitated fractions from alkaline (GA-p, LA-p) and aqueous extracts (GW-p, LW-p) exhibited low adhesion capacity, with detection times of 6.90–7.06 h, adhering 12%–34 % fewer bacteria than the positive control. Fractions from the aqueous extracts, LW-s

and GW-s, had no adhesion capacity, showed longer detection times (>7.4 h), and yielded similar results to those of the negative control (bovine serum albumin).

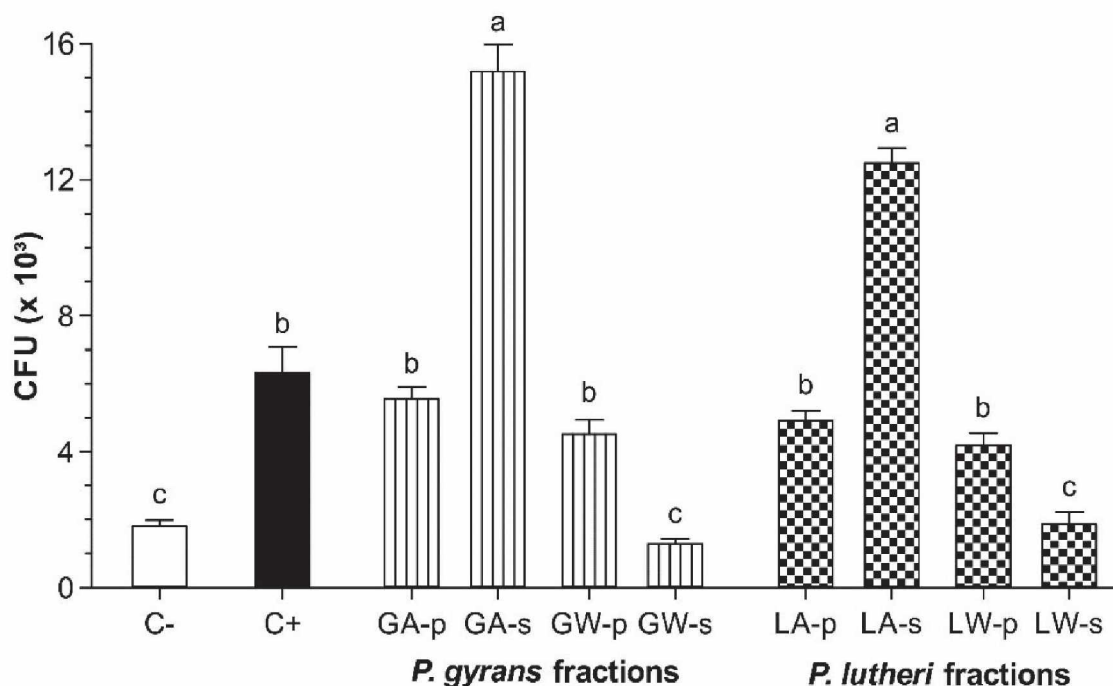


**Figure 6.** Number of *Salmonella Typhimurium* attached to wells coated with microalgal extracts in the adhesion assay. Each bar (CFU  $\pm$  SD) represents the average of three replicates from three independent *in vitro* assays according to the fitted equations (n = 9). Different letters indicate statistical differences (Tukey's test, p < 0.05).

## Discussion

Generally, polysaccharides, cell wall constituents, or storage carbohydrates produced by microalgae are mainly composed of glucose and are called glucans. Their glycosidic linkages vary among the families, classes, and divisions to which they belong. In the haptophytes and diatoms, the common storage polysaccharides are (1 $\rightarrow$ 3)- and/or (1 $\rightarrow$ 3),(1 $\rightarrow$ 6)- $\beta$ -glucans [48].

In haptophytes, storage  $\beta$ -glucans have been investigated only in a few species. Polysaccharides from *Isochrysis galbana*, *Pleurochrysis haptonemofera*, and *Emiliania huxleyi*, belonging to class Coccolithophyceae, showed a highly branched (1 $\rightarrow$ 3),(1 $\rightarrow$ 6)- $\beta$ -D-glucan with a (1 $\rightarrow$ 6)-linked  $\beta$ -D-Glcp backbone substituted at O-3 by single glucose units or rather short (up to tetrasaccharide) glucooligosaccharide chains [39,49,50], while

the polysaccharide from *Phaeocystis globosa* was described as a (1→3)-linked β-D-glucan substituted at O-6 by glucose residues [51]. In the present research, the glucans isolated from *P. gyraus* and *P. lutheri* showed similar structures as expected for species of the same genus. Linear (1→3)-linked β-glucans were identified in the cold-water-insoluble fraction, while highly branched β-glucans, constituted by a (1→3)-linked backbone with substitution at O-6, remained in the cold-water-soluble fraction of both species.

In addition to carbohydrates, proteins and lipids are abundant in most haptophytes. Renaud et al. [52] and Ponis et al. [7] found 24.2 %–32.5 % and 33.8 %–54.3 % protein contents in Coccolithophyceae and Pavlovophyceae species, respectively. Similar contents were found in the alkaline fractions obtained in this research (30.0 %–49.1 %). In these fractions, we also identified the glycosides SQG and DGG, as well as free fatty acids. The disruption process of the algal cell wall via the alkali treatment and high temperature used in this research saponified the native acylated forms, namely SQDG (sulfoquinovosyldiacylglycerol), DGDG (digalactosyldiacylglycerol), and TAG (triacylglycerol), generating water-soluble fragments, such as SQG, DGG, and sodium salts of fatty acids [42]. These molecules may interact with proteins, forming stable complexes not eliminated during the dialysis process [53]. Among lipids, the major lipid classes for *Pavlova* species are TAG and glycolipids. Tatsuzawa and Takizawa [54] reported the following for *P. lutheri*: 40 % TAG, 25 % MGDG (monogalactosyldiacylglycerol), 10 % SQDG, 8 % DGDG, and 6 % betaine lipids; Eichenberger and Gribi [55] also reported 42% TAG, 19% MGDG, 12% DGDG, 9 % SQDG, 6 % DGTA (diacylglyceryl hydroxymethyl-N,N,N-trimethyl-β-alanine), and 5 % DGCC (diacylglyceryl carboxyhydroxymethylcholine) for the same species. TAGs are neutral lipids mainly stored in vacuoles within the microalgal cell, while galactolipids and sulfolipids are constituents of chloroplast and extraplastid membranes, respectively [55,56].

Developing alternatives to antibiotics is especially challenging in the area of intestinal infection prevention. The anti-adherence strategy using analog receptors has gained increasing importance. Analog receptors resemble host intestinal receptors and act as decoys via bacteria adsorption, interrupting the adherence process. In this study, an *in vitro* model was utilized to evaluate the ability of microalgal extracts to specifically adhere *Salmonella* Typhimurium acting as analog receptor. Fractions with an adhesion

capacity were chemically distinct, indicating the presence of different bioactive molecules.

Alkaline fractions that exhibited the greatest adhesion capacity (LA-s, GA-s) did not have a high carbohydrate content (around 16 %) and exhibited heterogeneous monosaccharide composition with absolute content around 5 % glucose, 4 % galactose, and 2.3 % mannose. This observation suggests that adhesins specificity was not entirely a function of the total amount of particular saccharide structures. The *Salmonella* adhesion is mediated via protein–carbohydrate or a protein–protein interactions [57], thus proteins and glycosides (SQG and DGG) in alkaline fractions could be synergistically cooperating with polysaccharides binding to bacteria through other mechanisms. For *Salmonella* Typhimurium, the object of this study, protein–protein interactions are mediated by fimbrial and non-fimbrial adhesins and involve the extracellular matrix components of the host cell [58,59,60,61,62,63]. Several studies reported that milk and colostrum fractions containing proteins ( $\beta$ -lactoglobulin,  $\alpha$ -lactalbumin) and glycopeptides (glycomacropeptide) show anti-adherence properties against *Salmonella* Typhimurium, *Salmonella enteritidis*, enteropathogenic *Escherichia coli*, and enterohemorrhagic *E. coli*, among others [11,64,65,66]. Newburg et al. [67] showed that human-milk-derived sulfated glycolipids inhibited the *S. Typhimurium* pathogenesis *in vitro*. The high content of proteins observed in the active microalgal extracts and the presence of glycosides suggested that these molecules might also play an important role in the adhesion process.

The aqueous fractions, GW-p or LW-p, with an adhesion capacity similar to the positive control, were composed mainly of (1→3)-linked  $\beta$ -glucans, and it is possible that the type-1 adhesins—the most important adhesin found in *Salmonella*—recognized and bound to glucose present in these fractions. Bouckaert et al. [68] determined the binding affinities of the purified FimH lectin from *E. coli* for several hexoses. The lectin binding site is highly specific for mannose; however, their results showed that FimH can bind to other saccharides, such as fructose and glucose, but their affinity is reduced when compared to mannose. Furthermore, according to Hung et al. [69], the binding-receptor domain interacts with almost all mannose OH groups, indicating that a glycosidic linkage at O-3 may not be detrimental for the binding since the unit still contains other OH groups to interact. The fractions mainly composed of highly branched (1→3),(1→6)-linked  $\beta$ -glucan, LW-s and GW-s, did not present any potential to adhere to bacteria. This result suggests that unsubstituted O-6 was somehow important for the interaction with *S.*

Typhimurium. Hung et al. [69] reported that the O-6 of mannose directly interacts with the backbone of the Asp47 residue, the side-chain oxygen of Asn46 residue, and the NH<sub>2</sub> terminal group of the FimH receptor-binding domain, thereby the substitution at O-6 of glucans may have been deleterious for the binding affinity.

Ganner et al. [19] correlated the amount of mannan, glucan, and proteins of yeast cell wall fractions and yeast autolysate products from several strains with their binding capacity to *E. coli* and *S. Typhimurium*. For *Salmonella*, the binding affinity was highly correlated with the presence of glucans, whereas the mannan content was important for *E. coli* binding. In accordance with Ganner et al. [19], we believe that many factors influence the binding affinity to these pathogens, together with the mannan and/or glucan content. The polymer three-dimensional structure is also a critical factor for the adhesion process, considering that a pure standardized mannan did not bind to *E. coli* [70], and *E. coli* with mannose-specific adhesins did not colonize all mannose-containing tissues [71]. Furthermore, the adhesion process might involve other non-specific, hydrophobic or electrostatic interactions [72]. Adhesion is apparently due to a combination of factors, including saccharide presentation and dimensional structure [71]. It is likely that the 3-linked  $\beta$ -glucan three-dimensional structure, typical a triple-helix [73], could be favorable to bacteria binding.

The method used in the present study limits us in terms of explaining how the binding between the molecules present in the microalgal fractions and bacteria occurred or determining whether any unknown mechanism was involved. Nevertheless, our results strengthen the complexity of this subject and it seems clear that binding mechanisms are acting synergistically and/or other mechanisms not yet fully understood or unknown may be involved. Therefore, studies at a molecular level are necessary to elucidate the additional forces that might be involved in the binding mechanism between microalgal extracts and *Salmonella Typhimurium*. Finally, *in vivo* experiments with challenged animals could also contribute to validate the adhesion capacity of microalgal molecules and the study of their binding capacity.

## Conclusions

$\beta$ -glucans were isolated from aqueous extracts of *P. gyrans* and *P. lutheri*. Chemical and spectroscopic analyses showed linear (1 $\rightarrow$ 3)-linked  $\beta$ -D-glucans in the cold-water-precipitated fractions (GW-p, LW-p), whereas the cold-water-soluble fractions (GW-s, LW-s) presented branched  $\beta$ -D-glucans, which were constituted by a main chain of (1 $\rightarrow$ 3)-linked  $\beta$ -D-Glcp units and highly substituted at O-6 by single  $\beta$ -D-Glcp units or (1 $\rightarrow$ 6)-linked  $\beta$ -D-Glcp branches. In contrast, the alkaline extracts (GA-s, GA-p, LA-s, LA-p) were mainly composed of proteins, glycosides (SQG, DGG), and free fatty acids.

The use of microtitration-based *in vitro* bioassays allowed for the identification of extracts from *Haptophyta* microalgae that specifically adhered to *Salmonella* Typhimurium, highlighting the potential of these products as an alternative binding matrix for enteropathogens. Additionally, the results clearly indicate that the presence of the  $\beta$ -glucans and proteins could not be the unique factors responsible for the binding of *S.* Typhimurium to the microalgal extracts; other factors, such as the presence of glycosides, the polymers' three-dimensional structure, and other mechanisms that are still unknown, could be involved in the adhesion process. As such, further studies are necessary to determine the exact binding mechanism between the microalgae bioactive molecules and the enteropathogens.

## Patents

Nosedá, M.D.; Machado, T.W.M.; Nosedá, M.E.D.; Rodrigues, J.M. Extrato de microalgas marinhas com capacidade de aderência a bactérias patogênicas. BR102013010798-0.

## Author Contributions

T.W.M.M. and J.M.R. designed and performed the experiments, undertook the analysis and interpretation of data, and wrote the manuscript. T.R.M. assisted in the experiments and data analyses. M.E.R.D. revised all analyses and contributed to the conception and

design of the study. M.D.N. conceived, designed and supervised the study. All authors reviewed and approved the final manuscript.

## **Funding**

This work was supported by the Brazilian agencies: National Council for Scientific and Technological Development (CNPq) (Universal Calls grant numbers: 485980/2012-6, 462414/2014-0); Araucaria Foundation (PRONEX Carboidratos); Coordenação de Aperfeiçoamento de Pessoal de Nível Superior (CAPES), Finance Code 001.

## **Acknowledgments**

M.E.R.D. and M.D.N. are research members of CNPq. T.W.M.M., J.M.R., and T.R.M. acknowledge doctoral/postdoctoral scholarships from CNPq and CAPES. The authors are grateful to Professor Wagner Bonat for help with calculations related to the sigmoidal model and to Grupo Integrado de Aquicultura (GIA-UFPR) for assistance with the microalgae culture.

## **Conflicts of Interest**

The authors declare no conflict of interest.

## Supplementary Figures

**Figure 1.** 2D NMR COSY spectrum (400 MHz, Me<sub>2</sub>SO-*d*<sub>6</sub>, 70 °C) of GW-s.

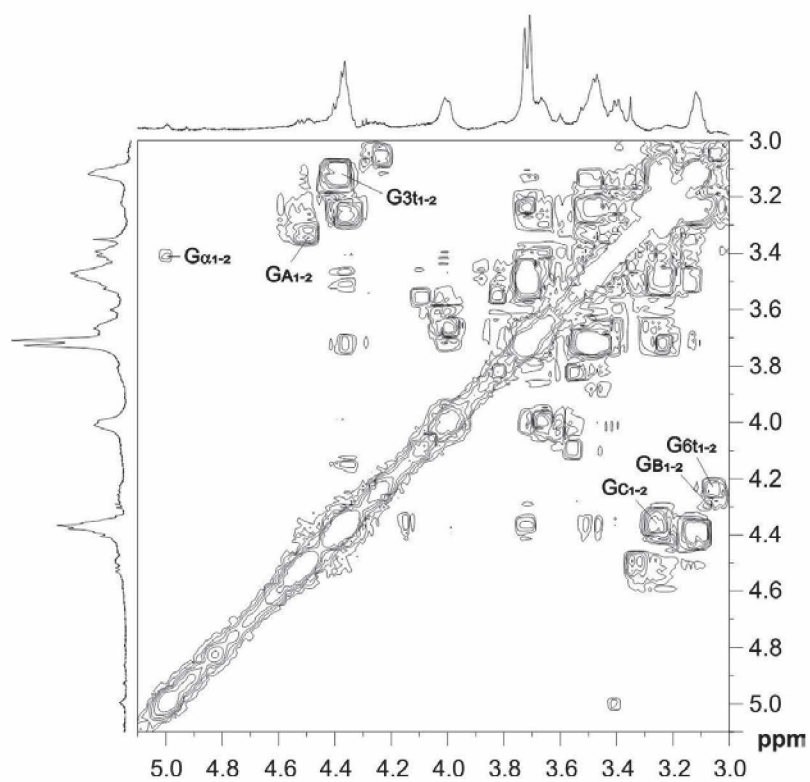
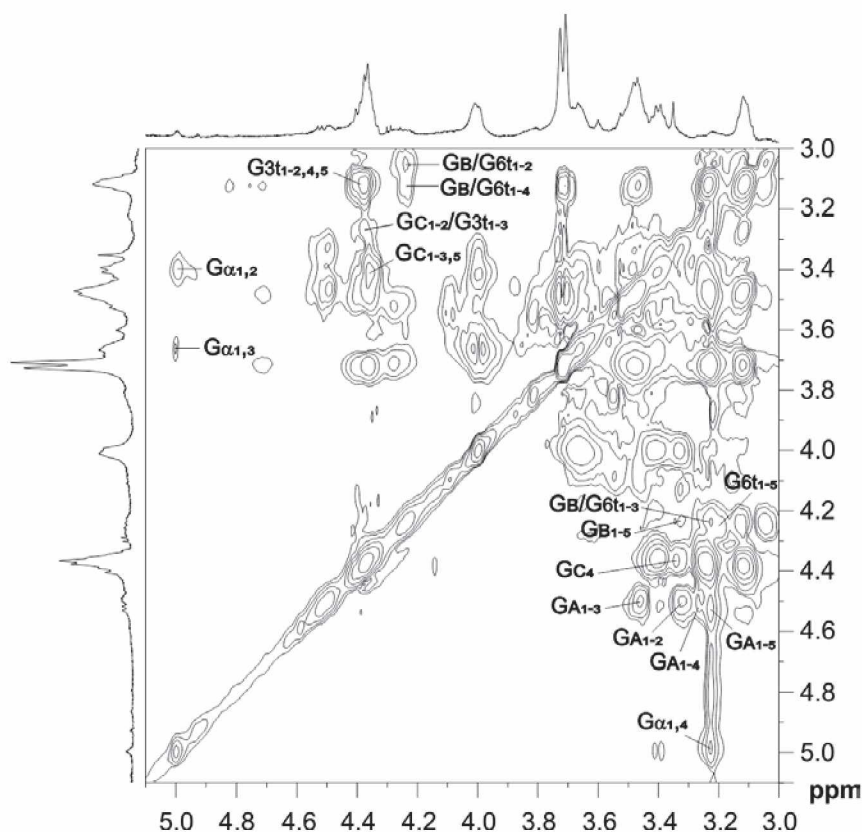


**Figure S2.** 2D NMR TOCSY spectrum (400 MHz, Me<sub>2</sub>SO-*d*<sub>6</sub>, 70 °C) of GW-s



## References

1. López, Y.; Cepas, V.; Soto, S.M. The marine ecosystem as a source of antibiotics. In *Grand Challenges in Marine Biotechnology*; Rampelotto, P.H., Trincone, A., Eds.; Springer: Cham, Switzerland, 2018; pp. 3–48. ISBN 978-3-319-69074-2.
2. Chu, W.L. Biotechnological applications of microalgae. *IeJSME* 2012, 6, S24–S37.
3. Villarruel-López, A.; Ascencio, F.; Nuño, K. Microalgae, a potential natural functional food source—A review. *Polish J. Food Nutr. Sci.* 2017, 67, 251–264.
4. Bendif, M.E.; Probert, I.; Hervé, A.; Billard, C.; Goux, D.; Lelong, C.; Cadoret, J.P.; Véron, B. Integrative taxonomy of the Pavlovophyceae (Haptophyta): A reassessment. *Protist* 2011, 162, 738–761.
5. Rehberg-Haas, S.; Meyer, S.; Lippemeier, S.; Schulz, C. A comparison among different Pavlova sp. products for cultivation of *Brachionus plicatilis*. *Aquaculture* 2015, 435, 424–430

6. Haas, S.; Bauer, J.L.; Adakli, A.; Meyer, S.; Lippemeier, S.; Schwarz, K.; Schulz, C. Marine microalgae *Pavlova viridis* and *Nannochloropsis* sp. as n-3 PUFA source in diets for juvenile European sea bass (*Dicentrarchus labrax* L.). *J. Appl. Phycol.* 2016, 28, 1011–1021.
7. Ponis, E.; Probert, I.; Véron, B.; Le Coz, J.R.; Mathieu, M.; Robert, R.; Coz, J.R.L.; Mathieu, M.; Robert, R. Nutritional value of six Pavlovophyceae for *Crassostrea gigas* and *Pecten maximus* larvae. *Aquaculture* 2006, 254, 544–553.
8. Bhalamurugan, G.L.; Valerie, O.; Mark, L. Valuable bioproducts obtained from microalgal biomass and their commercial applications: A review. *Environ. Eng. Res.* 2018, 23, 229–241.
9. de Jesus Raposo, M.F.; de Morais, A.M.B.; de Morais, R.M.S.C. Marine polysaccharides from algae with potential biomedical applications. *Mar. Drugs* 2015, 13, 2967–3028.
10. Xiao, R.; Zheng, Y. Overview of microalgal extracellular polymeric substances (EPS) and their applications. *Biotechnol. Adv.* 2016, 34, 1225–1244.
11. Maldonado-Gomez, M.X.; Lee, H.; Barile, D.; Lu, M.; Hutkins, R.W. Adherence inhibition of enteric pathogens to epithelial cells by bovine colostrum fractions. *Int. Dairy J.* 2015, 40, 24–32.
12. Quintero-Villegas, M.I.; Aam, B.B.; Rupnow, J.; Sorlie, M.; Eijsink, V.G.H.; Hutkins, R.W.; Sørlie, M.; Eijsink, V.G.H.; Hutkins, R.W. Adherence inhibition of enteropathogenic *Escherichia coli* by chitooligosaccharides with specific degrees of acetylation and polymerization. *J. Agric. Food Chem.* 2013, 61, 2748–2754.
13. Parkar, S.G.; Redgate, E.L.; Wibisono, R.; Luo, X.; Koh, E.T.H.; Schröder, R. Gut health benefits of kiwifruit pectins: Comparison with commercial functional polysaccharides. *J. Funct. Foods* 2010, 2, 210–218.
14. Gonzalez-Ortiz, G.; Perez, J.F.; Hermes, R.G.; Molist, F.; Jimenez-Diaz, R.; Martin-Orue, S.M. Screening the ability of natural feed ingredients to interfere with the adherence of enterotoxigenic *Escherichia coli* (ETEC) K88 to the porcine intestinal mucus. *Br. J. Nutr.* 2014, 111, 633–642.

15. Rodrigues, J.M.; Duarte, M.E.R.; Nosedá, M.D. Modified soybean meal polysaccharide with high adhesion capacity to *Salmonella*. *Int. J. Biol. Macromol.* 2019, 139, 1074–1084.
16. Ofek, I.; Sharon, N.; Abraham, S.N. Bacterial adhesion. In *The Prokaryotes*; Dworkin, M., Falkow, S., Rosenberg, E., Schleifer, K.H., Stackebrandt, E., Eds.; Springer: Singapore, 2006; Volume 2, pp. 16–31.
17. Laxminarayan, R.; Duse, A.; Wattal, C.; Zaidi, A.K.; Wertheim, H.F.; Sumpradit, N.; Vlieghe, E.; Hara, G.L.; Gould, I.M.; Goossens, H.; et al. Antibiotic resistance—the need for global solutions. *Lancet Infect. Dis.* 2013, 13, 1057–1098.
18. Kogan, G.; Kocher, A. Role of yeast cell wall polysaccharides in pig nutrition and health protection. *Livest. Sci.* 2007, 109, 161–165.
19. Ganner, A.; Stoiber, C.; Uhlik, J.T.; Dohnal, I.; Schatzmayr, G. Quantitative evaluation of *E. coli* F4 and *Salmonella typhimurium* binding capacity of yeast derivatives. *AMB Express* 2013, 3, 62–69.
20. Guzman-Murillo, M.A.; Ascencio, F. Anti-adhesive activity of sulphated exopolysaccharides of microalgae on attachment of red sore disease-associated bacteria and *Helicobacter pylori* to tissue culture cells. *Lett. Appl. Microbiol.* 2000, 30, 473–478.
21. Loke, M.F.; Lui, S.Y.; Ng, B.L.; Gong, M.; Ho, B. Antiadhesive property of microalgal polysaccharide extract on the binding of *Helicobacter pylori* to gastric mucin. *FEMS Immunol. Med. Microbiol.* 2007, 50, 231–238.
22. Guillard, R.R.L. Culture of phytoplankton for feeding marine invertebrates. In *Culture of Marine Invertebrate Animals*; Smith, W.L., Chanley, M.H., Eds.; Plenum Press: New York, NY, USA, 1975; pp. 29–60. ISBN 978-1-4615-8714-9.
23. Gorin, P.A.J.; Iacomini, M. Structural diversity of D-galacto-D-mannan components isolated from lichens having Ascomycetous mycosymbionts. *Carbohydr. Res.* 1985, 142, 253–261.
24. Lowry, O.H.; Rosebrough, N.J.; Farr, A.L.; Randall, R.J. Protein measurement with the Folin phenol reagent. *J. Biol. Chem.* 1951, 193, 265–275.

25. DuBois, M.; Gilles, K.A.; Hamilton, J.K.; Rebers, P.A.; Smith, F. Colorimetric method for determination of sugars and related substances. *Anal. Chem.* 1956, 28, 350–356.
26. Jansson, P.E.; Kenne, L.; Liedgren, H.; Lindberg, B.; Lönngrén, J. A practical guide to the methylation analysis of carbohydrates. *Chem. Commun. Univ. Stock.* 1976, 8, 1–75.
27. Ciucanu, I.; Kerek, F. A simple and rapid method for the permethylation of carbohydrates. *Carbohydr. Res.* 1984, 131, 209–217.
28. Bao, X.; Liu, C.; Fang, J.; Li, X. Structural and immunological studies of a major polysaccharide from spores of *Ganoderma lucidum* (Fr.) Karst. *Carbohydr. Res.* 2001, 332, 67–74.
29. Sasaki, G.L.; Gorin, P.A.J.; Souza, L.M.; Czelusniak, P.A.; Iacomini, M. Rapid synthesis of partially O-methylated alditol acetate standards for GC-MS: Some relative activities of hydroxyl groups of methyl glycopyranosides on Purdie methylation. *Carbohydr. Res.* 2005, 340, 731–739.
30. Ascêncio, S.D.; Orsato, A.; França, R.A.; Duarte, M.E.R.; Nosedá, M.D. Complete <sup>1</sup>H and <sup>13</sup>C NMR assignment of digeneaside, a low-molecular-mass carbohydrate produced by red seaweeds. *Carbohydr. Res.* 2006, 341, 677–682. [Google Scholar] [CrossRef]
31. Becker, P.M.; Galletti, S.; Roubos-van den Hil, P.J.; van Wikselaar, P.G. Validation of growth as measurand for bacterial adhesion to food and feed ingredients. *J. Appl. Microbiol.* 2007, 103, 2686–2696.
32. Ganner, A.; Stoiber, C.; Wieder, D.; Schatzmayr, G. Quantitative *in vitro* assay to evaluate the capability of yeast cell wall fractions from *Trichosporon mycotoxinivorans* to selectively bind gram negative pathogens. *J. Microbiol. Methods* 2010, 83, 168–174.
33. Batista, A.P.; Gouveia, L.; Bandarra, N.M.; Franco, J.M.; Raymundo, A. Comparison of microalgal biomass profiles as novel functional ingredient for food products. *Algal Res.* 2013, 2, 164–173.

34. Fernandes, T.; Fernandes, I.; Andrade, C.A.P.; Ferreira, A.; Cordeiro, N. Marine microalgae monosaccharide fluctuations as a stress response to nutrients inputs. *Algal Res.* 2017, 24, 340–346.
35. Marcilla, A.; Gómez-Siurana, A.; Gomis, C.; Chápuli, E.; Catalá, M.C.; Valdés, F.J. Characterization of microalgal species through TGA/FTIR analysis: Application to *Nannochloropsis* sp. *Thermochim. Acta* 2009, 484, 41–47.
36. Ponder, G.R.; Richards, G.N.; Stevenson, T.T. Influence of linkage position and orientation in pyrolysis of polysaccharides: A study of several glucans. *J. Anal. Appl. Pyrolysis* 1992, 22, 217–229.
37. Leng, E.; Costa, M.; Peng, Y.; Zhang, Y.; Gong, X.; Zheng, A.; Huang, Y.; Xu, M. Role of different chain end types in pyrolysis of glucose-based anhydro-sugars and oligosaccharides. *Fuel* 2018, 234, 738–745.
38. Dobruchowska, J.M.; Jonsson, J.O.; Fridjonsson, O.H.; Aevarsson, A.; Kristjansson, J.K.; Altenbuchner, J.; Watzlawick, H.; Gerwig, G.J.; Dijkhuizen, L.; Kamerling, J.P.; et al. Modification of linear ( $\beta$  1→3)-linked gluco-oligosaccharides with a novel recombinant beta-glucosyltransferase (trans-beta-glucosidase) enzyme from *Bradyrhizobium diazoefficiens*. *Glycobiology* 2016, 26, 1157–1170.
39. Sadovskaya, I.; Souissi, A.; Souissi, S.; Grard, T.; Lencel, P.; Greene, C.M.; Duin, S.; Dmitrenok, P.S.; Chizhov, A.O.; Shashkov, A.S.; et al. Chemical structure and biological activity of a highly branched (1→3,1→6)- $\beta$ -D-glucan from *Isochrysis galbana*. *Carbohydr. Polym.* 2014, 111, 139–148.
40. Kono, H.; Kondo, N.; Hirabayashi, K.; Ogata, M.; Totani, K.; Ikematsu, S.; Osada, M. NMR spectroscopic structural characterization of a water-soluble beta-(1→3, 1→6)-glucan from *Aureobasidium pullulans*. *Carbohydr. Polym.* 2017, 174, 876–886.
41. Lowman, D.W.; West, L.J.; Bearden, D.W.; Wempe, M.F.; Power, T.D.; Ensley, H.E.; Haynes, K.; Williams, D.L.; Kruppa, M.D. New Insights into the structure of (1→3,1→6)- $\beta$ -D-Glucan side chains in the *Candida glabrata* cell wall. *PLoS ONE* 2011, 6, e27614.

42. Sasaki, G.L.; Machado, M.J.; Tischer, C.A.; Gorin, P.A.J.; Iacomini, M. Glycosyldiacylglycerolipids from the lichen *Dictyonema glabratum*. *J. Nat. Prod.* 1999, 62, 844–847.
43. de Souza, L.M.; Iacomini, M.; Gorin, P.A.J.; Sari, R.S.; Haddad, M.A.; Sasaki, G.L. Glyco- and sphingophosphonolipids from the medusa *Phyllorhiza punctata*: NMR and ESI-MS/MS fingerprints. *Chem. Phys. Lipids* 2007, 145, 85–96.
44. Wang, H.; Li, Y.L.; Shen, W.Z.; Rui, W.; Ma, X.J.; Cen, Y.Z. Antiviral activity of a sulfoquinovosyldiacylglycerol (SQDG) compound isolated from the green alga *Caulerpa racemosa*. *Bot. Mar.* 2007, 50, 185–190.
45. Almoselhy, R.I.M.; Allam, M.H.; El-Kalyoubi, M.H.; El-Sharkawy, A.A. <sup>1</sup>H NMR spectral analysis as a new aspect to evaluate the stability of some edible oils. *Ann. Agric. Sci.* 2014, 59, 201–206.
46. Cavanagh, J.; Fairbrother, W.J.; Palmer, A.G.; Rance, M.; Skelton, N.J.B. Sequential assignment, structure determination, and other applications. In *Protein NMR Spectroscopy: Principles and Practice*; Cavanagh, J., Fairbrother, W.J., Palmer, A.G., Rance, M., Skelton, N.J.B., Eds.; Academic Press: Burlington, VT, USA, 2007; pp. 781–817. ISBN 978-0-12-164491-8.
47. Ma, L.; Yang, Y.; Yao, J.; Shao, Z.; Huang, Y.; Chen, X. Selective chemical modification of soy protein for a tough and applicable plant protein-based material. *J. Mater. Chem. B* 2015, 3, 5241–5248.
48. Myklestad, S.M.; Granum, E. Biology of (1,3)- $\beta$ -Glucans and related glucans in protozoans and chromistans. In *Chemistry, Biochemistry, and Biology of 1-3  $\beta$  Glucans and Related Polysaccharides*; Bacic, A., Fincher, G.B., Stone, B.A., Eds.; Academic Press: San Diego, CA, USA, 2009; pp. 353–385. ISBN 978-0-12-373971-1.
49. Hirokawa, Y.; Fujiwara, S.; Suzuki, M.; Akiyama, T.; Sakamoto, M.; Kobayashi, S.; Tsuzuki, M. Structural and physiological studies on the storage beta-polyglucan of haptophyte *Pleurochrysis haptoneofera*. *Planta* 2008, 227, 589–599.

50. Varum, K.M.; Kvam, B.J.; Myklestad, S.; Paulsen, B.S. Structure of a food-reserve  $\beta$ -D-glucan produced by the haptophyte alga *Emiliania huxleyi* (Lohmann) Hay and Mohler. *Carbohydr. Res.* 1986, 152, 243–248.
51. Janse, I.; van Rijssel, M.; van Hall, P.J.; Gerwig, G.J.; Gottschal, J.C.; Prins, R.A. The storage glucan of *Phaeocystis globosa* (Prymesiophyceae) cells. *J. Phycol.* 1996, 32, 382–387.
52. Renaud, S.M.; Van Thinh, L.; Parry, D.L. The gross chemical composition and fatty acid composition of 18 species of tropical Australian microalgae for possible use in mariculture. *Aquaculture* 1999, 170, 147–159.
53. Mauer, L. Heat Treatment for Food Proteins. In *Encyclopedia of Food Sciences and Nutrition*; Caballero, B., Trug, L., Finglas, P.M., Eds.; Academic Press: Oxford, UK, 2003; pp. 4868–4872. ISBN 978-0-12-227055-0.
54. Tatsuzawa, H.; Takizawa, E. Changes in lipid and fatty acid composition of *Pavlova lutheri*. *Phytochemistry* 1995, 40, 397–400.
55. Eichenberger, W.; Gribi, C. Lipids of *Pavlova lutheri*: Cellular site and metabolic role of DGCC. *Phytochemistry* 1997, 45, 1561–1567.
56. Thompson, G.A. Lipids and membrane function in green algae. *Biochim. Biophys. Acta Lipids Lipid Metab.* 1996, 1302, 17–45.
57. Shoaf-Sweeney, K.D.; Hutkins, R.W. Chapter 2 Adherence, anti-adherence, and oligosaccharides: Preventing pathogens from sticking to the host. *Adv. Food Nutr. Res.* 2008, 55, 101–161.
58. Romling, U.; Bian, Z.; Hammar, M.; Sierralta, W.D.; Normark, S. Curli fibers are highly conserved between *Salmonella typhimurium* and *Escherichia coli* with respect to operon structure and regulation. *J. Bacteriol.* 1998, 180, 722–731.
59. Wagner, C.; Barlag, B.; Gerlach, R.G.; Deiwick, J.; Hensel, M. The *Salmonella enterica* giant adhesin SiiE binds to polarized epithelial cells in a lectin-like manner. *Cell. Microbiol.* 2014, 16, 962–975.
60. Griessl, M.H.; Schmid, B.; Kassler, K.; Braunsmann, C.; Ritter, R.; Barlag, B.; Stierhof, Y.-D.; Sturm, K.U.; Danzer, C.; Wagner, C.; et al. Structural insight into

- the giant Ca<sup>2+</sup>-Binding Adhesin SiiE: Implications for the adhesion of *Salmonella enterica* to polarized epithelial cells. *Structure* 2013, 21, 741–752.
61. Dorsey, C.W.; Laarakker, M.C.; Humphries, A.D.; Weening, E.H.; Bäumlner, A.J. *Salmonella enterica* serotype Typhimurium MisL is an intestinal colonization factor that binds fibronectin. *Mol. Microbiol.* 2005, 57, 196–211.
  62. Weimer, B.C.; Chen, P.; Desai, P.T.; Chen, D.; Shah, J. Whole cell cross-linking to discover host–microbe protein cognate receptor/ligand pairs. *Front. Microbiol.* 2018, 9, 1585.
  63. Chowdhury, S.M.; Shi, L.; Yoon, H.; Ansong, C.; Rommereim, L.M.; Norbeck, A.D.; Auberry, K.J.; Moore, R.J.; Adkins, J.N.; Heffron, F.; et al. A method for investigating protein–protein interactions related to *Salmonella Typhimurium* pathogenesis. *J. Proteome Res.* 2009, 8, 1504–1514.
  64. Brück, W.M.; Kelleher, S.L.; Gibson, G.R.; Graverholt, G.; Lonnerdal, B.L. The effects of  $\alpha$ -lactalbumin and glycomacropeptide on the association of CaCo-2 cells by enteropathogenic *Escherichia coli*, *Salmonella typhimurium* and *Shigella flexneri*. *FEMS Microbiol. Lett.* 2006, 259, 158–162.
  65. Nakajima, K.; Tamura, N.; Kobayashi-Hattori, K.; Yoshida, T.; Hara-Kudo, Y.; Ikedo, M.; Sugita-Konishi, Y.; Hattori, M. Prevention of intestinal infection by glycomacropeptide. *Biosci. Biotechnol. Biochem.* 2005, 69, 2294–2301.
  66. Ouwehand, A.C.; Salminen, S.J.; Skurnik, M.; Conway, P.L. Inhibition of pathogen adhesion by  $\beta$ -lactoglobulin. *Int. Dairy J.* 1997, 7, 685–692.
  67. Newburg, D.S.; McCormick, B.; Chaturvedi, P.; Siber, A.M.; Warren, C.D. Inhibition of *Salmonella typhimurium* by human milk sulfatides. *Pediatr. Res.* 1999, 45, 116.
  68. Bouckaert, J.; Berglund, J.; Schembri, M.; De Genst, E.; Cools, L.; Wuhrer, M.; Hung, C.S.; Pinkner, J.; Slattegard, R.; Zavialov, A.; et al. Receptor binding studies disclose a novel class of high-affinity inhibitors of the *Escherichia coli* FimH adhesin. *Mol. Microbiol.* 2005, 55, 441–455.
  69. Hung, C.S.; Bouckaert, J.; Hung, D.; Pinkner, J.; Widberg, C.; DeFusco, A.; Auguste, C.G.; Strouse, R.; Langermann, S.; Waksman, G.; et al. Structural basis

- of tropism of *Escherichia coli* to the bladder during urinary tract infection. *Mol. Microbiol.* 2002, 44, 903–915.
70. Ganner, A.; Fink, L.; Schatzmayr, G. Quantitative *in vitro* assay to evaluate yeast products concerning their binding activity of enteropathogenic bacteria. *J. Anim. Sci.* 2008, 86, 54.
71. Ofek, I.; Doyle, R.J. Principles of Bacterial Adhesion. In *Bacterial Adhesion to Cells and Tissues*; Ofek, I., Doyle, R.J., Eds.; Springer: Boston, MA, USA, 1994; pp. 1–15. ISBN 978-1-4684-6435-1.
72. Ofek, I.; Hasty, D.L.; Sharon, N. Anti-adhesion therapy of bacterial diseases: Prospects and problems. *FEMS Immunol. Med. Microbiol.* 2003, 38, 181–191.
73. Sletmoen, M.; Stokke, B.T. Higher order structure of (1,3)- $\beta$ -D-Glucans and its influence on their biological activities and complexation abilities. *Biopolymers* 2008, 89, 310–321.

## Referências

- ABDULLAH, N.R.; SHARIF, F.; AZIZAN, N.H.; HAFIDZ, I.F.M.; SUPRAMANI, S.; USULDIN, S.R.A.; AHMAD, R.; WAN-MOHTAR, W. Pellet diameter of *Ganoderma lucidum* in a repeated-batch fermentation for the trio total production of biomass-exopolysaccharide-endopolysaccharide and its anti-oral cancer beta-glucan response. **AIMS microbiology** v. 6, n. 4, p. 379-400, 2020.
- ABREU, H.; SIMAS, F.F.; SMIDERLE, F.R.; SOVRANI, V.; DALLAZEN, J.L.; MARIA-FERREIRA, D.; WERNER, M.F.; CORDEIRO, L.M.C.; IACOMINI, M. Gelling functional property, anti-inflammatory and antinociceptive bioactivities of  $\beta$ -D-glucan from the edible mushroom *Pholiota nameko*. **International Journal of Biological Macromolecules**, v. 122, p. 1128-1135, 2019.
- ALASSALI, A.; CYBULSKA, I.; BRUDECKI, G. P.; FARZANAH, R. & THOMSEN, M. H. Methods for Upstream Extraction and Chemical Characterization of Secondary Metabolites from Algae Biomass. **Advanced Techniques in Biology and Medicine**, v.4, n.1, p.16, 2016.
- ALEKSEEVA, S.A.; SHEVCHENKO, N.M.; KUSAIKIN, M.I.; PONOMORENKO, L.P.; ISAKOV, V.V.; ZVIAGINTSEVA, T.N.; LIKHOSHVAI, E.V. Polysaccharides of diatoms occurring in lake Baikal. **Prikladnaia Biokhimiia i Mikrobiologiya**, n. 41, p. 213-219, 2005.
- ALLEN, E.L.; ULANET, D.B.; PIRMAN, D.; MAHONEY, C.E.; COCO, J.; SI, Y. et al. Smolen, Differential Aspartate Usage Identifies a Subset of Cancer Cells Particularly Dependent on OGDH. **Cell Reports**, v. 17, n. 3, p. 876-890, 2016.
- ALMOSELHY, R.I.M.; ALLAM, M.H.; EL-KALYUBI, M.H.; EL-SHARKAWY, A.A. <sup>1</sup>H NMR spectral analysis as a new aspect to evaluate the stability of some edible oils. **Annals of Agricultural Sciences**, n. 59, p. 201–206, 2014
- AL-SAFFAR, A.Z.; HADI, N.A.; KHALAF, H.M. Antitumor Activity of  $\beta$ -glucan Extracted from *Pleurotus eryngii*. **Indian Journal of Forensic Medicine & Toxicology** v. 14, n. 3, p. 2492-2499, 2020.
- AMARAL, A.E.; CARBONERO, E.R.; SIMÃO, R.D.C.G.; KADOWAKI, M.K.; SASSAKI, G.L. et al. An unusual water-soluble  $\beta$ -glucan from the basidiocarp of the fungus *Ganoderma resinaceum*. **Carbohydrate Polymers**, v. 72, n. 3, p. 473-478, 2008.
- AMARAL, S.D.C.; BARBIERI, S.F.; RUTHES, A.C.; BARK, J.M.; BROCHADO WINNISCHOFER, S.M.; SILVEIRA, J.L.M. Cytotoxic effect of crude and purified pectins from *Campomanesia xanthocarpa* Berg on human glioblastoma cells. **Carbohydrate polymers**, v. 224, p.115140, 2019.
- ANJUM, K.; SHAGUFTA, B.I.; ABBAS, S.Q.; PATEL, S.; KHAN, I.; SHAH, S.A.A.;

AKHTER, N.; HASSAN, S.S.U. Current status and future therapeutic perspectives of glioblastoma multiforme (GBM) therapy: A review. **Biomedicine & pharmacotherapy = Biomedecine & pharmacotherapie**, 92 (2017) 681-689.

ASCÊNCIO, S.D.; ORSATO, A.; FRANÇA, R.A.; DUARTE, M.E.R.; NOSEDA, M.D. Complete <sup>1</sup>H and <sup>13</sup>C NMR assignment of digeneaside, a low-molecular-mass carbohydrate produced by red seaweeds. **Carbohydrate Research**, v. 341, p. 677–682, 2006.

BAO, X.; LIU, C.; FANG, J.; LI, X. Structural and immunological studies of a major polysaccharide from spores of *Ganoderma lucidum* (Fr.) Karst. **Carbohydrate Research**, n. 332, p. 67–74, 2001.

BARANOSKI, A.; TEMPESTA OLIVEIRA, M.; SEMPREBON, S.C.; NIWA, A.M.; RIBEIRO, L.R.; MANTOVANI, M.S. Effects of sulfated and non-sulfated  $\beta$ -glucan extracted from *Agaricus brasiliensis* in breast adenocarcinoma cells - MCF-7. **Toxicology mechanisms and methods**, v. 25, n. 9, p. 672- 9, 2015.

BARSANTI, L. & GUALTIERI, P. **Algae: Anatomy, Biochemistry and Biotechnology**, 2014.

BARSANTI, L.; GUALTIERI, P. Paramylon, a potent immunomodulator from WZSL mutant of *Euglena gracilis*. **Molecules**, v. 24, n. 17, p. 3114, 2019.

BATISTA, A.P.; GOUVEIA, L.; BANDARRA, N.M.; FRANCO, J.M.; RAYMUNDO, A. Comparison of microalgal biomass profiles as novel functional ingredient for food products. **Algal Research**, 2013, 2, 164–173.

BRANDT, A.P.; GOZZI, G.J.; PIRESADO, R.; MARTINEZ, G.R.; DOS SANTOS CANUTO, A.V.; ECHEVARRIA, A.; DI PIETRO, A., CADENA S.M. Impairment of oxidative phosphorylation increases the toxicity of SYD-1 on hepatocarcinoma cells (HepG2). **Chemico-Biological Interactions**, n. 256 p. 154-160, 2016.

BRAY, F.; FERLAY, J.; SOERJOMATARAM, I.; SIEGEL, R.L.; TORRE, L.A.; JEMAL, A. Global cancer statistics 2018: GLOBOCAN estimates of incidence and mortality worldwide for 36 cancers in 185 countries. **CA: A Cancer Journal for Clinicians**, 68 (2018) 394-424

BECKER, P.M.; GALLETTI, S.; ROUBOS-VAN DEN HIL, P.J.; VAN WIKSELAAR, P.G. Validation of growth as measurand for bacterial adhesion to food and feed ingredients. **Journal of Applied Microbiology**, n. 103, p. 2686–2696, 2007.

BEKESCHUS, S.; EISENMANN, S.; SAGWAL, S.K.; BODNAR, Y.; MORITZ, J.; POSCHKAMP, B. et al. xCT (SLC7A11) expression confers intrinsic resistance to physical plasma treatment in tumor cells. **Redox Biology**, n. 30, p. 101423, 2020.

BENDIF, M.E.; PROBERT, I.; HERVÉ, A.; BILLARD, C.; GOUX, D.; LELONG, C.; CADORET, J.P.; VÉRON, B. Integrative taxonomy of the *Pavlovophyceae* (Haptophyta):

A reassessment. **Protist** n. 162, p. 738–761, 2011.

BERNAERTS, T.M.M.; GHEYSEN, L.; KYOMUGASHO, C.; JAMSAZZADEH KERMANI, Z.; VANDIONANT, S.; FOUBERT, I.; VAN LOEY, A.M. Comparison of microalgal biomasses as functional food ingredients: focus on the composition of cell wall related polysaccharides. **Algal Research**, n. 32, pp. 150-161, 2018.

BHALAMURUGAN, G.L.; VALERIE, O.; MARK, L. Valuable bioproducts obtained from microalgal biomass and their commercial applications: A review. **Environmental Engineering Research**, n. 23, p. 229–241, 2018.

BIRAY AVCI, C.; KURT, C. C.; TEPEDELEN, B. E.; OZALP, O.; GOKER, B.; MUTLU, Z.; GUNDUZ, C. Zoledronic acid induces apoptosis via stimulating the expressions of ERN1, TLR2, and IRF5 genes in glioma cells. **Tumour Biology**, v.37, n.5, p.6673-6679, 2016.

BOHN, J.; BEMILLER, J. (1→3)-β-D-glucans as biological response modifiers: a review of structure-functional activity relationships **Carbohydrate Polymers**, n. 28, pp. 3-14, 1995.

BONANNO, G. & ORLANDO-BONACA, M. Trace elements in Mediterranean seagrasses and macroalgae. A review. **Science of The Total Environment**, n. 618, p.1152-1159, 2018.

BOUCKAERT, J.; BERGLUND, J.; SCHEMBRI, M.; DE GENST, E.; COOLS, L.; WUHRER, M.; HUNG, C.S.; PINKNER, J.; SLATTEGARD, R.; ZAVIALOV, A.; et al. Receptor binding studies disclose a novel class of high-affinity inhibitors of the *Escherichia coli* FimH adhesin. **Molecular Microbiology**, n. 55, p. 441–455, 2005.

BOUISSIL, S.; PIERRE, G.; ALAOUI-TALIBI, Z. E.; MICHAUD, P.; EL MODAFAR, C. & DELATTRE, C. Applications of Algal Polysaccharides and Derivatives in Therapeutic and Agricultural Fields. **Current Pharmaceutical Design**, v.25, n.11, p.1187-1199, 2019.

BOUKID, F., CASTELLARI, M. Food and beverages containing algae and derived ingredients launched in the market from 2015 to 2019: a front-of-pack labeling perspective with a special focus on Spain. **Foods**, v. 10, n. 1, p. 173, 2021.

BRÜCK, W.M.; KELLEHER, S.L.; GIBSON, G.R.; GRAVERHOLT, G.; LONNERDAL, B.L. The effects of α-lactalbumin and glycomacropeptide on the association of CaCo-2 cells by enteropathogenic *Escherichia coli*, *Salmonella typhimurium* and *Shigella flexneri*. **FEMS Microbiology Letters** n. 259, p. 158–162, 2006.

BUCHI, D.D.F.; DE SOUZA, W. Internalization of surface components during Fc-receptor mediated phagocytosis by macrophages. **Cell Structure and Function**, n. 18, p. 399-407, 1993.

CAGNO, V.; TSELIGKA, E. D.; JONES, S. T. & TAPPAREL, C. Heparan Sulfate Proteoglycans and Viral Attachment: True Receptors or Adaptation Bias?. **Viruses**, v.11, p.7, 2019.

CAVANAGH, J.; FAIRBROTHER, W.J.; PALMER, A.G.; RANCE, M.; SKELTON, N.J.B. **Sequential assignment, structure determination, and other applications. In Protein NMR Spectroscopy: Principles and Practice**; Cavanagh, J., Fairbrother, W.J., Palmer, A.G., Rance, M., Skelton, N.J.B., Eds.; Academic Press: Burlington, VT, USA, pp. 781–817. ISBN 978-0-12-164491-8, 2007.

CASSOLATO, J.E.; NOSEDA, M.D.; PUJOL, C.A.; PELLIZZARI, F.M.; DAMONTE, E.B.; DUARTE, M.E. Chemical structure and antiviral activity of the sulfated heterorhamnan isolated from the green seaweed *Gayralia oxysperma*. **Carbohydrate Research**, n. 343, p. 3085-3095, 2008.

CHAN, G.C.; CHAN, W.K.; SZE, D.M. The effects of  $\beta$ -glucan on human immune and cancer cells. **Journal of Hematology & Oncology**, n. 2, p. 25, 2009.

CHAPMAN, R. L. Algae: the world's most important "plants"—an introduction. **Mitigation and Adaptation Strategies for Global Change**, v. 18, n. 1, p. 1573-1596, 2013.

CHEN, J.; THAN, A.; LI, N.; ANANTHANARAYANAN, A.; ZHENG, X.; XI, F. et al. Sweet graphene quantum dots for imaging carbohydrate receptors in live cells. **FlatChem**, v.5, p.25-32, 2017.

CHEN, L. & HUANG, G. Antitumor Activity of Polysaccharides: An Overview. **Current Drug Targets**, v.19, n.1, p.89-96, 2018.

CHEN, R.; SMITH-COHN, M.; COHEN, A.L.; COLMAN, H. Glioma subclassifications and their clinical significance. **Neurotherapeutics**, v. 14, n. 2, pp. 284-297, 2017.

CHEN, T.; CHEN, J.; ZHU, Y.; LI, Y.; WANG, Y.; CHEN, H.; KE, Y. CD163, a novel therapeutic target, regulates the proliferation and stemness of glioma cells via casein kinase 2. **Oncogene**, v.38, n.8, p.1183-1199, 2019.

CHEN, Y.; JIANG, X.; XIE, H.; LI, X.; & SHI, L. Structural characterization and antitumor activity of a polysaccharide from *Ramulus mori*. **Carbohydrated Polymers**, v.190, p. 232-239, 2018.

CHENGHUA, D.; XIANGLIANG, Y.; XIAOMAN, G.; YAN, W.; JINGYAN, Z.; HUIBI, X. A  $\beta$ -D-glucan from the sclerotia of *Pleurotus tuberregium* (Fr.) Sing. **Carbohydrate Research**, n. 328, p. 629-633, 2000.

CHIVIOTTI, A.; MOLINO, P., CRAWFORD, S.A.; TENG, R.; SPURCK, T.; WETHERBEE, R. The glucans extracted with warm water from diatoms are mainly derived from

intracellular chylolaminaran and not extracelullar polysaccharides. **European Journal of Phycology**, n. 39, p. 117-128, 2004.

CHOJNACKA, K.; WIECZOREK, P. P.; SCHROEDER, G.; MICHALAK, I. **Algae Biomass: Characteristics and Applications**: Springer, Cham, 2018.

CHOROMANSKA, A.; KULBACKA, J.; REMBIALKOWSKA, N.; PILAT, J.; OLEDZKI, R.; HARASYM, J.; SACZKO, J. Anticancer properties of low molecular weight oat  $\beta$ -glucan - an *in vitro* study. **International Journal of Biological Macromolecules**, n. 80, p. 23-28, 2015.

CHOROMANSKA, A.; KULBACKA, J.; HARASYM, J.; OLEDZKI, R.; SZEWCZYK, A.; SACZKO, J. High- and low-Molecular Weight oat  $\beta$ -Glucan Reveals Antitumor Activity in Human Epithelial Lung Cancer. **Pathology oncology research: POR** v. 24, n. 3, p. 583-592, 2018.

CHOWDHURY, S.M.; SHI, L.; YOON, H.; ANSONG, C.; ROMMEREIM, L.M.; NORBECK, A.D.; AUBERRY, K.J.; MOORE, R.J.; ADKINS, J.N.; HEFFRON, F. et al. A method for investigating protein-protein interactions related to *Salmonella* Typhimurium pathogenesis. **Journal of Proteome Research**, n. 8, p. 1504-1514, 2009.

CHU, W.L. **Biotechnological applications of microalgae**. *leJSME* n. 6, p.24- 37, 2012.

CIANCIA, M.; FERNÁNDEZ, P.V.; LELIAERT F. Diversity of Sulfated Polysaccharides from Cell Walls of Coenocytic Green Algae and Their Structural Relationships in View of Green Algal Evolution. **Frontiers in Plant Science**, n.11, 2020.

CIUCANU, I.; KEREK, F. A simple and rapid method for the permethylation of carbohydrates. **Carbohydrate Research**, n. 131, p. 209-217, 1984.

COMPTON, C. **Cancer Initiation, Promotion, and Progression and the Acquisition of Key Behavioral Traits**. In **Cancer: The Enemy from Within: A Comprehensive Textbook of Cancer's Causes, Complexities and Consequences** (pp. 25-48). Cham: Springer International Publishing, 2020.

COLODI, F. G.; DUCATTI, D.; NOSEDA, M. D.; DE CARVALHO, M. M.; WINNISCHOFER, S. & DUARTE, M. Semi-synthesis of hybrid ulvan-kappa-carrabiose polysaccharides and evaluation of their cytotoxic and anticoagulant effects. **Carbohydrate polymers**, v.267, p.118-161, 2021.

COLUSSE, G.A.; CARNEIRO, J.; DUARTE, M.E.R; DE CARVALHO, J.C.; NOSEDA, M.D. Advances in microalgal cell wall polysaccharides: a review focused on structure, production, and biological application. **Critical Reviews in Biotechnology**, n. 42, p. 562-577, 2021.

CORRÊA, D. D. O.; DUARTE, M. E. R. & NOSEDA, M. D. Biomass production and harvesting of *Desmodesmus subspicatus* cultivated in flat plate photobioreactor using chitosan as flocculant agent. **Journal of Applied Phycology**, v. 31, n. 2, p. 857-866,

2018.

CORRÊA, P. S.; MORAIS JÚNIOR, W. G.; MARTINS, A. A.; CAETANO, N. S. & MATA, T. M. Microalgae Biomolecules: Extraction, Separation and Purification Methods. **Processes**, v.9, n. 1, p.10, 2021.

CUI, Y.; ZHU, L.; LI, Y.; JIANG, S.; SUN, Q.; XIE, E.; CHEN, H.; ZHAO, Z.; QIAO, W.; XU, J.; DONG, C. Structure of a laminarin-type  $\beta$ -(1 $\rightarrow$ 3)-glucan from brown algae *Sargassum henslowianum* and its potential on regulating gut microbiota. **Carbohydrate polymers**, n. 255, p. 117389, 2021.

CUNHA DE PADUA, M.M.; SUTER CORREIA CADENA, S.M.; DE OLIVEIRA PETKOWICZ, C.L.; MARTINEZ, G.R.; MERLIN ROCHA, M.E.; MERCE, A.L.R.; NOLETO, G.R. Toxicity of native and oxovanadium (IV/V) galactomannan complexes on HepG2 cells is related to impairment of mitochondrial functions. **Carbohydrate polymers**, n. 173, p. 665-675, 2017.

CUNHA DE PADUA, M.M.; SUTER CORREIA CADENA, S.M.; DE OLIVEIRA PETKOWICZ, C.L.; MARTINEZ, G.R.; NOLETO, G. R. Galactomannan from *Schizolobium amazonicum* seed and its sulfated derivatives impair metabolism in HepG2 cells. **International Journal of Biological Macromolecules**, n.101, p.464-473, 2017.

DE CARVALHO, M. M.; DE FREITAS, R. A.; DUCATTI, D.; FERREIRA, L. G.; GONÇALVES, A. G.; COLODI, F. G.; MAZEPA, E.; ARANHA, E. M.; NOSEDA, M. D. & DUARTE, M. Modification of ulvans via periodate- chlorite oxidation: Chemical characterization and anticoagulant activity. **Carbohydrate polymers**, v.197, p.631–640, 2018.

DE CARVALHO, M. M.; NOSEDA, M. D.; DALLAGNOL, J.; FERREIRA, L. G.; DUCATTI, D.; GONÇALVES, A. G.; DE FREITAS, R. A. & DUARTE, M. Conformational analysis of ulvans from *Ulva fasciata* and their anticoagulant polycarboxylic derivatives. **International journal of biological macromolecules**, v.162, p.599–608, 2020.

DE CLERCK, O.; GUIRY, M. D.; LELIAERT, F.; SAMYN, Y. & VERBRUGGEN, H. Algal taxonomy: a road to nowhere? **Journal of Phycology**, v. 49, n. 2, p. 215-225, 2013.

DE SOUZA, L.M.; IACOMINI, M.; GORIN, P.A.J.; SARI, R.S.; HADDAD, M.A.; SASSAKI, G.L. Glyco- and sphingophosphonolipids from the medusa *Phyllorhiza punctata*: NMR and ESI-MS/MS fingerprints. **Chemistry and Physics of Lipids**, n. 145, p. 85–96, 2007.

DE JESUS RAPOSO, M.F.; DE MORAIS, A.M.M.B.; DE MORAIS, R.M.S.C. **Bioactivity and applications of polysaccharides from marine microalgae**. K. Ramawat, J.M. Mérillon (Eds.), Polysaccharides, Springer, Cham. p. 1-38, 2014.

DE JESUS RAPOSO, M.F.; DE MORAIS, A.M.B.; DE MORAIS, R.M.S.C. Marine polysaccharides from algae with potential biomedical applications. **Marine Drugs**, n. 13, p. 2967–3028, 2015.

DEBIAGI, P. E. A., TRINCHERA, M., FRASSOLDATI, A., FARAVELLI, T., VINU, R. & RANZI, E. Algae characterization and multistep pyrolysis mechanism. **Journal of Analytical and Applied Pyrolysis**, v.128, p.423- 436, 2017.

DELGADO-LOPEZ, P.D. & CORRALES-GARCIA, E.M. Survival in glioblastoma: a review on the impact of treatment modalities. **Clinical and Translational Oncology**, v.18, n. 11, p. 1062-1071, 2016.

DOBRUCHOWSKA, J.M.; JONSSON, J.O.; FRIDJONSSON, O.H.; AEVARSSON, A.; KRISTJANSSON, J.K.; ALTENBUCHNER, J.; WATZLAWICK, H.; GERWIG, G.J.; DIJKHUIZEN, L.; KAMERLING, J.P.; et al. Modification of linear  $\beta$  (1 $\rightarrow$ 3)-linked gluco-oligosaccharides with a novel recombinant beta-glucosyltransferase (trans-beta-glucosidase) enzyme from *Bradyrhizobium diazoefficiens*. **Glycobiology** n. 26, p. 1157–1170, 2016.

DODGSON, K.S.; PRICE, R.G. A note on the determination of the ester sulphate content of sulphated polysaccharides. **The Biochemical journal**, v. 84, n. 1, p. 106-10, 1962.

DORSEY, C.W.; LAARAKKER, M.C.; HUMPHRIES, A.D.; WEENING, E.H.; BÄUMLER, A.J. *Salmonella enterica* serotype Typhimurium MisL is an intestinal colonization factor that binds fibronectin. **Molecular Microbiology**, n. 57, p. 196–211, 2005.

DUBOIS, M.; GILLES, K.A.; HAMILTON, J.K.; REBERS, P.A.; SMITH, F. Colorimetric method for determination of sugars and related substances. **Analytical Chemistry**, v. 28, n. 350–356, 1956.

EICHENBERGER, W.; GRIBI, C. Lipids of *Pavlova lutheri*: Cellular site and metabolic role of DGCC. **Phytochemistry**, n. 45, p. 1561–1567, 1997.

EL-OSTA, H.; CIRCU, M.L. Mitochondrial ROS and Apoptosis, in: L.M. Buhlman (Ed.) **Mitochondrial Mechanisms of Degeneration and Repair in Parkinson's Disease**, Springer International Publishing, Cham, pp. 1-23, 2016.

ESCALIANTE, L.; BUSATO, B.; PETKOWICZ, C.L.O.; CADENA, S.; NOLETO, G.R. Cytotoxic effect of xyloglucan and oxovanadium (IV/V) xyloglucan complex in HepG2 cells. **International Journal of Biological Macromolecules**, n.185, p.40-48, 2021.

FARIAS, C.L.A.; MARTINEZ, G.R.; CADENA, S.; MERCE, A.L.R.; DE OLIVEIRA PETKOWICZ, C.L.; NOLETO, G.R. Cytotoxicity of xyloglucan from *Copaifera langsdorffii* and its complex with oxovanadium (IV/V) on B16F10 cells. **International Journal of Biological Macromolecules**, n.121, p.1019-1028, 2019.

FERNANDES, T.; FERNANDES, I.; ANDRADE, C.A.P.; FERREIRA, A.; CORDEIRO, N. Marine microalgae monosaccharide fluctuations as a stress response to nutrients inputs.

**Algal Research**, n. 24, v. 340–346, 2017.

FERREIRA, L.G.; DA SILVA, A.C.R.; NOSEDA, M.D.; FULY, A.L.; DE CARVALHO, M.M.; FUJII, M.T.; SANCHEZ, E.F.; CARNEIRO, J.; DUARTE, M.E.R. Chemical structure and snake antivenom properties of sulfated agarans obtained from *Laurencia dendroidea* (Ceramiales, Rhodophyta). **Carbohydrate polymers**, n. 218, p. 136-144, 2019.

FERREIRA, S. S.; PASSOS, C. P.; MADUREIRA, P.; VILANOVA, M. & COIMBRA, M. A. Structure-function relationships of immunostimulatory polysaccharides: A review. **Carbohydrate Polymers**, v.132, p.378-396, 2015.

FILISSETTI-COZZI, T.M.C.C.; CARPITA, N.C. Measurement of uronic acids without interference from neutral sugars, **Analytical Biochemistry**, v. 197, n. 1, p. 157-162, 1991.

FORD, C.W.; PERCIVAL, E.E. Carbohydrates of *Phaeodactylum tricornutum*. **Journal of the Chemical Society**, p. 7042–7046, 1965.

FORKINK, M.; MANJERI, G.R.; LIEMBURG-APERS, D.C.; NIBBELING, E.; BLANCHARD, M.; WOJTALA, A.; SMEITINK, J.A.; WIECKOWSKI, M.R.; WILLEMS, P.H.; KOOPMAN, W.J. Mitochondrial hyperpolarization during chronic complex I inhibition is sustained by low activity of complex II, III, IV and V. **Biochimica et Biophysica Acta (BBA)**, n.1837, p.1247-1256, 2014.

FUCHS, B.C.; BODE, B.P. Amino acid transporters ASCT2 and LAT1 in cancer: partners in crime?. **Seminars in Cancer Biology**, v. 15, n. 4, p. 254-66, 2005.

FURNEAUX, R.H.; STEVENSON, T.T. The xylogalactan sulfate from *Chondria macrocarpa* (Ceramiales, Rhodophyta). **Hydrobiologia**, v. 204, p. 615-620, 1990.

GANDHIRAJAN, R.K.; MEYER, D.; SAGWAL, S.K.; WELTMANN, K.D.; VON WOEDTKE, T.; BEKESCHUS, S. The amino acid metabolism is essential for evading physical plasma-induced tumour cell death, **British Journal of Cancer** v. 124, n. 11, p. 1854-1863, 2021.

GANNER, A.; FINK, L.; SCHATZMAYR, G. Quantitative *in vitro* assay to evaluate yeast products concerning their binding activity of enteropathogenic bacteria. **Journal of Animal Science**, n. 86, p. 54, 2008.

GANNER, A.; STOIBER, C.; WIEDER, D.; SCHATZMAYR, G. Quantitative *in vitro* assay to evaluate the capability of yeast cell wall fractions from *Trichosporon mycotoxinivorans* to selectively bind gram negative pathogens. **Journal of Microbiological Methods**, n. 83, p. 168–174, 2010.

GANNER, A.; STOIBER, C.; UHLIK, J.T.; DOHNAL, I.; SCHATZMAYR, G. Quantitative evaluation of *E. coli* F4 and *Salmonella typhimurium* binding capacity of yeast derivatives. **AMB Express**, n. 3, p. 62–69, 2013.

GARCÍA-POZA, S.; LEANDRO, A.; COTAS, C.; COTAS, J.; MARQUES, J. C.; PEREIRA, L. & GONÇALVES, A. M. M. The Evolution Road of Seaweed Aquaculture: Cultivation Technologies and the Industry 4.0. **International Journal of Environmental Research and Public Health**, v. 17, n. 18, p. 6528, 2020.

GRAHAM, J. E.; WILCOX, L. W. & GRAHAM, L. E. **Algae**. San Francisco, 2009.

GONZALEZ-ORTIZ, G.; PEREZ, J.F.; HERMES, R.G.; MOLIST, F.; JIMENEZ-DIAZ, R.; MARTIN-ORUE, S.M. Screening the ability of natural feed ingredients to interfere with the adherence of enterotoxigenic *Escherichia coli* (ETEC) K88 to the porcine intestinal mucus. **British Journal of Nutrition**, n.111, p. 633–642, 2014.

GORIN, P.A.J.; IACOMINI, M. Structural diversity of D-galacto-D-mannan components isolated from lichens having *Ascomycetous mycosymbionts*. **Carbohydrate Research**, n. 142, v. 253–261, 1985.

GRANUM, E.; MYKLESTAD, S.M. A simple combined method for determination of  $\beta$ -(1→3)-glucan and cell wall polysaccharides in diatoms. **Hydrobiologia**, n. 477, p. 155–161, 2002.

GRIESSL, M.H.; SCHMID, B.; KASSLER, K.; BRAUNSMANN, C.; RITTER, R.; BARLAG, B.; STIERHOF, Y.D.; STURM, K.U.; DANZER, C.; WAGNER, C.; et al. Structural insight into the giant Ca<sup>2+</sup>-Binding Adhesin SiiE: Implications for the adhesion of *Salmonella enterica* to polarized epithelial cells. **Structure**, n. 21, p. 741–752, 2013.

GUILLARD, R.R.L. **Culture of phytoplankton for feeding marine invertebrates**. In **Culture of Marine Invertebrate Animals**; Smith, W.L., CHANLEY, M.H., Eds.; Plenum Press: New York, NY, USA, pp. 29–60. ISBN 978-1-4615-8714- 9, 1975.

GUNTUKU, L.; NAIDU, V.G.; YERRA, V.G. Mitochondrial Dysfunction in Gliomas: Pharmacotherapeutic Potential of Natural Compounds. **Current Neuropharmacology**, n.14, p. 567–583, 2016.

GUZMAN-MURILLO, M.A.; ASCENCIO, F. Anti-adhesive activity of sulphated exopolysaccharides of microalgae on attachment of red sore disease-associated bacteria and *Helicobacter pylori* to tissue culture cells. **Letters in Applied Microbiology**, n. 30, p. 473–478, 2000.

HAAS, S.; BAUER, J.L.; ADAKLI, A.; MEYER, S.; LIPPEMEIER, S.; SCHWARZ, K.; SCHULZ, C. Marine microalgae *Pavlova viridis* and *Nannochloropsis* sp. as n-3 PUFA source in diets for juvenile European sea bass (*Dicentrarchus labrax* L.). **Journal of Applied Phycology**, n. 28, p. 1011–1021, 2016.

HARDING, S. E.; TOMBS, M. P.; ADAMS, G. G.; PAULSEN, B. S.; INNGJERDINGEN, K. T., & BARSETT, H. **An Introduction to Polysaccharide Biotechnology**. (2nd ed.). Boca Raton, 2017.

HEIMANN, K. & HUERLIMANN, R. **Chapter 3 - Microalgal Classification: Major Classes and Genera of Commercial Microalgal Species.** In S.-K. Kim (Ed.), **Handbook of Marine Microalgae** (pp. 25-41). Academic Press, 2015.

HIROKAWA, Y.; FUJIWARA, S.; SUZUKI, M.; AKIYAMA, T.; SAKAMOTO, M.; KOBAYASHI, S.; TSUZUKI, M. Structural and physiological studies on the storage  $\beta$ -polyglucan of haptophyte *Pleurochrysis haptoneofera*. **Planta**, n. 227, p. 589–599, 2008.

HU, Y.; CHEN, J.; HU, G.; YU, J.; ZHU, X.; LIN, Y.; CHEN, S.; YUAN, J. Statistical research on the bioactivity of new marine natural products discovered during the 28 years from 1985 to 2012. **Marine drugs**, v. 13, n. 1, p. 202-21, 2015.

HUANG, J.; YU, J., TU, L.; HUANG, N.; LI, H.; LUO, Y. Isocitrate Dehydrogenase Mutations in Glioma: From Basic Discovery to Therapeutics Development. **Frontiers in Oncology**, n. 9, p. 506, 2019.

HUANG, G.; CHEN, F.; YANG, W. & HUANG, H. Preparation, deproteinization and comparison of bioactive polysaccharides. **Trends in Food Science & Technology**, v. 109, p. 564-568, 2021.

HUNDSHAMMER, C.; BRAEUER, M.; MULLER, C. A.; HANSEN, A. E.; SCHILLMAIER, M.; DUWEL, S.; SCHWAIGER, M. Simultaneous characterization of tumor cellularity and the Warburg effect with PET, MRI and hyperpolarized ( $^{13}\text{C}$ -MRSI). **Theranostics**, v. 8, n. 17, p. 4765-4780, 2018.

HUNG, C.S.; BOUCKAERT, J.; HUNG, D.; PINKNER, J.; WIDBERG, C.; DEFUSCO, A.; AUGUSTE, C.G.; STROUSE, R.; LANGERMANN, S.; WAKSMAN, G.; et al. Structural basis of tropism of *Escherichia coli* to the bladder during urinary tract infection. **Molecular Microbiology**, n. 44, p. 903–915, 2002.

HUSSAIN, P.R.; RATHER, S.A.; SURADKAR, P.P. Structural characterization and evaluation of antioxidant, anticancer and hypoglycemic activity of radiation degraded oat (*Avena sativa*)  $\beta$ -glucan. **Radiation Physics and Chemistry**, n. 144, p. 218-230, 2018.

IBAÑEZ, E. & CIFUENTES, A. Benefits of using algae as natural sources of functional ingredients. **Journal of the Science of Food and Agriculture**, v. 93, n. 4, p. 703-709, 2013.

JANSE, I.; VAN RIJSSEL, M.; VAN HALL, P.J.; GERWIG, G.J.; GOTTSCHAL, J.C.; PRINS, R.A. The storage glucan of *Phaeocystis globosa* (Prymesioophyceae) cells. **Journal of Phycology** n. 32, p. 382–387, 1996.

JANSSON, P.E.; KENNE, L.; LIEDGREN, H.; LINDBERG, B.; LÖNNGREN, J. **A practical guide to the methylation analysis of carbohydrates.** Chem. Commun. Univ. Stock. v. 8, p. 1–75, 1976.

JEFFREY, S.; WRIGHT, S. & ZAPATA, M. **Microalgal classes and their signature**

**pigments.** In C. L. In S. Roy, E. Egeland, & G. Johnsen (Ed.), **Phytoplankton Pigments: Characterization, Chemotaxonomy and Applications in Oceanography** (pp. 3-77), 2011.

JIN, Y.; LI, P.; WANG, F.  $\beta$ -glucans as potential immunoadjuvants: a review on the adjuvanticity, structure-activity relationship and receptor recognition properties. **Vaccine**, n. 36, p. 5235-5244, 2018.

KARKI, P.; ANGARDI, V.; MIER, J.C.; ORMAN, M.A. A Transient Metabolic State In Melanoma Persister Cells Mediated By Chemotherapeutic Treatments. **bioRxiv**, 2021.

KARTIK, A.; AKHIL, D.; LAKSHMI, D.; PANCHAMOORTHY GOPINATH, K.; ARUN, J.; SIVARAMAKRISHNAN, R.; PUGAZHENDHI, A. A critical review on production of biopolymers from algae biomass and their applications. **Bioresource Technology**, v. 329, 2021.

KHAN, T.; DATE, A.; CHAWDA, H. & PATEL, K. Polysaccharides as potential anticancer agents-A review of their progress. **Carbohydrate Polymers**, v. 210, p. 412-428, 2019.

KIM, D.; RAHHAL, N. & RADEMACHER, C. Elucidating Carbohydrate-Protein Interactions Using Nanoparticle-Based Approaches. **Frontiers in Chemistry**, v.9, p.265, 2021.

KIM, M.J.; HONG, S.Y.; KIM, S.K.; CHEONG, C.; PARK, H.J.; CHUN, H.K. et al.  $\beta$ -glucan enhanced apoptosis in human colon cancer cells SNU-C4. **Nutrition Research and Practice**, n. 3, p. 180-184, 2009.

KIM, Y.T.; KIM, E.H.; CHEONG, C.; WILLIAMS, D.L.; KIM, C.W.; LIM, S.T. Structural characterization of  $\beta$ -D-(1 $\rightarrow$ 3,1 $\rightarrow$ 6)-linked glucans using NMR spectroscopy. **Carbohydrate Research**, n. 328, pp. 331-341, 2000.

KOGAN, G.; KOCHER, A. Role of yeast cell wall polysaccharides in pig nutrition and health protection. **Livestock Science**, n. 109, v. 161–165, 2007.

KONO, H.; KONDO, N.; HIRABAYASHI, K.; OGATA, M.; TOTANI, K.; IKEMATSU, S.; OSADA, M. NMR spectroscopic structural characterization of a water-soluble  $\beta$ -(1 $\rightarrow$ 3, 1 $\rightarrow$ 6)-glucan from *Aureobasidium pullulans*. **Carbohydrate Polymers**, n. 174, p. 876–886, 2017.

KOYANDE, A.K.; CHEW, K.W.; RAMBABU, K.; TAO, Y.; CHU, D.T.; SHOW, P.L. Microalgae: A potential alternative to health supplementation for humans. **Food Science and Human Wellness**, v. 8, n. 1, p. 16-24, 2019.

KULICKE, W.M.; LETTAU, A.; THIELKING, H. Correlation between immunological activity, molar mass, and molecular structure of different (1 $\rightarrow$ 3)- $\beta$ -D-glucans. **Carbohydrate Research**, n. 297, p. 135-143, 1997.

KUMAR, B. R.; THANGAVEL, M. P. M.; SUDHAKAR, K. R.; ABDUL-SATTAR, N.; BRINDHADEVI, K. & PUGAZHENDHI, A. A state-of-the-art review on the cultivation of algae for energy and other valuable products: Application, challenges, and opportunities. **Renewable and Sustainable Energy Reviews**, v.138, 2021.

LAXMINARAYAN, R.; DUSE, A.; WATTAL, C.; ZAIDI, A.K.; WERTHEIM, H.F.; SUMPRADIT, N.; VLIEGHE, E.; HARA, G.L.; GOULD, I.M.; GOOSSENS, H.; et al. Antibiotic resistance-the need for global solutions. **The Lancet Infectious Diseases**, n. 13, v. 1057–1098, 2013.

LEÃO BARROS, M.B.; PINHEIRO, D.D.R., Borges B.D.N., Mitochondrial DNA Alterations in Glioblastoma (GBM). **International journal of molecular sciences**, n. 22, 2021.

LEE, R. **Basic Characteristics of the Algae. In Phycology.**: Cambridge University Press, 2018.

LEGENTIL, L.; PARIS, F.; BALLEST, C.; TROUVELOT, S.; DAIRE, X.; VETVICKA, V.; FERRIERES, V. Molecular interactions of  $\beta$ -(1→3)-glucans with their receptors. **Molecules**, n. 20, p. 9745-9766, 2015.

LENG, E.; COSTA, M.; PENG, Y.; ZHANG, Y.; GONG, X.; ZHENG, A.; HUANG, Y.; XU, M. Role of different chain end types in pyrolysis of glucose-based anhydro-sugars and oligosaccharides. **Fuel**, n. 234, p. 738–745, 2018.

LEVASSEUR, W.; PERRE, P.; & POZZOBON, V. A review of high value-added molecules production by microalgae in light of the classification. **Biotechnology Advances**, n. 41, p. 107545, 2020.

LI, F.; WEI, Y.; ZHAO, J.; YU, G.; HUANG, L. & LI, Q. Transport mechanism and subcellular localization of a polysaccharide from *Cucurbita Moschata* across Caco-2 cells model. **International Journal of Biological Macromolecules**, n. 182, p.1003-1014, 2021.

LI, H.; LEI, B.; XIANG W.; WANG, H.; FENG, W.; LIU, Y.; QI, S. Differences in Protein Expression between the U251 and U87 Cell Lines. **Turkish Neurosurgery**, v. 27, n. 6, p. 894-903, 2017.

LI, W.; SONG, K.; WANG, S.; ZHANG, C.; ZHUANG, M.; WANG, Y.; LIU, T. Anti-tumor potential of astragalus polysaccharides on breast cancer cell line mediated by macrophage activation. **Materials Science and Engineering: C**, n. 98, p. 685-695, 2019.

LI, W.; HU, X.; WANG, S.; JIAO, Z.; SUN, T.; LIU, T.; SONG, K. Characterization and anti-tumor bioactivity of *astragalus* polysaccharides by immunomodulation. **International Journal of Biological Macromolecules**, n. 145, p. 985-997, 2020.

LIU, J.; DANG, H.; WANG, X.W. The significance of intertumor and intratumor heterogeneity in liver cancer. **Experimental & Molecular Medicine**, n. 50, e416, 2018.

LIU, W. B.; XIE, F.; SUN, H. Q.; MENG, M.; & ZHU, Z. Y. Antitumor effect of polysaccharide from *Hirsutella sinensis* on human non-small cell lung cancer and nude mice through intrinsic mitochondrial pathway. **International Journal of Biological Macromolecules**, v. 99, p. 258-264, 2017.

LIU, W.B.; XIE, F.; SUN, H.Q.; MENG, M.; ZHU, Z.Y. Anti-tumor effect of polysaccharide from *Hirsutella sinensis* on human non-small cell lung cancer and nude mice through intrinsic mitochondrial pathway. **International Journal of Biological Macromolecules**, n. 99, p. 258-264, 2017.

LOKE, M.F.; LUI, S.Y.; NG, B.L.; GONG, M.; HO, B. Antiadhesive property of microalgal polysaccharide extract on the binding of *Helicobacter pylori* to gastric mucin. **FEMS Immunology and Medical Microbiology**, n. 50, v. 231–238, 2007.

LÓPEZ, Y.; CEPAS, V.; SOTO, S.M. **The marine ecosystem as a source of antibiotics. In Grand Challenges in Marine Biotechnology**; Rampelotto, P.H., Trincone, A., Eds.; Springer: Cham, Switzerland, pp. 3–48. ISBN 978-3-319-69074-2, 2018.

LOWMAN, D.W.; WEST, L.J.; BEARDEN, D.W.; WEMPE, M.F.; POWER, T.D.; ENSLEY, H.E.; HAYNES, K.; WILLIAMS, D.L.; KRUPPA, M.D. New insights into the structure of (1→3,1→6)-β-D-Glucan side chains in the *Candida glabrata* cell wall. **PLoS ONE** n. 6, p. 27614, 2011.

LOWRY, O.H.; ROSEBROUGH, N.J.; FARR, A.L.; RANDALL, R.J. Protein measurement with the Folin phenol reagent. **Journal of Biological Chemistry**, n. 193, p. 265–275, 1951.

MA, L.; YANG, Y.; YAO, J.; SHAO, Z.; HUANG, Y.; CHEN, X. Selective chemical modification of soy protein for a tough and applicable plant protein-based material. **Journal of Materials Chemistry B** n. 3, p. 5241–5248, 2015.

MALDONADO-GOMEZ, M.X.; LEE, H.; BARILE, D.; LU, M.; HUTKINS, R.W. Adherence inhibition of enteric pathogens to epithelial cells by bovine colostrum fractions. **International Dairy Journal**, n. 40, p. 24–32, 2015.

MANOYLOV, K. M. Taxonomic identification of algae (morphological and molecular): species concepts, methodologies, and their implications for ecological bioassessment. **Journal of Phycology**, v. 50, n. 3, p. 409-424, 2014.

MARCILLA, A.; GÓMEZ-SIURANA, A.; GOMIS, C.; CHÁPULI, E.; CATALÁ, M.C.; VALDÉS, F.J. Characterization of microalgal species through TGA/FTIR analysis: Application to *Nannochloropsis sp.* **Thermochimica Acta**, n. 484, p. 41–47, 2009.

MARTÍNEZ ANDRADE, K.A.; LAURITANO, C.; ROMANO, G.; IANORA, A. Marine Microalgae with Anti- Cancer Properties. **Marine drugs**, v. 16, n. 5, 2018.

MAUER, L. **Heat Treatment for Food Proteins. In Encyclopedia of Food Sciences and Nutrition**; Caballero, B., Trug, L., Finglas, P.M., Eds.; Academic Press: Oxford, UK, pp. 4868–4872. ISBN 978-0-12-227055-0, 2003.

MAZEPA, E.; NOSEDA, M. D.; FERREIRA, L. G.; DE CARVALHO, M. M.; GONÇALVES, A. G.; DUCATTI, D.; DE L BELLAN, D.; GOMES, R. P.; TRINDADE, E.; FRANCO, C.; PELLIZZARI, F. M., WINNISCHOFER, S., & DUARTE, M. Chemical structure of native and modified sulfated heterorhamnans from the green seaweed *Gayralia brasiliensis* and their cytotoxic effect on U87MG human glioma cells. **International journal of biological macromolecules**, v.187, p.710–721, 2021.

MCCONVILLE, M.; BACIC, A.; CLARKE, A. Structural studies of chrysolaminaran from the ice diatom *Stauroneis amphioxys* (Gregory). **Carbohydrate Research**, n. 153, p. 330-333, 1986.

MENDES, G.S.; DUARTE, M.E.; COLODI, F.G.; NOSEDA, M.D.; FERREIRA, L.G.; BERTE, S.D.; CAVALCANTI, J.F.; SANTOS, N.; ROMANOS, M.T. Structure and anti-metapneumovirus activity of sulfated galactans from the red seaweed *Cryptonemia seminervis*. **Carbohydrate polymers**, n. 101, p. 313- 23, 2014.

MENSHOVA, R. V.; ERMAKOVA, S. P.; ANASTYUK, S. D.; ISAKOV, V. V.; DUBROVSKAYA, Y. V.; KUSAYKIN, M. I.; et al. Structure, enzymatic transformation and anticancer activity of branched high molecular weight laminaran from brown alga *Eisenia bicyclis*. **Carbohydrate Polymers**, v.99, p.101-109, 2014.

MIAZEK, K.; KRATKY, L.; SULC, R.; JIROUT, T.; AGUEDO, M.; RICHEL, A. & GOFFIN, D. Effect of Organic Solvents on Microalgae Growth, Metabolism and Industrial Bioproduct Extraction: A Review. **International Journal of Molecular Sciences**, v. 18, n. 7, p. 1429, 2017.

MICHALAK, I. & CHOJNACKA, K. Algae as production systems of bioactive compounds. **Engineering in Life Sciences**, v. 15, n. 2, p. 160-176, 2015.

MISSIROLI, S.; PERRONE, M.; GENOVESE, I.; PINTON, P. & GIORGI, C. Cancer metabolism and mitochondria: Finding novel mechanisms to fight tumours. **EBioMedicine**, n. 59, p. 102943, 2020.

MOHAMMED, A. S. A.; NAVEED, M. & JOST, N. Polysaccharides; Classification, Chemical Properties, and Future Perspective Applications in Fields of Pharmacology and Biological Medicine (A Review of Current Applications and Upcoming Potentialities). **Journal of Polymers and the environment**, p.1-13, 2021.

MORETAO, M.; ZAMPRONIO, A.R.; GORIN, P.A.J.; IACOMINI, M.; OLIVEIRA, M.B.M. Induction of secretory and tumoricidal activities in peritoneal macrophages activated by an acidic heteropolysaccharide (ARAGAL) from the gum of *Anadenanthera colubrina* (angico branco). **Immunology Letters**, n. 93, p. 189-197, 2004.

MOTALN, H.; KOREN, A.; GRUDEN, K.; RAMSAK, Z.; SCHICHOR, C.; LAH, T.T. Heterogeneous glioblastoma cell cross-talk promotes phenotype alterations and enhanced drug resistance. **Oncotarget**, n.6, p.40998- 41017, 2015.

MURAD, H.; HAWAT, M.; EKHTIAR, A.; ALJAPAWA, A.; ABBAS, A.; DARWISH, H.; SBENATI, O.; GHANNAM, A. Induction of G1-phase cell cycle arrest and apoptosis pathway in MDA-MB-231 human breast cancer cells by sulfated polysaccharide extracted from *Laurencia papillosa*. **Cancer Cell International**, n.16, p.39, 2016.

MYKLESTAD, S.M.; GRANUM, E. **Biology of (1,3)- $\beta$ -Glucans and related glucans in protozoans and chromistans**. In **Chemistry, Biochemistry, and Biology of 1-3  $\beta$  Glucans and Related Polysaccharides**; Bacic, A., Fincher, G.B., Stone, B.A., Eds.; Academic Press: San Diego, CA, USA, pp. 353–385. ISBN 978-0-12- 373971-1, 2009.

NAKAJIMA, K.; TAMURA, N.; KOBAYASHI-HATTORI, K.; YOSHIDA, T.; HARA-KUDO, Y.; IKEDO, M.; SUGITA-KONISHI, Y.; HATTORI, M. Prevention of intestinal infection by glycomacropeptide. **Bioscience, Biotechnology and Biochemistry**, n. 69, p. 2294–2301, 2005.

NARALA, R. R.; GARG, S.; SHARMA, K. K.; THOMAS-HALL, S. R.; DEME, M.; LI, Y. & SCHENK, P. M. Comparison of Microalgae Cultivation in Photobioreactor, Open Raceway Pond, and a Two-Stage Hybrid System. **Frontiers in Energy Research**, v. 4, n. 29, 2016.

NEWBURG, D.S.; MCCORMICK, B.; CHATURVEDI, P.; SIBER, A.M.; WARREN, C.D. Inhibition of *Salmonella typhimurium* by human milk sulfatides. **Pediatric Research**, n. 45, p. 116, 1999.

NEWMAN, J.C.; VERDIN, E.  $\beta$ -Hydroxybutyrate: A Signaling Metabolite. **Annual Review of Nutrition**, n. 37, p. 51-76, 2017.

NIEMCZYK, E.; ŻYSZKA-HABERECHE, B.; DRZYZGA, D.; LENARTOWICZ, M. & LIPOK, J. **Algae in Biotechnological Processes**. In K. Chojnacka, P. P. Wieczorek, G. Schroeder & I. Michalak (Eds.), *Algae Biomass: Characteristics and Applications: Towards Algae-based Products* (pp. 33-48). Cham: Springer International Publishing, 2018.

NIKOLOVA, B.; SEMKOVA, S.; TSONEVA, I.; ANTOV, G.; IVANOVA, J.; VASILEVA, I.; KARDALEVA, P.; STOINEVA, I.; CHRISTOVA, N.; NACHEVA, L.; KABAIVANOVA, L. Characterization and potential antitumor effect of a heteropolysaccharide produced by the red alga *Porphyridium sordidum*. **Engineering in Life Sciences**, v. 19, n. 12, p. 978-985, 2019.

NOLFI-DONEGAN, D.; BRAGANZA, A.; SHIVA, S. Mitochondrial electron transport chain: Oxidative phosphorylation, oxidant production, and methods of measurement. **Redox Biology**, n.37, p.101674, 2020.

NOVAK, M.; VETVICKA, V. Glucans as biological response modifiers. **Endocrine, Metabolic & Immune Disorders - Drug Targets**, n. 9, p. 67-75, 2009.

OFEK, I.; DOYLE, R.J. **Principles of Bacterial Adhesion**. In **Bacterial Adhesion to Cells and Tissues**; Ofek, I., Doyle, R.J., Eds.; Springer: Boston, MA, USA, pp. 1–15.

ISBN 978-1-4684-6435-1, 1994.

OFEK, I.; SHARON, N.; ABRAHAM, S.N. **Bacterial adhesion. In The Prokaryotes;** Dworkin, M., Falkow, S., Rosenberg, E., Schleifer, K.H., Stackebrandt, E., Eds.; Springer: Singapore, v. 2, pp. 16–31, 2006.

OFEK, I.; HASTY, D.L.; SHARON, N. Anti-adhesion therapy of bacterial diseases: Prospects and problems. **FEMS Immunology and Medical Microbiology**, n. 38, p. 181–191, 2003.

OKAZAKI, M.; ADACHI, Y.; OHNO, N.; YADOMAE, T. Structure-activity relationship of (1→3)- $\beta$ -D-glucans in the induction of cytokine production from macrophages *in vitro*. **Biological and Pharmaceutical Bulletin**, n. 18, p. 1320-1327, 1995.

OOI, V.E.; LIU, F. Immunomodulation and anti-cancer activity of polysaccharide-protein complexes. **Current Medicinal Chemistry**, n. 7, p. 715-729, 2000.

OSTROM, Q.T.; BAUCHET, L.; DAVIS, F.G.; DELTOUR, I.; FISHER, J.L et al. The epidemiology of glioma in adults: a “state of the science” review. **Neuro-Oncology**, v. 16 n. 7, pp. 896-913, 2014.

OUWEHAND, A.C.; SALMINEN, S.J.; SKURNIK, M.; CONWAY, P.L. Inhibition of pathogen adhesion by  $\beta$ -lactoglobulin. **International Dairy Journal**, n. 7, p. 685–692, 1997.

PAINTER, T.J. Algal polysaccharides. G.O. Aspinall (Ed.), **The Polysaccharides** (1st), 2, Academic Press (1983), pp. 195-285

PALACIOS, I.; GARCIA-LAFUENTE, A.; GUILLAMON, E.; VILLARES, A. Novel isolation of water-soluble polysaccharides from the fruiting bodies of *Pleurotus ostreatus* mushrooms. **Carbohydrate Research**, n. 358, p. 72-7, 2012.

PARK, S.J.; SMITH, C.P.; WILBUR, R.R.; CAIN, C.P.; KALLU, S.R.; VALASAPALLI, S.; SAHOO, A.; GUDA, M.R.; TSUNG, A.J.; VELPULA, K.K. An overview of MCT1 and MCT4 in GBM: small molecule transporters with large implications. **American Journal of Cancer Research**, v. 8, n. 10, p. 1967-1976, 2018.

PARKAR, S.G.; REDGATE, E.L.; WIBISONO, R.; LUO, X.; KOH, E.T.H.; SCHRÖDER, R. Gut health benefits of kiwifruit pectins: Comparison with commercial functional polysaccharides. **Journal of Functional Foods** n. 2, p. 210–218, 2010.

PAULSEN, B.S.; MYKLESTAD, S. Structural studies of the reserve glucan produced by the marine diatom *Skeletonema costatum* (Grev.) Cleve. **Carbohydrate Research**, n. 62, p. 386-388, 1978.

PAVLOVA, N. N. & THOMPSON, C. B. The Emerging Hallmarks of Cancer Metabolism. **Cell Metabolism**, v. 23, n. 1, p. 27-47, 2016.

PAW, I.; CARPENTER, R. C.; WATABE, K.; DEBINSKI, W.; & LO, H. W. Mechanisms regulating glioma invasion. **Cancer letters**, v. 362, n. 1, p. 1–7, 2015.

PIRES ADO, R.; RUTHES, A.C.; CADENA, S.M.; ACCO, A.; GORIN, P.A.; IACOMINI, M. Cytotoxic effect of *Agaricus bisporus* and *Lactarius rufus*  $\beta$ -D-glucans on HepG2 cells, **International Journal of Biological Macromolecules** n. 58, p. 95-103, 2013.

POLISETTY, R. V.; GAUTAM, P.; GUPTA, M. K.; SHARMA, R.; GOWDA, H.; RENU, D et al. Microsomal membrane proteome of low grade diffuse astrocytomas: Differentially expressed proteins and candidate surveillance biomarkers. **Scientific Reports**, v.6, p.26882, 2016.

PONDER, G.R.; RICHARDS, G.N.; STEVENSON, T.T. Influence of linkage position and orientation in pyrolysis of polysaccharides: A study of several glucans. **Journal of Analytical and Applied Pyrolysis**, n. 22, p. 217–229, 1992.

PONIS, E.; PROBERT, I.; VÉRON, B.; LE COZ, J.R.; MATHIEU, M.; ROBERT, R.; COZ, J.R.L.; MATHIEU, M.; ROBERT, R. Nutritional value of six Pavlovophyceae for *Crassostrea gigas* and *Pecten maximus* larvae. **Aquaculture**, n. 254, p. 544–553, 2006.

PORPORATO, P.; FILIGHEDDU, N.; PEDRO, J. M. B.; KROEMER, G. & GALLUZZI, L. Mitochondrial metabolism and cancer. **Cell Research**, v. 28, n. 3, p. 265-280, 2018.

QIANG, W.; XIAOJING, S.; AIMIN, S.; HUI, H.; YING, Y.; LI, L.; LING, F.; HONGZHI, L.  $\beta$ -glucans: relationships between modification, conformation and functional activities. **Molecules**, n. 22, p. 257-269, 2017.

QUINTERO-VILLEGAS, M.I.; AAM, B.B.; RUPNOW, J.; SORLIE, M.; EIJSINK, V.G.H.; HUTKINS, R.W.; SØRLIE, M.; EIJSINK, V.G.H.; HUTKINS, R.W. Adherence inhibition of enteropathogenic *Escherichia coli* by chitooligosaccharides with specific degrees of acetylation and polymerization. **Journal of Agricultural and Food Chemistry**, n. 61, p. 2748– 2754, 2013.

RADULOVICH, R.; NEORI, A.; VALDERRAMA, D.; REDDY, C. R. K.; CRONIN, H. & FORSTER, J. **Farming of seaweeds**. In D. J. T. Brijesh K. Tiwari (Ed.), *Seaweed Sustainability* (pp. 27-59). Academic Press, 2015.

RAHMAN, D.Y.; SARIAN, F.D.; VAN WIJK, A.; MARTINEZ-GARCIA, M.; VAN DER MAAREL, M.J.E.C. Thermostable phycocyanin from the red microalga *Cyanidioschyzon merolae*, a new natural blue food colorant. **Journal of Applied Phycology**, v. 29, n. 3, pp. 1233-1239, 2017.

RAIMUNDO, S.C.; PATTATHIL, S.; EBERHARD, S.; HAHN, M.G.; POPPER, Z.A.  $\beta$ -1,3-Glucans are components of brown seaweed (*Phaeophyceae*) cell walls. **Protoplasma**, v. 254, n. 2, p. 997-1016, 2017.

RAMESH, H.P.; YAMAKI, K.; TSUSHIDA, T. Effect of fenugreek (*Trigonella foenum-graecum* L.) galactomannan fractions on phagocytosis in rat macrophages and on proliferation and IgM secretion in HB4C5 cells. **Carbohydrate Polymers**, n. 50, p. 79-83, 2002.

RASCHKE, W.C.; BAIRD, S.; RALPH, P.; NAKOINZ, I. Functional macrophage cell lines transformed by abelson leukemia virus. **Cell**, n. 15, p. 261-267, 1978.

RAZAK, N.A.; ABU, N.; HO, W.Y.; et al. Cytotoxicity of eupatorin in MCF-7 and MDA-MB-231 human breast cancer cells via cell cycle arrest, anti-angiogenesis and induction of apoptosis. **Scientific Reports**, n. 9, p. 1514, 2019.

REHBERG-HAAS, S.; MEYER, S.; LIPPEMEIER, S.; SCHULZ, C. A comparison among different Pavlova sp. products for cultivation of *Brachionus plicatilis*. **Aquaculture** n. 435, p. 424-430, 2015.

REILLY, T.P.; BELLEVUE, F.H.; WOSTER, P.M.; SVENSSON, C.K. Comparison of the *in vitro* cytotoxicity of hydroxylamine metabolites of sulfamethoxazole and dapsone. **Biochemical Pharmacology**, v. 55, n. 6, p. 803-10, 1998.

REN, Y.; BAI, Y.; ZHANG, Z.; CAI, W. & DEL RIO FLORES, A. The Preparation and Structure Analysis Methods of Natural Polysaccharides of Plants and Fungi: A Review of Recent Development. **Molecules**, v. 24, n. 17, p. 3122, 2019.

RENAUD, S.M.; VAN THINH, L.; PARRY, D.L. The gross chemical composition and fatty acid composition of 18 species of tropical Australian microalgae for possible use in mariculture. **Aquaculture** n. 170, p. 147-159, 1999.

RENDUELES, O.; KAPLAN, J. B. & GHIGO, J. M. Antibiofilm polysaccharides. **Environmental Microbiology**, v.15, n.2, p.334-346, 2013.

RICCIO, G.; LAURITANO, C. Microalgae with immunomodulatory activities. **Marine Drugs**, v. 18, n. 1, 2019.

RICO, M.; GONZÁLEZ, A. G.; SANTANA-CASIANO, M.; GONZÁLEZ-DÁVILA, M.; PÉREZ-ALMEIDA, N. & DE TANGIL, M. S. **Production of Primary and Secondary Metabolites Using Algae**. In B. N. Tripathi & D. Kumar (Eds.), **Prospects and Challenges in Algal Biotechnology** (pp. 311- 326). Singapore: Springer Singapore, 2017.

RODRIGUES, J.M.; DUARTE, M.E.R.; NOSEDA, M.D. Modified soybean meal polysaccharide with high adhesion capacity to *Salmonella*. **International Journal of Biological Macromolecules** n. 139, v. 1074-1084, 2019.

ROLLAND-SABATÉ, I.A. **High-Performance Size-Exclusion Chromatography coupled with on-line Multi-angle Laser Light Scattering (HPSEC-MALLS)**, in: Martin Masuelli, D. Renard. (Eds.), **Advances in Physicochemical Properties of Biopolymers**

(Part 1), Bentham Science Publisher, pp. 92-136, 2017.

ROMLING, U.; BIAN, Z.; HAMMAR, M.; SIERRALTA, W.D.; NORMARK, S. Curli fibers are highly conserved between *Salmonella typhimurium* and *Escherichia coli* with respect to operon structure and regulation. **Journal of Bacteriology**, n. 180, p. 722–731, 1998.

ROPELLATO, J.; CARVALHO, M.M.; FERREIRA, L.G.; NOSEDA, M.D.; ZUCONELLI, C.R.; GONCALVES, A.G.; DUCATTI, D.R.B.; KENSKI, J.C.N.; NASATO, P.L.; WINNISCHOFER, S.M.B.; DUARTE, M.E.R. Sulfated heterorhamnans from the green seaweed *Gayralia oxysperma*: partial depolymerization, chemical structure and antitumor activity, **Carbohydrate polymers**, n.117, p.476-485, 2015.

RUIJTER, J.M.; RAMAKERS, C.; HOOGAARS, W.M.; KARLEN, Y.; BAKKER, O.; VAN DEN HOFF, M.J.; MOORMAN, A.F. Amplification efficiency: linking baseline and bias in the analysis of quantitative PCR data. **Nucleic Acids Research**, n.37, p.45, 2009.

RUSSO, R.; BARSANTI, L.; EVANGELISTA, V.; FRASSANITO, A.M.; LONGO, V. et al. *Euglena gracilis* paramylon activates human lymphocytes by upregulating pro-inflammatory factors **Food Science & Nutrition**, v. 5, n. 2, p. 205-214, 2017.

RUTCKEVISKI, R.; CORSO, C.R.; ROMÁN-OCHOA, Y.; CIPRIANI, T.R.; CENTA, A.; SMIDERLE, F.R. *Agaricus bisporus*  $\beta$ -(1→6)-D-glucan induces M1 phenotype on macrophages and increases sensitivity to doxorubicin of triple negative breast cancer cells. **Carbohydrate Polymers**, n. 278, 2022.

SADOVSKAYA, I.; SOUISSI, A.; SOUISSI, S.; GRARD, T.; LENCEL, P.; GREENE, C.M.; DUIN, S.; DMITRENOK, P.S.; CHIZHOV, A.O.; SHASHKOV, A.S.; et al. Chemical structure and biological activity of a highly branched (1→3,1→6)- $\beta$ -D-glucan from *Isochrysis galbana*. **Carbohydrate Polymers**, n. 111, p. 139–148, 2014.

SALINAS-SALAZAR, C., SAUL GARCIA-PEREZ, J., CHANDRA, R., CASTILLO-ZACARIAS, C., IQBAL, H. M. N., & PARRA-SALDÍVAR, R. **Methods for Extraction of Valuable Products from Microalgae Biomass**. In M. A. Alam & Z. Wang (Eds.), **Microalgae Biotechnology for Development of Biofuel and Wastewater Treatment** (pp. 245-263). Singapore: Springer Singapore, 2019.

SALMEAN, A.A.; DUFFIEUX, D.; HARHOLT, J.; QIN, F.; MICHEL, G.; CZJZEK, M.; WILLATS, W.G.T., HERVE C. Insoluble (1→3), (1→4)-  $\beta$ -D-glucan is a component of cell walls in brown algae (Phaeophyceae) and is masked by alginates in tissues. **Scientific Reports**, v. 7, n. 1, p. 2880, 2017.

SARRAZY, V.; VEDRENNE, N.; BILLET, F.; BORDEAU, N.; LEPREUX, S., VITAL, A., et al. TLR4 signal transduction pathways neutralize the effect of Fas signals on glioblastoma cell proliferation and migration. **Cancer Letters**, v.311, n.2, p.195-202, 2011.

SASSAKI, G.L.; MACHADO, M.J.; TISCHER, C.A.; GORIN, P.A.J.; IACOMINI, M. Glycosyldiacylglycerolipids from the lichen *Dictyonema glabratum*. **Journal of Natural**

**Products**, n. 62, p. 844–847, 1999.

SASSAKI, G.L.; GORIN, P.A.J.; SOUZA, L.M.; CZELUSNIAK, P.A.; IACOMINI, M. Rapid synthesis of partially O-methylated alditol acetate standards for GC-MS: Some relative activities of hydroxyl groups of methyl glycopyranosides on Purdie methylation. **Carbohydrate Research**, n. 340, p. 731–739, 2005.

SELESU, N. F. H.; V. DE OLIVEIRA, T.; CORRÊA, D. O.; MIYAWAKI, B.; MARIANO, A. B.; VARGAS, J. V. C. & VIEIRA, R. B. Maximum microalgae biomass harvesting via flocculation in large scale photobioreactor cultivation. **The Canadian Journal of Chemical Engineering**, v. 94, n. 2, p. 304-309, 2016.

SHAO, P.; PEI, Y.; FANG, Z.; SUN, P. Effects of partial desulfation on antioxidant and inhibition of DLD cancer cell of *Ulva fasciata* polysaccharide. **International Journal of Biological Macromolecules**, n. 65, p. 307-13, 2014.

SHAO, P.; LIU, J.; CHEN, X.; FANG, Z. & SUN, P. Structural features and antitumor activity of a purified polysaccharide extracted from *Sargassum horneri*. **International Journal of Biological Macromolecules**, v. 73, p. 124-130, 2015.

SHOAF-SWEENEY, K.D.; HUTKINS, R.W. Chapter 2 **Adherence, anti-adherence, and oligosaccharides: Preventing pathogens from sticking to the host**. *Advances in Food and Nutrition Research* 55, 101–161, 2008.

SINGH, P. K.; SRIVASTAVA, A. K.; DEV, A.; KAUNDAL, B.; CHOUDHURY, S. R.; & KARMAKAR, S. (1→3)  $\beta$ -Glucan anchored, paclitaxel loaded chitosan nanocarrier endows enhanced hemocompatibility with efficient anti-glioblastoma stem cells therapy. **Carbohydrate Polymers**, v.180, p.365-375, 2018.

SKJANES, K.; REBOURS, C. & LINDBLAD, P. Potential for green microalgae to produce hydrogen, pharmaceuticals and other high value products in a combined process. **Critical Reviews in Biotechnology**, v. 33, n. 2, p. 172-215, 2013.

SKJERMO, J.; STØRSETH, T.; HANSEN, K.; HANDÅ A.; ØIE G.. Evaluation of  $\beta$ -(1→3, 1→6)-glucans and high-M alginate used as immunostimulatory dietary supplement during first feeding and weaning of Atlantic cod [*Gadus morhua* L] **Aquaculture**, n. 261, pp. 1088-1101, 2006.

SLETMOEN, M.; STOKKE, B.T. Higher order structure of (1,3)- $\beta$ -D-Glucans and its influence on their biological activities and complexation abilities. **Biopolymers**, n. 89, p. 310–321, 2008.

SPINELLI, J.B.; HAIGIS, M.C. The multifaceted contributions of mitochondria to cellular metabolism. **Nature Cell Biology**, v. 20, n. 7, p. 745-754, 2018.

STEPHEN, A. M. & PHILLIPS, G. O. **Food Polysaccharides and Their Applications**

CRC Press, 2006.

STIGER, V.; N. BOURGOUGNON, E. DESLANDES, Chapter 8 - **Carbohydrates From Seaweeds.**, in: I.L. Joël Fleurence (Ed.) *Seaweed in Health and Disease Prevention*, Academic Press, 2016.

STIRK, W. A.; BÁLINT, P.; VAMBE, M.; LOVÁSZ, C.; MOLNÁR, Z.; VAN STADEN, J. & ÖRDÖG, V. Effect of cell disruption methods on the extraction of bioactive metabolites from microalgal biomass. **Journal of Biotechnology**, v. 307, 2020.

STØRSETH, T.; HANSEN, K.; SKJERMO, J.; KRANE, J. Characterization of a  $\beta$ -D-(1 $\rightarrow$ 3)-glucan from the marine diatom *Chaetoceros mülleri* by high-resolution magic-angle spinning NMR spectroscopy on whole algal cells. **Carbohydrate Research**, n. 339, p. 421-424, 2004.

TAN, J. S.; LEE, S. Y.; CHEW, K. W.; LAM, M. K.; LIM, J. W.; HO, S.H. & SHOW, P. L. A review on microalgae cultivation and harvesting, and their biomass extraction processing using ionic liquids. **Bioengineered**, v. 11, n. 1, p. 116-129, 2020.

TATSUZAWA, H.; TAKIZAWA, E. Changes in lipid and fatty acid composition of *Pavlova lutheri*. **Phytochemistry**, n.40, p.397–400, 1995.

TENNANT, D. A.; DURAN, R. V. & GOTTLIEB, E. Targeting metabolic transformation for cancer therapy. **Nature Reviews Cancer**, v. 10, n. 4, p. 267-277, 2010.

THOMPSON, G.A. Lipids and membrane function in green algae. **Biochimica et Biophysica Acta (BBA) - Lipids and Lipid Metabolism**. n. 1302, p. 17–45 1996.

TIAN, Y.; ZHAO, Y.; ZENG, H.; ZHANG, Y. & ZHENG, B. Structural characterization of a novel neutral polysaccharide from *Lentinus giganteus* and its antitumor activity through inducing apoptosis. **Carbohydrate Polymers**, v. 154, p. 231-240, 2016.

URBANI R.; MAGALETTI E.; SIST, P.; CICERO A.  $\beta$ -D-glucans in the induction of cytokine production from macrophages *in vitro*. **Biological and Pharmaceutical Bulletin**, n. 18, p. 1320-1327, 2006.

VALIZADEH, K. & DAVARPANA, A. Design and construction of a micro-photo bioreactor in order to dairy wastewater treatment by micro-algae: parametric study. **Energy Sources, Part A: Recovery, Utilization, and Environmental Effects**, v. 42, n. 5, p. 611-624, 2020.

VANDER HEIDEN, M. G. Targeting cancer metabolism: a therapeutic window opens. **Nature Reviews Drug Discovery**, v. 10, n. 9, p. 671-684, 2011.

VARUM, K.M.; KVAM, B.J.; MYKLESTAD, S.; PAULSEN, B.S. Structure of a food-reserve  $\beta$ -D-glucan produced by the haptophyte alga *Emiliania huxleyi* (Lohmann) Hay and Mohler. **Carbohydrate Research**, v. 152, p. 243–248, 1986.

VASAN, K.; WERNER, M. & CHANDEL, N. S. Mitochondrial Metabolism as a Target for Cancer Therapy. **Cell Metabolism**, v. 32, n. 3, p. 341-352, 2020.

VETTORE, L.; WESTBROOK, R.L.; TENNANT, D.A. New aspects of amino acid metabolism in cancer. **British Journal of Cancer**, v. 122, n. 2, p. 150-156, 2020.

VILLARRUEL-LÓPEZ, A.; ASCENCIO, F.; NUÑO, K. Microalgae, a potential natural functional food source—A review. **Polish Journal of Food and Nutrition Science**, n. 67, p. 251–264, 2017.

VISHCHUK, O.S.; ERMAKOVA, S.P.; ZVYAGINTSEVA, T.N. Sulfated polysaccharides from brown seaweeds *Saccharina japonica* and *Undaria pinnatifida*: isolation, structural characteristics, and antitumor activity. **Carbohydrate research**, v. 346, n. 17, p. 2769-76, 2011.

VOGLER, B.W.; BRANNUM, J.; CHUNG, J.W.; SEGER, M.; POSEWITZ, M.C. Characterization of the *Nannochloropsis gaditana* storage carbohydrate: a 1,3- $\beta$ -glucan with limited 1,6-branching. **Algal Research**, n. 36, p. 152-158, 2018.

WAGNER, C.; BARLAG, B.; GERLACH, R.G.; DEIWICK, J.; HENSEL, M. The *Salmonella enterica* giant adhesin SiiE binds to polarized epithelial cells in a lectin-like manner. **Cellular Microbiology**, n. 16, p. 962–975, 2014.

WANG, H.; LI, Y.L.; SHEN, W.Z.; RUI, W.; MA, X.J.; CEN, Y.Z. Antiviral activity of a sulfoquinovosyldiacylglycerol (SQDG) compound isolated from the green alga *Caulerpa racemosa*. **Botanica Marina**, n. 50, p.185–190, 2007.

WANG, H.M. D.; CHEN, C.C.; HUYNH, P. & CHANG, J.S. Exploring the potential of using algae in cosmetics. **Bioresource Technology**, v. 184, p. 355-362, 2015.

WANG, Z.; XIE, J.; SHEN, M.; NIE, S.; XIE, M. Sulfated modification of polysaccharides: Synthesis, characterization and bioactivities. **Trends in Food Science & Technology**, n.74, p. 147-157, 2018.

WEIMER, B.C.; CHEN, P.; DESAI, P.T.; CHEN, D.; SHAH, J. Whole cell cross-linking to discover host–microbe protein cognate receptor/ligand pairs. **Frontiers in Microbiology**, n. 9, p. 1585, 2018.

WELLER, M.; WICK, W.; ALDAPE, K.; BRADA, M.; BERGER, M.; PFISTER, S. M., et al. Glioma. **Nature Reviews Disease Primers**, n. 1, p. 15017, 2015.

WOLF, A.; AGNIHOTRI, S.; MICALLEF, J.; MUKHERJEE, J.; SABHA, N.; CAIRNS, R., HAWKINS, C.; GUHA, A. Hexokinase 2 is a key mediator of aerobic glycolysis and promotes tumor growth in human glioblastoma multiforme. **Journal of Experimental Medicine**, v. 208, n. 2, p. 313-26, 2011.

WUFUER, R.; BAI, J.; LIU, Z.; ZHOU, K.; TAOERDAHONG, H. Biological activity of *Brassica rapa* L. polysaccharides on RAW 264.7 macrophages and on tumor cells. **Bioorganic & Medicinal Chemistry**, v. 28, n. 7, 2020.

XIAO, R.; ZHENG, Y. Overview of microalgal extracellular polymeric substances (EPS) and their applications. **Biotechnology Advances**, n. 34, p. 1225–1244, 2016.

XIE, L.; SHEN, M.; HONG, Y.; YE, H.; HUANG, L. & XIE, J. Chemical modifications of polysaccharides and their antitumor activities. **Carbohydrate Polymers**, v.229, p.115436, 2020.

XIE, N.; ZHANG, L.; GAO, W.; HUANG, C.; HUBER, P.E.; ZHOU, X.; LI, C.; SHEN, G.; ZOU, B. NAD (+) metabolism: pathophysiologic mechanisms and therapeutic potential, **Signal transduction and targeted therapy**, v. 5, n. 1, p. 227, 2020.

XU, H.; ZOU, S. & XU, X. The  $\beta$ -glucan from *Lentinus edodes* suppresses cell proliferation and promotes apoptosis in estrogen receptor positive breast cancers. **Oncotarget**, v.8, n.49, p.86693-86709, 2017.

YIN, Y.; ZHAO, X.; JIA, LI, H.; JIANG, X.; SHAN, Y. et al. A  $\beta$ -glucan from *Durvillaea antarctica* has immunomodulatory effects on RAW 264.7 macrophages via toll-like receptor 4. **Carbohydrate Polymers**, n. 191, p. 255-265, 2018.

YOUNG, S.H.; YE, J.; FRAZER, D.G.; SHI, X.; CASTRANOVA, V. Molecular mechanism of tumor necrosis factor-alpha production in (1 $\rightarrow$ 3)- $\beta$ -D-glucan (zymosan)-activated macrophages. **Journal of Biological Chemistry**, n. 276, pp. 20781-20787, 2001.

ZENG, T.; CUI, D. & GAO, L. Glioma: an overview of current classifications, characteristics, molecular biology and target therapies. **Frontiers in Bioscience (Landmark Ed)**, v. 20, p. 1104-1115, 2015.

ZHANG, H.; LI, C.; LAI, P.F.H.; CHEN, J.; XIE, F.; XIA, Y.; AI, L. Fractionation, chemical characterization and immunostimulatory activity of  $\beta$ -glucan and galactoglucan from *Russula vinosa* Lindblad. **Carbohydrate Polymers**, n. 256, 2021.

ZHAO, L.; CHEN, Y.; REN, S.; HAN, Y.; CHENG, H. Studies on the chemical structure and antitumor activity of an exopolysaccharide from *rhizobium* sp. N613. **Carbohydrate Research**, n. 345, p. 637-643, 2010.

ZHENG, X.; ZOU, S.; XU, H.; LIU, Q.; SONG, J.; XU, M.; XU, X.; ZHANG, L. The linear structure of  $\beta$ -glucan from baker's yeast and its activation of macrophage-like RAW264.7 cells. **Carbohydrate Polymers**, n. 148, p. 61-68, 2016.

ZHOU, X.; LIU, X.; HUANG, L. Macrophage-mediated tumor cell phagocytosis: opportunity for nanomedicine intervention. **Advanced Functional Materials**, n. 31, p. 1-18, 2021.

ZIELKE, C.; LU, Y.; POINSOT, R. & NILSSON, L. Interaction between cereal beta-glucan and proteins in solution and at interfaces. **Colloids Surface B Biointerfaces**, v.162, p.256-264, 2018.

ZOROVA, L.D.; POPKOV, V.A.; PLOTNIKOV, E.Y.; SILACHEV, D.N.; PEVZNER, I.B., et al. Mitochondrial membrane potential. **Analytical Biochemistry**, n. 552, p. 50-59, 2018.